PNL-2588
UC-71

COMPLIMENTARY COPY
FROM
TECHNICAL INFORMATION OPERATION
DO NOT RETURN

An Assessment of the Risk of Transporting Spent Nuclear Fuel by Truck

November 1978

Prepared for the U.S. Department of Energy
under Contract EY-76-C-06-1830

Pacific Northwest Laboratory
Operated for the U.S. Department of Energy
by Battelle Memorial Institute

Battelle

PNL-2588

NOTICE

This report was prepared as an account of work sponsored by the United States Government. Neither the United States nor the Department of Energy, nor any of their employees, nor any of their contractors, subcontractors, or their employees, makes any warranty, express or implied, or assumes any legal liability or responsibility for the accuracy, completeness or usefulness of any information, apparatus, product or process disclosed, or represents that its use would not infringe privately owned rights.

The views, opinions and conclusions contained in this report are those of the contractor and do not necessarily represent those of the United States Government or the United States Department of Energy.

PACIFIC NORTHWEST LABORATORY
operated by
BATTELLE
for the
UNITED STATES DEPARTMENT OF ENERGY
Under Contract EY-76-C-06-1830

Printed in the United States of America
Available from
National Technical Information Service
United States Department of Commerce
5285 Port Royal Road
Springfield, Virginia 22151

Price: Printed Copy $____*; Microfiche $3.00

*Pages	NTIS Selling Price
001-025	$4.00
026-050	$4.50
051-075	$5.25
076-100	$6.00
101-125	$6.50
126-150	$7.25
151-175	$8.00
176-200	$9.00
201-225	$9.25
226-250	$9.50
251-275	$10.75
276-300	$11.00

PNL-2588
UC-71

3 3679 00049 2357

AN ASSESSMENT OF THE RISK OF TRANSPORTING SPENT NUCLEAR FUEL BY TRUCK

H. K. Elder
Project Coordinator

Technical Contribution
W. B. Andrews
J. R. Friley
J. F. Johnson
R. A. McCann
R. E. Rhoads

November 1978

Prepared for
The U.S. Department of Energy
Under Contract EY-76-C-06-1830

Pacific Northwest Laboratory
Richland, Washington 99352

ACKNOWLEDGMENTS

The authors would like to acknowledge the assistance provided by D. L. Strenge of PNL for his input to the section on environmental consequences. The authors would also like to thank those persons who reviewed the draft version of this document and provided valuable comments toward development of this final report.

CONTENTS

FIGURES

FIGURES (contd)

TABLES

1.0 INTRODUCTION

Radioactive materials, in a variety of physical and chemical forms, have been routinely transported between various nuclear facilities. The safety record for these shipments has been excellent. As the nuclear industry grows, it is expected that the number of shipments made annually will increase. To insure the health and safety of the general public, industry and government agencies are continually improving their level of understanding of the safety-related aspects of transporting energy materials including nuclear materials.

Research programs are one method of improving the level of understanding. Such a research program is being conducted by Pacific Northwest Laboratory (PNL) for the Transportation Branch of the Department of Energy in the Division of Environmental Control Technology. The objective of this continuing program is to develop a methodology for quantitatively assessing the safety of transporting energy materials and to apply it to current and future shipping systems. Risk analysis was the technique selected for this assessment. Through analysis of risk, consequences of postulated releases of energy materials during transport can be put into perspective by viewing the events relative to their expected frequency of occurrence.

Risk, as used in the context of this report, is the product of the probability of a release of material to the environment and the consequences resulting from the release. There are two measures of the risk that are of importance in a risk assessment. The first is a numerical value which is the sum of the risk associated with each particular loss. This is the total risk. In order to perform the summation, all risks have to be expressed with respect to the same time interval (e.g., per year). Although the total risk is an important measure, it gives only the loss that would be expected on the average during the reference time interval. The range of losses which could be experienced is not discernable. For example, the risk associated with an accident that occurs once a year and results in one fatality is the same (i.e., one fatality/year) as that from an accident which occurs once in ten years but results in ten fatalities.

In a plot of the expected frequency of N or more fatalities as a function of N, these two accidents would appear as discrete points. The second measure of risk is a curve called a risk spectrum, which is generated by connecting such points. The risks associated with two activities are similar only if they have the same total risk (risk magnitude) and the same risk spectrum. Both risk measures are used in this report.

The risk methodology was initially applied to the shipment of plutonium[1] by truck and has subsequently been applied to the shipment of plutonium by rail[2] and air,[3] the shipment of gasoline by truck,[4] and the shipment of uranium hexafluoride by truck and rail.[5] This report presents the results of an assessment of the risk of transporting spent nuclear fuel by truck. The general risk methodology used in this assessment as well as the previous risk studies is also reviewed.

REFERENCES

1. T. I. McSweeney, R. J. Hall et al., An Assessment of the Risk of Transporting Plutonium Oxide and Liquid Plutonium Nitrate by Truck. BNWL-1846, Battelle, Pacific Northwest Laboratories, Richland, WA, August 1975.

2. R. J. Hall et al., An Assessment of the Risk of Transporting Plutonium Dioxide and Liquid Plutonium Nitrate by Train. BNWL-1996, Battelle, Pacific Northwest Laboratories, Richland, WA, February 1977.

3. T. I. McSweeney, J. F. Johnson, An Assessment of the Risk of Transporting Plutonium Dioxide by Cargo Aircraft. BNWL-2030, Battelle, Pacific Northwest Laboratories, Richland, WA, June 1977.

4. R. E. Rhoads et al., An Assessment of the Risk of Transporting Gasoline by Truck. PNL-2133, Battelle, Pacific Northwest Laboratories, Richland, WA, November 1978.

5. C. A. Geffen et al., An Assessment of the Risk of Transporting Uranium Hexafluoride by Truck and Train. PNL-2211, Battelle, Pacific Northwest Laboratories, Richland, WA, August, 1978.

2.0 SUMMARY

This report is the sixth in a series of studies of the risk of transporting potentially hazardous energy materials.[a] The report presents an assessment of the risk of shipping spent nuclear fuel by truck.

The general risk assessment methodology used in this study is the same as that developed for the first study in this series.[1] The methodology is summarized in Section 3. The assessment includes the risks from release of spent fuel materials and radioactive cask cavity cooling water due to transportation accidents. The contribution to the risk of package misclosure and degradation during normal transport was also considered.

The report is sectioned to correspond to the specific analysis steps of the risk assessment model. The transportation system and accident environment are described in Sections 4 and 5. Calculation of the response of the shipping system to forces produced in transportation accidents are presented in Section 6 and the results of a survey to determine the condition of the package during transport are presented in Section 7. Sequences of events that could lead to a release of radioactive material from the shipping cask during transportation are postulated in Section 8 using fault tree analysis. These release sequences are evaluated in Sections 9 through 11, to determine both the likelihood and the possible consequences of each release. Supportive data and analyses are given in the appendices.

The results of the risk assessment have been related to a time in the mid-1980's, when it is projected that nuclear plants with an electrical generating capacity of 100 GW will be operating in the U.S. Because there is some uncertainty about the future development of the nuclear fuel cycle, two alternative transportation scenarios are considered: (1) the "once through" fuel cycle where all spent fuel is shipped to interim storage, and (2) the fuel reprocessing scenario where all spent fuel is shipped to reprocessing plants. Additional assumptions used for the analysis are:

(a) The others are listed as references 1, 3, 4, 5, and 6.

- Shipping systems and regulations are the same as in 1978.
- Twenty percent of the spent fuel transported in the reference year is shipped by truck.
- Spent fuel is assumed to be shipped either 180 days or 4 years after discharge from the reactor.
- The spent fuel is shipped in a legal weight truck cask with a capacity of one PWR or 2 BWR spent fuel elements.

The shipping system description developed from these assumptions is summarized in Table 2.1. Other shipping conditions or different shipping regulations could result in different risks than reported in this study. However, the methodology is capable of analyzing the risks under any shipping conditions.

TABLE 2.1 Summary of Shipping Characteristics for Spent Fuel by Truck in Mid-1980's

Spent Fuel Per Shipment (MTHM):[a]	
PWR	0.461
BWR	0.394
Shipment: Origin/Destination:	
Once Through Fuel Cycle	Reactor/Interim Storage
Reprocessing Fuel Cycle	Reactor/Reprocessing Plant
Material Shipped Per Year (MTHM):	380
Number of Shipments Per Year by Truck:	885
Average Shipment Distance (km):	
Once Through Fuel Cycle	690 (430 mi.)
Reprocessing Fuel Cycle	930 (580 mi.)
Accident Probability (Number/km):	1.5×10^{-6}

(a) Metric tons of heavy metal (uranium plus plutonium) in the fuel.

For shipments from reactors to interim storage facilities, it is estimated that a truck carrying spent fuel will be involved in an accident that would not be severe enough to result in a release of spent fuel material about once in 1.1 years. It was estimated that an accident that could result in a small release of radioactive material (primarily contaminated cooling water) would occur once in about 40 years. This accident would not be expected to result in measurable doses to the general public. The frequency of an accident resulting in one or more latent cancer fatalities from release of radioactive materials during a truck shipment of spent fuel to interim storage was estimated to be once in 41,000 years. No accidents were found that would result in acute fatalities from releases of radioactive material.

The risk for spent fuel shipments from reactors to reprocessing plants was found to be about 20% less than the risk for shipments to interim storage. Although the average shipment distance for the reprocessing case is larger, the risk is somewhat lower because the shipping routes, on average, are through less populated sections of the country. Given the uncertainty in the location of future fuel cycle facilities, this difference is judged to be insignificant.

The potential consequences of the postulated releases were estimated based on the characteristics and amount of radioactive material released to the environs, the probable weather conditions at the time of the accident, and the population density downwind from the accident scene. The likelihood and the consequences for these postulated releases have been coupled and expressed as risk spectra.

The risk spectrum for truck shipment of spent fuel to interim storage is shown in Figure 2.1 for the number of shipments projected for the United States in the mid-1980's. The risk spectrum is a plot of the estimated number of latent cancer fatalities vs the estimated frequency of an event resulting in that number of fatalities or greater. For example, the estimated probability that a truck carrying 180-day cooled spent fuel will be involved in an accident resulting in one or more latent cancer fatalities during the reference year is 2.2×10^{-5} and the estimated probability of an event resulting in five or more fatalities is 5.0×10^{-6}. Shipping only fuel that had

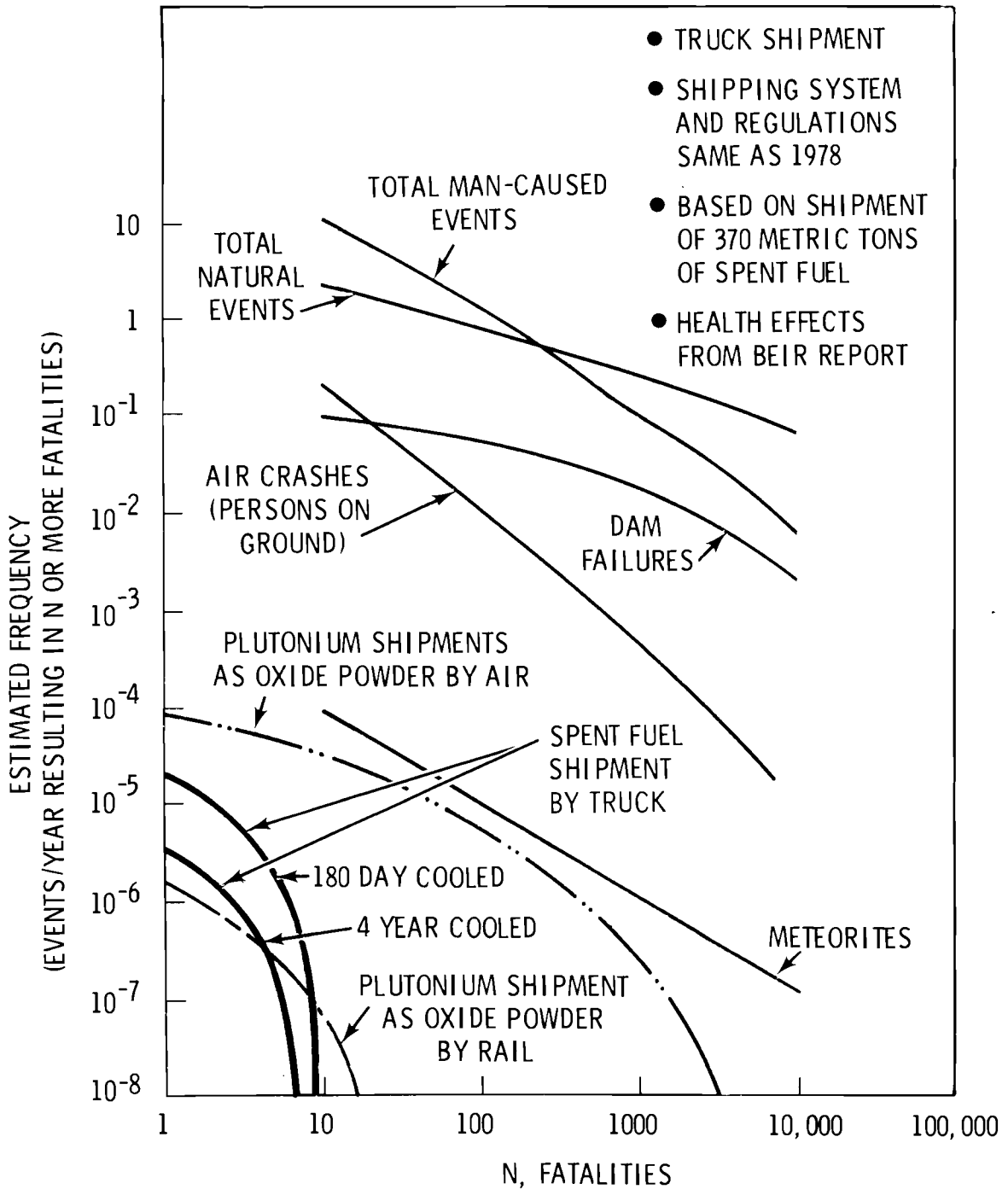

FIGURE 2.1. Risk Spectra for Spent Fuel Shipments in the Mid-1980's for the Entire United States

been cooled 4 years would reduce the probability of one or more deaths to 3.6×10^{-6}. Risk spectra for other risks to which society is exposed[2] and from transportation of other radioactive materials[3,4] have been included in the figure for comparison. The risk from transporting spent fuel by truck in the reference year is seen to be much less than the risk to society from natural events or man-caused events and comparable to the risks from transporting plutonium.

The spent fuel transported by truck in the reference year will have generated about 10^{11} kwhr of electricity or enough to provide the annual electric energy requirement for a population of about 8 million. Considering the substantial benefits derived from the fuel, it is the opinion of the authors that the current spent fuel transportation system poses acceptable risks to the public.

Additional perspective may be gained on the risk of transporting spent fuel by truck by comparing the total risk and the risk to any individual in society with similar numbers for other risk-producing activities and natural events. The total risk from transporting 180-day cooled spent fuel by truck in the reference year is 4.5×10^{-5} fatalities. An individual in the population at risk would have one chance in 6×10^{11} of suffering a latent cancer fatality from a release of radioactive material from a truck carrying spent fuel in the reference year. Table 2.2 presents a comparison of these numbers to other risk-producing events in the U.S. The risks from transporting spent fuel by truck in the reference year are seen to be much less than the risks from other man-caused events and lower than the risk from infrequent natural disasters such as meteorites.

Sensitivity studies were performed to determine the important contributors to the risk of spent fuel shipment by truck. These studies are described in Section 11. Impact forces were found to contribute to about 69% of the releases, and failure by fire contributed to about 28%, while accidents involving casks with nonstandard packaging conditions contributed to only about 3% of the releases in the basic risk assessment. To illustrate the sensitivity of the risk to the release fractions, it was assumed that all release fractions were increased by a factor of ten. This case represents an analysis

TABLE 2.2 Average Total and Individual Risk in the United States from Various Accident and Natural Disasters

Event	Total Risk (Fatalities/Year)[a]	Individual[b] Risk
All Accidents	103,030	1 in 2,000
Motor Vehicle Accidents	46,700	1 in 4,000
Air Crashes	1,552	1 in 130,000
Dam Failures	35[c]	1 in 5,700,000
Air Crashes (Persons on Ground)	6[d]	1 in 33,000,000[e]
Meteorites	1.0×10^{-3}[f]	1 in 2×10^{11}
Spent Fuel Truck Shipments	4.5×10^{-5}	1 in 6×10^{11}[e]

(a) Based on 1975 statistics unless otherwise noted.
(b) Based on total U.S. population.
(c) Average for dam failures 1889-1972 (Reference 2).
(d) Average for years 1960-1973 (Reference 2).
(e) Based on population at risk.
(f) Estimate based on information from Reference 2.

that is believed to be very conservative. This was shown to increase the risk by a factor of eight.

Modifying the reference cask to reduce the effects of fire by replacing the rupture disk with a pressure relief valve was found to reduce the risk level by 24%.

REFERENCES

1. T. I. McSweeney, R. J. Hall et al., An Assessment of the Risk of Transporting Plutonium Oxide and Liquid Plutonium Nitrate by Truck. BNWL-1846 Battelle, Pacific Northwest Laboratories, Richland, WA, August 1975.

2. Reactor Safety Study. "An Assessment of Accident Risks in U.S. Commercial Nuclear Power Plant." WASH 1400, U.S. Nuclear Regulatory Commission Washington DC, October 1975.

3. R. J. Hall et al., An Assessment of the Risk of Transporting Plutonium Dioxide and Liquid Plutonium Nitrate by Train. BNWL-1996, Battelle, Pacific Northwest Laboratories, Richland, WA, February 1977.

4. T. I. McSweeney and J. F. Johnson, An Assessment of the Risk of Transporting Plutonium Dioxide by Cargo Aircraft. BNWL-2030, Battelle, Pacific Northwest Laboratories, Richland, WA, June 1977.

5. R. E. Rhoads et al., An Assessment of the Risk of Transporting Gasoline by Truck. PNL-2133, Battelle, Pacific Northwest Laboratories, Richland, WA, November 1978.

6. C. A. Geffen, et al., An Assessment of the Risk of Transporting Uranium Hexafluoride by Truck and Train. PNL-2211, Battelle, Pacific Northwest Laboratories, Richland, WA, August, 1978.

3.0 TRANSPORTATION RISK ASSESSMENT METHODOLOGY

This risk assessment represents the sixth in a series of analyses of the transportation of hazardous energy materials. The history of the methodology and a brief summary of the risk assessment model used in all studies to date will be presented below.

3.1 HISTORY

The risk methodology used in this and earlier risk transportation studies evolved from a number of risk analysis models originally developed for use in the nuclear industry. Initially, the risk methodology was suggested as a method of selecting an acceptable site for nuclear power facilities.[1] Accident frequencies were expressed in the form of reactor years between radioactive material releases and consequences were expressed in terms of curies of radioactive material released.

Developments in the area of the health effects of exposure to radiation allowed the eventual use of individual mortality as the measurement of release consequences in later studies.[2, 3, 4] The units of risk became the probability of an individual mortality in any operation year. Analyses[5, 6] were further expanded to show that the risk level individuals are willing to accept is related to the benefits received by the individual. If the benefits are significantly higher, then the risk level the individual is willing to accept is also higher.

The use of health effects to express risk allows a variety of technologies to be meaningfully compared. In the Reactor Safety Study,[7] the risk of operating a nuclear power plant was compared to the risks from natural disasters and man-caused events.

The risk assessment methodologies discussed above have been limited to analyses of fixed facilities. These facilities have a well-defined population distribution and the population in the immediate vicinity of the plant

(the exclusion area) is controlled by the facility operator. The population distribution in the vicinity of a transportation accident, however, is highly variable. Transportation accidents may occur in rural areas (with very low population densities) in suburban areas or in urban areas (with relatively high population densities). Since transportation accidents can occur at virtually any location along the shipping route, a variety of geographic and meteorological conditions can also be encountered. The variability in the population distribution, geography and meteorology for transportation accidents adds a degree of complexity not found in risk assessments of fixed sites.

A number of methodologies have been developed to analyze the transport of hazardous materials. One, used by the University of Southern California[8] in a study for the Department of Transportation is based on accident case histories. This technique, however, cannot be applied to all energy material shipments because in many cases the accident experience is extremely limited or the accident data have not been collected in a way that permits accurate risk assessments.

A second technique developed by Holmes and Narver was used to determine the risk of transporting bioweapons[9] and radioactive material.[10] These analyses were performed for shipments of material along a selected route. This methodology is limited in that one average number for the risk is obtained. It would also be beneficial to know how the risk varies with route, weather, population, material form, and accident severity. The variability of risk with possible transport conditions could then be considered.

3.2 RISK ASSESSMENT MODEL

The risk assessment model used in the analysis of the transport of energy materials is described below. The methodology used in the PNL risk studies provides flexibility not available in previous transportation risk studies since it permits the risk to be analyzed for a spectrum of population densities and weather conditions that can be encountered along shipping routes.

The transportation risk assessment model provides a systematic method for handling the data required to analyze the safety of the transporation of hazardous materials. The model uses one fundamental equation:

$$R = \sum_i R_i \qquad (3\text{-}1)$$

The total system risk R is the sum of the risks of all accidental releases as denoted by the subscript i. Only accidental releases are considered in the model. The risk of an individual release is the product of the consequences of the release and the probability of its occurrence. In the current formulation of the model, each term in Equation 1 is expanded into two expressions which have more physical significance. The expanded equation for R_i is:

$$R_i = \left(A\ F_{R_i} \times P_{R_i}\right) \times \left(\sum_q C_{E_{i,q}} \times P_{E_q}\right) \qquad (3\text{-}2)$$

The first expression, $A\ F_{R_i} \times P_{R_i}$, can be thought of as a probabilistic source term for each identified release sequence. The first factor in this term, $A\ F_{R_i}$, represents the amount of material released in the i^{th} release sequence. It is the product of the amount of material present in a shipment (A) and the fraction of that material lost to the environment in the i^{th} release sequence (F_{R_i}). This factor can be considered a source term for the i^{th} chain of events or failures which end with a release of material. The second factor, P_{R_i}, is the probability that the release sequence will happen during transport.

The second expression in equation $2(\sum_q C_{Ei,q} \times P_{Eq})$, represents the consequences of a unit release of material (unit source term) under probabilistically weighted weather conditions and population distributions. The consequences of a unit release of material are evaluated in the expression $C_{E_{i,q}}$. The subscript q is added to show that this factor is a function of the specific weather conditions existing at the time of the release and the population exposed to the release. The consequences can be expressed in a variety of ways, depending on the material being studied. Risk comparisons can be made most advantageously if the consequences are expressed as health

effects. The final factor in this expression, P_{E_g}, is the joint probability of encountering a particular set of weather conditions within a specific population zone.

The methodology used to provide input data for solution of the above equations involves four components:

- System Description
- Release Sequence Identification
- Release Sequence Evaluation
- Risk Calculation and Assessment

These four components, shown graphically in Figure 3.1, are described in detail below. Step numbers correspond to the number shown in the figure.

3.2.1 System Description

The system description can be considered the what, how, when, and where component. The risk assessment is as good as the knowledge of the system through which the material is being shipped. Most of the information is already available or easily derived. A complete description of the transportation system generally consists of seven steps, which are shown in Figure 3.1.

Projected industry characteristics are determined in Step 1. Included in this segment is a description of projected facilities and industry needs for the reference year. Material type, amounts, origins, and destinations are specified in the second step. The third step presents a description of the important physical and chemical characteristics of the material being shipped. For example, an important property of liquid materials is the vapor pressure exerted as a result of elevated temperatures in an accident environment. Powdered materials require specification of the particle size distribution. For radioactive materials, the radionuclide inventory must also be specified.

In the remaining four steps, the transportation system is described. In Step 4, the transportation mode is specified, and the vehicles used are described. Weight and space limitations (and in the case of radioactive

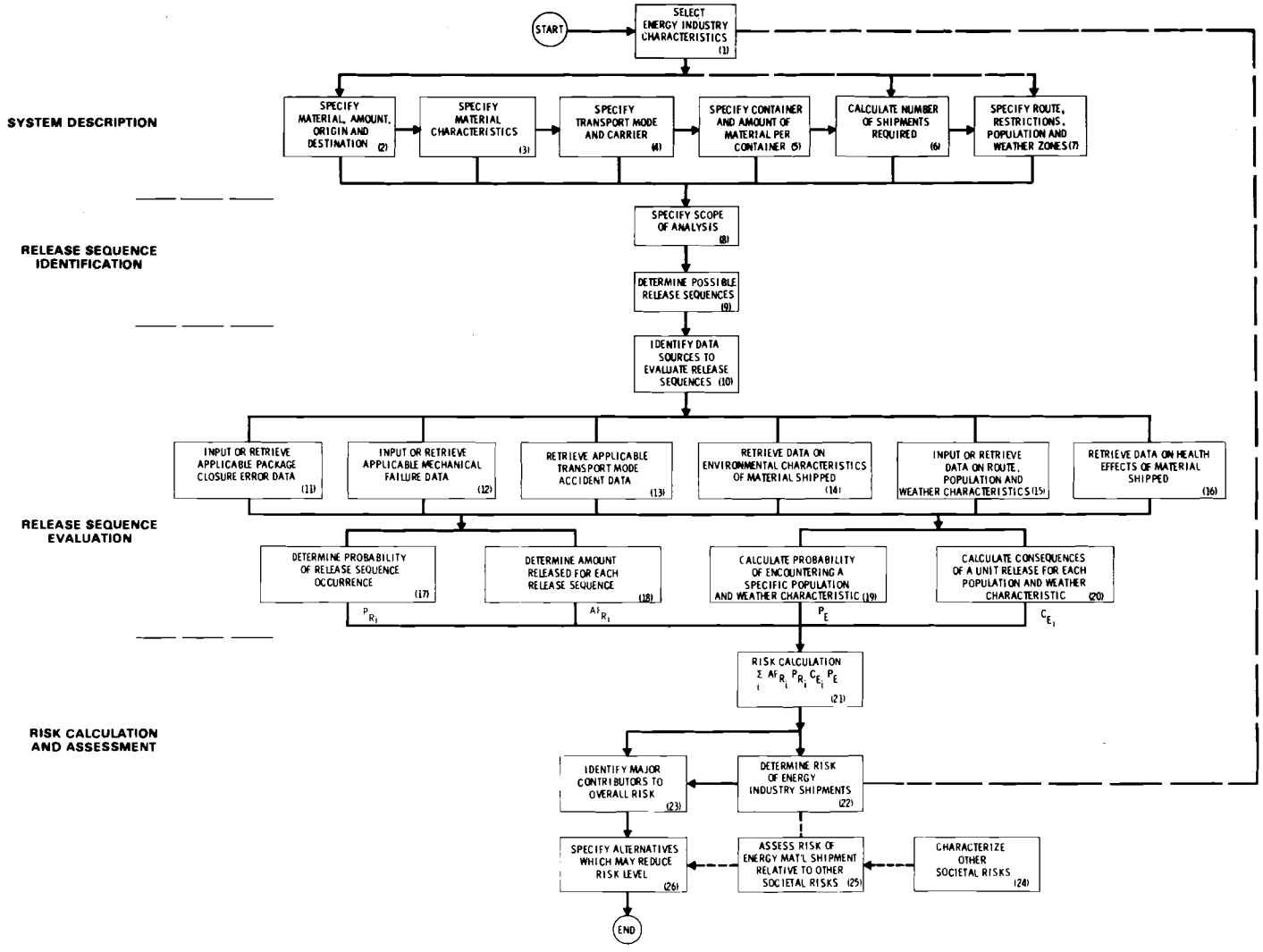

FIGURE 3.1. Model to Calculate the Risk of Shipping Energy Materials

materials shipments, heat, geometry, dose and criticality limits) must be specified here so that amount of material per shipment and the required number of shipments can be calculated.

The container used to carry the material is considered in Step 5. For DOE specification or approved containers, only the container designation is needed to completely describe the container. Nonstandard containers require sufficient input to permit evaluation of failure paths later in the analysis. Step 6 of the system description involves the calculation of the number of shipments required to transport the amounts of material specified in Step 2, in the vehicles and containers given in Steps 4 and 5.

In the final step of the system description, the shipping route is divided and each segment is described in terms of type of route, shipping restrictions, population and weather characteristics. With the completion of this step, the entire transportation system has been described.

3.2.2 Release Sequence Identification

The next component in the risk assessment process is the identification of the sequences of events that could lead to release of material from the transport vehicle. These sequences of events called release sequences, may be identified in a variety of ways. It is felt that the most complete listings of release sequences are obtained by deductive reasoning processes that work backwards from a release through the possible chain of events that could produce the release. Fault tree analysis provides a systematic method for performing these deductive reasoning processes. The fault tree that is constructed in these analyses also provides a compact notation for displaying large numbers of release sequences. Computer codes such as the MFAULT[14] code used at PNL, can be used to quickly and accurately perform the Boolean "cut sets" required for subsequent steps in the analysis.

Before the possible release sequences are identified (Step 9), the scope of the analysis must be delineated (Step 8). Only those release sequences within the selected scope of analysis are evaluated in subsequent steps in the model. Completed studies using this risk assessment model have considered releases from two general causes. In addition to releases caused by forces

produced in transportation accidents, releases resulting from package closure errors, substandard packaging construction or deterioration in packaging condition resulting from the normal transportation environment have been considered. Failure associated with deliberate sabotage or diversion attempts have not been considered.

3.2.3 Release Sequence Evaluation

The release sequences which have been identified are evaluated to determine the factors needed to evaluate Equation 3.2. The source term and environmental consequences evaluations are performed separately.

The release sequence factors (denoted by the subscript "R" in Equation 3.2) represent the probability that material will be released in an accident and the amount of the material released. The evaluation of these factors requires the information from four data bases, shown in Figure 1 as Steps 11-14. These data bases are:

- Package Closure Error Data (11)
- Mechanical Failure Data (12)
- Transport Mode Accident Data (13)
- Data on Environmental Characteristics of Material Shipped (14)

Package closure data (Step 11) can be obtained in several ways. One method that has been used is to survey facilities routinely receiving the material under study. Physical container tests and mechanical failure analyses are used to develop data in Step 12. Studies already completed using the PNL model have used both accident environment information developed at Sandia Laboratories[11] and Department of Transportation accident data to satisfy Step 13. The behavior of the material in the environment (Step 14) depends entirely upon the material under consideration.

With the information from Steps 11 to 14, the probability of a release is evaluated and the source term for each release is characterized (Steps 17 and 18 in Figure 3.1). Generally the probability of a release sequence occurring is evaluated first and the source term is then determined for the release

sequences. Release fractions (F_{RI}) used for various release sequences and environmental conditions are determined after carefully examining the individual release sequences.

The environmental terms in Equation 3.2 are denoted by a subscript E. The factor P_E represents the probability that a given set of weather and population density characteristics will be encountered. The factor C_{E_i} represents the consequences of a unit release occurring in the region characterized by the weather and population density used to determine P_E. When analyzing releases involving radioactive materials, the consequences are initially calculated as a population dose in units of man-rem to a selected organ of reference and then converted to health effects.

The evaluation of these two environmental consequences terms requires input from three data bases:

- Data on Environmental Characteristics of Material Shipped (14)
- Data on Route, Population, and Weather Characteristics (15)
- Data on Potential Health Effects of Material Shipped (16)

The environmental behavior characteristics and health effects from exposure to the released material is a function of the material itself and must be developed individually for each study. Data for Step 15 are available from many compilations including U.S. Census data[12] and summaries of regional weather data compiled by the U.S. Weather Bureau.[13]

Information from Steps 14 to 16 is used to evaluate the probability of experiencing a given set of weather conditions and population characteristics. These evaluations are shown as Steps 19 and 20 in Figure 3.1. The P_E term in Equation 3.2 is the probability associated with the weather and population characteristics. The expanded form of this term is given:

$$P_{E_{j,k,l}} = P_{j/k} \times P_k \times P_l. \qquad (3\text{-}3)$$

The subscripts j, k and l refer to the multiplicity of environmental conditions which could exist at the location of the accident. For example, the variable $P_{j/k}$ may be the probability of experiencing the j^{th} atmospheric

stability classification when the K^{th} windspeed exists, the variable P_k the probability of encountering the k^{th} windspeed category and the variable P_1 the probability of encountering a specified population distribution.

3.2.4 Risk Calculation and Assessment

The final component in the risk assessment is to sum and evaluate the risks associated with the applicable release sequences. The steps involved in this component are shown graphically in Figure 3.1.

The overall risk calculation for each release sequence is described by Equations 3.1 and 3.2. These release sequence risks are added to determine the risk associated with individual shipping routes. The risks for individual routes are next weighted according to the amounts being shipped along each route. The overall transportation risk (total risk) is the sum of risks from these weighted individual routes. At this point, the risk can also be expressed in terms of a risk spectrum (plot of magnitude of consequence versus frequency of events resulting in that consequence or a more severe consequence).

Comparative analysis of the individual risk terms permits identification of those sequences of events that are major contributors to the overall risk (Step 23). From this list of sequences, changes which could reduce the overall risk may be suggested.

Comparing the risk levels obtained in the analysis to risk levels from other technologies or the natural environment places the calculated risk levels in perspective. Step 24 provides values for other societal risks and comparisons are made in Step 25. If it is determined that the calculated risk is unacceptable, alternatives which may reduce the risk level can be specified (Step 26).

REFERENCES

1. F. R. Farmer, "Reactor Safety and Siting: A Proposed Risk Criterion." Nuclear Safety, 8:539, 1967.

2. H. J. Otway and R. C. Erdmann, "Reactor Siting and Design from a Risk Viewpoint." Nuclear Engineering and Design, 13:365, 1970.

3. M. Meleis and R. C. Erdmann, "The Development of Reactor Siting Criteria Based Upon Risk Probability." Nuclear Safety, 13:22, 1972.

4. G. D. Bell, "Safety Criteria," Quantitative Safety Analysis, Nuclear Engineering and Design, 13:183-244, 1970.

5. C. Starr, "Benefit-Cost Studies in Socio-Technical Systems," Proceedings of Conference on Hazard Evaluation and Risk Analysis, Houston, TX, 18-19 August 1971, National Academy of Sciences, Washington DC.

6. C. Starr, M. A. Greenfield and D. F. Hausknecht, "A Comparison of Public Health Risks: Nuclear vs Oil Fired Power Plants," Nuclear News, 15(10): 37, 1972.

7. Reactor Safety Study, WASH-1400, U.S. Nuclear Regulatory Commission, Washington DC, October 1975.

8. G. P. Jones and R. W. Barrow, Risk Analysis in Hazardous Materials Transportation. RAPO-72-106, U.S. Department of Transportation, Office of Hazardous Materials, Washington DC, November 1972.

9. B. J. Garrick, W. C. Gekler, O. C. Baldonado, H. K. Elder and J. E. Shapley, A Risk Model for the Transport of Hazardous Materials. HN-204, Holmes and Narver, Inc., Los Angeles, CA, August 1969.

10. C. V. Hodge and O. C. Baldonado, "Risk Analysis of Shipments in the Nuclear Power Industry." Proceedings of the 4th International Symposium on Packaging and Transportation of Radioactive Materials, CONF-740901, September 22-27, 1974.

11. R. K. Clarke et al., Severities of Transport Accidents. SLA-74-0001, Sandia Laboratories, Albuquerque, NM, July 1976.

12. U.S. Bureau of the Census, County and City Data Book, 1967, (A Statistical Abstract Supplement). U.S. Department of Commerce, Washington DC, 1967.

13. U.S. Weather Bureau, Climatological Data Summaries. U.S. Department of Commerce National Climatic Center, Asheville, NC.

14. P. J. Pelto, W. L. Purcell, MFAULT: A Computer Code for Analyzing Fault Trees. BNWL-2145, Battelle, Pacific Northwest Laboratories, Richland, WA, November 1977.

4.0 SPENT FUEL SHIPPING SYSTEM

The risk assessment model discussed in Section 3 is based on a specific set of shipping requirements for the material being transported. The shipping requirements include the projected amounts of material to be shipped and the number, origin and destination of shipments in the time period being studied. This evaluation is based on the number of operating power reactors to allow comparisons to be made with the relative risks involved in shipping other fuel cycle materials determined in earlier studies.[1, 2, 3, 4] Because of uncertainties in the future development of the nuclear fuel cycle, risk assessments for two spent fuel shipping scenarios, the "once through" fuel cycle and fuel reprocessing, were made in this study. Spent fuel shipping models for the two cases are presented in Section 4.3. A brief description of the spent fuel shipping cask is given in Section 4.4.

4.1 NUCLEAR INDUSTRY ASSUMPTIONS

The analysis in this study is based on the spent fuel shipping requirements for a nuclear industry consisting of 100 nuclear reactors, each with 1,000 Megawatt electrical capacity (i.e., a total installed nuclear generating capacity of 100 Gigawatts electrical). This capacity level will probably be reached in the early to mid-1980's at the presently projected rate of growth. Fuel cycle facilities operating in the mid-1980's are assumed to be the same as those operating or in the planning or construction phase during 1977-78. The regulations governing shipping are assumed to be the same as in 1978. No significant changes in the nuclear industry are assumed to occur which would change the amounts of materials projected in the mid-1980's. The industry characteristic assumptions used in this evaluation are summarized in Table 4.1. A plant capacity factor of approximately 65% is assumed. The amount of fuel shipped per year from the 100 reactors is estimated to be 1854 metric tons of heavy metal.[5] Converting this to the number of fuel assemblies shipped per year gives 2680 PWR fuel assemblies and 3275 BWR fuel assemblies shipped per year.

TABLE 4.1. Nuclear Industry Assumptions

	PWR	BWR
Number of Operating Power Reactors[a]	67	33
Reactor Generating Capacity	1000 MWe	1000 MWe
Capacity Factor	65%	65%
Total Weight of Fuel Shipped per yr[b]	1236 MTHM	618 MTHM
Number of Assemblies Shipped per yr from Reactors to Interim Storage or Reprocessing Plants	2680	3275
Uranium plus Fission Product per Assembly	461.4 kg	197.0 kg

(a) Two-thirds of reactors are assumed to be PWR.
(b) Based on data derived from Reference 5.

4.2 TRANSPORTATION SCENARIO

Spent nuclear fuel may either be stored or reprocessed and used as additional reactor fuel. The reprocessing of spent nuclear fuel is currently the subject of national and international debate. At the present time, reprocessing has been indefinitely deferred in the U.S. However, for completeness this study assesses the risk for spent fuel shipping scenarios associated with both the "once through" and the reprocessing fuel cycles.

4.2.1 "Once Through" Fuel Cycle

In the "once through" fuel cycle, spent fuel elements from nuclear power plants are shipped to an intermediate storage facility, and eventually sent to a permanent disposal facility. Irradiated fuel elements are cooled in a fuel storage basin at the nuclear reactor for at least six months after discharge. The fuel is then shipped by rail or truck to an interim storage facility. Some fuel may remain in reactor storage basins for longer than six months before shipment. After storage for about six years, the irradiated elements can then be packaged and shipped to a permanent disposal facility. No location or

number of Federal repositories have been determined at this time and they will not be ready to receive spent fuel until after the mid-1980's; thus, those shipments are not considered in this study.

It is assumed that there are four interim spent fuel storage facilities in operation in the United States in the reference year. These are assumed to be located at:

- Morris, Illinois
- Barnwell, South Carolina
- Oak Ridge, Tennessee
- Hanford, Washington

4.2.2 Spent Fuel Reprocessing

In the reprocessing fuel cycle, spent fuel is transported from reactors to a chemical reprocessing plant where the residual fissionable material is separated for eventual recycle in fresh reactor fuel. For purposes of this study, this scenario differs from the "once through" fuel cycle case only in the shipment destinations. For the reprocessing scenario, it was assumed that reprocessing facilities were located in Barnwell, SC and Oak Ridge, TN.

4.3 SPENT FUEL SHIPPING MODEL

To determine estimated shipping route distances from reactors to spent fuel storage facilities or fuel reprocessing plants, a model shipping system was developed. Existing and proposed reactors[6] were grouped according to type (PWR or BWR) and location, and distances from these groups to the nearest assumed interim storage or reprocessing facility were calculated. Locations of the reactor groups, spent fuel storage facilities and reprocessing plants are shown in Figure 4.1. Estimates of the amounts of spent fuel shipped per year from each reactor group were made based on the number, size and type of reactors in each group. From these amounts, the number of assemblies shipped were calculated. For this study, it was assumed that 20% of the spent fuel transported during the reference time period is shipped by truck and that the fuel is shipped at either 180 days or 4 years after discharge from the reactor.

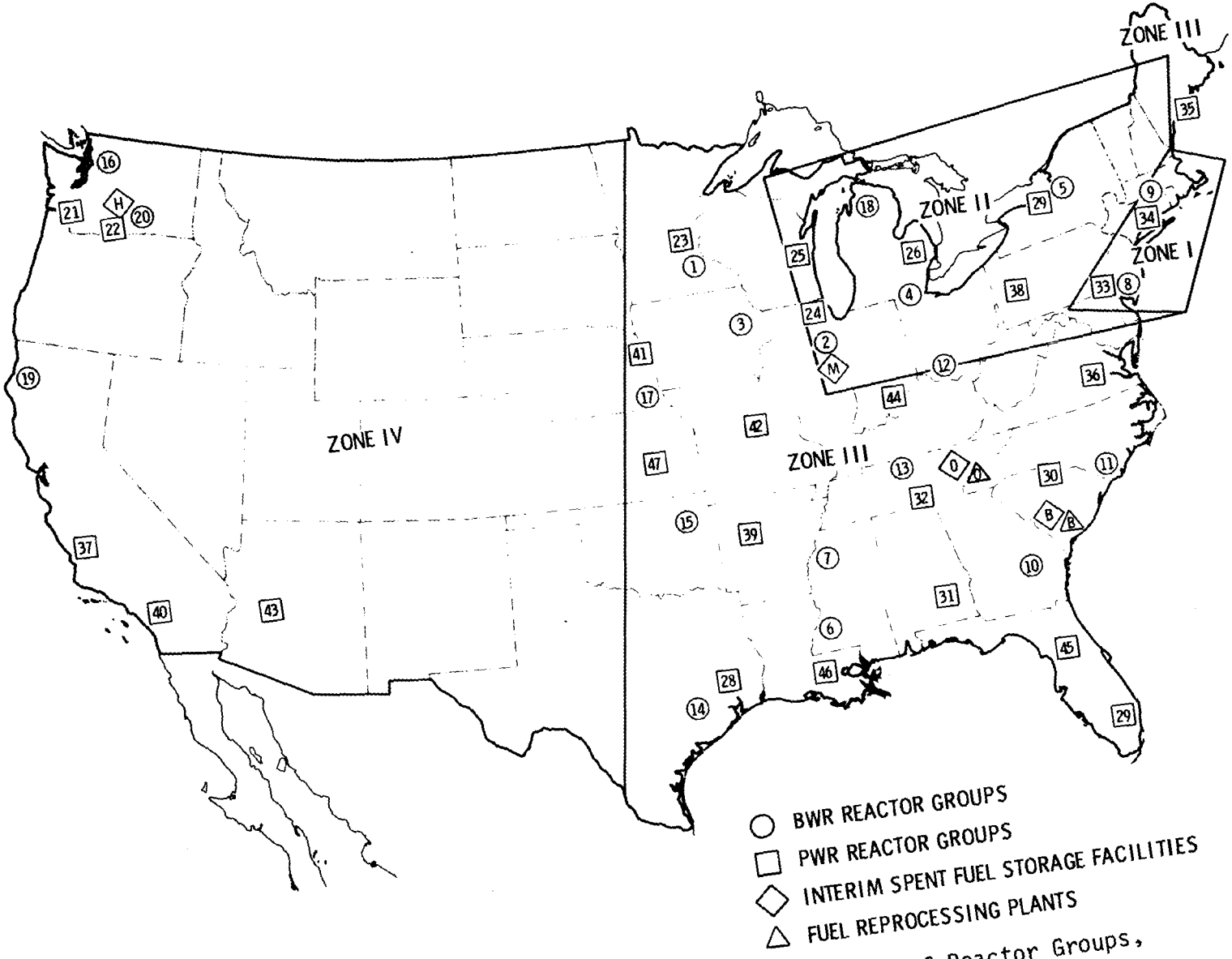

FIGURE 4.1. U.S. Population Zones with Locations of Reactor Groups, Spent Fuel Storage Facilities and Reprocessing Plants

Both of these cooling time periods after discharge were analyzed in the study. It was further assumed that shipments made in the mid-1980's would be on primary roads by licensed shippers. Table 4.2 shows the shipping characteristics assumed for analysis including the estimated shipping distances and number of truck shipments. Details of the calculations of spent fuel shipping requirements are presented in Appendix H.

TABLE 4.2 Shipping Characteristics for Spent Fuel by Truck

	Once Through Fuel Cycle	Spent Fuel Reprocessing
Shipment Origin/Destination	Reactor/ Interim Storage	Reactor/ Reprocessing Plant
Age of Fuel at Shipment (Time after Discharge from Reactor)	180 days and 4 years	180 days
Number of Shipments per Year by Truck	885	885
Average Shipment Distance (Km)	690 (430 mi.)	930 (580 mi.)

4.4 REFERENCE CASK DESCRIPTION

Shipments of spent fuel are assumed to be made in a reference truck cask designed to transport one PWR or two BWR fuel assemblies. The approximate loaded cask weight is 23 MT (50,000 lbs). The cask has an overall length of 544 cm (214 in.) and a diameter of 96 cm (38 in.). The cask cavity has a length of 452 cm (178 in.) and a diameter of 34 cm (13.5 in.). Interchangeable fuel baskets provide the cask with a capacity of one PWR or two BWR fuel assemblies.

The primary cask cavity consists of a nominal 0.8 cm (5/16 in.) stainless steel pressure shell surrounded by a lead gamma shield 16.8 cm (6-5/8 in.) thick and a stainless steel penetration barrier 3.2 cm (1-1/4 in.) thick. Neutron shielding is provided by a borated water-antifreeze solution contained in a 11.4 cm (4-1/2 in.) thick compartmentalized tank which surrounds the

cask. An expansion chamber for the shield tank accommodates temperature sheathed balsa wood at each end of the cask given protection from impact damage.

The container has a single lid, attached with high-strength bolts and sealed with teflon O-rings. The closure requires a lifting spider, special tools and O-ring pressure test equipment. Two valve-type drain closures are provided.

Heat rejection is by convection through the water coolant in the cavity to the inner wall, conduction to the neutron shield, convection to the outer wall, and convection plus radiation to the atmosphere. Maximum heat rejection capacity is 11.5 kW. Maximum design conditions for the inner cavity during normal transport [i.e., 55°C (130°F)] direct sunlight, still air, maximum fuel burnup, minimum fuel cooling period) are 174°C (345°F) and 10 atm (150 psig). The primary cavity is designed to withstand temperature and pressure conditions of 278°C (532°F) and 67 atm (984 psig) under the fire accident condition [1/2 hr at a temperature of 800°C (1475°F)].

A detailed description of the reference spent fuel shipping cask is given in Appendix A.

REFERENCES

1. T. I. McSweeney, R. J. Hall, et al., An Assessment of the Risk of Transporting Plutonium Oxide and Liquid Plutonium Nitrate by Truck, BNWL-1846, Battelle, Pacific Northwest Laboratories, Richland, WA, September 1975.

2. R. J. Hall, et al., An Assessment of the Risk of Transporting Plutonium Dioxide and Liquid Plutonium Nitrate by Train, BNWL-1996, Battelle, Pacific Northwest Laboratories, Richland, WA, February 1976.

3. J. F. Johnson and T. I. McSweeney, An Assessment of the Risk of Transporting Plutonium Dioxide by Cargo Aircraft, BNWL-2030, Battelle, Pacific Northwest Laboratories, Richland, WA, June 1977.

4. J. F. Johnson, et al., An Assessment of the Risk of Transporting Uranium Hexafluoride by Truck and Train, PNL-2211, Battelle, Pacific Northwest Laboratories, Richland, WA, August 1978.

5. C. M. Heeb, et al., ENFORM: An Energy Information System, BNWL-2195, Battelle, Pacific Northwest Laboratories, Richland, WA, March 1977.

6. Nuclear News, 20(10):73. August 1977.

5.0 TRANSPORT ACCIDENT ENVIRONMENT

Failure of a container during an accident occurs when the forces generated in an accident exceed the mechanical strength of a container. The forces or stresses which may be generated in the truck accident environment and their likelihood of occurrence are discussed in this section. The estimated mechanical strength of the reference spent fuel cask is discussed in Section 6. The use of the results from Sections 5 and 6 to estimate the likelihood of container failure in an accident is demonstrated in Section 9.

The truck accident environment data summarized here were developed by Sandia Laboratories.[1] These data represent the most comprehensive accident environment information currently available. In Sandia's analysis the accident environment is categorized by five accident stresses: impact, crush, puncture, fire, and immersion. Impact forces act over periods of a few milliseconds whereas crush forces can exist for several seconds following the accident. Impact forces are applied to one side whereas crush forces are applied from several directions. Impact and crush forces are adequately differentiated by comparing the force exerted by a hammer blow to the same force exerted by a press. Puncture stresses occur when a container is struck by an object that has potential for penetrating the container.

The following paragraphs briefly summarize the Sandia results. The likelihood of an accident is discussed first. Sections discussing the fire, impact, crush, immersion and puncture environments follow.

5.1 TRUCK ACCIDENT RATES

Truck accidents as defined by Sandia[1] include all accidents that result in fatalities, injuries or property damage of $250 or more. The accident rate selected by Sandia which will be used for this study was 1.5×10^{-6} accidents per truck kilometer. This rate was based on accident frequency data prepared by the Bureau of Motor Carrier Safety of the U.S. Department of Transportation, which is compiled from individual reports by large interstate motor carriers. The selected study period covered data for the years 1969 through 1972.

5.2 FIRE ENVIRONMENT

Fire accident environment data used in this study were developed by Sandia.[1] Based on the Sandia compilation of the truck accident environment, fire can be expected to occur in 1.6% of all truck accidents. The fire temperature has an expected range of 760 to 1320°C with a mean value of about 1010°C (1850°F) and the duration of the fire can range from a few minutes to several hours. The expected duration of fires for truck transport of large packages is shown in Figure 5.1. The temperature selected as representative for the truck fire environment is 1010°C. Because of the fire pool sizes and general nature of the truck accidents used in the Sandia analysis, it was conservatively assumed that in all truck accidents involving fires, the cargo was exposed to the fire.

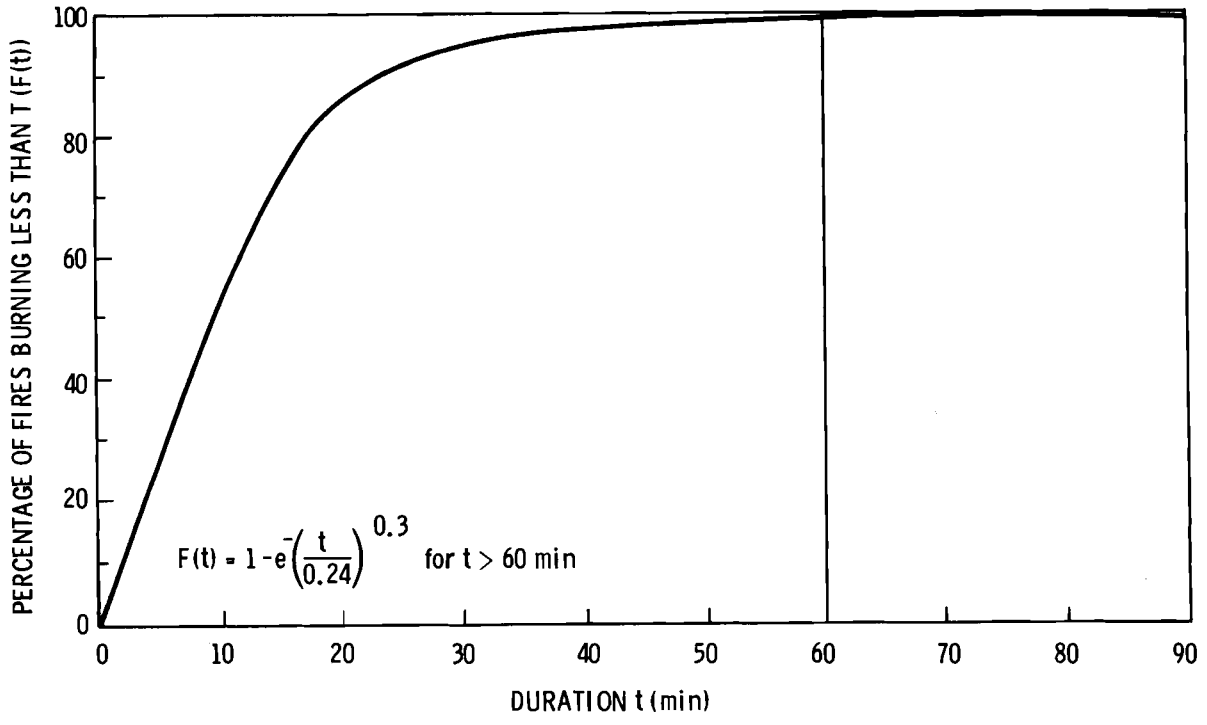

FIGURE 5.1. Cumulative Distribution of Fire-Accident Duration for Truck Transport of Large Packages[1]

5.3 IMPACT ENVIRONMENT

Impact forces are produced in about 80% of all truck accidents.[1] The impact environment for an accident involving a large container such as a spent fuel cask is taken from information developed at Sandia Laboratories.[1] The statistical information analyzed by Sandia was developed from the Bureau of Motor Carrier Safety (BMCS) data. The impact accident environment information was developed from the statistical data base using a Monte Carlo computer simulation. The results of this analysis for a truck with a gross weight of 36,300 kg (80,000 lbs) are presented in Figures 5.2 and 5.3. Figure 5.2 presents the magnitude of the velocity change versus expected frequency of occurrence in a collision accident. Figure 5.3 presents the portion of Figure 5.2 for velocities above 40 kph in greater detail. Table 5.1 contains the basic information plotted in Figures 5.2 and 5.3 for the 40-ton vehicle. The values in Figure 5.3 are computed as 1 minus the value listed in Table 5.1.

The transport vehicle structure, the package tiedown system, and the target impacted will all affect the severity of the impact environment to which a large package like a spent fuel cask could be subjected. In low velocity collision accidents the truck structure will act to mitigate the impact, however, in high velocity collisions, the truck structure may not have much effect. The effects of target hardness have been factored into the Monte Carlo analysis results reported in Figures 5.2 and 5.3 and Table 5.1. For smaller transport vehicle weights, larger velocity changes occur more frequently than for larger vehicles. This indicates that there are fewer large substantial targets which represent a threat to the large vehicles. Hard targets for large trucks include trains, other large trucks of equal or greater size and massive fixed objects such as bridge abutments and tunnel faces.

5.4 CRUSH ENVIRONMENT

The truck crush environment is difficult to quantify. The Sandia study[1] arbitrarily defined crush as "essentially static force acting on a container because of the containers' position underneath the truck." Static crush results from a container resting between the ground and an overturned truck or other heavy structure. Sandia analysis determined the probability of a

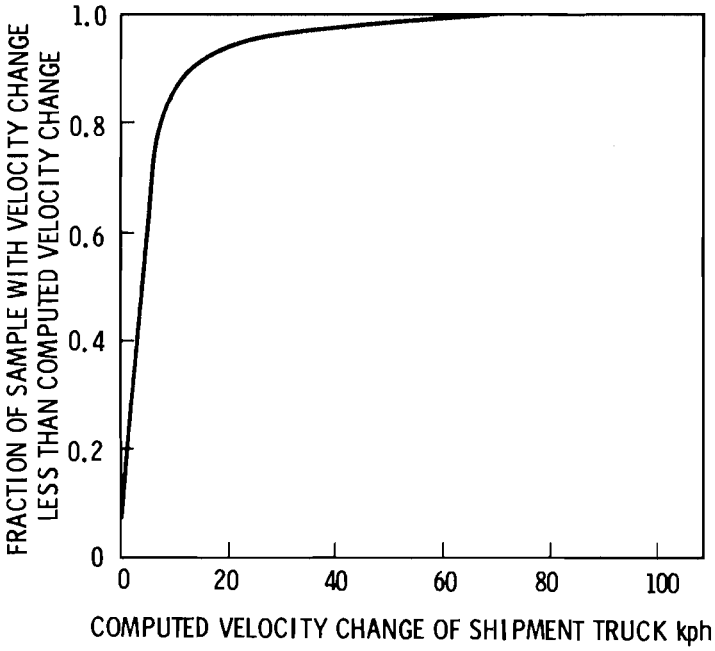

FIGURE 5.2. Expected Maximum Velocity Change Given a Truck Cask System Subjected to a Random Accident Sample (Reference 1) [Truck Gross Weight 36,300 kg (80,000 lb)]

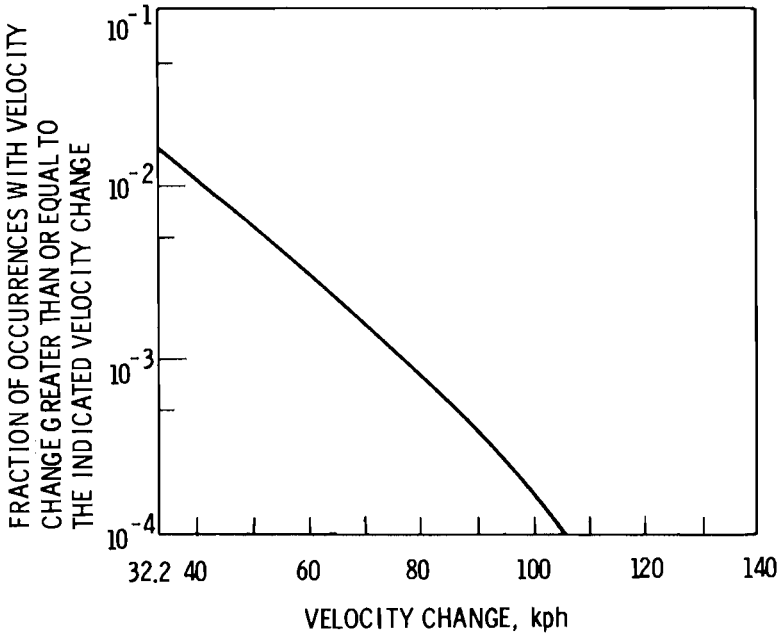

FIGURE 5.3. Velocity Change Due to Impact in a Highway Transportation Collision Accident Reference 1) [Truck Gross Weight 36,300 kg (80,000 lb)]

TABLE 5.1. Velocity Change Due to Impact in a Highway Transportation Collision Accident

Velocity Change Due to Impact (mph)[a]	Cumulative Fraction of Sample With a Velocity Change Less Than or Equal to Indicated Velocity Change for Each Over-the-Road Transport Vehicle Weight (in tons)[b]						
	10	15	20	25	30	40	50
5	0.5038	0.6220	0.7146	0.7813	0.8248	0.8711	0.8962
10	0.7541	0.8489	0.8881	0.9104	0.9256	0.9454	0.9579
15	0.8759	0.9173	0.9386	0.9520	0.9610	0.9721	0.9782
20	0.9244	0.9508	0.9642	0.9723	0.9775	0.9834	0.9872
25	0.9528	0.9997	0.9782	0.9828	0.9859	0.9899	0.9923
30	0.9701	0.9810	0.9859	0.9890	0.9911	0.9936	0.9949
35	0.9809	0.9876	0.9910	0.9931	0.9945	0.9959	0.9966
40	0.9878	0.9921	0.9945	0.9950	0.9965	0.9973	0.9978
45	0.9922	0.9951	0.9966	0.9973	0.9977	0.9983	0.9987
50	0.9951	0.9970	0.9978	0.9983	0.9986	0.9990	0.9994
55	0.9970	0.9982	0.9987	0.9990	0.9996	0.9996	0.9998
60	0.9981	0.9989	0.9992	0.9995	0.9998	0.9998	0.9999
65	0.9989	0.9994	0.9996	0.9997	0.9999	0.9999	
70	0.9993	0.9996	0.9998	0.9999			
75	0.9996	0.9998	0.9999				
80	0.9997	0.9999					
85	0.9998						
90	0.9999						

(a) mph x 1.609 = kph.
(b) tons x 907.2 = kg.

container encountering accident related crushing forces during transport and an estimate of the severity of those forces.

The static loading placed on a large package as a result of crush forces was found to be insignificant when compared to the structural capacities of accident resistant containers.[1]

5.5 IMMERSION ENVIRONMENT

No actual data are available from which it is possible to infer the probability of large package cargo being immersed. However estimates can be made of the relative significance of the immersion environment in terms of its probability of occurrence. In the Sandia analysis, three types of events were considered: 1) accident during bridge crossing; 2) roadside ditch immersions; and 3) accidents in which the truck leaves the road and enters an adjacent body of water.

Immersion was shown to be a very infrequent occurrence. It was predicted that only 1 accident in 3,000 will involve immersion of the package and the probability of immersion to depths greater than 40 feet is of the order of 10^{-13} per package transport kilometer. Because spent fuel casks are designed to operate at elevated internal pressure, they can be expected to withstand pressures from immersion that are much greater than a 40-foot immersion depth.

5.6 PUNCTURE ENVIRONMENT

An adequate description of the puncture environment could not be esta blished from existing data or current analytical methods. Sandia performed an analysis of the puncture threat in large package railroad accidents by use of railroad tank car puncture data. The puncture threat in the rail environment was considered by Sandia to be greater than that in the highway environment because of the presence of the railcar coupler as a potential puncture probe and the substantial weight of railcars compared to the weight of autos, trucks, and stationary objects. The response of truck transported packages to puncture threats was estimated based upon the analysis of the rail transport environment. Table 5.2 presents the results of the Sandia analysis in terms of the probability that a package will be punctured and the probability of a puncture

TABLE 5.2 Probability That a Spent Fuel Cask Will Be Punctured

Package Wall[a] Thickness (cm)	Probability per Transport kilometer	Probability of a Puncture Situation Given a Collision Accident
1 (0.4 in.)	2.75×10^{-9}	2.21×10^{-1}
1.27 (0.5 in.)	2.71×10^{-9}	2.18×10^{-1}
1.91 (0.75 in.)	2.54×10^{-9}	2.04×10^{-1}
2.54 (1.0 in.)	2.04×10^{-9}	1.64×10^{-1}
3.18 (1.25 in.)	1.17×10^{-9}	9.38×10^{-2}
3.81 (1.5 in.)	3.58×10^{-10}	2.88×10^{-2}
4.45 (1.75 in.)	4.93×10^{-11}	3.97×10^{-3}
5.08 (2.0 in.)	2.87×10^{-11}	2.31×10^{-3}
6.35 (2.5 in.)	-	4.36×10^{-8}
7.62 (3.0 in.)	-	5.56×10^{-12}

(a) Mild Steel Package Wall Assumed

situation given a truck accident for different package wall thickness. The puncture threat is relatively small for large packages with accident resistant designs such as rail casks. Packages with a one-inch equivalent steel thickness have a puncture probability of about 2×10^{-9} per transport kilometer.

REFERENCE

1. A. W. Dennis, J. T. Foley, W. F. Hartman and D. W. Larson, Severities of Transportation Accidents Involving Large Packages. SAND77-0001 Sandia Laboratories, Albuquerque, NM, May 1978.

6.0 PACKAGE FAILURE THRESHOLDS

The environment imposed on large containers during truck accidents has been described in the previous section. Package response to the most significant stresses imposed in highway accidents is estimated in terms of "failure thresholds." Estimates of the failure thresholds for the truck transported spent fuel cask are presented in this section. A failure threshold is the level of applied thermal or mechanical stresses that produce a release of radioactivity in an accident. Failure points of containers are distributed in stress level. There is a most probable level that will result in failure, but in any group of "identical" containers there are some that will fail above or below this most probable value. The results of this section must be used in conjunction with other information on the stresses to which the package may be exposed in order to assess whether or not the package will fail in the accident environment. These assessments are made in Sections 9 and 11.

The package failure threshold estimates presented here were obtained using mathematical analysis, engineering estimates and the results of a full scale test of a water cooled truck cask.[1] The analysis that was performed provides results that are within the overall accuracy range of the risk assessment and it is believed that they provide a conservative estimate of the system risk. The results represent estimates of failure thresholds obtained in using elastic and energy absorption theories of structure behavior. The failure estimates obtained using these methods are believed to be less than the actual strength of the container if tests to failure had been performed. The degree of conservatism is unknown. Analysis can be performed to show the sensitivity of the overall system risk to various assumptions and calculational techniques. Based on the sensitivity studies discussed in Section 11, the techniques used to estimate failure thresholds do not appear to introduce significant error into the risk assessment. The failure threshold should not, however, be used in assessing cask integrity for purposes other than those for which they are used in this analysis.

The truck cask analyzed in this report is described in Appendix A. The detailed stress analysis for the package and spent fuel is given in Appendix F (Calculations of Mechanical Failure Thresholds for Reference Cask). Details of

the thermal calculations for the cask in fire and loss of cavity coolant situations are presented in Appendix G (Thermal Analysis of Reference Cask).

Two barriers to release of radioactive material are present for the spent fuel cask. These barriers are the fuel rod cladding and the spent fuel cask body. Relatively small amounts of activity are present in the cavity coolant and are released if the cask body is breached. All larger releases of radioactivity from the cask must breach both the fuel and the cask. The failure thresholds estimated in this section are derived for both the fuel and cask.

The most significant types of accident-imposed stresses which affect the spent fuel cask and fuel are:

- End Impact
- Side Impact
- Fire
- Impact followed by Fire

The response of the cask and fuel to each type of stress associated with the accident environment is calculated independently.

The puncture threat is based on the equivalent steel thickness of large packages so no failure thresholds were required. No analysis of the response of the cask to the immersion environment was performed because the accident environment analysis showed that it was not significant.

6.1 RESULTS OF MECHANICAL ANALYSIS

Cask failure analysis considered for this risk assessment were of two types. The first uses dynamic elastic and energy absorption analyses to predict failure thresholds which are assumed for purposes of this study to result in cask failure due to distortion of sealing surfaces and cavity penetration closure devices. Venting of the cask cavity by dynamic overpressurization of the rupture disk was also considered. The second failure type uses an energy absorption model and assumptions of material behavior to estimate impact velocities which could result in a breach of the cask cavity to the surrounding atmosphere. Energy requirements for these types of failure are then used to calculate minimum cask impact velocities.

Fuel cladding mechanical failure thresholds were calculated using elastic and energy absorption models. Irradiated material properties were considered in the analysis. Internal pressure and dynamic loadings were the principal stress contributors.

Failure thresholds for accidents considered in the mechanical analysis included: 1) end impact onto a rigid planar target, 2) end impact to over pressurize the rupture disk, 3) side impact onto a flat rigid target, 4) side impact onto a column, 5) crushing of cask, 6) end impact resulting in a large breach of cask body and 7) fuel pin failure thresholds for both end and side impact. These types of accidents were considered to be the most significant with respect to contribution towards the total risk of transporting spent fuel. All postulated accident conditions which could cause cask failure were in excess of cask licensing requirements. Minimum failure velocities for the various mechanical environments are presented in Table 6.1. The indicated velocities are cask impact velocities with no consideration of energy absorption by the tractor trailer equipment. This is considered to be conservative at lower impact velocities where the tractor-trailer system could absorb a significant amount of energy. However, at higher velocity collisions, the energy absorbed by the transport system would probably be negligible. A rigid planar target was assumed for all the mechanical failure thresholds shown in Table 6.1 except the side impact onto a column. This is believed to be conservative since very few rigid planar targets exist in the real world. The impact accident environment data presented in Section 5.3 takes into account the relative hardness of targets in the Monte Carlo simulation techniques used to derive the data. The neutron shield would fail during any significant impact accident which would result in damage to the cask. No crushing environments were identified which could fail the cask body.

Fuel cladding failure thresholds are reported in Table 6.2. The end impact results in a cladding failure due to shear stresses. Side impacts cause failures in tension with the fuel supported as a beam between the grid spacers.

TABLE 6.1 Summary of Spent Fuel Cask Mechanical Failure Threshold Estimates[a]

	Target	Cask Velocity km/hr (mph)	Failure Type
End Impact	Rigid Plane	78.1 (48.5)	Seal to Cask Cavity
	Rigid Plane	153 (95.5)	Larger Opening to Cask Cavity
	Rigid Plane	61.0 (37.9)	Rupture Disk Venting
Side Impact	Rigid Plane	64.7 (40.2)	Seal to Cask Cavity
	Rigid 1.5 m Column	20.1 (12.5)	Opening to Cask Cavity

(a) Taken from Appendix F

TABLE 6.2 Summary of Spent Fuel Cladding Mechanical Failure Threshold Estimates[a]

	Cask Velocity km/hr (mph)	
End Impact	66.7 (41.4)	Rods Fail at a Single Point
Side Impact	45.1 (28.0)	Possible Multiple Cladding Failures on Each Rod

(a) Taken from Appendix F

6.2 RESULTS OF THE THERMAL ANALYSIS

The thermal analysis was performed with a special purpose computer code designed to analyze radiation and conduction heat transfer in detail and include an estimate of the effects of convection. Thermal failures of both the cask and fuel cladding were considered for several fire and loss of coolant situations. Thermal failure of the cask due to fire was assumed to occur when a cask component fails and radioactive material can be released to the atmosphere. The various basic events that lead to failure are identified in Section 8 through development of fault trees. The thermal analysis was conservatively based on the maximum decay heat load PWR fuel that can be carried in the reference cask. The analysis provides the information to determine the duration of a fire to cause various types of thermal failure and the time to failure for loss of coolant from other accident forces.

The cavity coolant was assumed to be lost from the cask when the mean cavity temperature reached 290°C. This is based on the rupture disk set to relieve the pressure at 76 atmospheres for saturated conditions. It was determined that the cask rupture disk would fail from overpressurization in about 2.5 hours after the cask was exposed to a 1010°C fire for 15 minutes. As the fuel temperature increases due to self-heating after the coolant is lost, the pressure in the fuel pins increases. This results in a hoop stress in the fuel pin cladding. Fuel pin failure occurs when the hoop stress exceeds the creep rupture strength of the Zircaloy 4 tubing. Smith[2] estimated that some PWR cladding will fail above 565°C and all fuel elements would fail above 675°C.

Data from seal manufacturers indicates that the teflon O-ring closure seal could withstand temperatures of 280°C (540°F) for a period of 48 hours. The seal can also withstand somewhat higher temperatures for shorter periods of time. For purposes of this analysis, the closure seal was conservatively assumed to fail if the temperature exceeds 320°C for longer than one hour. Considering the cask geometry, it was conservatively assumed that the seal would be at about the same temperature as the inner wall. It was then determined from the curves in Appendix G that a fire greater than 30 minutes duration at 1010°C would result in temperatures sufficient to fail the closure seal.

The drain valves and vent valve have teflon seals. Data on teflon valve seals indicate that failure would occur if the temperature exceeds 280°C (540°F). The valves are well protected from thermal stresses and it is difficult to predict what temperature they would be at during accident conditions. It was conservatively assumed that a fire duration of 30 minutes would fail the valve seals. Table 6.3 presents failure thresholds for the fire accident. It was conservatively assumed that loss of cavity coolant would occur in less than 2.5 hours for any seal failure due to fire.

TABLE 6.3. Thermal Failure Thresholds

Type of Failure	Minimum Duration of Fire[a] to Cause Failure
Loss of Coolant from Rupture Disk	15 min.
Closure Seal	30 min.
Drain Valve Seal	30 min.
Vent Valve Seal	30 min.

(a) All fires assumed to be 1010°C (1850°F).

Table 6.4 presents the length of time to failure of the reference cask and fuel elements for several cases analyzed in Appendix G. For cases with the coolant intact at the beginning of a 1010°C fire, the coolant is lost in less than 50 minutes. Case 3, an initial loss of coolant implies that the cask seals have failed allowing the coolant to drain from the cavity. Accident Case 6 shows that a fire which lasts longer than 15 minutes at 1010°C will result in release of the coolant. The column in Table 6.4 for time to fuel cladding failure is the length of time following a loss of coolant at which the first and last fuel elements fail by creep rupture. If an extreme mechanical impact precedes the fire, then all cladding may be initially failed.

The information in Table 6.4 is used in the analysis to determine the length of time over which the release occurs for the various fire accident cases, impact followed by fire, and the loss of coolant case. In all cases

except the impact case, the significant release occurs over a period of time from 0.5 to 1.5 hours. For the impact case, an instantaneous release is conservatively assumed to occur.

All fire situations considered in this study exceed the cask licensing requirements.

TABLE 6.4. Time to Thermal Failure for Reference Spent Fuel Cask and Fuel

Accident Case	Time of Loss of Coolant (hr)	Time to Fuel Cladding Failures (hr)	
		Time to Initial Failure	Time to Failure of All Cladding
1. 1/2-Hour Fire[a] at 1010°C (1850°F)	∿0.8	2.2	3.4
2. 2-Hour Fire[a] at 1010°C	∿0.6	1.9	2.4
3. No Fire with[b] an Initial Loss of Cavity Coolant	∿0	2.1	3.5
4. 1/2-Hour Fire[a] at 1010°C with an Initial Loss of Cavity Coolant	∿0	2.0	3.1
5. 2-Hour Fire at[a] 1010°C with an Initial Loss of Cavity Coolant	∿0	1.8	2.3
6. Minimum Duration[b] Fire to Cause Loss of Cavity Coolant	∿2.5 Hours for a 15-Minute 1010°C Fire	4.5	6.0

(a) Time zero at start of fire.
(b) Time zero when loss of coolant occurs.

REFERENCES

1. M. Huerta, Analysis, Scale Modeling, and Full Scale Tests of a Truck Spent-Nuclear-Fuel Shipping System in High Velocity Impacts Against a Rigid Barrier SAND 77-0270 Sandia Laboratories, Albuquerque, NM, April 1978.

2. C. W. Smith, Calculated Fuel Rod Perforation Temperatures Commercial Power Reactor Fuels. NEDO 10093, General Electric Company, San Jose, CA, September 1969.

7.0 CONDITIONS OF SPENT FUEL CASK DURING TRANSPORT

To perform a detailed risk analysis of spent fuel transport, it was necessary to determine the package condition during normal transport. A survey was conducted of companies and government laboratories which have received spent fuel for storage or processing. The survey was performed to obtain a data bank of conditions of the cask during transport for use in the risk analysis. The results of this survey are presented in this section.

7.1 SCOPE OF SURVEY

The initial step in developing the survey was to determine the information which was needed for the data bank. Determination of the package condition information required was carried out simultaneously with development of the release sequence evaluation fault trees shown in Section 8.

The analysis traced the steps of package loading and closure and the normal transport environment to identify all conditions that could affect package containment integrity. Based on the information identified in the analysis, questionnaires were prepared for use in the survey of the nuclear industry. The survey covers the time period from 1970 to 1977 with most of the available data in the period 1973 to 1976.

7.1.1 Packages Included in Survey

The purpose of this survey was to provide the broadest possible data base to evaluate packaging conditions during transport. Thus a broad class of spent fuel shipping casks were covered in the survey including both truck and rail casks. Most commercial spent fuel casks will accept either PWR or BWR spent fuel by using different fuel baskets, however, some are designed only for a particular type of fuel. Table 7.1 gives information about commercial shipping casks that are currently licensed and available for LWR spent fuel shipments in the United States.

TABLE 7.1. Licensed and Available Shipping Casks for Current Generation LWR Spent Fuel

Cask Designation	Number of Assemblies PWR	Number of Assemblies BWR	Approximate Loaded Cask Weight, MT	Usual Transport Mode	Shielding Gamma	Shielding Neutron	Cavity Coolant	Maximum Heat Removal kW	Status
NFS-4 (NAC-1)	1	2	23	Truck	Lead and steel	Borated water antifreeze	Water	11.5	6 casks available
NFS-5	2	3	25	Truck	Uranium and steel	Borated water and antifreeze	Water	24.7	SAR submitted
NLI 1/2	1	2	22	Truck	Lead, uranium and steel	Water	Helium	10.6	5 casks available
TN-8	3		36	Truck[a]	Lead and steel	Borated solid resin	Air	35.5	Licensed
TN-9		7	36	Truck[a]	Lead and steel	Borated solid resin	Air	24.5	Licensed
IF-300	7	18	63	Rail[b]	Uranium and steel	Water and antifreeze	Water	76[c]	4 casks available
NLI 10/24	10	24	88	Rail	Lead and steel	Water	Helium	97[d]	2 casks available

(a) Overweight permit required.
(b) Truck shipment for short distances with overweight permit.
(c) Licensed decay heat load is 62 kW.
(d) Licensed decay heat load is 70 kW.

Since the number of commercial cask shipments that have occurred in the United States has been limited, the survey included other noncommercial casks that have been used to ship spent reactor fuel. The material shipped in these casks were similar to commercial fuel. The type of packaging and handling of the casks were also similar. The results presented in this study include the entire survey, both commercial and noncommercial fuel shipments. When differences occurred in the data, if possible, that data relating to commercial fuel was relied on more heavily than the noncommercial fuel. By including as much data as possible, a broader data base for the survey could be obtained.

Specific commercial spent fuel containers covered in the survey are: NFS-4, NLI 1/2, IF-100, and IF-200 truck casks and the IF-300 rail cask. The survey includes noncommercial casks used by government laboratories and the Naval reactors program.

7.1.2 Sites Included in Survey

The companies and laboratories asked to participate in the survey included:

General Electric Company
Morris Operation
Morris, Illinois

Nuclear Fuel Services, Inc.
West Valley, New York

Allied Chemical Corporation
Idaho Chemical Programs
Operation Office
Idaho Falls, Idaho

E. I. duPont de Nemours
Savannah River Laboratory
Aiken, South Carolina

U.S. Energy Research and
Development Administration
Pittsburgh Naval Reactors Office
West Mifflin, Pennsylvania

7.2 RESULTS OF SURVEY

A copy of the questionnaire with overall results of the survey is shown in Table 7.2. The total number of shipments covered in the survey from 1970-77 is 3,795 shipments. This includes 3,581 truck and 214 rail shipments. It should be emphasized that in the experience sampled by the survey, a complete loss of packaging integrity of a spent fuel cask has never been observed.

There have been several accidents involving spent fuel casks; however, no radioactive material has been released in these accidents.[1, 2] The survey does not include data on any casks that were involved in accidents. Supplementary information obtained from the survey respondents used in the analysis is provided in the comments section of Table 7.2.

Even though the information obtained in the survey provides a reasonably good base for the risk assessment model, certain limitations should be recognized. First, for the most part, the observations were made by personal recollections. Consequently, the time period of the observations were not entirely certain. Secondly, in the years since 1971, Quality Assurance (QA) and Quality Control (QC) requirements have been strengthened by the NRC resulting in a significant reduction in packaging errors. Considering these factors, the results presented in Table 7.2 are believed to represent the best available data on present day spent fuel handling and packaging conditions.

TABLE 7.2. Spent Fuel Cask Shipping Survey Results

	Total No. of Truck and Rail Shipments	Truck Casks	Rail Casks
A. Shipments of Spent Fuel Received			
1977	399	384	15
1976	532	482	50
1975	613	594	19
1974	453	429	24
1973	541	522	19
1972	489	470	19
1971	371	350	21
1970	397	350	47
Pre-1970 (If Available)	144	0	144
Total 1970-77	3,795	3,581	214
Total	3,939	3,581	358

	Truck and Rail Shipments	Truck Casks	Rail Casks
B. General Condition of Shipments (1970 - 1977)			
1. What was the maximum cask internal pressure on arrival?	0-35[1] psig	18 psig	35 psig
2. Number of casks received with coolant pressure above normal operating range.	0	0	0
3. Number of casks designed with impact limiters received with impact limiters not installed.	0	0	0
4. Number of casks designed with impact limiters received with impact limiters not installed correctly.	1 of 536[2]	1 of 536[2]	0
5. Number of casks received with cask hold-down broken or failed during shipment.	9[3]	9[3]	0
6. Number of casks received with cask hold-down not safety wired at time of shipment.	0	0	0
7. Number of casks received with low fuel cooling water level (not shipped dry).	0	0	0
8. Number of licensed "dry" shipments of spent fuel casks.	98	55	43
9. Number of casks received with low neutron shield water levels (casks which have neutron shield water).	0	0	0
10. Number of casks containing spent fuel subjected to freezing with damage caused by freezing.	0	0	0
11. Number of casks received with higher external radiation readings than permitted on shipment release survey.	5	5	0
12. Number of casks received with shipping damage incurred in route. (Note damage which was incurred in comments section.)	0	0	0
13. Number of casks dropped during handling procedure. (Note details of any damage in comments section.)	0	0	0

[1] If accurate numbers are not available, approximate values or estimates based on best recollections can be used and are requested. If you have any questions about completing this form, please contact H. K. Elder, Battelle-Northwest, Richland, Washington 99352 (509) 946-3638 FTS 444-7411 (Ext. 946-3638).

[2] Please identify any casks listed here in the comments section.

TABLE 7.2. (contd)

	Truck and Rail Shipments	Truck Casks	Rail Casks
C. Cask Lid Condition			
1. Number of casks received with closure bolts not properly torqued (overtorqued/undertorqued).	6(4)	6(4)	0
2. Number of casks received with missing closure bolts.	1	1	0
a. Number of closure bolts missing.	1(5)	1(5)	0
3. Number of casks received with closure bolts damaged in transit.	0	0	0
D. Closure Seal Condition			
1. Number of casks received with closure seal damaged in transit.	0	0	0
2. Number of casks received with closure seal not installed properly.	0	0	0
3. Number of casks received with incorrect closure seal installed.	0	0	0
4. Number of casks received with closure seal leaking.	1	1	0
E. Cavity Penetration Conditions			
1. Number of casks received requiring defective drain valve replacement.	2(6)	2(6)	0
2. Number of casks received requiring defective vent valve replacement.	2(7)	2(7)	0
3. Number of casks received requiring defective pressure relief device replacement.	7(8)	1(8)	6(8)
4. Number of casks received with drain valve not closed.	0	0	0
5. Number of casks received with vent valve not closed.	2	2	0
6. Number of casks received with drain valve not installed properly.	0	0	0
8. Number of casks received with pressure relief device not installed properly.	0	0	0
9. Number of casks received with cavity penetration damaged during transit. (Note details of damage in comments section.)	0	0	0
10. Number of casks received with drain valve requiring replacement due to wear.	10	10	0
11. Number of casks received with vent valve requiring replacement due to wear.	5	5	0

(Additional information or details on survey are shown below.)

Comments:

(1) Pressure in casks ranged from 0 to 35 psig.

(2) 1 of 536 truck casks designed with impact limiters was received with impact limiter not installed correctly.

(3) 9 truck cask shipments had loosened tiedowns on shipment arrival. No failures of tiedowns occurred.

(4) 6 truck cask shipments had bolts which were undertorqued.

(5) Cask with bolts missing had 6 bolts total on the cask.

(6) 2 drain valves were replaced due to leakage which occurred when testing before shipment.

(7) 2 vent valves were found defective after pressure testing before shipment and were replaced.

(8) 1 truck cask pressure relief valve replaced after testing 6 rail cask pressure relief valves replaced due to defect with relief mechanism.

REFERENCES

1. J. W. Langhaar, "Transport Experience with Radioactive Materials," Proceedings of the International Symposium on the Management of Wastes from the LWR Fuel Cycle, CONF-76-0701, Denver, Co, July 1976.

2. A. E. Grella, "A Review of Five Years Accident Experience in the U.S. Involving Nuclear Transportation (1971-1975)." International Symposium on the Design, Construction and Testing of Packaging for the Safe Transport of Radioactive Materials, IAEA-SR-10, Vienna, Austria, August 1976.

8.0 RELEASE SEQUENCE IDENTIFICATION

Several transportation accidents have been reported[1,2] in which spent fuel truck casks have been subjected to severe accident environments. None of these accidents has resulted in a release of the package contents. Therefore, possible ways that releases could occur (release sequences) from truck casks must be identified through analysis of the shipping system. The information presented in Sections 5.0, 6.0 and 7.0 gives a basis for identifying events or combinations of events which could result in the release of spent fuel to the environment.

In this section a formalized procedure for identifying combinations of conditions which could result in a release is presented. The first step in the procedure is to develop fault trees using the techniques described in Section 8.1. Fault trees developed for truck shipment of spent fuel are presented in Section 8.2. The second step in the procedure is to develop a list of release sequences from the fault tree. The development of these sequences is discussed in Section 8.3.

8.1 FAULT TREE CONSTRUCTION

The fault tree analysis technique was developed in the 1960's in the aerospace industry to identify design deficiencies before actual space flight of the equipment. Basically the procedure is to assume a failure and work backwards to identify component failures which could cause or contribute to the failure. The fault tree failure sequences are then related to individual components for which failure data are available. In practice, fault trees seldom are developed to that degree. What occurs instead is development of fault trees in terms of basic system modules. Such a fault tree is called a Top Level Fault Tree since it usually identifies only large systems which could result in a failure. Table 8.1 gives the various fault tree symbols and their meanings and use.

TABLE 8.1. Fault Tree Symbolism

Symbol	Meaning and Use
 output / inputs	"AND" logic gate. The simultaneous occurrence of inputs is required to cause an output.
 output / inputs	"OR" logic gate. The occurrence of any one of the inputs will result in an output.
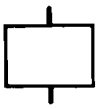	Fault event that results from the logical operation of two or more fault events. It is always the output from a logic gate.
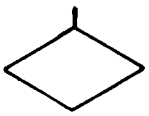	Inferred fault event. Any failure except a primary failure which is not developed further due to lack of information, time or money or due to the low probability of occurrence. It can also be used where other analyses give sufficient information to indicate that further analysis would be redundant.
Output 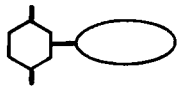 Input	"Inhibit" gate. The condition specified in the oval is required for an input fault event to result in an output event. This condition is frequently a design limit which will not transmit a failure until the design limits have been exceeded.
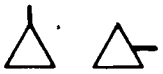	Transfer symbol denoting that failure also impacts on other branches of fault tree. A line at the apex of the triangle represents a "transfer in." A line in the side represents a "transfer out." A number is placed in the triangle to identify transfer locations.
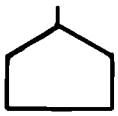	"House" defines an event that must occur, or is expected to occur, due to design and normal operating conditions.

The fault tree analysis applied to transportation of spent fuel involves postulation of a release of radioactive contents during transport and then examination of the series of events which must have occurred to cause the release. This form of reasoning is thought to be more inclusive than beginning with an initiating event and working toward a release, (i.e., constructing accident scenarios or decision trees). The tree which is developed is then broken down into all the possible release sequences. In effect, all the accident scenarios will be obtained from the fault tree. When properly applied, the accident scenarios obtained from using the fault tree methodology are likely to be more complete than the alternative method of trying to list all accident scenarios without the aid of any formalized reasoning process. The tree constructed using the fault tree methodology is used as the basis for estimating the total release probability.

8.2 FAULT TREE FOR SHIPMENT OF SPENT FUEL

The fault trees for shipments of spent fuel in the reference cask described in Appendix A are developed for truck transport on primary roads in the United States. The analysis considers the combined effects of the truck accident environment and packaging condition. The effects of sabotage or theft are not considered. Based on these criteria, the fault tree shown in Figures 8.1, Sheets 1 through 10, was developed to determine applicable failure sequences for the reference cask design. Pacific Northwest Laboratory's computer code ACORN[3] was used to plot the fault tree.

For spent fuel, both barriers between the radioactive fission products in the fuel rods and man's environment were considered. All significant releases of radioactivity from the cask would have to breach both the fuel cladding and the cask. There are two other types of release sequences covered in the fault trees which could occur that do not involve breaching of both barriers. They do not result in significant release but are included in the tree for completeness of the analysis. These are: 1) release of very small amount of radioactivity that could be in the cavity coolant water from small cask leaks and 2) loss of neutron shield water which could result in

a direct radiation dose to individuals located close to the cask for a significant period of time. It is assumed that the public is excluded from the immediate area surrounding the cask in an accident situation.

Figure 8.1, Sheet 1, shows the top of the fault tree. The top event on the tree is the postulated release of radioactive material to the environment during spent fuel shipment. Radioactive releases, to the environment occur through release of material from one of the main components of the cask. Detailed fault trees for the failure of various cask components are shown in Figure 8.1, Sheets 2 through 13. Cask components through which releases of radioactive material could occur are: the cask lid, closure seal, cask wall, pressure relief device, drain valve and the vent valve.

Releases from the cask components occur from: 1) accident forces which cause failure of the component and release radioactive material from the fuel and 2) loss of coolant from the component failure caused by accidents or closure errors which result in release of radioactive material. Both the cask component and the fuel may fail from the same accident event or they may fail from different events. Loss of cavity coolant may result from accident forces which fail one of the cask components or packaging errors which result in a loss of coolant. Loss of coolant failure sequences may result in release of radioactivity in the cavity coolant itself or coolant activity plus fission products escaping from overheated fuel rods.

Each of the fault tree branches for the different cask components are then further broken down to basic events which can be assigned failure probabilities.

The list of identified events or failure elements used in the fault tree which could contribute to a release are shown in Table 8.2. These elements are designated in the fault tree as "X" with associated numerical designations and descriptive titles. Elements which have further development in the fault tree are designated by "A". The descriptive titles for the "A" elements are given in Table 8.3. The fault events in the tree designated by the circle symbol were not analyzed individually because of lack of information or because they were not considered to be significant events. They are included in the fault tree only for completeness in illustrating all the conditions considered in developing the tree.

SPENT FUEL CASK TRUCK SHIPMENT FAULT TREE

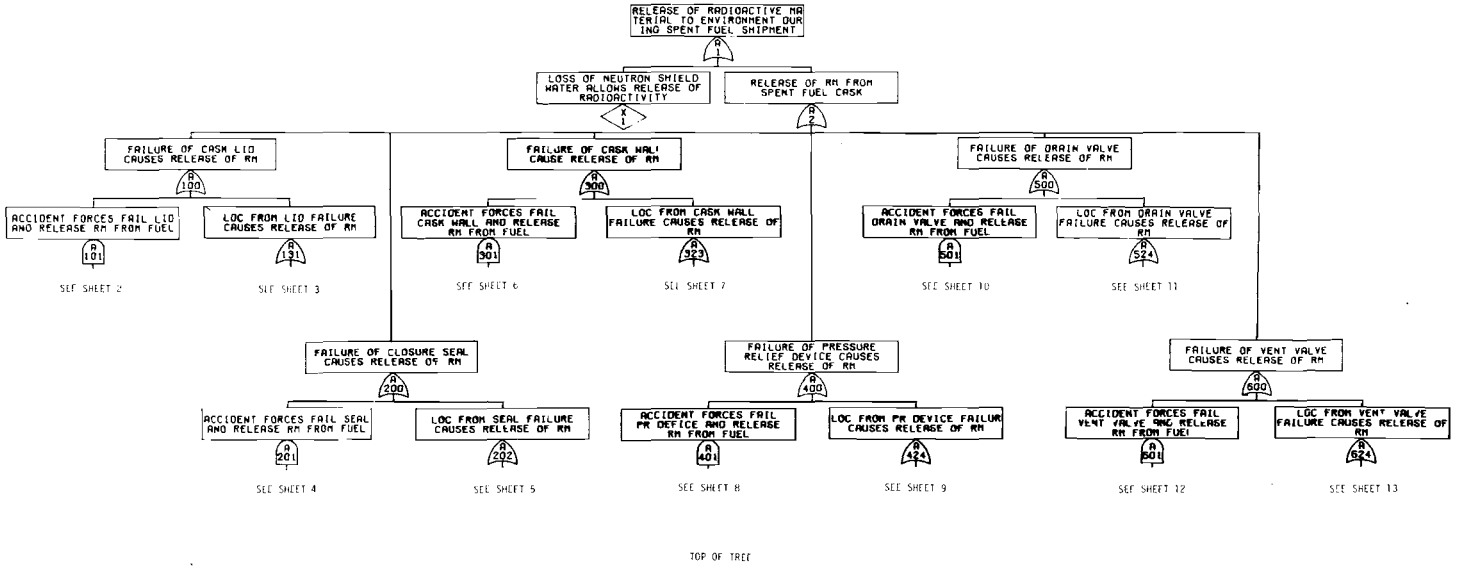

FIGURE 8.1. Fault Tree for the Shipment of Spent Fuel by Truck (Sheet 1)

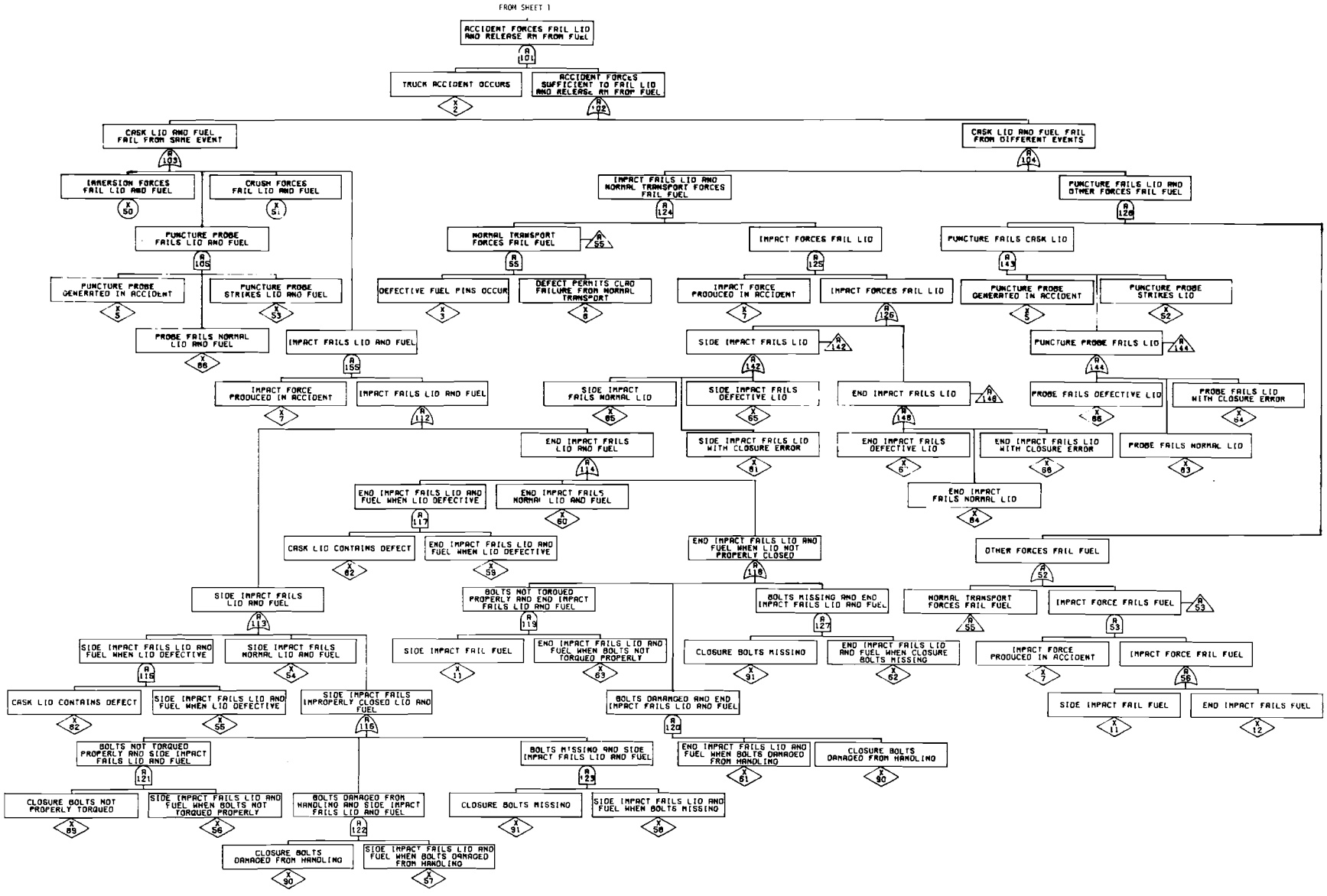

FIGURE 8.1. Sheet 2

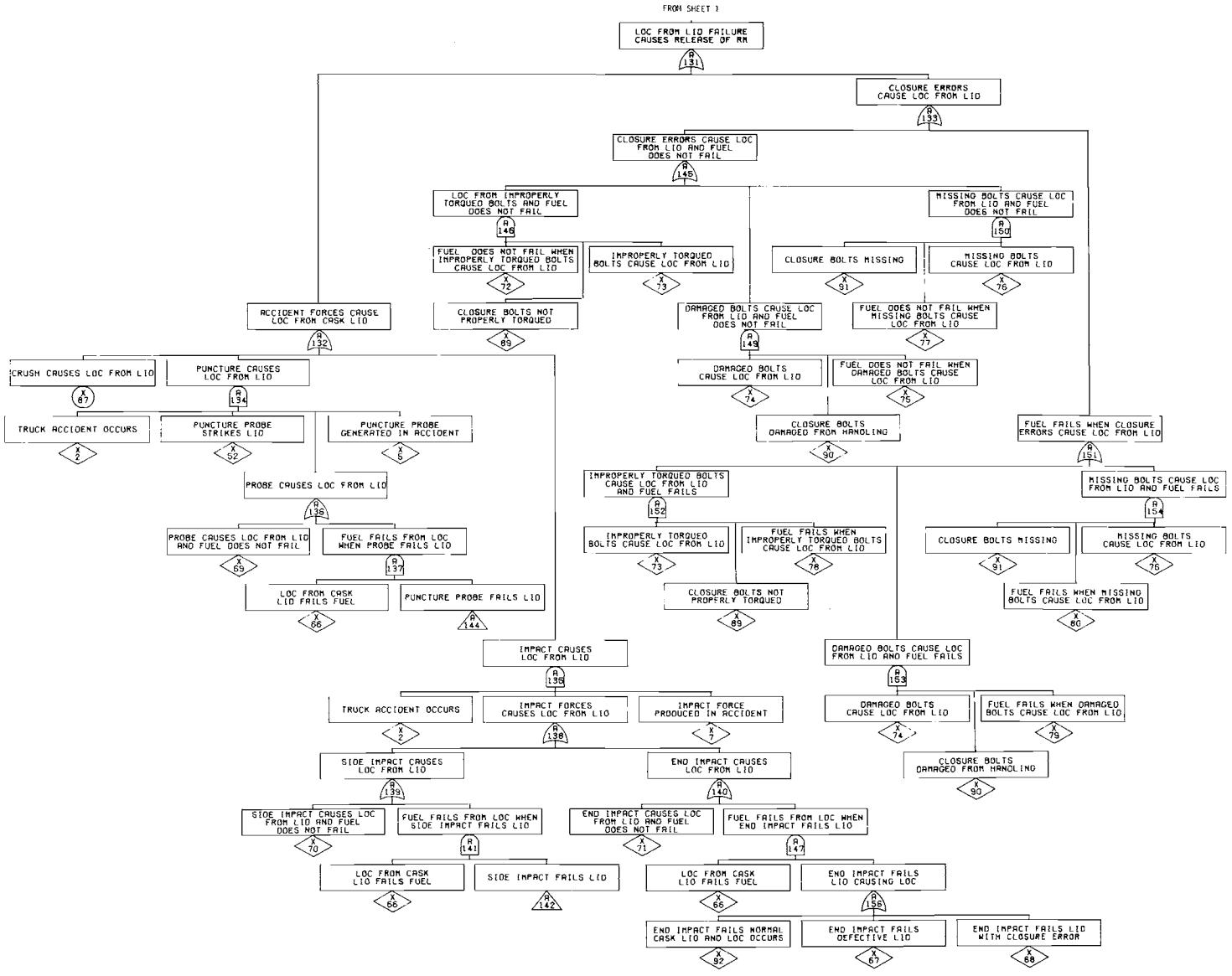

FIGURE 8.1. Sheet 3

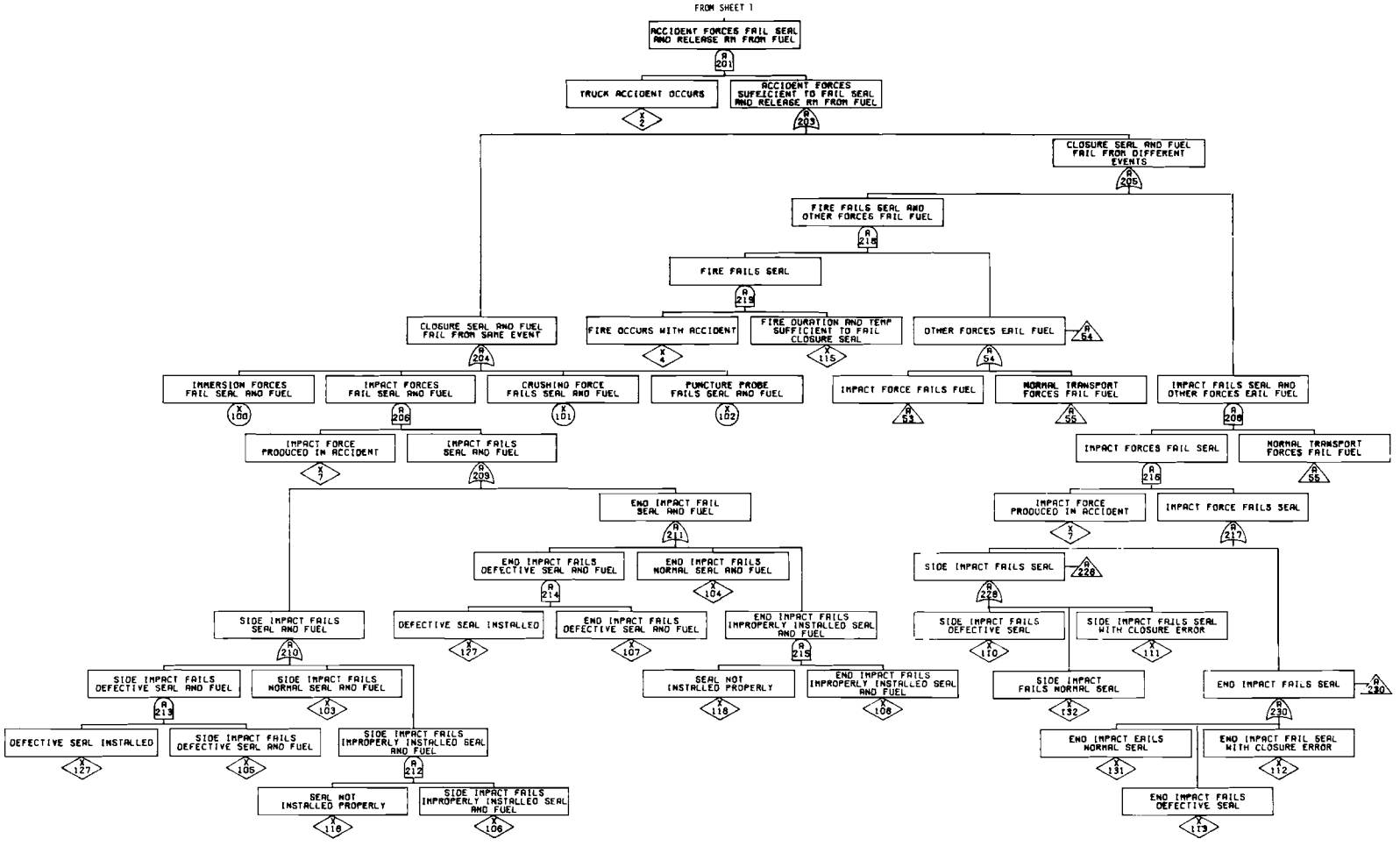

FIGURE 8.1. Sheet 4

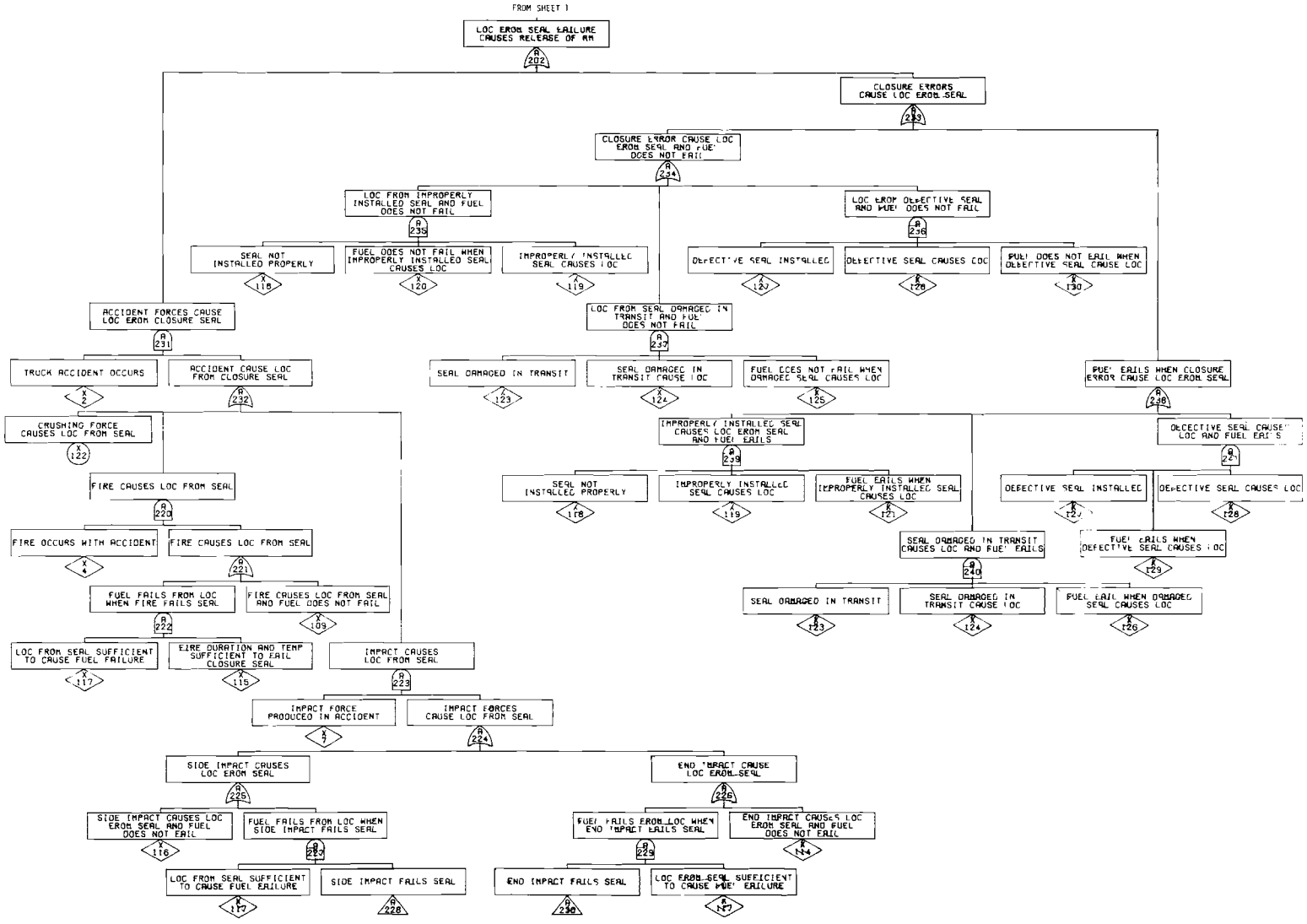

FIGURE 8.1. Sheet 5

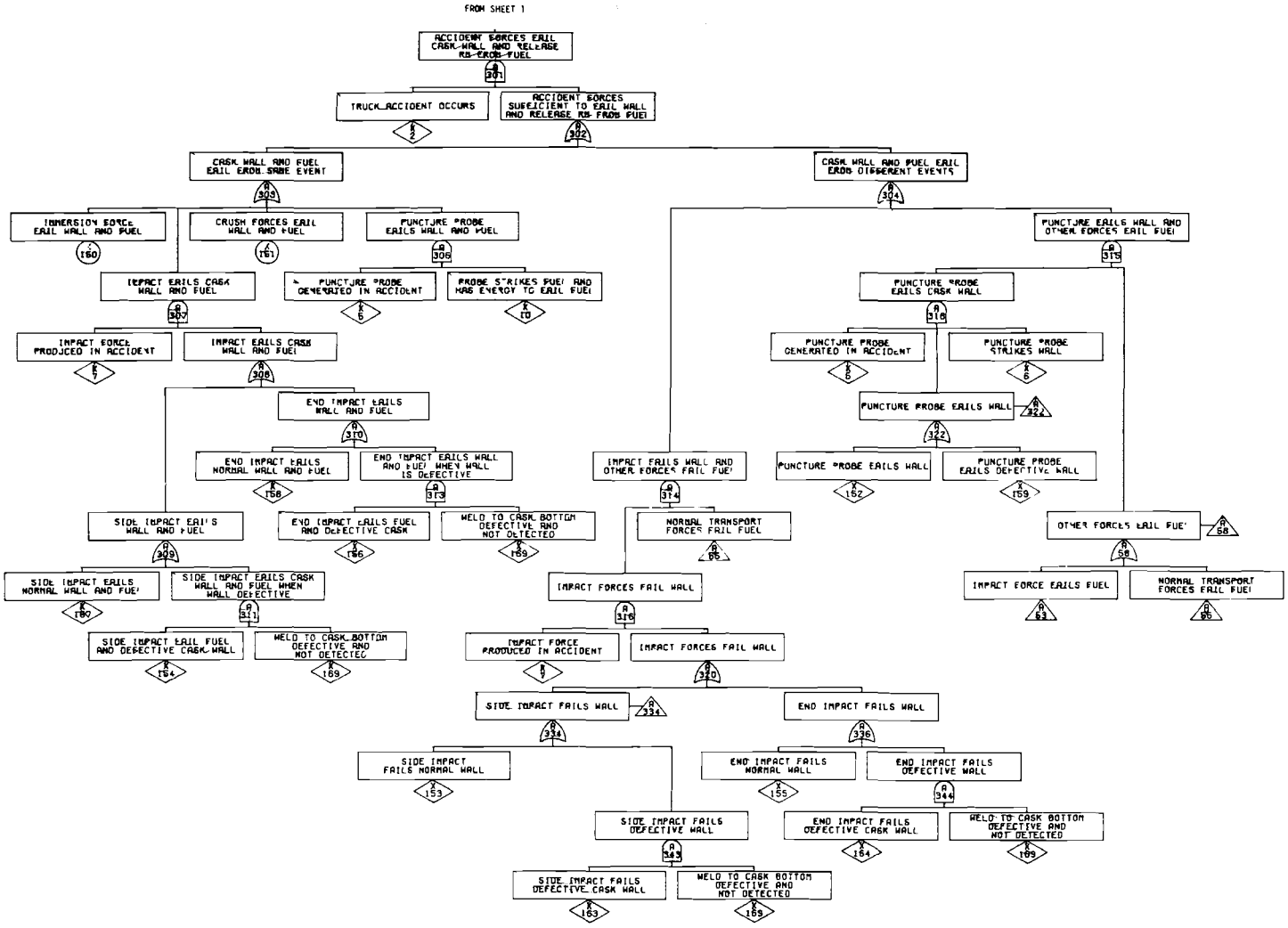

FIGURE 8.1. Sheet 6

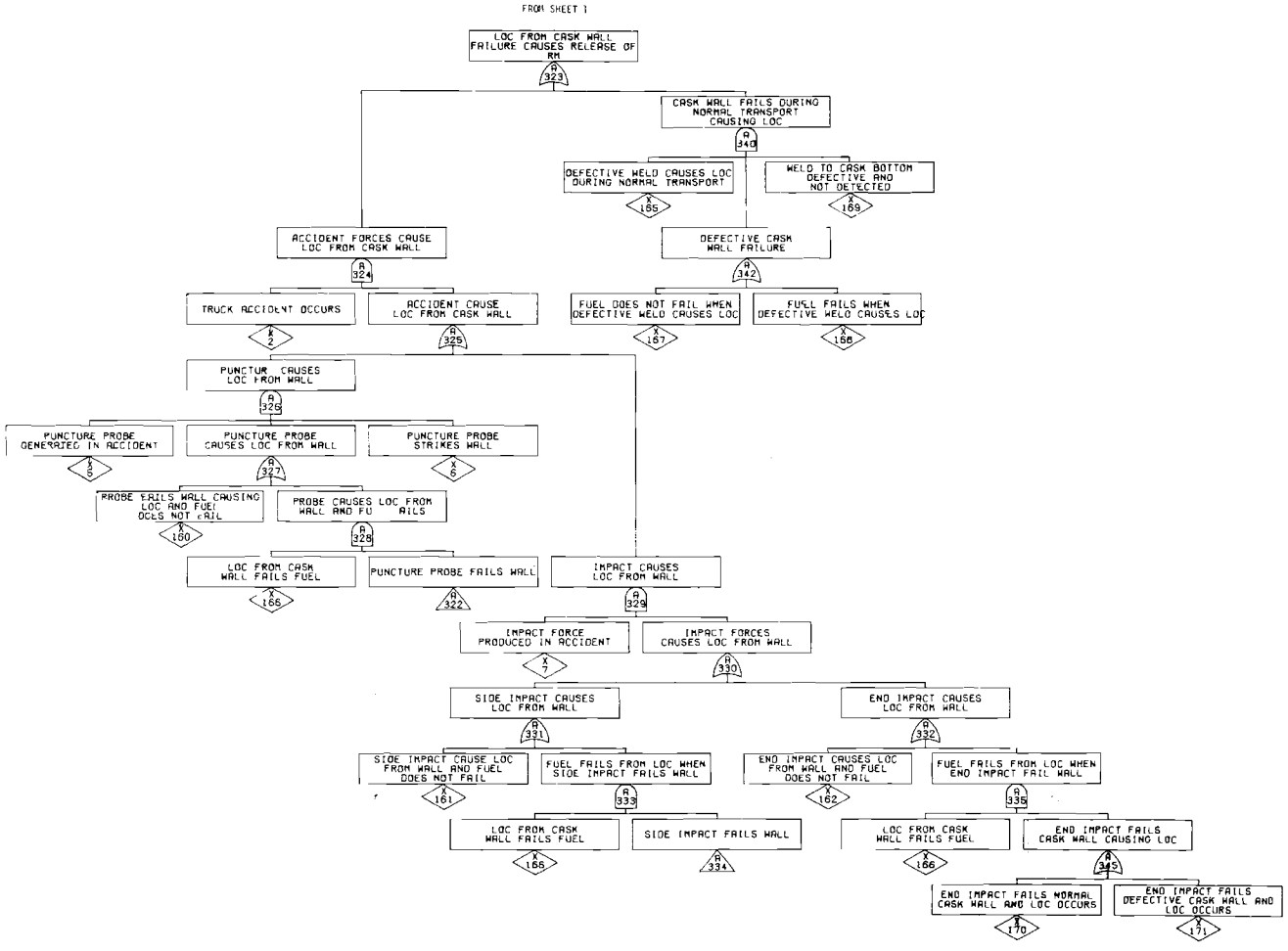

FIGURE 8.1. Sheet 7

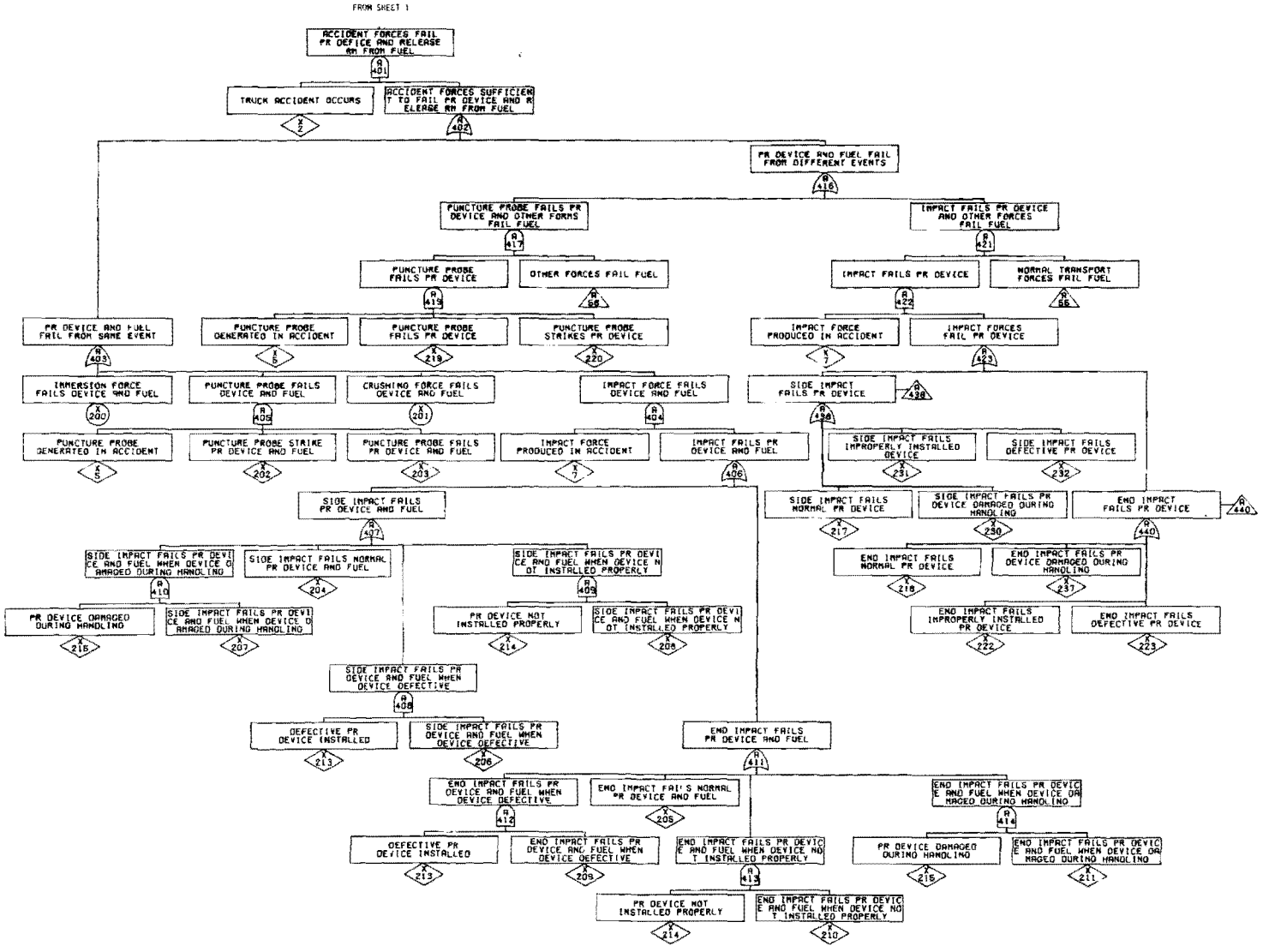

FIGURE 8.1. Sheet 8

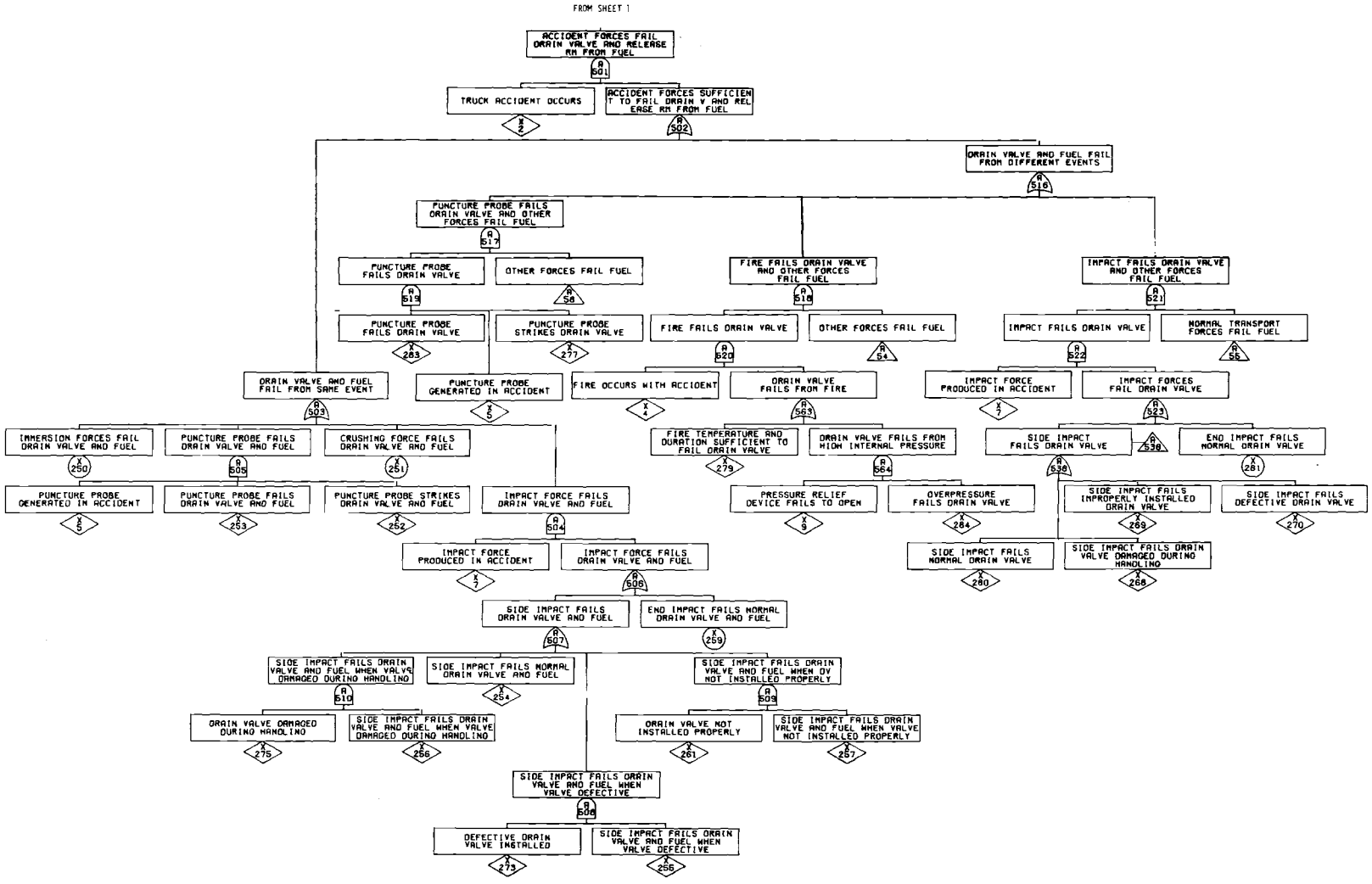

FIGURE 8.1. Sheet 10

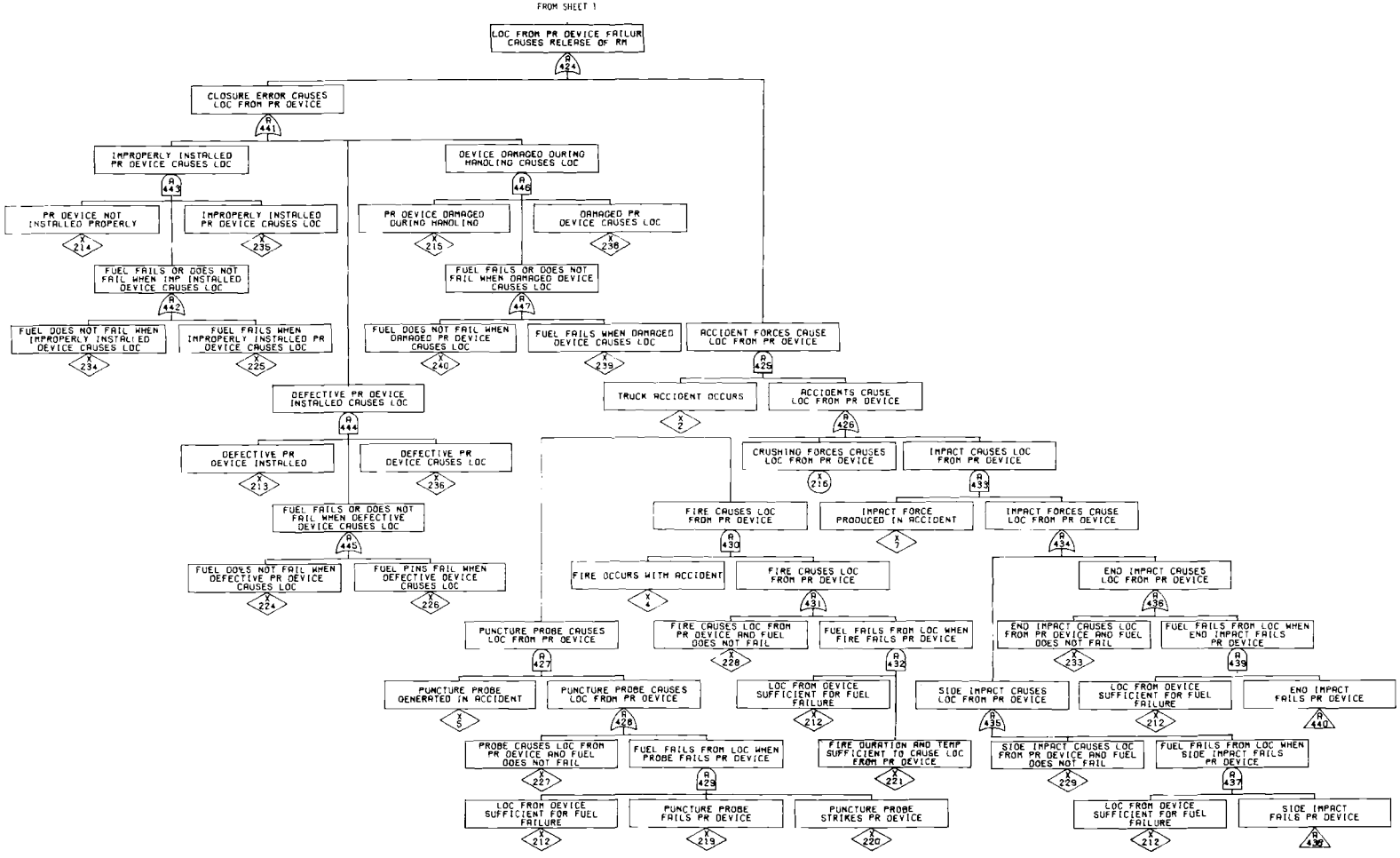

FIGURE 8.1. Sheet 9

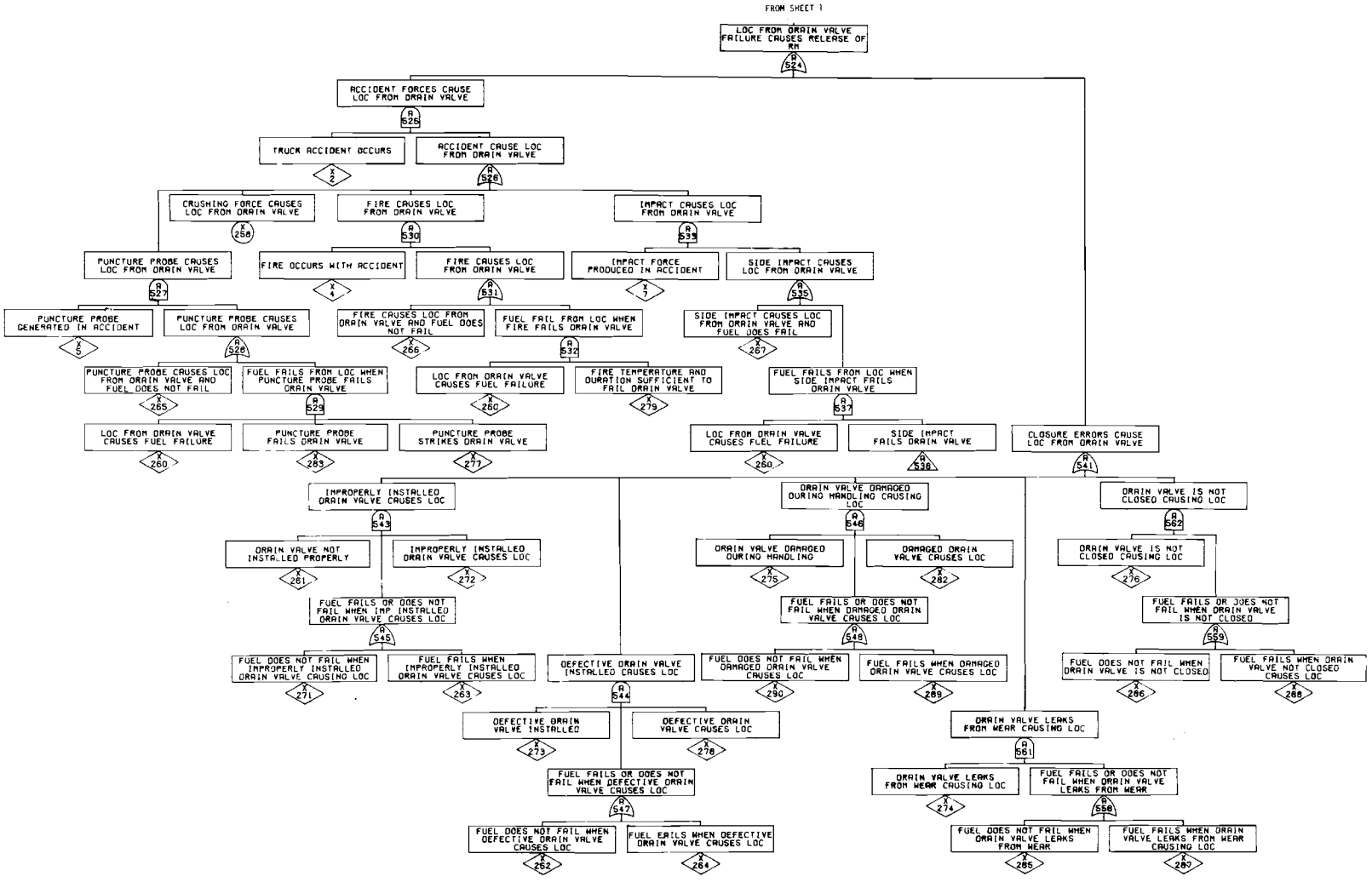

FIGURE 8.1. Sheet 11

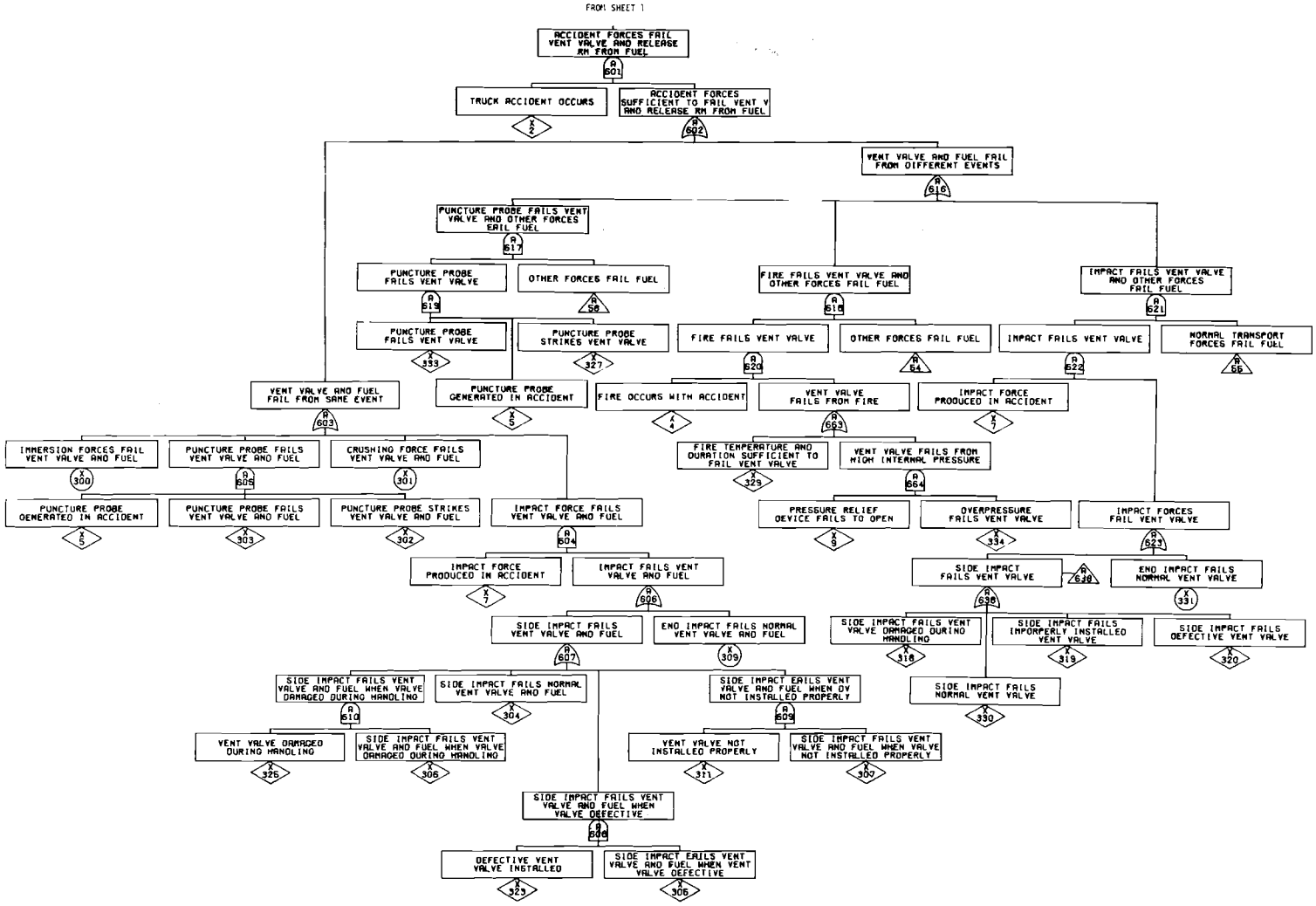

FIGURE 8.1. Sheet 12

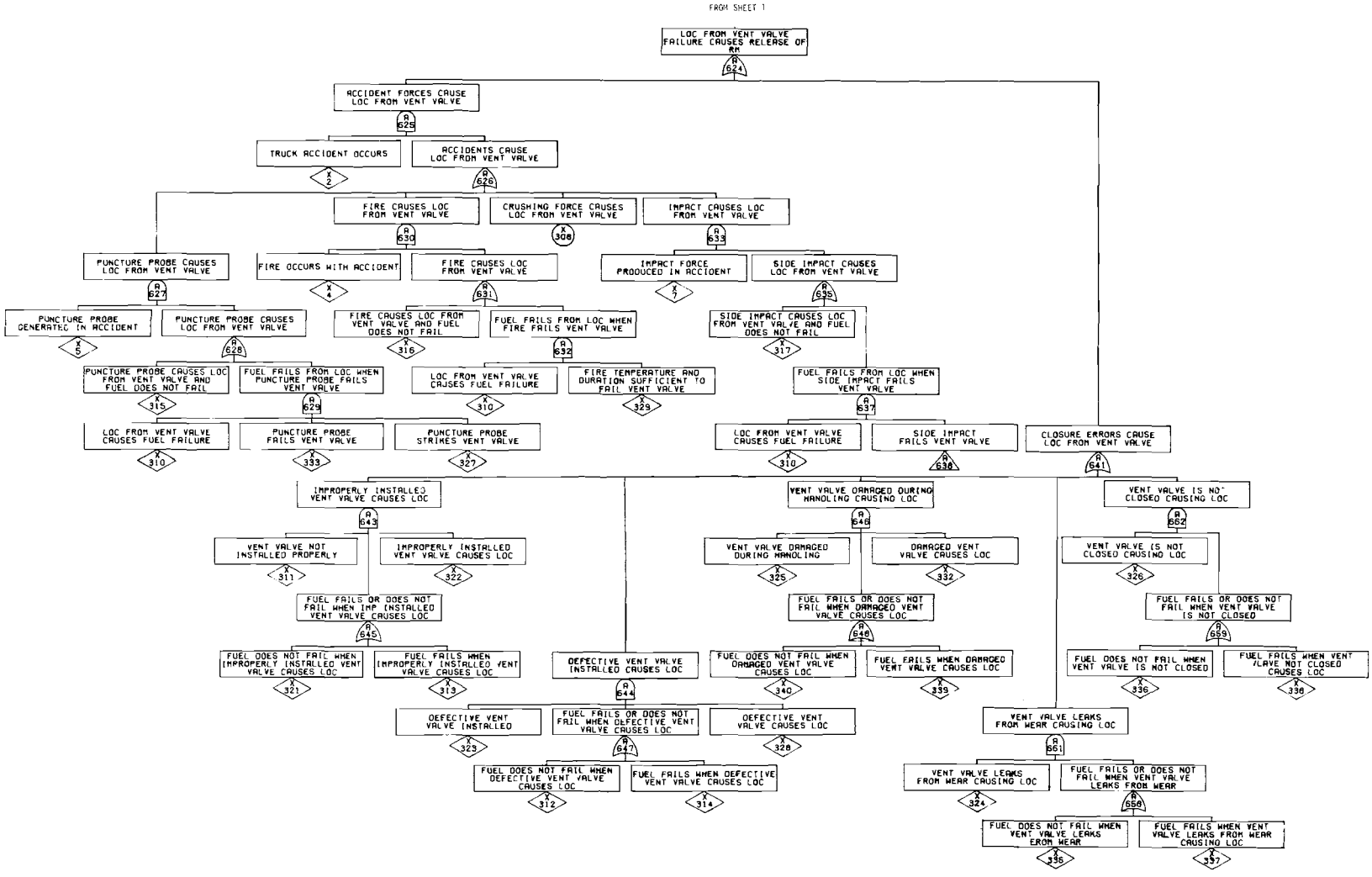

FIGURE 8.1. Sheet 13

TABLE 8.2. Listing of Basic Events for Analysis of Spent Fuel

X 1 LOSS OF NEUTRON SHIELD WATER ALLOWS RELEASE OF RADIOACTIVITY
X 2 TRUCK ACCIDENT OCCURS
X 3 DEFECTIVE FUEL PINS OCCUR
X 4 FIRE OCCURS WITH ACCIDENT
X 5 PUNCTURE PROBE GENERATED IN ACCIDENT
X 6 PUNCTURE PROBE STRIKES WALL
X 7 IMPACT FORCE PRODUCED IN ACCIDENT
X 8 DEFECT PERMITS CLAD FAILURE FROM NORMAL TRANSPORT
X 9 PRESSURE RELIEF DEVICE FAILS TO OPEN
X 10 PROBE STRIKES FUEL AND HAS ENERGY TO FAIL FUEL
X 11 SIDE IMPACT FAIL FUEL
X 12 END IMPACT FAILS FUEL
X 50 IMMERSION FORCES FAIL LID AND FUEL
X 51 CRUSH FORCES FAIL LID AND FUEL
X 52 PUNCTURE PROBE STRIKES LID
X 53 PUNCTURE PROBE STRIKES LID AND FUEL
X 54 SIDE IMPACT FAILS NORMAL LID AND FUEL
X 55 SIDE IMPACT FAILS LID AND FUEL WHEN LID DEFECTIVE
X 56 SIDE IMPACT FAILS LID AND FUEL WHEN BOLTS NOT TORQUED PROPERLY
X 57 SIDE IMPACT FAILS LID AND FUEL WHEN BOLTS DAMAGED FROM HANDLING
X 58 SIDE IMPACT FAILS LID AND FUEL WHEN BOLTS MISSING
X 59 END IMPACT FAILS LID AND FUEL WHEN LID DEFECTIVE
X 60 END IMPACT FAILS NORMAL LID AND FUEL
X 61 END IMPACT FAILS LID AND FUEL WHEN BOLTS DAMAGED FROM HANDLING
X 62 END IMPACT FAILS LID AND FUEL WHEN CLOSURE BOLTS MISSING
X 63 END IMPACT FAILS LID AND FUEL WHEN BOLTS NOT TORQUED PROPERLY
X 64 PROBE FAILS LID WITH CLOSURE ERROR
X 65 SIDE IMPACT FAILS DEFECTIVE LID
X 66 LOC FROM CASK LID FAILS FUEL
X 67 END IMPACT FAILS DEFECTIVE LID
X 68 END IMPACT FAILS LID WITH CLOSURE ERROR
X 69 PROBE CAUSES LOC FROM LID AND FUEL DOES NOT FAIL
X 70 SIDE IMPACT CAUSES LOC FROM LID AND FUEL DOES NOT FAIL
X 71 END IMPACT CAUSES LOC FROM LID AND FUEL DOES NOT FAIL
X 72 FUEL DOES NOT FAIL WHEN IMPROPERLY TORQUED BOLTS CAUSE LOC FROM LID
X 73 IMPROPERLY TORQUED BOLTS CAUSE LOC FROM LID
X 74 DAMAGED BOLTS CAUSE LOC FROM LID
X 75 FUEL DOES NOT FAIL WHEN DAMAGED BOLTS CAUSE LOC FROM LID
X 76 MISSING BOLTS CAUSE LOC FROM LID
X 77 FUEL DOES NOT FAIL WHEN MISSING BOLTS CAUSE LOC FROM LID
X 78 FUEL FAILS WHEN IMPROPERLY TORQUED BOLTS CAUSE LOC FROM LID
X 79 FUEL FAILS WHEN DAMAGED BOLTS CAUSE LOC FROM LID
X 80 FUEL FAILS WHEN MISSING BOLTS CAUSE LOC FROM LID
X 81 SIDE IMPACT FAILS LID WITH CLOSURE ERROR
X 82 CASK LID CONTAINS DEFECT
X 83 PROBE FAILS NORMAL LID
X 84 END IMPACT FAILS NORMAL LID
X 85 SIDE IMPACT FAILS NORMAL LID
X 86 PROBE FAILS DEFECTIVE LID

(cont'd) TABLE 8.2. Listing of Basic Events for Analysis of Spent Fuel

X 87 CRUSH CAUSES LOC FROM LID
X 88 PROBE FAILS NORMAL LID AND FUEL
X 89 CLOSURE BOLTS NOT PROPERLY TORQUED
X 90 CLOSURE BOLTS DAMAGED FROM HANDLING
X 91 CLOSURE BOLTS MISSING
X 92 END IMPACT FAILS NORMAL CASK LID AND LOC OCCURS
X 100 IMMERSION FORCES FAIL SEAL AND FUEL
X 101 CRUSHING FORCE FAILS SEAL AND FUEL
X 102 PUNCTURE PROBE FAILS SEAL AND FUEL
X 103 SIDE IMPACT FAILS NORMAL SEAL AND FUEL
X 104 END IMPACT FAILS NORMAL SEAL AND FUEL
X 105 SIDE IMPACT FAILS DEFECTIVE SEAL AND FUEL
X 106 SIDE IMPACT FAILS IMPROPERLY INSTALLED SEAL AND FUEL
X 107 END IMPACT FAILS DEFECTIVE SEAL AND FUEL
X 108 END IMPACT FAILS IMPROPERLY INSTALLED SEAL AND FUEL
X 109 FIRE CAUSES LOC FROM SEAL AND FUEL DOES NOT FAIL
X 110 SIDE IMPACT FAILS DEFECTIVE SEAL
X 111 SIDE IMPACT FAILS SEAL WITH CLOSURE ERROR
X 112 END IMPACT FAIL SEAL WITH CLOSURE ERROR
X 113 END IMPACT FAILS DEFECTIVE SEAL
X 114 END IMPACT CAUSES LOC FROM SEAL AND FUEL DOES NOT FAIL
X 115 FIRE DURATION AND TEMP SUFFICIENT TO FAIL CLOSURE SEAL
X 116 SIDE IMPACT CAUSES LOC FROM SEAL AND FUEL DOES NOT FAIL
X 117 LOC FROM SEAL SUFFICIENT TO CAUSE FUEL FAILURE
X 118 SEAL NOT INSTALLED PROPERLY
X 119 IMPROPERLY INSTALLED SEAL CAUSES LOC
X 120 FUEL DOES NOT FAIL WHEN IMPROPERLY INSTALLED SEAL CAUSES LOC
X 121 FUEL FAILS WHEN IMPROPERLY INSTALLED SEAL CAUSES LOC
X 122 CRUSHING FORCE CAUSES LOC FROM SEAL
X 123 SEAL DAMAGED IN TRANSIT
X 124 SEAL DAMAGED IN TRANSIT CAUSE LOC
X 125 FUEL DOES NOT FAIL WHEN DAMAGED SEAL CAUSES LOC
X 126 FUEL FAIL WHEN DAMAGED SEAL CAUSES LOC
X 127 DEFECTIVE SEAL INSTALLED
X 128 DEFECTIVE SEAL CAUSES LOC
X 129 FUEL FAILS WHEN DEFECTIVE SEAL CAUSES LOC
X 130 FUEL DOES NOT FAIL WHEN DEFECTIVE SEAL CAUSE LOC
X 131 END IMPACT FAILS NORMAL SEAL
X 132 SIDE IMPACT FAILS NORMAL SEAL
X 150 IMMERSION FORCE FAIL WALL AND FUEL
X 151 CRUSH FORCES FAIL WALL AND FUEL
X 152 PUNCTURE PROBE FAILS WALL
X 153 SIDE IMPACT FAILS NORMAL WALL
X 154 SIDE IMPACT FAIL FUEL AND DEFECTIVE CASK WALL
X 155 END IMPACT FAILS NORMAL WALL
X 156 END IMPACT FAILS FUEL AND DEFECTIVE CASK
X 157 SIDE IMPACT FAILS NORMAL WALL AND FUEL
X 158 END IMPACT FAILS NORMAL WALL AND FUEL
X 159 PUNCTURE PROBE FAILS DEFECTIVE WALL
X 160 PROBE FAILS WALL CAUSING LOC AND FUEL DOES NOT FAIL
X 161 SIDE IMPACT CAUSE LOC FROM WALL AND FUEL DOES NOT FAIL

(cont'd) TABLE 8.2. Listing of Basic Events for Analysis of Spent Fuel

X 162 END IMPACT CAUSES LOC FROM WALL AND FUEL DOES NOT FAIL
X 163 SIDE IMPACT FAILS DEFECTIVE CASK WALL
X 164 END IMPACT FAILS DEFECTIVE CASK WALL
X 165 DEFECTIVE WELD CAUSES LOC DURING NORMAL TRANSPORT
X 166 LOC FROM CASK WALL FAILS FUEL
X 167 FUEL DOES NOT FAIL WHEN DEFECTIVE WELD CAUSES LOC
X 168 FUEL FAILS WHEN DEFECTIVE WELD CAUSES LOC
X 169 WELD TO CASK BOTTOM DEFECTIVE AND NOT DETECTED
X 170 END IMPACT FAILS NORMAL CASK WALL AND LOC OCCURS
X 171 END IMPACT FAILS DEFECTIVE CASK WALL AND LOC OCCURS
X 200 IMMERSION FORCE FAILS DEVICE AND FUEL
X 201 CRUSHING FORCE FAILS DEVICE AND FUEL
X 202 PUNCTURE PROBE STRIKE PR DEVICE AND FUEL
X 203 PUNCTURE PROBE FAILS PR DEVICE AND FUEL
X 204 SIDE IMPACT FAILS NORMAL PR DEVICE AND FUEL
X 205 END IMPACT FAILS NORMAL PR DEVICE AND FUEL
X 206 SIDE IMPACT FAILS PR DEVICE AND FUEL WHEN DEVICE DEFECTIVE
X 207 SIDE IMPACT FAILS PR DEVICE AND FUEL WHEN DEVICE DAMAGED DURING HANDLING
X 208 SIDE IMPACT FAILS PR DEVICE AND FUEL WHEN DEVICE NOT INSTALLED PROPERLY
X 209 END IMPACT FAILS PR DEVICE AND FUEL WHEN DEVICE DEFECTIVE
X 210 END IMPACT FAILS PR DEVICE AND FUEL WHEN DEVICE NOT INSTALLED PROPERLY
X 211 END IMPACT FAILS PR DEVICE AND FUEL WHEN DEVICE DAMAGED DURING HANDLING
X 212 LOC FROM DEVICE SUFFICIENT FOR FUEL FAILURE
X 213 DEFECTIVE PR DEVICE INSTALLED
X 214 PR DEVICE NOT INSTALLED PROPERLY
X 215 PR DEVICE DAMAGED DURING HANDLING
X 216 CRUSHING FORCES CAUSES LOC FROM PR DEVICE
X 217 SIDE IMPACT FAILS NORMAL PR DEVICE
X 218 END IMPACT FAILS NORMAL PR DEVICE
X 219 PUNCTURE PROBE FAILS PR DEVICE
X 220 PUNCTURE PROBE STRIKES PR DEVICE
X 221 FIRE DURATION AND TEMP SUFFICIENT TO CAUSE LOC FROM PR DEVICE
X 222 END IMPACT FAILS IMPROPERLY INSTALLED PR DEVICE
X 223 END IMPACT FAILS DEFECTIVE PR DEVICE
X 224 FUEL DOES NOT FAIL WHEN DEFECTIVE PR DEVICE CAUSES LOC
X 225 FUEL FAILS WHEN IMPROPERLY INSTALLED PR DEVICE CAUSES LOC
X 226 FUEL PINS FAIL WHEN DEFECTIVE DEVICE CAUSES LOC
X 227 PROBE CAUSES LOC FROM PR DEVICE AND FUEL DOES NOT FAIL
X 228 FIRE CAUSES LOC FROM PR DEVICE AND FUEL DOES NOT FAIL
X 229 SIDE IMPACT CAUSES LOC FROM PR DEVICE AND FUEL DOES NOT FAIL
X 230 SIDE IMPACT FAILS PR DEVICE DAMAGED DURING HANDLING
X 231 SIDE IMPACT FAILS IMPROPERLY INSTALLED DEVICE
X 232 SIDE IMPACT FAILS DEFECTIVE PR DEVICE
X 233 END IMPACT CAUSES LOC FROM PR DEVICE AND FUEL DOES NOT FAIL
X 234 FUEL DOES NOT FAIL WHEN IMPROPERLY INSTALLED DEVICE CAUSES LOC

(cont'd) TABLE 8.2. Listing of Basic Events for Analysis of Spent Fuel

X 235 IMPROPERLY INSTALLED PR DEVICE CAUSES LOC
X 236 DEFECTIVE PR DEVICE CAUSES LOC
X 237 END IMPACT FAILS PR DEVICE DAMAGED DURING HANDLING
X 238 DAMAGED PR DEVICE CAUSES LOC
X 239 FUEL FAILS WHEN DAMAGED DEVICE CAUSES LOC
X 240 FUEL DOES NOT FAIL WHEN DAMAGED PR DEVICE CAUSES LOC
X 250 IMMERSION FORCES FAIL DRAIN VALVE AND FUEL
X 251 CRUSHING FORCE FAILS DRAIN VALVE AND FUEL
X 252 PUNCTURE PROBE STRIKES DRAIN VALVE AND FUEL
X 253 PUNCTURE PROBE FAILS DRAIN VALVE AND FUEL
X 254 SIDE IMPACT FAILS NORMAL DRAIN VALVE AND FUEL
X 255 SIDE IMPACT FAILS DRAIN VALVE AND FUEL WHEN VALVE DEFECTIVE
X 256 SIDE IMPACT FAILS DRAIN VALVE AND FUEL WHEN VALVE DAMAGED DURING HANDLING
X 257 SIDE IMPACT FAILS DRAIN VALVE AND FUEL WHEN VALVE NOT INSTALLED PROPERLY
X 258 CRUSHING FORCE CAUSES LOC FROM DRAIN VALVE
X 259 END IMPACT FAILS NORMAL DRAIN VALVE AND FUEL
X 260 LOC FROM DRAIN VALVE CAUSES FUEL FAILURE
X 261 DRAIN VALVE NOT INSTALLED PROPERLY
X 262 FUEL DOES NOT FAIL WHEN DEFECTIVE DRAIN VALVE CAUSES LOC
X 263 FUEL FAILS WHEN IMPROPERLY INSTALLED DRAIN VALVE CAUSES LOC
X 264 FUEL FAILS WHEN DEFECTIVE DRAIN VALVE CAUSES LOC
X 265 PUNCTURE PROBE CAUSES LOC FROM DRAIN VALVE AND FUEL DOES NOT FAIL
X 266 FIRE CAUSES LOC FROM DRAIN VALVE AND FUEL DOES NOT FAIL
X 267 SIDE IMPACT CAUSES LOC FROM DRAIN VALVE AND FUEL DOES FAIL
X 268 SIDE IMPACT FAILS DRAIN VALVE DAMAGED DURING HANDLING
X 269 SIDE IMPACT FAILS IMPROPERLY INSTALLED DRAIN VALVE
X 270 SIDE IMPACT FAILS DEFECTIVE DRAIN VALVE
X 271 FUEL DOES NOT FAIL WHEN IMPROPERLY INSTALLED DRAIN VALVE CAUSING LOC
X 272 IMPROPERLY INSTALLED DRAIN VALVE CAUSES LOC
X 273 DEFECTIVE DRAIN VALVE INSTALLED
X 274 DRAIN VALVE LEAKS FROM WEAR CAUSING LOC
X 275 DRAIN VALVE DAMAGED DURING HANDLING
X 276 DRAIN VALVE IS NOT CLOSED CAUSING LOC
X 277 PUNCTURE PROBE STRIKES DRAIN VALVE
X 278 DEFECTIVE DRAIN VALVE CAUSES LOC
X 279 FIRE TEMPERATURE AND DURATION SUFFICIENT TO FAIL DRAIN VALVE
X 280 SIDE IMPACT FAILS NORMAL DRAIN VALVE
X 281 END IMPACT FAILS NORMAL DRAIN VALVE
X 282 DAMAGED DRAIN VALVE CAUSES LOC
X 283 PUNCTURE PROBE FAILS DRAIN VALVE
X 284 OVERPRESSURE FAILS DRAIN VALVE
X 285 FUEL DOES NOT FAIL WHEN DRAIN VALVE LEAKS FROM WEAR
X 286 FUEL DOES NOT FAIL WHEN DRAIN VALVE IS NOT CLOSED
X 287 FUEL FAILS WHEN DRAIN VALVE LEAKS FROM WEAR CAUSING LOC
X 288 FUEL FAILS WHEN DRAIN VALVE NOT CLOSED CAUSES LOC

(cont'd) TABLE 8.2. Listing of Basic Events for Analysis of Spent Fuel

X 289 FUEL FAILS WHEN DAMAGED DRAIN VALVE CAUSES LOC
X 290 FUEL DOES NOT FAIL WHEN DAMAGED DRAIN VALVE CAUSES LOC
X 300 IMMERSION FORCES FAIL VENT VALVE AND FUEL
X 301 CRUSHING FORCE FAILS VENT VALVE AND FUEL
X 302 PUNCTURE PROBE STRIKES VENT VALVE AND FUEL
X 303 PUNCTURE PROBE FAILS VENT VALVE AND FUEL
X 304 SIDE IMPACT FAILS NORMAL VENT VALVE AND FUEL
X 305 SIDE IMPACT FAILS VENT VALVE AND FUEL WHEN VENT VALVE DEFECTIVE
X 306 SIDE IMPACT FAILS VENT VALVE AND FUEL WHEN VALVE DAMAGED DURING HANDLING
X 307 SIDE IMPACT FAILS VENT VALVE AND FUEL WHEN VALVE NOT INSTALLED PROPERLY
X 308 CRUSHING FORCE CAUSES LOC FROM VENT VALVE
X 309 END IMPACT FAILS NORMAL VENT VALVE AND FUEL
X 310 LOC FROM VENT VALVE CAUSES FUEL FAILURE
X 311 VENT VALVE NOT INSTALLED PROPERLY
X 312 FUEL DOES NOT FAIL WHEN DEFECTIVE VENT VALVE CAUSES LOC
X 313 FUEL FAILS WHEN IMPROPERLY INSTALLED VENT VALVE CAUSES LOC
X 314 FUEL FAILS WHEN DEFECTIVE VENT VALVE CAUSES LOC
X 315 PUNCTURE PROBE CAUSES LOC FROM VENT VALVE AND FUEL DOES NOT FAIL
X 316 FIRE CAUSES LOC FROM VENT VALVE AND FUEL DOES NOT FAIL
X 317 SIDE IMPACT CAUSES LOC FROM VENT VALVE AND FUEL DOES NOT FAIL
X 318 SIDE IMPACT FAILS VENT VALVE DAMAGED DURING HANDLING
X 319 SIDE IMPACT FAILS IMPORPERLY INSTALLED VENT VALVE
X 320 SIDE IMPACT FAILS DEFECTIVE VENT VALVE
X 321 FUEL DOES NOT FAIL WHEN IMPROPERLY INSTALLED VENT VALVE CAUSES LOC
X 322 IMPROPERLY INSTALLED VENT VALVE CAUSES LOC
X 323 DEFECTIVE VENT VALVE INSTALLED
X 324 VENT VALVE LEAKS FROM WEAR CAUSING LOC
X 325 VENT VALVE DAMAGED DURING HANDLING
X 326 VENT VALVE IS NOT CLOSED CAUSING LOC
X 327 PUNCTURE PROBE STRIKES VENT VALVE
X 328 DEFECTIVE VENT VALVE CAUSES LOC
X 329 FIRE TEMPERATURE AND DURATION SUFFICIENT TO FAIL VENT VALVE
X 330 SIDE IMPACT FAILS NORMAL VENT VALVE
X 331 END IMPACT FAILS NORMAL VENT VALVE
X 332 DAMAGED VENT VALVE CAUSES LOC
X 333 PUNCTURE PROBE FAILS VENT VALVE
X 334 OVERPRESSURE FAILS VENT VALVE
X 335 FUEL DOES NOT FAIL WHEN VENT VALVE LEAKS FROM WEAR
X 336 FUEL DOES NOT FAIL WHEN VENT VALVE IS NOT CLOSED
X 337 FUEL FAILS WHEN VENT VALVE LEAKS FROM WEAR CAUSING LOC
X 338 FUEL FAILS WHEN VENT VLAVE NOT CLOSED CAUSES LOC
X 339 FUEL FAILS WHEN DAMAGED VENT VALVE CAUSES LOC
X 340 FUEL DOES NOT FAIL WHEN DAMAGED VENT VALVE CAUSES LOC

TABLE 8.3. Listing of Input Labels for Rectangles for Analysis of Spent Fuel

```
A   1 RELEASE OF RADIOACTIVE MATERIAL TO ENVIRONMENT DURING
      SPENT FUEL SHIPMENT
A   2 RELEASE OF RM FROM SPENT FUEL CASK
A  52 OTHER FORCES FAIL FUEL
A  53 IMPACT FORCE FAILS FUEL
A  54 OTHER FORCES FAIL FUEL
A  55 NORMAL TRANSPORT FORCES FAIL FUEL
A  56 IMPACT FORCE FAIL FUEL
A  58 OTHER FORCES FAIL FUEL
A 100 FAILURE OF CASK LID CAUSES RELEASE OF RM
A 101 ACCIDENT FORCES FAIL LID AND RELEASE RM FROM FUEL
A 102 ACCIDENT FORCES SUFFICIENT TO FAIL LID AND RELEASE RM FROM FUEL
A 103 CASK LID AND FUEL FAIL FROM SAME EVENT
A 104 CASK LID AND FUEL FAIL FROM DIFFERENT EVENTS
A 105 PUNCTURE PROBE FAILS LID AND FUEL
A 112 IMPACT FAILS LID AND FUEL
A 113 SIDE IMPACT FAILS LID AND FUEL
A 114 END IMPACT FAILS LID AND FUEL
A 115 SIDE IMPACT FAILS LID AND FUEL WHEN LID DEFECTIVE
A 116 SIDE IMPACT FAILS IMPROPERLY CLOSED LID AND FUEL
A 117 END IMPACT FAILS LID AND FUEL WHEN LID DEFECTIVE
A 118 END IMPACT FAILS LID AND FUEL WHEN LID NOT PROPERLY CLOSED
A 119 BOLTS NOT TORQUED PROPERLY AND END IMPACT FAILS LID AND FUEL
A 120 BOLTS DAMAMGED AND END IMPACT FAILS LID AND FUEL
A 121 BOLTS NOT TORQUED PROPERLY AND SIDE IMPACT FAILS LID AND FUEL
A 122 BOLTS DAMAGED FROM HANDLING AND SIDE IMPACT FAILS LID AND FUEL
A 123 BOLTS MISSING AND SIDE IMPACT FAILS LID AND FUEL
A 124 IMPACT FAILS LID AND NORMAL TRANSPORT FORCES FAIL FUEL
A 125 IMPACT FORCES FAIL LID
A 126 IMPACT FORCES FAIL LID
A 127 BOLTS MISSING AND END IMPACT FAILS LID AND FUEL
A 128 PUNCTURE FAILS LID AND OTHER FORCES FAIL FUEL
A 131 LOC FROM LID FAILURE CAUSES RELEASE OF RM
A 132 ACCIDENT FORCES CAUSE LOC FROM CASK LID
A 133 CLOSURE ERRORS CAUSE LOC FROM LID
A 134 PUNCTURE CAUSES LOC FROM LID
A 135 IMPACT CAUSES LOC FROM LID
A 136 PROBE CAUSES LOC FROM LID
A 137 FUEL FAILS FROM LOC WHEN PROBE FAILS LID
A 138 IMPACT FORCES CAUSES LOC FROM LID
A 139 SIDE IMPACT CAUSES LOC FROM LID
A 140 END IMPACT CAUSES LOC FROM LID
A 141 FUEL FAILS FROM LOC WHEN SIDE IMPACT FAILS LID
A 142 SIDE IMPACT FAILS LID
A 143 PUNCTURE FAILS CASK LID
A 144 PUNCTURE PROBE FAILS LID
A 145 CLOSURE ERRORS CAUSE LOC FROM LID AND FUEL DOES NOT FAIL
```

(cont'd) TABLE 8.3. Listing of Input Labels for Rectangles for Analysis of Spent Fuel

A 146 LOC FROM IMPROPERLY TORQUED BOLTS AND FUEL DOES NOT FAIL
A 147 FUEL FAILS FROM LOC WHEN END IMPACT FAILS LID
A 148 END IMPACT FAILS LID
A 149 DAMAGED BOLTS CAUSE LOC FROM LID AND FUEL DOES NOT FAIL
A 150 MISSING BOLTS CAUSE LOC FROM LID AND FUEL DOES NOT FAIL
A 151 FUEL FAILS WHEN CLOSURE ERRORS CAUSE LOC FROM LID
A 152 IMPROPERLY TORQUED BOLTS CAUSE LOC FROM LID AND FUEL FAILS
A 153 DAMAGED BOLTS CAUSE LOC FROM LID AND FUEL FAILS
A 154 MISSING BOLTS CAUSE LOC FROM LID AND FUEL FAILS
A 155 IMPACT FAILS LID AND FUEL
A 156 END IMPACT FAILS LID CAUSING LOC
A 200 FAILURE OF CLOSURE SEAL CAUSES RELEASE OF RM
A 201 ACCIDENT FORCES FAIL SEAL AND RELEASE RM FROM FUEL
A 202 LOC FROM SEAL FAILURE CAUSES RELEASE OF RM
A 203 ACCIDENT FORCES SUFFICIENT TO FAIL SEAL AND RELEASE RM FROM FUEL
A 204 CLOSURE SEAL AND FUEL FAIL FROM SAME EVENT
A 205 CLOSURE SEAL AND FUEL FAIL FROM DIFFERENT EVENTS
A 206 IMPACT FORCES FAIL SEAL AND FUEL
A 208 IMPACT FAILS SEAL AND OTHER FORCES FAIL FUEL
A 209 IMPACT FAILS SEAL AND FUEL
A 210 SIDE IMPACT FAILS SEAL AND FUEL
A 211 END IMPACT FAIL SEAL AND FUEL
A 212 SIDE IMPACT FAILS IMPROPERLY INSTALLED SEAL AND FUEL
A 213 SIDE IMPACT FAILS DEFECTIVE SEAL AND FUEL
A 214 END IMPACT FAILS DEFECTIVE SEAL AND FUEL
A 215 END IMPACT FAILS IMPROPERLY INSTALLED SEAL AND FUEL
A 216 IMPACT FORCES FAIL SEAL
A 217 IMPACT FORCE FAILS SEAL
A 218 FIRE FAILS SEAL AND OTHER FORCES FAIL FUEL
A 219 FIRE FAILS SEAL
A 220 FIRE CAUSES LOC FROM SEAL
A 221 FIRE CAUSES LOC FROM SEAL
A 222 FUEL FAILS FROM LOC WHEN FIRE FAILS SEAL
A 223 IMPACT CAUSES LOC FROM SEAL
A 224 IMPACT FORCES CAUSE LOC FROM SEAL
A 225 SIDE IMPACT CAUSES LOC FROM SEAL
A 226 END IMPACT CAUSE LOC FROM SEAL
A 227 FUEL FAILS FROM LOC WHEN SIDE IMPACT FAILS SEAL
A 228 SIDE IMPACT FAILS SEAL
A 229 FUEL FAILS FROM LOC WHEN END IMPACT FAILS SEAL
A 230 END IMPACT FAILS SEAL
A 231 ACCIDENT FORCES CAUSE LOC FROM CLOSURE SEAL
A 232 ACCIDENT CAUSE LOC FROM CLOSURE SEAL
A 233 CLOSURE ERRORS CAUSE LOC FROM SEAL
A 234 CLOSURE ERROR CAUSE LOC FROM SEAL AND FUEL DOES NOT FAIL
A 235 LOC FROM IMPROPERLY INSTALLED SEAL AND FUEL DOES NOT FAIL
A 236 LOC FROM DEFECTIVE SEAL AND FUEL DOES NOT FAIL
A 237 LOC FROM SEAL DAMAGED IN TRANSIT AND FUEL DOES NOT FAIL

(cont'd) TABLE 8.3. Listing of Input Labels for Rectangles for Analysis of Spent Fuel

A 238 FUEL FAILS WHEN CLOSURE ERROR CAUSE LOC FROM SEAL
A 239 IMPROPERLY INSTALLED SEAL CAUSES LOC FROM SEAL AND FUEL FAILS
A 240 SEAL DAMAGED IN TRANSIT CAUSES LOC AND FUEL FAILS
A 241 DECECTIVE SEAL CAUSES LOC AND FUEL FAILS
A 300 FAILURE OF CASK WALL CAUSE RELEASE OF RM
A 301 ACCIDENT FORCES FAIL CASK WALL AND RELEASE RM FROM FUEL
A 302 ACCIDENT FORCES SUFFICIENT TO FAIL WALL AND RELEASE RM FROM FUEL
A 303 CASK WALL AND FUEL FAIL FROM SAME EVENT
A 304 CASK WALL AND FUEL FAIL FROM DIFFERENT EVENTS
A 305 PUNCTURE PROBE FAILS WALL AND FUEL
A 307 IMPACT FAILS CASK WALL AND FUEL
A 308 IMPACT FAILS CASK WALL AND FUEL
A 309 SIDE IMPACT FAILS WALL AND FUEL
A 310 END IMPACT FAILS WALL AND FUEL
A 311 SIDE IMPACT FAILS CASK WALL AND FUEL WHEN WALL DEFECTIVE
A 313 END IMPACT FAILS WALL AND FUEL WHEN WALL IS DEFECTIVE
A 314 IMPACT FAILS WALL AND OTHER FORCES FAIL FUEL
A 315 PUNCTURE FAILS WALL AND OTHER FORCES FAIL FUEL
A 316 IMPACT FORCES FAIL WALL
A 318 PUNCTURE PROBE FAILS CASK WALL
A 320 IMPACT FORCES FAIL WALL
A 322 PUNCTURE PROBE FAILS WALL
A 323 LOC FROM CASK WALL FAILURE CAUSES RELEASE OF RM
A 324 ACCIDENT FORCES CAUSE LOC FROM CASK WALL
A 325 ACCIDENT CAUSE LOC FROM CASK WALL
A 326 PUNCTURE CAUSES LOC FROM WALL
A 327 PUNCTURE PROBE CAUSES LOC FROM WALL
A 328 PROBE CAUSES LOC FROM WALL AND FUEL FAILS
A 329 IMPACT CAUSES LOC FROM WALL
A 330 IMPACT FORCES CAUSES LOC FROM WALL
A 331 SIDE IMPACT CAUSES LOC FROM WALL
A 332 END IMPACT CAUSES LOC FROM WALL
A 333 FUEL FAILS FROM LOC WHEN SIDE IMPACT FAILS WALL
A 334 SIDE IMPACT FAILS WALL
A 335 FUEL FAILS FROM LOC WHEN END IMPACT FAIL WALL
A 336 END IMPACT FAILS WALL
A 340 CASK WALL FAILS DURING NORMAL TRANSPORT CAUSING LOC
A 342 DEFECTIVE CASK WALL FAILURE
A 343 SIDE IMPACT FAILS DEFECTIVE WALL
A 344 END IMPACT FAILS DEFECTIVE WALL
A 345 END IMPACT FAILS CASK WALL CAUSING LOC
A 400 FAILURE OF PRESSURE RELIEF DEVICE CAUSES RELEASE OF RM
A 401 ACCIDENT FORCES FAIL PR DEFICE AND RELEASE RM FROM FUEL
A 402 ACCIDENT FORCES SUFFICIENT TO FAIL PR DEVICE AND RELEASE RM FROM FUEL
A 403 PR DEVICE AND FUEL FAIL FROM SAME EVENT
A 404 IMPACT FORCE FAILS DEVICE AND FUEL
A 405 PUNCTURE PROBE FAILS DEVICE AND FUEL
A 406 IMPACT FAILS PR DEVICE AND FUEL

(cont'd) TABLE 8.3. Listing of Input Labels for Rectangles for Analysis of Spent Fuel

A 407 SIDE IMPACT FAILS PR DEVICE AND FUEL
A 408 SIDE IMPACT FAILS PR DEVICE AND FUEL WHEN DEVICE DEFECTIVE
A 409 SIDE IMPACT FAILS PR DEVICE AND FUEL WHEN DEVICE NOT INSTALLED PROPERLY
A 410 SIDE IMPACT FAILS PR DEVICE AND FUEL WHEN DEVICE DAMAGED DURING HANDLING
A 411 END IMPACT FAILS PR DEVICE AND FUEL
A 412 END IMPACT FAILS PR DEVICE AND FUEL WHEN DEVICE DEFECTIVE
A 413 END IMPACT FAILS PR DEVICE AND FUEL WHEN DEVICE NOT INSTALLED PROPERLY
A 414 END IMPACT FAILS PR DEVICE AND FUEL WHEN DEVICE DAMAGED DURING HANDLING
A 416 PR DEVICE AND FUEL FAIL FROM DIFFERENT EVENTS
A 417 PUNCTURE PROBE FAILS PR DEVICE AND OTHER FORMS FAIL FUEL
A 419 PUNCTURE PROBE FAILS PR DEVICE
A 422 IMPACT FAILS PR DEVICE
A 423 IMPACT FORCES FAIL PR DEVICE
A 421 IMPACT FAILS PR DEVICE AND OTHER FORCES FAIL FUEL
A 424 LOC FROM PR DEVICE FAILUR CAUSES RELEASE OF RM
A 425 ACCIDENT FORCES CAUSE LOC FROM PR DEVICE
A 426 ACCIDENTS CAUSE LOC FROM PR DEVICE
A 427 PUNCTURE PROBE CAUSES LOC FROM PR DEVICE
A 428 PUNCTURE PROBE CAUSES LOC FROM PR DEVICE
A 429 FUEL FAILS FROM LOC WHEN PROBE FAILS PR DEVICE
A 430 FIRE CAUSES LOC FROM PR DEVICE
A 431 FIRE CAUSES LOC FROM PR DEVICE
A 432 FUEL FAILS FROM LOC WHEN FIRE FAILS PR DEVICE
A 433 IMPACT CAUSES LOC FROM PR DEVICE
A 434 IMPACT FORCES CAUSE LOC FROM PR DEVICE
A 435 SIDE IMPACT CAUSES LOC FROM PR DEVICE
A 436 END IMPACT CAUSES LOC FROM PR DEVICE
A 437 FUEL FAILS FROM LOC WHEN SIDE IMPACT FAILS PR DEVICE
A 438 SIDE IMPACT FAILS PR DEVICE
A 439 FUEL FAILS FROM LOC WHEN END IMPACT FAILS PR DEVICE
A 440 END IMPACT FAILS PR DEVICE
A 441 CLOSURE ERROR CAUSES LOC FROM PR DEVICE
A 442 FUEL FAILS OR DOES NOT FAIL WHEN IMP INSTALLED DEVICE CAUSES LOC
A 443 IMPROPERLY INSTALLED PR DEVICE CAUSES LOC
A 444 DEFECTIVE PR DEVICE INSTALLED CAUSES LOC
A 445 FUEL FAILS OR DOES NOT FAIL WHEN DEFECTIVE DEVICE CAUSES LOC
A 446 DEVICE DAMAGED DURING HANDLING CAUSES LOC
A 447 FUEL FAILS OR DOES NOT FAIL WHEN DAMAGED DEVICE CAUSES LOC
A 500 FAILURE OF DRAIN VALVE CAUSES RELEASE OF RM
A 501 ACCIDENT FORCES FAIL DRAIN VALVE AND RELEASE RM FROM FUEL
A 502 ACCIDENT FORCES SUFFICIENT TO FAIL DRAIN V AND RELEASE RM FROM FUEL
A 503 DRAIN VALVE AND FUEL FAIL FROM SAME EVENT
A 504 IMPACT FORCE FAILS DRAIN VALVE AND FUEL
A 505 PUNCTURE PROBE FAILS DRAIN VALVE AND FUEL
A 506 IMPACT FORCE FAILS DRAIN VALVE AND FUEL

(cont'd) TABLE 8.3. Listing of Input Labels for Rectangles for Analysis of Spent Fuel

A 507 SIDE IMPACT FAILS DRAIN VALVE AND FUEL
A 508 SIDE IMPACT FAILS DRAIN VALVE AND FUEL WHEN VALVE DEFECTIVE
A 509 SIDE IMPACT FAILS DRAIN VALVE AND FUEL WHEN DV NOT INSTALLED PROPERLY
A 510 SIDE IMPACT FAILS DRAIN VALVE AND FUEL WHEN VALVE DAMAGED DURING HANDLING
A 516 DRAIN VALVE AND FUEL FAIL FROM DIFFERENT EVENTS
A 517 PUNCTURE PROBE FAILS DRAIN VALVE AND OTHER FORCES FAIL FUEL
A 518 FIRE FAILS DRAIN VALVE AND OTHER FORCES FAIL FUEL
A 519 PUNCTURE PROBE FAILS DRAIN VALVE
A 520 FIRE FAILS DRAIN VALVE
A 521 IMPACT FAILS DRAIN VALVE AND OTHER FORCES FAIL FUEL
A 522 IMPACT FAILS DRAIN VALVE
A 523 IMPACT FORCES FAIL DRAIN VALVE
A 524 LOC FROM DRAIN VALVE FAILURE CAUSES RELEASE OF RM
A 525 ACCIDENT FORCES CAUSE LOC FROM DRAIN VALVE
A 526 ACCIDENT CAUSE LOC FROM DRAIN VALVE
A 527 PUNCTURE PROBE CAUSES LOC FROM DRAIN VALVE
A 528 PUNCTURE PROBE CAUSES LOC FROM DRAIN VALVE
A 529 FUEL FAILS FROM LOC WHEN PUNCTURE PROBE FAILS DRAIN VALVE
A 530 FIRE CAUSES LOC FROM DRAIN VALVE
A 531 FIRE CAUSES LOC FROM DRAIN VALVE
A 532 FUEL FAIL FROM LOC WHEN FIRE FAILS DRAIN VALVE
A 533 IMPACT CAUSES LOC FROM DRAIN VALVE
A 535 SIDE IMPACT CAUSES LOC FROM DRAIN VALVE
A 537 FUEL FAILS FROM LOC WHEN SIDE IMPACT FAILS DRAIN VALVE
A 538 SIDE IMPACT FAILS DRAIN VALVE
A 541 CLOSURE ERRORS CAUSE LOC FROM DRAIN VALVE
A 543 IMPROPERLY INSTALLED DRAIN VALVE CAUSES LOC
A 544 DEFECTIVE DRAIN VALVE INSTALLED CAUSES LOC
A 545 FUEL FAILS OR DOES NOT FAIL WHEN IMP INSTALLED DRAIN VALVE CAUSES LOC
A 546 DRAIN VALVE DAMAGED DURING HANDLING CAUSING LOC
A 547 FUEL FAILS OR DOES NOT FAIL WHEN DEFECTIVE DRAIN VALVE CAUSES LOC
A 548 FUEL FAILS OR DOES NOT FAIL WHEN DAMAGED DRAIN VALVE CAUSES LOC
A 558 FUEL FAILS OR DOES NOT FAIL WHEN DRAIN VALVE LEAKS FROM WEAR
A 559 FUEL FAILS OR DOES NOT FAIL WHEN DRAIN VALVE IS NOT CLOSED
A 561 DRAIN VALVE LEAKS FROM WEAR CAUSING LOC
A 562 DRAIN VALVE IS NOT CLOSED CAUSING LOC
A 563 DRAIN VALVE FAILS FROM FIRE
A 564 DRAIN VALVE FAILS FROM HIGH INTERNAL PRESSURE
A 600 FAILURE OF VENT VALVE CAUSES RELEASE OF RM
A 601 ACCIDENT FORCES FAIL VENT VALVE AND RELEASE RM FROM FUEL
A 602 ACCIDENT FORCES SUFFICIENT TO FAIL VENT V AND RELEASE RM FROM FUEL
A 603 VENT VALVE AND FUEL FAIL FROM SAME EVENT
A 604 IMPACT FORCE FAILS VENT VALVE AND FUEL
A 605 PUNCTURE PROBE FAILS VENT VALVE AND FUEL
A 606 IMPACT FAILS VENT VALVE AND FUEL

(cont'd) TABLE 8.3. Listing of Input Labels for Rectangles for Analysis of Spent Fuel

A 607 SIDE IMPACT FAILS VENT VALVE AND FUEL
A 608 SIDE IMPACT FAILS VENT VALVE AND FUEL WHEN VALVE DEFECTIVE
A 609 SIDE IMPACT FAILS VENT VALVE AND FUEL WHEN DV NOT INSTALLED PROPERLY
A 61[illegible] SIDE IMPACT FAILS VENT VALVE AND FUEL WHEN VALVE DAMAGED DURING HANDLING
A 616 VENT VALVE AND FUEL FAIL FROM DIFFERENT EVENTS
A 617 PUNCTURE PROBE FAILS VENT VALVE AND OTHER FORCES FAIL FUEL
A 618 FIRE FAILS VENT VALVE AND OTHER FORCES FAIL FUEL
A 619 PUNCTURE PROBE FAILS VENT VALVE
A 620 FIRE FAILS VENT VALVE
A 621 IMPACT FAILS VENT VALVE AND OTHER FORCES FAIL FUEL
A 622 IMPACT FAILS VENT VALVE
A 623 IMPACT FORCES FAIL VENT VALVE
A 624 LOC FROM VENT VALVE FAILURE CAUSES RELEASE OF RM
A 625 ACCIDENT FORCES CAUSE LOC FROM VENT VALVE
A 626 ACCIDENTS CAUSE LOC FROM VENT VALVE
A 627 PUNCTURE PROBE CAUSES LOC FROM VENT VALVE
A 628 PUNCTURE PROBE CAUSES LOC FROM VENT VALVE
A 629 FUEL FAILS FROM LOC WHEN PUNCTURE PROBE FAILS VENT VALVE
A 630 FIRE CAUSES LOC FROM VENT VALVE
A 631 FIRE CAUSES LOC FROM VENT VALVE
A 632 FUEL FAILS FROM LOC WHEN FIRE FAILS VENT VALVE
A 633 IMPACT CAUSES LOC FROM VENT VALVE
A 635 SIDE IMPACT CAUSES LOC FROM VENT VALVE
A 637 FUEL FAILS FROM LOC WHEN SIDE IMPACT FAILS VENT VALVE
A 638 SIDE IMPACT FAILS VENT VALVE
A 641 CLOSURE ERRORS CAUSE LOC FROM VENT VALVE
A 643 IMPROPERLY INSTALLED VENT VALVE CAUSES LOC
A 644 DEFECTIVE VENT VALVE INSTALLED CAUSES LOC
A 645 FUEL FAILS OR DOES NOT FAIL WHEN IMP INSTALLED VENT VALVE CAUSES LOC
A 646 VENT VALVE DAMAGED DURING HANDLING CAUSING LOC
A 647 FUEL FAILS OR DOES NOT FAIL WHEN DEFECTIVE VENT VALVE CAUSES LOC
A 648 FUEL FAILS OR DOES NOT FAIL WHEN DAMAGED VENT VALVE CAUSES LOC
A 658 FUEL FAILS OR DOES NOT FAIL WHEN VENT VALVE LEAKS FROM WEAR
A 659 FUEL FAILS OR DOES NOT FAIL WHEN VENT VALVE IS NOT CLOSED
A 661 VENT VALVE LEAKS FROM WEAR CAUSING LOC
A 662 VENT VALVE IS NOT CLOSED CAUSING LOC
A 663 VENT VALVE FAILS FROM FIRE
A 664 VENT VALVE FAILS FROM HIGH INTERNAL PRESSURE

8.3 RELEASE SEQUENCES

The fault tree can be thought of as a compact notation for identifying and displaying large numbers of release sequences. For larger trees, it is often helpful to utilize computer programs to perform the Boolean algebra that reduces the fault tree to a series of release sequences or "cut sets". The computer code MFAULT[4] was used for this analysis.

A listing of the release sequences identified from the transportation of spent fuel by truck fault tree analysis is presented in Table 9.1 of Section 9.2. Analysis of the fault tree indicated the presence of several hundred release sequences for this particular reference cask design and transport mode. The cut sets presented in Table 9.1 have been screened by the program MFAULT using a probability cutoff and only those which are expected to occur at least once in every 10^{15} shipments are presented. Duplicate cut sets are automatically eliminated by the computer code. To keep the amount of analysis to a reasonable level, the top 198 cut sets or release sequences were retained for evaluation using the probability cutoff option. The retained cut sets were then used to determine the shipping system risk. The level of analysis accounts for the significant release sequences in the fault tree.

REFERENCES

1. J. W. Langhaar, "Transport Experience with Radioactive Materials." Proceedings of the International Symposium on the Management of Wastes from the LWR Fuel Cycle, CONF-76-0701, Denver, Co, July 1976.

2. A. E. Grella, "A Review of Five Years Accident Experience in the U.S. Involving Nuclear Transportation (1971-1975)." International Symposium on the Design, Construction and Testing of Packaging for the Safe Transport of Radioactive Materials, IAEA-SR-10, Vienna, Austria, August 1976.

3. J. L. Carter, ACORN a Program for Plotting Fault Trees. BNWL-2144, Battelle, Pacific Northwest Laboratories, Richland, WA, October 1977.

4. P. J. Pelto, W. L. Purcell, MFAULT: A Computer Program for Analyzing Fault Trees. BNWL-2145, Battelle, Pacific Northwest Laboratories, Richland, WA, November 1977.

9.0 RELEASE SEQUENCE EVALUATION

A fault tree for the truck shipment of spent fuel in the reference cask was presented in the previous chapter. From the fault tree, a set of release sequences can be identified. For example, the occurrence of the following events is one release sequence which will result in a loss of radioactive material from the cask.

X2 Truck Accident Occurs

X4 Fire Occurs with Accident

X212 Fire Duration and Temperature Sufficient to Cause Loss of Coolant from Pressure Releaf Device

X221 Loss of Coolant from Pressure Relief Device Sufficient for Fuel Failure

The fault tree can be thought of as a compact notation for summarizing several thousand release sequences. As shown in Figure 9.1, based on the release

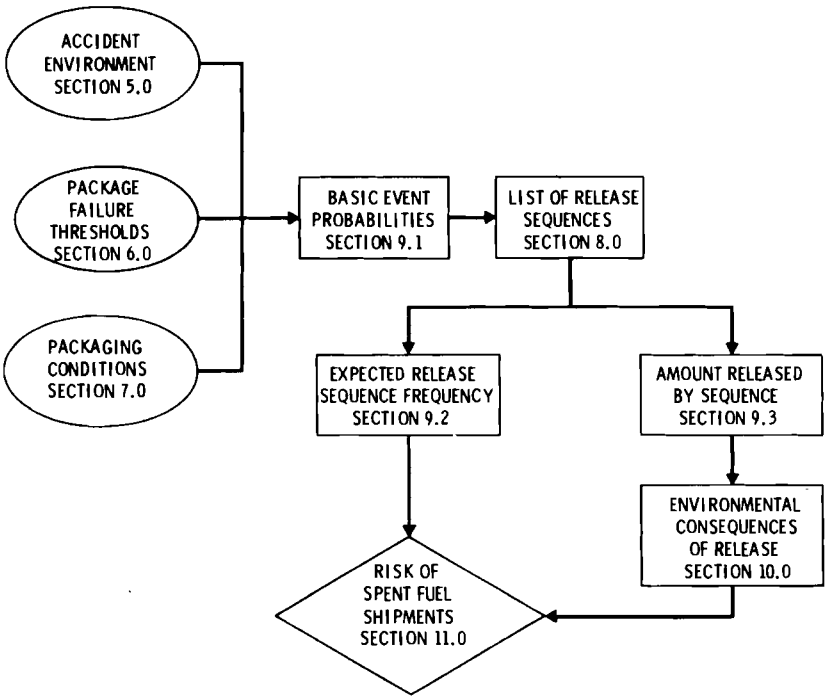

FIGURE 9.1. Remaining Steps in the Risk Evaluation

sequences, both the occurrence frequency and the amount released (release fraction) must be determined for each release sequence to complete the risk evaluation. The basic data required to evaluate all release sequences are presented in this section.

The basic event probabilities and release fractions are fundamental to the analysis. The fault trees in Section 8 were developed to a point where data on basic events could be obtained through either analysis or survey. The estimated basic event probabilities are presented in Section 9.1. The probability data are then used to develop the information on release sequence probabilities summarized in Section 9.2. Release fractions are evaluated in Section 9.3.

9.1. BASIC EVENT PROBABILITIES

A sequential description of failure probability estimates for spent fuel shipments in the configuration considered in this risk assessment is presented in this section. The number sequence used here corresponds to the numbering sequence used in the fault trees. Events numbered from 1 to 340 were identified in the fault tree shown in Figure 8.1 of Section 8. Table 8.1 listed the events as they are titled and keyed in the fault tree. Since the fault tree is made up of several similar branches, a numbering system was used to help identify the different branches of the tree. Events numbered 1 through 12 identify various basic accident probabilities and fuel failure probabilities. Events which describe failure of the cask lid are numbered 50 through 92. Those events which are concerned with failure of the closure seal are numbered 100 through 132. Failure events for the cask wall are listed with numbers 150 through 169. Event numbers 200 through 240 are for events covering the pressure relief device, 250 through 290 for the drain valve and 300 through 340 for the vent valve. The explanation "not used" following an event number simply means that the event number was not used in the numbering sequence.

The expected frequency of the release sequences identified from the fault tree is obtained by taking the product of the probabilities of each event in the sequence. In all cases the best available information was used in determining failure event probabilities. Estimates of the probabilities for each event are presented in the following paragraphs.

Loss of Neutron Shield Water Allows Release of Radioactivity (X1)

The amount of radioactivity released in an accident involving loss of neutron shield water would be negligible. Loss of cask neutron shield water would also result in an increase of neutron flux outside the cask. However, total loss of neutron shielding can be postulated for the reference cask without exceeding post accident radiation dose rate limits in the regulatory criteria of 10CFR71.[1] Since the public is assumed to be excluded from the immediate area surrounding the cask in an accident situation, no risk would result. Because the consequences of this accident are not significant, this event was not analyzed and a probability of zero was used.

Truck Accident Occurs (X2)

The accident frequency for truck transport used in this study which is presented in Section 5.1 is one accident every 640,000 km or an accident rate of 1.5×10^{-6} truck accidents per km.[2] The estimated average shipping distances from Section 4.3 for the two transportation scenarios used in this study are 690 km and 930 km. For 690 km shipping distance, the expected accident frequency is 1.1×10^{-3} accidents per shipment and 1.5×10^{-3} accidents per shipment for a 930 km shipping distance. These values were used in the analysis.

Defective Fuel Pins Occur (X3)

It is conservatively assumed in nuclear reactor plant safety analysis reports that 1% of the fuel pins are defective[3] and will leak fission products after reactor operation. Thus it is assumed that some failed fuel will always be present in the cask and the probability of this event was set at 1.0.

Fire Occurs with Accident (X4)

Based on accident environment data presented in Section 5.2, the occurrence rate of fire in truck accidents was estimated to be 0.016 fires per truck accident.[2] It was assumed that the spent fuel cask was exposed to the fire in all accidents involving fire.

Accident Generates Puncture Probe (X5)

The frequency of a puncture situation in truck accidents given a collision accident, is given in Reference 2. The rate of 2.5×10^{-2} puncture situations per truck accident was used for this event.

Puncture Probe Strike Cask Wall (X6)

Puncture rate data summarized in Section 5.6 gives the frequency of puncture given a puncture situation for equivalent steel thickness of the spent fuel cask.[2] All puncture probes generated in truck accidents are conservatively assumed to strike the cask wall. This event was therefore assigned a probability of 1.0.

Impact Force Produced in Accident (X7)

Data presented in Section 5.3 shows that 80% of truck accidents involve impact with another vehicle or a stationary object. Therefore, an expected frequency of 0.8 collision accidents per truck accident was used for this event.

Defect Permits Clad Failure from Normal Transport (X8)

No data are available for this event. Information on irradiated fuel shipment and storage of more than 200 spent fuel assemblies has shown that no significant leakage from the fuel to the cask coolant occurred and none of the fuel bundles were damaged in transit.[4] Occurrence of event X8 is considered to be very unlikely and it was therefore assigned a low probability of 1×10^{-4} per shipment.[a]

Pressure Relief Device Fails to Open (X9)

It is assumed that the relief valve in the pressure relief device would have to open to relieve any excess pressure generated in the cask. The rupture disk was conservatively assumed not to relieve the pressure if the

(a) An analysis was performed to determine the sensitivity of the total release probability to the probability value used for this event. It was found that increasing this event probability by a factor of 10 raised the total release probability by less than 0.01 percent. This is well within the overall accuracy of the analysis.

valve failed closed. Data available in Reference 5 showed a failure rate for relief valves of 1×10^{-5} failures per demand. This value was used for component X9.

Puncture Probe Strikes Cask and Fuel and Has Energy to Fail Fuel (X10)

The probability that a puncture probe will strike the fuel pins was calculated based on the ratio of the projected area of the fuel to the projected area of the spent fuel cask. The rate of occurrence was determined to be 0.63. To fail the fuel pins, a puncture probe would have to penetrate into the cask cavity. Data summarized in Section 5.6 gives the estimated probability of a puncture situation given a collision accident in terms of equivalent steel thickness of the container. The reference spent fuel cask has an equivalent steel thickness of about 1.95 inches of mild steel. From this it was determined that component X10, the frequency of puncture that could fail the fuel, would be 8.8×10^{-5} per puncture situation.

Side Impact Fails Fuel Pins (X11)

Mechanical failure thresholds summarized in Section 6 showed that a side impact at a cask velocity greater than 45 kph on a flat unyielding surface would cause failure of the fuel pins. Data summarized in Section 5, for the accident environment are based on truck-trailer systems and the impact frequency data are based on the transport system impact velocity. For the side impact case, it was assumed that the cask and truck impact velocities were the same. Data presented in Figure 5.3 showed that the probability of a collision accident resulting in an impact velocity of 45 kph or greater would be 6.4×10^{-3} per collision accident. The probability of a side-on impact is given in Reference 2 as 0.145. The probability of this event is then 9.3×10^{-4}.

End Impact Fails Fuel Pins (X12)

From Section 6, the fuel pin mechanical failure threshold velocity for end-impact was estimated to be about 67 kph. Full scale tests performed by Sandia[5] have shown that a truck trailer system will absorb a certain amount of energy in the system in a collision. Thus the velocity of the truck could be significantly higher than the cask velocity at impact. For the end impact case, it was conservatively assumed that the cask velocity and the transport

system velocity are the same. Data developed by Sandia for the accident environment were based on velocity change of the truck transport system and the impact frequency data were based on transport system impact velocity. The probability of an end-impact is 0.855.[2] Using Figure 5.3, and the probability of an end-impact, the occurrence frequency for this event was estimated to be 5.5×10^{-3} collisions per collision accident.

(X13) to (X49) Not Used

Immersion Forces Fail Lid and Fuel (X50)

Failure by immersion is not believed to be significant in accidents involving spent fuel casks.[2] Therefore, this event was not analyzed and was assigned a probability of zero.

Crush Forces Fail Lid and Fuel (X51)

Crush forces are not considered to be significant in the transport accident environment of spent fuel casks as described in Section 5.4.[2] This event was therefore given a probability of zero for this analysis.

Puncture Probe Strikes Cask Lid (X52)

The probability of a puncture probe striking the cask lid was determined by taking the ratio of surface area of the lid to the cask. This gives the percentage of puncture probes that would strike the lid given that the puncture probe strikes the cask. Thus the expected frequency for this event was estimated to be 2×10^{-2}.

Puncture Probe Strikes Cask Lid and Fuel Pins (X53)

The probability that a puncture probe will strike the cask lid and the fuel pins was calculated based on event X52 and the ratio of the projected area of the fuel to the projected area of the spent fuel cask which was determined to be 0.63. The rate of occurrence of this event was thus 1.3×10^{-2}.

Side Impact Fails Normal Lid and Fuel (X54)

Failure threshold data from Table 6.1 show that a velocity change of 65 kph in a collision onto a rigid planar surface is required to fail the cask lid (event X85) and a velocity change of 48 kph to fail the fuel (event X11).

The velocity change required to fail both the lid and the fuel would be the same as that to fail the lid, 65 kph. Potential failures from impact with a rigid column were also considered in the failure threshold calculations. Data on the frequency of encountering various impact targets along different types of highway[6] was examined to determine the potential importance of this event. It was found that even though the failure threshold is lower for impact with a rigid column, these failures are not important when compared with impact against a rigid plane because of the infrequent occurrence of large columnar targets along highways. The probability of this event was then taken to be the same as that for X85, 3.9×10^{-4}.

Side Impact Fails Lid and Fuel When Lid Defective (X55)

The probability of a side impact failing both the fuel and a defective lid was estimated to be twice as likely as the probability of failing a normal lid and fuel. Thus a value of 7.8×10^{-4} was used for this event.[a]

Side Impact Fails Lid and Fuel When Bolts Not Torqued Properly (X56)

The probability of a side impact failing both the fuel and a lid with bolts not torqued properly was estimated to be twice as likely as the probability of failing a normal lid and fuel. Thus a value of 7.8×10^{-4} was used for this event.[b]

(a) An analysis was performed to determine the sensitivity of the total release probability to the probability value used for this event. It was found that increasing this event probability by a factor of 10 raised the total release probability by less than 0.01%. This is well within the overall accuracy of the analysis.

(b) An analysis was performed to determine the sensitivity of the total release probability to the probability value used for this event. It was found that increasing this event probability by a factor of 10 raised the total release probability by less than 0.1%. This is well within the overall accuracy of the analysis.

Side Impact Fails Lid and Fuel When Bolts Damaged From Handling (X57)

The probability of a side impact failing both fuel and the lid with damaged bolts was estimated to be two times more probable than failing a normal lid and fuel (event X54). This event was assigned a value of 7.8×10^{-4}.(a)

Side Impact Fails Lid and Fuel When Bolts Missing (X58)

The probability of a side impact failing both fuel and the lid with bolts missing was estimated to be twice as likely as failing a normal lid and fuel (event 54). This event was then given a value of 7.8×10^{-4}.(a)

End Impact Fails Lid and Fuel When Lid Defective (X59)

The probability of an end impact failing the fuel and a defective lid was estimated to be two times more likely than the probability of failing a normal lid and fuel. Event X59 was therefore given a value of 1.7×10^{-4}.(a)

End Impact Fails Normal Lid and Fuel (X60)

Failure threshold data from Table 6.1 show a velocity change of 150 kph to fail the cask lid and 67 kph for the fuel. Thus a velocity change of 150 kph would be required to fail both the lid and fuel. The probability of this event was then taken to be 8.5×10^{-5}.

End Impact Lid and Fuel When Bolts Damaged from Handling (X61)

The probability of an end impact failing the fuel and a lid with damaged bolts was estimated to be two times more likely to occur than a normal lid. The probability of event X61 was then taken to be 1.7×10^{-4}.(a)

End Impact Fails Lid and Fuel When Closure Bolts Missing (X62)

An end impact causing failure of the fuel and lid with bolts missing was estimated to occur twice as frequently as a normal lid. The probability of this event was then estimated to be 1.7×10^{-4}.(a)

(a) An analysis was performed to determine the sensitivity of the total release probability to the probability value used for this event. It was found that increasing this event probability by a factor of 10 raised the total release probability by less than 0.1%. This is well within the overall accuracy of the analysis.

End Impact Fails Lid and Fuel When Bolts Not Torqued Properly (X63)

An end impact causing failure of the fuel and lid with bolts not properly torqued was assumed to occur twice as frequently as a normal lid. The probability of the event was then estimated to be 1.7×10^{-4}.(a)

Puncture Probe Fails Lid with Closure Error (X64)

The probability of a puncture probe failing the lid with a closure error was estimated to be two times more likely than the probability of failing a normal lid (event X83). The probability of a defective lid was estimated to be 3.0×10^{3} (see event X65). Thus a value of 6.0×10^{11} was used for event X64.(a)

Side Impact Fails Defective Lid (X65)

The probability of a side impact failing a defective lid was estimated to be two times more probable than the likelihood of failing a normal lid (event X85). Quality control in manufacturing operations is estimated to have a probability of 3×10^{3} that a defective component will not be detected. It is assumed that this value is representative of the probability that the cask lid contains a defect which could affect the impact strength. Thus a value of 2.3×10^{6} was used for this event.(a)

Loss of Coolant from Cask Lid Fails Fuel (X66)

If a loss of cavity coolant occurs and no action is taken to restore the coolant, fuel cladding failures will occur from self-heating of the fuel elements. This is shown in the thermal analysis summarized in Section 6.2. If a coolant loss occurs, it is shown in Table 6.4 that it would take about two hours until fuel failure starts to occur. If coolant was restored during that time, no fuel would fail and only the cavity coolant activity or fuel which was damaged initially in the accident would be released. Since no data are available to determine the probability of restoring the cavity coolant, the probability of fuel pin failure was conservatively set at 1.0 given that a loss of coolant occurs.

(a) An analysis was performed to determine the sensitivity of the total release probability value used for this event. It was found that increasing this event probability by a factor of 10 raised the total release probability by less than 0.1%. This is well within the overall accuracy of the analysis.

End Impact Force Fails Defective Cask Lid (X67)

The probability of an impact force failing a defective lid was estimated to be two times more probable than the impact force to fail a standard cask lid. The probability of a defective lid which could affect the impact strength is assumed to be 3.0×10^{-3} (see event X65). Thus the probability that an impact force would fail a defective cask lid was estimated to be 5.1×10^{-7} per collision accident based on the value used for X84.[a]

End Impact Fails Lid with Closure Error (X68)

A probability of 1.7×10^{4} was used for an end impact failing a lid with closure error (see event X67). The probability of a closure error is estimated to be 1.5×10^{3} (see event X89). Therefore the probability of this event was estimated to be 2.6×10^{7}.[a]

Puncture Probe Causes LOC from Lid and Fuel Does Not Fail (X69)

A puncture probe causing a loss of coolant was determined in event X83 to have a probability of 1.0×10^{8}. The thermal analysis summarized in Section 6.2 shows that when cavity coolant is lost it takes approximately two hours before fuel pin failure starts to occur. If coolant is restored before two hours has elapsed, then fuel failure would be prevented and only coolant activity would be released. No data are available to estimate the probability of restoring the coolant, so a conservative value of 0.1 was assumed for this occurrence. Thus event X69 was assigned a value of 1×10^{9}.

Side Impact Causes LOC from Lid and Fuel Does Not Fail (X70)

A side impact causing a loss of coolant determined for event X85 to have a probability of 3.9×10^{4}. A probability of 0.1 was used for the estimated frequency of restoring the coolant (see event X69). This event was then assigned a value of 4.0×10^{5}.

(a) An analysis was performed to determine the sensitivity of the total release probability to the probability value used for this event. It was found that increasing this event probability by a factor of 10 raised the total release probability by less than 0.01%. This is well within the overall accuracy of the analysis.

End Impact Causes LOC from Lid and Fuel Does Not Fail (X71)

The probability of an end impact causing a loss of coolant taken from event X84 is 8.5×10^{-5}. A probability of 0.1 was used for the probability of restoring the coolant (see event X69). This event was given a value of 8.5×10^{-6}.

Fuel Does Not Fail When Improperly Torqued Bolts Cause LOC from Lid (X72)

The probability of fuel failure when improperly torqued bolts cause loss of coolant from the lid is 3×10^{-3} (see event X78). The probability that the fuel does not fail is one minus the failure probability. This event was thus assigned a value of 1.0.

Improperly Torqued Bolts Cause LOC from Lid (X73)

Data for event X89 give the frequency of occurrence of improperly torqued bolts, but do not indicate that leakage occurred. It was conservatively assumed that 1% of those failures would result in significant leakage. Thus the rate for event X73 was set at 1.0×10^{2} per cask shipment.(a)

Damaged Bolts Cause LOC from Lid (X74)

Failure of closure bolts in handling does not indicate that release of coolant would occur. It was conservatively assumed that 1% of the failures would result in a significant release. Thus event X74 was given a value of 1.0×10^{2}.(a)

Fuel Does Not Fail when Damaged Bolts Cause LOC from Lid (X75)

A probability of 1.0 was used for this event (see event X72).

(a) An analysis was performed to determine the sensitivity of the total release probability to the probability value used for this event. It was found that increasing this event probability by a factor of 10 raised the total release probability by less than 0.1%. This is well within the overall accuracy of the analysis.

Missing Closure Bolts Cause LOC from Lid (X76)

The fact that some closure bolts were missing in the survey does not indicate that leakage would occur. It was conservatively assumed that 1% of the failures would result in leakage. This event was therefore given a value of 1.0×10^{-2}.(a)

Fuel Does Not Fail When Missing Closure Bolts Cause LOC from Lid (X77)

A probability of 1.0 was used for this event (see event X72).

Fuel Fails When Improperly Torqued Bolts Cause LOC from Lid (X78)

Calculations in Appendix G on thermal analysis show that approximately two hours after a loss of coolant, fuel clad failure will occur due to creep rupture. For fuel failure to occur, the truck operator must fail to detect that coolant leaks out of the cask. The driver is required to examine the shipment at least once every four hours during transit. Human failure rate data from Reference 5 show that general errors of human omission have an estimated rate of 10^{-2}. It is conservatively assumed for this event that after the coolant is lost, it is not restored. A value of 3.0×10^{-3} failures per cask shipment was used for this event.

Fuel Fails When Damaged Bolts Cause LOC from Lid (X79)

A probability of 3.0×10^{-3} per shipment was used for this event, (see event X78).

Fuel Fails When Missing Bolts Cause LOC from Lid (X80)

A probability of 3.0×10^{-3} per shipment was used for this event, (see event X78).

Side Impact Fails Lid with Closure Error (X81)

The probability of a side impact failing a lid with a closure error is estimated to be two times more probable than the likelihood of failing a

(a) An analysis was performed to determine the sensitivity of the total release probability to the probability value used for this event. It was found that increasing this event probability by a factor of 10 raised the total release probability by less than 0.1%. This is well within the overall accuracy of the analysis.

normal lid (event X85). The probability of a closure error is assumed to be 1.5×10^{-3} (see event X89). Thus a value of 1.2×10^{-6} was used for event X81.[a]

Cask Lid Contains Defect (X82)

Leak and rupture assessments for passive hardware in Reference 5 show that the probability of failure for a flange or large pipe is on the order of 10^{-8} per hour of operation. Assuming that average trip takes one day, the probability of a cask lid defect large enough to allow a release (Event X82) was given a value of 5×10^{-7} per shipment.

Puncture Probe Fails Normal Cask Lid (X83)

Based on data presented in Reference 2 summarized in Table 5.2, the estimated frequency of puncture to fail the cask lid, assuming an equivalent steel thickness of 2.5 inches, was estimated to be about 1.0×10^{-8} per puncture situation.

End Impact Fails Normal Cask Lid (X84)

From Section 6.1, the velocity change for the cask lid in the end impact case resulting in a large breach of the lid was estimated to be about 150 kph (see Table 6.1). The probability that a cask will be accelerated in the direction of the axis in an accident is 0.855[2] which is taken to be the probability of an end impact. Based on a 36,000 kg (80,000 lb) tractor trailer cask system, the probability that a cask lid will experience impact forces exceeding 150 kph velocity change was estimated to be less than 1.0×10^{-4} per collision accident. Therefore, this event was estimated to have a frequency of 8.5×10^{-5} per collision accident for a large breach of the cask lid.

(a) An analysis was performed to determine the sensitivity of the total release probability to the probability value used for this event. It was found that increasing this event probability by a factor of 10 raised the total release probability by less than 0.01%. This is well within the overall accuracy of the analysis.

Side Impact Fails Normal Cask Lid (X85)

Failure threshold data summarized in Table 6.1 show that a velocity change of 65 kph is required to cause a failure of the cask in a side impact onto a flat surface. It is assumed that the cask lid would fail at that impact velocity. The probability that the cask will be accelerated perpendicular to its axis is 0.145.[2] This is taken as the probability of a side-on impact. The probability of a velocity change of 65 kph or greater in a collision accident as given in Figure 5.3 is 2.7×10^{-3}. The probability of this event is then 3.9×10^{-4} per collision accident.

Puncture Probe Fails Defective Lid (X86)

The probability of a puncture probe failing a defective lid was estimated to be two times more likely than the probability of failing a normal lid (event X83). The probability of a defective lid was estimated to be 3.0×10^{-3} (see event X65). Thus a value of 6×10^{-11} per puncture situation was used for event X86.

Crushing Force Causes LOC from Lid (X87)

Crush forces are not considered to be significant in the transport accident environment as discussed in Section 5.4. This event was given a probability of zero for this analysis.

Puncture Probe Fails Normal Lid and Fuel (X88)

The probability of a probe failing the cask lid (event X83) was estimated to be about 10^{-8} per puncture situation and for the fuel about 10^{-4} per puncture situation. The probability of this event was therefore estimated to range from 10^{-8} to 10^{-12}. If the failures are totally dependent, the combined failure rate would be 10^{-8}. It is assumed for this event that the probability of a puncture probe causing failure of both lid and fuel was 1.0×10^{-9}.

Closure Bolts Not Properly Torqued (X89)

Data obtained from the survey of spent fuel shipments indicated that a frequency of 1.5×10^{-3} per cask shipment occurred for this event. The occurrence rate assumed for element X89 was then 1.5×10^{-3} per cask shipment.

Closure Bolts Damaged from Handling (X90)

No incidence of closure bolt damage was included in the survey. Based on a 50% confidence level for the sample size involved, this packaging error rate was estimated to be 9.7×10^{-4} per cask shipment. Thus event X90 was assumed to have a rate of 9.7×10^{-4} per cask shipment.

Closure Bolts Missing (X91)

Data from the survey indicated a frequency for missing bolts of 2.8×10^{-4} per cask shipment occurred. Based on a 50% confidence level, the value of this event was estimated to be 2.4×10^{-3} per cask shipment.

End Impact Fails Normal Lid Resulting in LOC (X92)

From Section 6.1, the velocity change for the cask lid in the end impact case resulting in loss of coolant was estimated to be about 100 kph. The probability a cask will be accelerated in the direction of the axis in an accident is 0.855.[2] This is taken to be the probability of an end impact. From Figure 5.3, the probability that a cask lid will experience impact forces of 100 kph or greater was estimated to be 2.0×10^{-4} per collision accident. Therefore, this event was estimated to have a frequency of 1.7×10^{-4} per collision accident.

(X93) to (X99) Not Used

Immersion Forces Fail Seal and Fuel (X100)

A probability of zero was used for this event (see event X50).

Crushing Force Fails Seal and Fuel (X101)

A probability of zero was used for this event (see event X51).

Puncture Probe Fails Seal and Fuel (X102)

The probability of a puncture probe failing both the seal and fuel was not believed to be significant. Therefore, the event was not analyzed and was assigned a probability of zero.

Side Impact Fails Normal Seal and Fuel (X103)

A velocity change of 95 kph is required to fail the seal in a side impact and 48 kph to fail the fuel. The velocity change required to fail

both the seal and fuel would be 65 kph. From event X132, the probability of failure for a 65 kph velocity change is 3.9×10^{-4} per collision accident. This value was used for event X103.

End Impact Fails Normal Seal and Fuel (X104)

A velocity change of 78 kph is required to fail the seal in an end impact and 63 kph to fail the fuel. Thus a velocity change of 78 kph would be required to fail both seal and fuel. The probability for this event was then assumed to be 8.5×10^{-4} based on data in Figure 5.3.

Side Impact Fails Defective Seal and Fuel (X105)

A side impact failure of both the fuel and a defective seal was estimated to be twice the probability of failing a normal seal (event X103). A value of 7.8×10^{-4} per collision accident was used for this event.(a)

Side Impact Fails Improperly Installed Seal and Fuel (X106)

This event was assigned a probability of 7.8×10^{-4} (see event X105).(a)

End Impact Fails Defective Seal and Fuel (X107)

An end impact which failed both the fuel and a defective seal was estimated to be twice as probable as a normal seal (event X103). A value of 1.7×10^{-3} failures per collision accident was used for this event.(a)

End Impact Fails Improperly Installed Seal and Fuel (X108)

This event was given a probability of 1.7×10^{-5}(see event X107).(a)

Fire Causes LOC from Seal and Fuel Does Not Fail (X109)

A fire causing a failure of the seal with loss of coolant and fuel failure was determined to have a probability of 4.2×10^{-2} in event X115.

(a) An analysis was performed to determine the sensitivity of the total release probability to the probability value used for this event. It was found that increasing this event probability by a factor of 10 raised the total release probability by less than 0.1% This is well within the overall accuracy of the analysis.

A value of 0.1 is estimated for the probability of restoring coolant following an accident (see event X69). This event was therefore assigned a probability of 4.2×10^{-3}.

Side Impact Fails Defective Seal (X110)

It is assumed that a defective seal would fail from side impact twice as frequently as a normal seal (event X132). The probability that a closure seal will have a defect that affects the impact failure threshold is taken to be the same as the probability of installing a defective seal. A value of 3.0×10^{-3} is used (see event X127). Thus a value of 2.3×10^{-6} failures per collision accident was used for event X110.(a)

Side Impact Fails Seal with Closure Error (X111)

It is assumed that a seal with a closure error would fail from impact twice as frequently as a normal seal. The probability that the seal will have a closure error that affects the impact failure threshold is taken to be the same as the probability of an improperly installed seal (event X118). That value is 9.7×10^{-4}. The probability of this event was then estimated to be 7.6×10^{-7}.(a)

End Impact Fails Seal with Closure Error (X112)

The probability of a seal closure error failing from impact was assigned a probability of 3.0×10^{-3} (see event X113). The probability of a closure error affecting the seal failure threshold was taken to be 9.7×10^{-4} (see event X111). Thus the probability of event X112 was estimated to be 3.3×10^{-7}.(a)

End Impact Fails Defective Seal (X113)

It is assumed that a defective seal would fail from end impact twice as frequently as a normal seal, giving a probability of 3.4×10^{-4} (see event

---

(a) An analysis was performed to determine the sensitivity of the total release probability to the probability value used for this event. It was found that increasing this event probability by a factor of 10 raised the total release probability by less than 0.01%. This is well within the overall accuracy of the analysis.

X131). The probability of a defective seal that affects the impact failure threshold is taken to be 3.0×10^{-3} (see event X110). Therefore, a value of 1.0×10^{-6} failures per collision accident was then used for this event.[a]

End Impact Causes LOC from Seal and Fuel Does Not Fail (X114)

An end impact which causes a loss of coolant was determined to have a probability of 8.5×10^{-4} in event X131. A value of 0.1 was used for the probability of restoring cavity coolant (see event X69). This event was therefore given a probability of 8.5×10^{-5}.

Fire Duration and Temperature Sufficient to Fail Closure Seal (X115)

For purposes of this analysis, it is conservatively assumed that the seal will fail if the temperature exceeds 320°C for longer than one hour as summarized in Section 6.2. As shown in Table 6.3, the fire must be greater than 30 minutes in length to exceed 320°C at the inner wall. This is shown in the thermal analysis in Appendix G. In Figure 5.1, the probability that a truck fire duration will exceed 30 minutes is given as 4.2×10^{-2}. This value was used as the probability that a truck fire will fail the closure seal.

Side Impact Causes LOC from Seal and Fuel Does Not Fail (X116)

A side impact causing a loss of coolant was determined in event X132 to have a probability of 3.9×10^{-4} per collision accident. A value of 0.1 was used for the estimated frequency of restoring the coolant (see event X69). Therefore, a probability of 3.9×10^{-5} was assigned to this event.

Loss of Coolant from Seal Sufficient to Cause Fuel Failure (X117)

A probability of 1.0 was used for this event (see event X66).

(a) An analysis was performed to determine the sensitivity of the total release probability to the probability value used for this event. It was found that increasing this event probability by a factor of 10 raised the total release probability by less than 0.01%. This is well within the overall accuracy of the analysis.

Seal Not Installed Properly (X118)

The survey of packaging errors showed no occurrences of incorrectly installed closure seals. A frequency rate of 9.7×10^{-4} per cask at a 50% confidence level was used for this event.

Improperly Installed Seal Causes LOC (X119)

Event X118 gives the failure rate for an improperly installed seal based on data from the shipping survey summarized in Section 7. The survey results did not indicate that loss of coolant occurred due to handling errors. It was conservatively assumed that 1% of the improperly installed closure seals would result in significant leakage. The probability for this event was then set at 1.0×10^{-2} per cask shipment.(a)

Fuel Does Not Fail When Improperly Installed Seal Causes LOC (X120)

The probability of fuel failure when an improperly installed seal causes loss of cavity coolant is 3.0×10^{-3} (see event X121). The probability that fuel does not fail is one minus the probability of failure. Therefore, this event was given a conservative value of 1.0.

Fuel Fails When Improperly Installed Seal Causes LOC (X121)

A probability of 3.0×10^{-3} was used for this event (see event X78).

Crushing Force Causes LOC from Seal (X122)

A probability of zero was used for this event (see event X87).

Seal Damaged During Transit (X123)

The packaging survey showed no occurrence of closure seals being damaged in transit of truck casks. An occurrence frequency of 9.7×10^{-4} per cask at a 50% confidence level was used for this event.

(a) An analysis was performed to determine the sensitivity of the total release probability to the probability value used for this event. It was found that increasing this event probability by a factor of 10 raised the total release probability by less than 0.01%. This is well within the overall accuracy of the analysis.

Seal Damaged in Transit Causes LOC (X124)

This event was assigned a value of 1.0×10^{-2} per cask shipment (see event X119).

Fuel Does Not Fail When Damaged Seal Causes LOC (X125)

This event was given a value of 1.0 (see event X120).

Fuel Fails When Damaged Seal Causes LOC (X126)

This event assigned a probability of 3.0×10^{-3} failures per cask shipment (see event X78).

Defective Seal Installed (X127)

The probability of installing a defective seal was estimated to be the same as the human error failure rate for items contained in a checklist given in Reference 5. The error rate for this event was estimated to be 3×10^{-3} per shipment.

Defective Seal Causes LOC (X128)

This event was assigned a probability of 1.0×10^{-2} per cask shipment (see event X119).

Fuel Fails When Defective Seal Causes LOC (X129)

This event was assigned a probability of 3.0×10^{-3} failures per cask shipment (see event X78).

Fuel Does Not Fail When Defective Seal Causes LOC (X130)

This event was given a value of 1.0 (see event X120).

End Impact Fails Normal Seal (X131)

An impact failure of the cask seal was estimated (see Section 6.1) to have a failure threshold velocity of 78 kph for an end impact. Based on data from Sandia for an 80,000 lb truck trailer cask transport system summarized in Figure 5.3, the probability that the cask will experience a velocity change of 78 kph or greater was estimated to be 1.0×10^{-3} per collision accident. The probability that the cask will be impacted along its axis is 0.855.[2] The total probability for this event is then 8.5×10^{-4} per collision accident.

Side Impact Fails Normal Seal (X132)

Failure thresholds summarized in Section 6.1 show that a velocity change of 65 kph would be required to cause failure of the cask seal in a side impact onto a flat surface. The probability that the cask will be accelerated perpendicular to its axis in a side-on impact is 0.145.[2] The probability of a velocity change of 65 kph or greater in a collision accident is given in Figure 5.3 as 2.7×10^{-3}. The probability of this event is then estimated to be 3.9×10^{-4} per collision accident.

(X133) to (X149) Not Used

Immersion Forces Fail Wall and Fuel (X150)

A probability of zero was used for this event (see event X50).

Crush Forces Fail Wall and Fuel (X151)

A probability of zero was used for this event (see event X51).

Puncture Probe Fails Wall (X152)

Data on puncture of large packages gives rates for puncture situations per truck accident on the basis of equivalent steel thickness of the package. The equivalent steel thickness of the reference cask was determined to be about 1.95 inches of mild steel. Reference 2 shows that the frequency of puncture that could fail the cask cavity wall would be 1.4×10^{-4} failures per puncture situation.

Side Impact Fails Normal Wall (X153)

Information summarized in Section 6.1 shows that a velocity change of 65 kph is required to fail the cask in a side-on impact. The probability that the cask will be impacted perpendicular to its axis is given as 0.145. The probability of a velocity change of 65 kph or greater in a collision accident is given in Figure 5.3 as 2.7×10^{-3}. The total probability estimated for this event was then 3.9×10^{-4} per collision accident.

Side Impact Fails Fuel and Defective Cask Wall (X154)

A side impact failure of both the fuel and a defective cask wall was estimated to be twice as probable as a normal wall (event X153). A value of 7.8×10^{-4} per collision accident was used for the event.(a)

End Impact Fails Normal Wall (X155)

Information presented in Section 6.1 shows that a velocity change of 150 kph is required to fail the cask sufficiently for a large breach to occur. The probability that the cask experiences an end-on impact is 0.855 (see event X84). The probability of a velocity change of 150 kph or greater in a collision accident was estimated from Figure 5.3 to be 1.0×10^{-4}. Therefore, the probability of this event was estimated to be 8.5×10^{-5} for a large breach of the cask wall.

End Impact Fails Fuel and Defective Cask (X156)

An end impact which fails both the fuel and a defective cask was estimated to be two times as probable as a failure of a normal wall. A value of 1.7×10^{-4} for the large breach was used for this event.(a)

Side Impact Fails Normal Wall and Fuel (X157)

A velocity change of 65 kph is required to fail the wall and 45 kph to fail the fuel. The velocity change required to fail both the wall and fuel would be 65 kph. From event X153, the probability of failure for a 65 kph velocity change were shown to be 3.9×10^{-4}. This value was used for event X157.

End Impact Fails Normal Wall and Fuel (X158)

It is assumed for this study that a velocity change of 150 kph is required to cause a large breach of the cask which would result in a sub-

(a) An analysis was performed to determine the sensitivity of the total release probability to the probability value used for this event. It was found that increasing this event probability by a factor of 10 raised the total release probability by less than 0.1%. This is well within the overall accuracy of the analysis.

substantial opening of the cask cavity. The fuel is assumed to fail at 67 kph. A velocity change of 150 kph would thus be required to fail both the wall and fuel. The probability for this event was then assumed to be 8.5×10^{-5} for a large breach to occur (see event X155).

Puncture Probe Fails Defective Wall (X159)

A failure from puncture of a defective wall was estimated to be twice as probable as a normal wall. A value of 2.8×10^{-4} is used (two times greater than event X152). The probability of a defective wall which could affect the puncture strength is taken to be the same as a manufacturing defect (see event X171). Therefore, a value of 8.4×10^{-7} was used for this event.(a)

Puncture Probe Fails Wall Causing LOC and Fuel Does Not Fail (X160)

A puncture failure of the cask wall resulting in a loss of coolant was determined in event X152 to have a probability of 1.4×10^{-4}. From event X69, the probability of restoring the coolant following an accident was estimated to be 0.1. Therefore, a value of 1.4×10^{-5} was used for this event.(a)

Side Impact Causes LOC from Wall and Fuel Does Not Fail (X161)

A side impact which causes a loss of coolant was determined to have a probability of 3.9×10^{-4} from event X153. A probability of 0.1 was used for the estimated frequency of restoring the coolant (see event X69). This event was then given a value of 3.9×10^{-5}.(a)

End Impact Causes LOC from Wall and Fuel Does Not Fail (X162)

The probability of loss of coolant from the cask wall caused by an end impact was estimated to be 8.5×10^{-4} based on a velocity of 78 kph. A value of 0.1 was used for the probability of restoring the coolant (see event X69). This event was then assigned a probability of 8.5×10^{-5}.(a)

(a) An analysis was performed to determine the sensitivity of the total release probability to the probability value used for this event. It was found that increasing this event probability by a factor of 10 raised the total release probability by less than 0.01%. This is well within the overall accuracy of the analysis.

Side Impact Fails Defective Cask Wall (X163)

A side impact failure of a defective cask wall was estimated to be twice as probable as a normal wall. Thus, a value of 7.8×10^{-4} was used for this event (twice that of event X153).[a]

End Impact Fails Defective Cask Wall (X164)

An end impact failure of a defective cask wall was estimated to be twice as frequent as a normal wall. Thus, a value of 1.7×10^{-4} (twice that of event X155) was used for this event.[a]

Defective Weld Causes LOC During Normal Transport (X165)

No data are available for this event. A weld defective enough to cause leakage of cask coolant should be detected during inspections to meet quality requirements. It is remotely possible that such a weld could be missed before the cask would be put into service and fail during transport resulting in a loss of coolant. For that reason, a low probability of occurrence of 10^{-4} per shipment was used for this event.[a]

Loss of Coolant from Cask Wall Causes Fuel Failure (X166)

A probability of 1.0 was assigned to this event (see event X66).

Fuel Does Not Fail When Defective Weld Causes LOC (X167)

This event was given a value of 1.0 (see event X120).

Fuel Fails When Defective Weld Causes LOC (X168)

This event was assigned a probability of 3.0×10^{-3} failures per cask shipment (see event X78).

(a) An analysis was performed to determine the sensitivity of the total release probability to the probability value used for this event. It was found that increasing this event probability by a factor of 10 raised the total release probability by less than 0.1%. This is well within the overall accuracy of the analysis.

Weld to Cask Bottom Defective During Transport (X169)

Data on welds for reactor containments for Reference 5 give a value of 1×10^{-7} serious leaks per hour. Assuming one day of operation per shipment, the welds would have a probability of failure of 2.4×10^{-6} per shipment.

End Impact Fails Normal Wall and LOC Occurs (X170)

Failure threshold data summarized in Section 6.1 show that a velocity change of 78 kph in an end impact would be required to fail the cask sufficiently for leakage to occur. The probability of end-on impact is 0.855 (see event X84). The probability of a velocity change of 78 kph or greater in a collision accident is given in Figure 5.3 as 1.0×10^{-3}. Therefore, the probability of this event was estimated to be 8.5×10^{-4} per collision accident for a small breach of the cask wall.

End Impact Fails Defective Cask Wall and LOC Occurs (X171)

An end impact failure of a defective cask was estimated to be twice as frequent as a normal wall. This gives a value of 1.7×10^{-3} (twice that of event X170). The probability that the cask wall will have a defect that weakens it structurally is taken to be the same as the probability of a manufacturing defect. A value of 3.0×10^{-3} is used (see event X65). Therefore, the probability of this event was estimated to be 5.1×10^{-6} per collision accident.[(a)]

(X172) to (X199) Not Used

Immersion Force Fails Device and Fuel (X200)

A probability of zero was used for this event (see event X50).

(a) An analysis was performed to determine the sensitivity of the total release probability to the probability value used for this event. It was found that increasing this event probability by a factor of 10 raised the total release probability by less than 0.01%. This is well within the overall accuracy of the analysis.

Crushing Force Fails Device and Fuel (X201)

A probability of zero was used for this event (see event X51).

Puncture Probe Strikes PR Device and Fuel (X202)

The probability that a puncture probe will strike the pressure relief device is 1.8×10^{-3} (event X220) and to strike the fuel, 0.63 (see event X10). The probability of this event was then estimated to be 1.1×10^{-3}.

Puncture Probe Fails PR Device and Fuel (X203)

The probability that a puncture probe fails the pressure relief device is 8.5×10^{-2} (event X219) and the fuel 1.4×10^{-4} (event X152). The probability of this event was then estimated to be 1.2×10^{-5} per puncture situation.

Side Impact Fails Normal PR Device and Fuel (X204)

A velocity change of 65 kph is required to fail the relief device and 45 kph to fail the fuel in the side impact case. The velocity change required to fail both the device and fuel would be 65 kph. From event X217, the probability of failure is 3.9×10^{-4} per collision accident for that velocity change.

End Impact Fails Normal PR Device and Fuel (X205)

A velocity change of 61 kph is required to fail the device and 67 kph to fail the fuel. Thus, a velocity of 67 kph would be required to fail both the device and fuel. The probability for this event was then assumed to be 2.1×10^{-3} per collision accident.

Side Impact Fails PR Device and Fuel when Device Defective (X206)

A side impact failure of the fuel and a defective pressure relief device was estimated to be twice as probable as a normal relief device. A value of 7.8×10^{-4} (twice that of event X204) was used for this event.[a]

(a) An analysis was performed to determine the sensitivity of the total release probability to the probability value used for this event. It was found that increasing this event probability by a factor of 10 raised the total release probability by less than 0.1%. This is well within the overall accuracy of the analysis.

Side Impact Fails PR Device and Fuel when Device Damaged During Handling (X207)

A side impact failure of both the fuel and a damaged pressure relief device was estimated to be twice the probability of failing a normal relief device. A value of 7.8×10^{-4} (twice that of event X204) was used for this event.(a)

Side Impact Fails PR Device and Fuel when Device Not Installed Properly (X208)

A side impact failure of the fuel and an improperly installed pressure relief device was estimated to be twice as frequent as a normal device. A value of 7.8×10^{-4} (twice that of event X204) was used for this event.(a)

End Impact Fails PR Device and Fuel when Device Defective (X209)

It is assumed that the fuel and a defective pressure relief device would fail from an end-on impact twice as frequently as a normal device. A value of 4.2×10^{-3} (twice that of event X205) was used for this event.(a)

End Impact Fails PR Device and Fuel when Device Not Installed Properly (X210)

It is assumed that the fuel and an improperly installed pressure relief device would fail from an end impact twice as frequently as a normal relief device. A value of 4.2×10^{-3} (twice that of event X205) was used for this event.(a)

End Impact Fails PR Device and Fuel when Device Damaged During Handling (X211)

It is assumed that the fuel and a damaged device would fail twice as frequently as a normal device. A value of 4.2×10^{-3} (twice that of event X205) was used for this event.(a)

Loss of Coolant from PR Device Sufficient to Fail Fuel (X212)

A probability of 1.0 was used for this event (see event X66).

(a) An analysis was performed to determine the sensitivity of the total release probability to the probability value used for this event. It was found that increasing this event probability by a factor of 10 raised the total release probability by less than 0.1%. This is well within the overall accuracy of the analysis.

Defective PR Device Installed (X213)

The survey showed that one cask was received with a defective pressure relief device which required replacement out of a total of about 3580 truck shipments. It was learned that no shipments covered in the survey involved overpressurization of the cask where in a pressure relief device would be actuated. It was then conservatively assumed that the defective pressure relief device would have resulted in a release of radioactivity; thus, the probability of this event was estimated to be 2.8×10^{-4} per shipment.

Pressure Relief Device Not Installed Properly (X214)

No cases of improper installation of a pressure relief device were found in the survey. Based on a 50% confidence limit, a value of 1.9×10^{-4} was estimated for this event.

Pressure Relief Device Damaged During Handling (X215)

No cases of damage to the pressure relief device during handling were found in the survey. Based on a 50% confidence limit, a value of 1.9×10^{-4} was estimated for this event.

Crushing Forces Cause LOC from PR Device (X216)

A probability of zero was used for this event (see event X87).

Side Impact Fails Normal PR Device (X217)

Threshold side-impact velocity changes, to fail the pressure relief device were assumed to be the same as that required to fail the cask seal, event X132. Based on a velocity change of 65 kph and a side impact probability of 0.145, the probability of this event was set at 3.9×10^{-4} per truck collision accident.

End Impact Fails Normal PR Device (X218)

Failure thresholds for end impact, summarized in Section 6.1, show that a velocity change of 61 kph would be required to cause venting of the pressure relief device due to water hammer effect. Failure of the valve body would occur at some higher impact velocity change. It is assumed that once the relief device vented in the end impact case, it would not be reseated

because of the rupture disk feature. The probability of a velocity change of 61 kph or greater in a collision accident is given in Figure 5.3 as 3.1×10^{-3}. Including the probability of an end impact from event X84, the probability of this event was then estimated to be 2.6×10^{-3} per collision accident.

Puncture Probe Fails PR Device (X219)

The equivalent steel thickness of the pressure relief device was estimated to be about 1.25 cm. Based on data in Table 5.2 using the equivalent steel thickness, it was estimated that the frequency of puncture that would fail the pressure relief device would be approximately 8.5×10^{-2} per puncture situation.

Puncture Probe Strikes PR Device (X220)

Puncture data from Reference 2 summarized in Section 5.6 give the probability of a puncture situation for large packages, given a truck collision accident. The probability that a puncture probe strikes the pressure relief device given that a puncture probe strikes the cask is based on the projected area of the valve compared to the projected area of the cask. It was estimated that the probability of a puncture probe striking the pressure relief device would be 1.8×10^{-3}.

Fire Duration and Temperature Sufficient to Cause LOC from PR Device (X221)

The rupture disk was assumed to relieve pressure at 76 atmospheres (1115 psi). The thermal analysis, summarized in Section 6.2, showed that a 15-minute or greater duration fire at 1010°C would result in a pressure exceeding the device rupture pressure and a loss of cavity coolant. From Figure 5.2, the probability of a fire exceeding 15 minutes is about 0.25. The probability of this event was then taken to be 0.25.

End Impact Fails Improperly Installed PR Device (X222)

It is assumed that an improperly installed pressure relief device would fail from an end impact twice as frequently as a normal relief device. This gives a value of 5.2×10^{-3} (twice that of event X218). The probability of

having an improperly installed device is 1.9×10^{-4} (event X231). Therefore, the probability of this event was estimated to be 1.0×10^{-6} per collision accident.[a]

End Impact Fails Defective PR Device (X223)

It is assumed that a defective pressure relief device will fail from end impact twice as frequently as a normal relief device. A value of 5.2×10^{-3} (twice that of event X218) is used. The probability of a defective device is 2.8×10^{-4} (event X232). Then the probability of this event was taken to be 1.5×10^{-6}.[a]

Fuel Does Not Fail when Defective PR Device Causes LOC (X224)

The probability of fuel failure when a defective pressure relief device causes loss of cavity coolant is 3.0×10^{-3} (see event X226). The probability that the fuel does not fail is one minus the probability of failure. Therefore, this event was given a conservative value of 1.0.

Fuel Fails when Improperly Installed PR Device Causes LOC (X225)

A probability of 3.0×10^{-3} failures per cask shipment was used for this event (see event X78).

Fuel Fails when Defective Device Causes LOC (X226)

A probability of 3.0×10^{-3} failure per cask shipment was used for this event (see event X78).

Puncture Probe Causes LOC from PR Device and Fuel Does Not Fail (X227)

The probability that a puncture probe fails the pressure relief device is assumed to be 8.5×10^{-2} punctures per puncture situation (see event X219). The probability of restoring the coolant is assumed to be 0.1 (see event X69). Therefore, a value of 8.5×10^{-3} was used for this event.

(a) An analysis was performed to determine the sensitivity of the total release probability to the probability value used for this event. It was found that increasing this event probability by a factor of 10 raised the total release probability by less than 0.01%. This is well within the overall accuracy of the analysis.

Fire Causes LOC from PR Device and Fuel Does Not Fail (X228)

The probability that a fire accident causes a loss of coolant from the pressure relief valve is assumed to be 0.25 (see event X221). The probability of restoring the coolant is assumed to be 0.1 (see event X69). Therefore, the value used for this event was 2.5×10^{-2}.

Side Impact Causes LOC from PR Device and Fuel Does Not Fail (X229)

A side impact causing failure of the pressure relief device was determined in event X217 to have a probability of 3.9×10^{-4}. This would result in a loss of cavity coolant. A value of 0.1 was used for the estimated frequency of restoring the coolant (see event X69). Therefore, a probability of 3.9×10^{-5} was assigned to this event.

Side Impact Fails PR Device Damaged During Handling (X230)

It is assumed that a damaged pressure relief device would fail from a side impact twice as frequently as a normal relief device. This gives a value of 7.8×10^{-4} per collision accident (twice that of event X217). The probability that a device will be damaged sufficiently to affect its impact threshold is taken to be the same as the probability of damage during handling. A value of 1.9×10^{-4} is used (event 215). Therefore a value of 1.4×10^{-7} was used for this event.[a]

Side Impact Fails Improperly Installed Device (X231)

It is assumed that an improperly installed pressure relief device would fail from a side impact twice as frequently as a normal relief device. This gives a value of 7.8×10^{-4} collisions per collision accident (twice that of event X217). The probability of an improperly installed device will affect the impact failure threshold is 1.9×10^{-4} (event X214). Thus a probability of 1.4×10^{-7} per collision accident was used for this event.[a]

(a) An analysis was performed to determine the sensitivity of the total release probability to the probability value used for this event. It was found that increasing this event probability by a factor of 10 raised the total release probability by less than 0.01%. This is well within the overall accuracy of the analysis.

Side Impact Fails Defective PR Device (X232)

It is assumed that a defective pressure relief device would fail from a side impact twice as frequently as a normal relief device. This gives a value of 7.8×10^{-4} collisions per collision accident (twice that of event X217). The probability that a defective device will affect the impact failure threshold is 2.8×10^{-4} (event X213). Therefore, the probability of this event was estimated to be 2.2×10^{-7}.(a)

End Impact Causes LOC from PR Device and Fuel Does Not Fail (X233)

An end impact causing failure of the pressure relief device resulting in a loss of coolant was determined in event X218 to have a probability of 2.6×10^{-3}. A value of 0.1 was used for the estimated frequency of restoring the coolant (see event X69). Therefore, a probability of 2.6×10^{-4} was assigned to this event.(b)

Fuel Does Not Fail when Improperly Installed Device Causes LOC (X234)

A probability of 1.0 was used for this event (see event X224).

Improperly Installed PR Device Causes LOC (X235)

Event X214 gives the failure rate for an improperly installed pressure relief device based on data from the shipping survey summarized in Section 7. The survey results did not indicate that loss of coolant occurred due to any handling errors. It is conservatively assumed that 1% of the improperly installed relief devices would result in significant leakage. The rate for this event was then set at 1.0×10^{-2} per shipment.(b)

(a) An analysis was performed to determine the sensitivity of the total release probability to the probability value used for this event. It was found that increasing this event probability by a factor of 10 raised the total release probability by less than 0.01%. This is well within the overall accuracy of the analysis.

(b) An analysis was performed to determine the sensitivity of the total release probability to the probability value used for this event. It was found that increasing this event probability by a factor of 10 raised the total release probability by less than 0.1%. This is well within the overall accuracy of the analysis.

Defective PR Device Causes LOC (X236)

A probability of 1.0×10^{-2} was used for this event (see event X235).[a]

End Impact Fails PR Device Damaged During Handling (X237)

It is assumed that a damaged pressure relief device would fail from an end impact twice as frequently as a normal relief device. A value of 5.2×10^{-3} (twice that of event X218) is used. The probability of a damaged device affecting the impact failure threshold is 1.9×10^{-4} (event X230). Therefore, the probability of this event was estimated to be 1.0×10^{-6}.[b]

Damaged PR Device Causes LOC (X238)

A probability of 1.0×10^{-2} was used for this event (see event X235).[a]

Fuel Fails When Damaged Device Causes LOC (X239)

A probability of 3.0×10^{-3} failures per cask shipment was used for this event (see event X78).

Fuel Does Not Fail When Damaged Device Causes LOC (X240)

A probability of 1.0 was used for this event (see event X224).

(X241) to (X249) Not Used

Immersion Force Fails Drain Valve and Fuel (X250)

A probability of zero was used for this event (see event X50).

Crushing Force Fails Drain Valve and Fuel (X251)

A probability of zero was used for this event (see event X51).

(a) An analysis was performed to determine the sensitivity of the total release probability to the probability value used for this event. It was found that increasing this event probability by a factor of 10 raised the total release probability by less than 0.1%. This is well within the overall accuracy of the analysis.

(b) An analysis was performed to determine the sensitivity of the total release probability to the probability value used for this event. It was found that increasing this event probability by a factor of 10 raised the total release probability by less than 0.01%. This is well within the overall accuracy of the analysis.

Puncture Probe Strikes Drain Valve and Fuel (X252)

The probability that a puncture probe will strike the drain valve is 1.8×10^{-3} (event X277) and to strike the fuel 0.63 (event X10). The probability of this event was then estimated to be 1.1×10^{-3}.

Puncture Probe Fails Drain Valve and Fuel (X253)

The probability that a puncture probe fails the drain valve is 8.5×10^{-2} (event X283) and the fuel 1.4×10^{-4} (event X152). The probability of this event was then estimated to be 1.2×10^{-5} per puncture situation.

Side Impact Fails Normal Drain Valve and Fuel (X254)

A velocity change of 65 kph is required to fail the drain valve and 45 kph to fail the fuel in the side impact case. The velocity change required to fail both the drain valve and fuel would be 65 kph. From event X280, the probability of failure is 9.7×10^{-5} per collision accident for that velocity change.

Side Impact Fails Drain Valve and Fuel when Valve Defective (X255)

A side impact failure of the fuel and a defective drain valve was estimated to be twice as probable as a normal drain valve. A valve of 1.9×10^{-4} (twice that of event X254) was used for this event.(a)

Side Impact Fails Drain Valve and Fuel when Valve Damaged During Handling (X256)

A side impact failure of both the fuel and a damaged drain valve was estimated to be twice the probability of failing a normal drain valve. A value of 1.9×10^{-4} (twice that of event X254) was used for this event.(a)

Side Impact Fails Drain Valve and Fuel when Valve Not Installed Properly (X257)

A side impact failure of the fuel and an improperly installed drain valve was estimated to be twice as frequent as a normal valve. A valve of 1.9×10^{-4} (twice that of event X254) was used for this event.(a)

(a) An analysis was performed to determine the sensitivity of the total release probability to the probability value used for this event. It was found that increasing this event probability by a factor of 10 raised the total release probability by less than 0.1%. This is well within the overall accuracy of the analysis.

Crushing Force Causes LOC from Drain Valve (X258)

A probability of zero was used for this event (see event X87).

End Impact Fails Normal Drain Valve and Fuel (X259)

This event was given a probability of zero (see event X281).

Loss of Coolant from Drain Valve Sufficient to Fail Fuel (X260)

A probability of 1.0 was used for this event (see event X66).

Drain Valve Not Installed Properly (X261)

No cases of improper installation of drain valves were found in the survey. Based on a 50% confidence limit, a value of 1.9×10^{-4} was then estimated for this event.

Fuel Does Not Fail when Defective Drain Valve Causes LOC (X262)

The probability of fuel failure when a defective drain valve causes loss of cavity coolant is 3.0×10^{-3} (see event X264). The probability that fuel does not fail is one minus the probability of failure. Therefore, this event was given a conservative value of 1.0.

Fuel Fails when Improperly Installed Drain Valve Causes LOC (X263)

A probability of 3.0×10^{-3} failures per cask shipment was used for this event (see event X78).

Fuel Fails when Defective Drain Valve Causes LOC (X264)

A probability of 3.0×10^{-3} failures per cask shipment was used for this event (see event X78).

Puncture Probe Causes LOC from Drain Valve and Fuel Does Not Fail (X265)

The probability that a puncture probe fails the drain valve is assumed to be 8.5×10^{-2} per puncture situation (see event X283). The probability

---

(a) An analysis was performed to determine the sensitivity of the total release probability to the probability value used for this event. It was found that increasing this event probability by a factor of 10 raised the total release probability by less than 0.1%. This is well within the overall accuracy of the analysis.

of restoring the coolant is assumed to be 0.1 (see event X69). Therefore, a value of 8.5×10^{-3} was used for this event.

Fire Causes LOC from Drain Valve and Fuel Does Not Fail (X266)

The probability that a fire accident fails the drain valve is assumed to be 1.0×10^{-7} (see event X279). The probability of restoring the coolant is assumed to be 0.1 (see event X69). Therefore, the value used for this event was 1.0×10^{-8}.

Side Impact Causes LOC from Drain Valve and Fuel Does Not Fail (X267)

A side impact causing failure of the drain valve was determined in event X280 to have a probability of 9.7×10^{-5}. This would result in a loss of cavity coolant. A value of 0.1 was used for the estimated frequency of restoring the coolant (see event X69). Therefore, a probability of 9.7×10^{-6} was assigned to this event.

Side Impact Fails Drain Valve Damaged During Handling (X268)

It is assumed that a damaged drain valve would fail from a side impact twice as frequently as a normal drain valve. A value of 1.9×10^{-4} per collision accident (twice that of event X280) is used. The probability that a damaged drain valve will be weakened so that the impact failure threshold is reduced is taken to be the same as a damaged valve (event X275). A valve of 1.9×10^{-4} is used. Therefore, the probability of this event was estimated to be 3.2×10^{-8} per collision accident.[a]

Side Impact Fails Improperly Installed Drain Valve (X269)

It is assumed that an improperly installed drain valve would fail from a side impact twice as frequently as a normal drain valve. This value of 1.9×10^{-4} per collision accident (twice that of event X280) is used. The

(a) An analysis was performed to determine the sensitivity of the total release probability to the probability value used for this event. It was found that increasing this event probability by a factor of 10 raised the total release probability by less than 0.01%. This is well within the overall accuracy of the analysis.

probability that an improperly installed drain valve will weaken the impact failure threshold strength is taken to be 1.9×10^{-4} (event X261). Therefore, the probability of this event was taken to be 3.2×10^{-8}.[a]

Side Impact Fails Defective Drain Valve (X270)

It is assumed that a defective drain valve would fail from a side impact twice as frequently as a normal drain valve. Thus, a value of 1.9×10^{-4} per collision accident (twice that of event X280) is used. The probability that a defective valve will affect the impact failure threshold is estimated to be 5.5×10^{-4} (event X273). The probability of event X270 was then estimated to be 1.1×10^{-7} per collision accident.[a]

Fuel Does Not Fail when Improperly Installed Drain Valve Causes LOC (X271)

A probability of 1.0 was used for this event (see event X262).

Improperly Installed Drain Valve Causes LOC (X272)

Event X261 gives the failure rate for an improperly installed drain valve based on data from the shipping survey summarized in Section 7. The survey results did not indicate that loss of coolant occurred due to any handling errors. It is conservatively assumed that 1% of the improperly installed drain valves would result in significant leakage. The rate for this event was then set at 1.0×10^{-2} per shipment.[b]

Defective Drain Valve Installed (X273)

Results of the survey showed that two cask shipments out of 3,580 truck shipments had been installed with a defective drain valve. The probability of this event was then estimated to be 5.5×10^{-4} per shipment.

(a) An analysis was performed to determine the sensitivity of the total release probability to the probability value used for this event. It was found that increasing this event probability by a factor of 10 raised the total release probability by less than 0.01%. This is well within the overall accuracy of the analysis.

(b) An analysis was performed to determine the sensitivity of the total release probability to the probability value used for this event. It was found that increasing this event probability by a factor of 10 raised the total release probability by less than 0.1%. This is well within the overall accuracy of the analysis.

Drain Valve Leaks from Water Causing LOC (X274)

Information provided on this event in the survey showed that 10 drain valves required replacement due to wear in all of the truck shipments. This gives a frequency of occurrence of about 2.8×10^{-3} per cask shipment. combining this rate with the probability of a loss of coolant due to a packaging or handling error (see event X272) gives a probability for this event of 2.8×10^{-5}.(a)

Drain Valve Damaged During Handling (X275)

No cases of damage to the drain valve during handling were found in the survey. Based on a 50% confidence limit, a value of 1.9×10^{-4} was estimated for this event.

Drain Valve Not Closed Causing LOC (X276)

No incidence of casks received with drain valves not closed were reported in the survey. At a 50% confidence level based on the sample size involved, it would be expected that this packaging error would occur at a rate of 1.9×10^{-4} per cask shipment. Combining this rate with the probability of a loss of coolant occuring due to a packaging error (see event X272) gives a probability for this event of 1.9×10^{-6} per shipment.(b)

Puncture Probe Strikes Drain Valve (X277)

Puncture data summarized in Section 5.6 gives the probability of a puncture situation for large packages given a truck collision accident. The probability that a puncture probe strikes the drain valve given that the puncture probe strikes the cask is based on the projected area of the valve

---

(a) An analysis was performed to determine the sensitivity of the total release probability to the probability value used for this event. It was found that increasing this event probability by a factor of 10 raised the total release probability by less than 0.1%. This is well within the overall accuracy of the analysis.

(b) An analysis was performed to determine the sensitivity of the total release probability to the probability value used for this event. It was found that increasing this event probability by a factor of 10 raised the total release probability by less than 0.01%. This is well within the overall accuracy of the analysis.

compared to the projected area of the cask. It was estimated that the probability of the puncture probe striking the drain valve would be 1.8×10^{-3}.

Defective Drain Valve Causes LOC (X278)

A probability of 1.0×10^{2} was used for this event (see event X272).[a]

Fire Temperature and Duration Sufficient to Fail Drain Valve (X279)

The drain valves have teflon valve seats with a secondary metal seal downstream that prevents leakage. Teflon valve seats can be operated at temperatures up to 285°C. It is conservatively estimated for this event that the teflon valve seats fail if the temperature rises above 285°C. It is assumed that the valve temperature is about equal to the inner wall temperature determined in the thermal analysis. From Section 6.2, it can be seen that a fire must exceed about 30 minutes for the temperature at the valve to cause failure. The probability of a fire exceeding 30-minute length is about 4.2×10^{-2}. The drain valve has a secondary metal seal to prevent leakage and the probability of the secondary metal seal failing is taken to be about 2.4×10^{-6}.[7] Thus, the probability of this event was taken to be about 1.0×10^{-7}.

Side Impact Fails Normal Drain Valve (X280)

A side-on collision is required for the drain valve to experience impact forces. Threshold side impact velocity changes for drain valve were conservatively assumed to be the same as that required to fail the cask seal. It is also assumed that the impact must occur at the location of the drain valve in the probability of impacting the drain valve. Based on a velocity change of 65 kph and a side impact probability of 0.145 (see event X85), the probability of this event was then set at 9.7×10^{-5} per collision accident.

(a) An analysis was performed to determine the sensitivity of the total release probability to the probability value used for this event. It was found that increasing this event probability by a factor of 10 raised the total release probability by less than 0.1%. This is well within the overall accuracy of the analysis.

End Impact Fails Normal Drain Valve (X281)

The drain valves are imbedded in the cask bottom and are very well protected from end impact forces. It is assumed that only impacts which would cause a large breach of the cask cavity could fail the drain valve. Therefore, this event was not analyzed, and a probability of zero was used.

Damaged Drain Valve Causes LOC (X282)

A probability of 1.0×10^{-2} was used for this event (see event X272).[a]

Puncture Probe Fails Drain Valve (X283)

The equivalent steel thickness of the drain valve was estimated to be about 1.25 cm. Based on data in Table 5.2, it was determined that the frequency of puncture that could fail the drain valve would be approximately 8.5×10^{-2} per puncture situation.

Overpressure Fails Drain Valve (X284)

It was conservatively assumed that the drain valve would fail if the pressure exceeds the design pressure of the pressure relief device on the cask. The thermal analysis summarized in Section 6.2 showed that the system would reach 76 atmospheres with a fire of about 15 minutes. The probability of the fire exceeding 15 minutes was determined to be about 0.25. Therefore, the occurrence rate for event X284 was set at 2.5×10^{-1} per fire accident.

Fuel Does Not Fail when Drain Valve Leaks from Wear (X285)

A probability of 1.0 was used for this event (see event X262).

Fuel Does Not Fail when Drain Valve Is Not Closed (X286)

A probability of 1.0 was used for this event (see event X262).

(a) An analysis was performed to determine the sensitivity of the total release probability to the probability value used for this event. It was found that increasing this event probability by a factor of 10 raised the total release probability by less than 0.1%. This is well within the overall accuracy of the analysis.

Fuel Fails when Drain Valve Leaks from Wear Causing LOC (X287)

A probability of 3.0×10^{-3} failures per cask shipment was used for this event (see event X78).

Fuel Fails when Drain Valve Not Closed Causes LOC (X288)

A probability of 3.0×10^{-3} failures per cask shipment was used for this event (see event X78).

Fuel Fails when Damaged Drain Valve Causes LOC (X289)

A probability of 3.0×10^{-3} failures per cask shipment was used for this event (see event X78).

Fuel Does Not Fail when Damaged Drain Valve Causes LOC (X290)

A probability of 1.0 was used for this event (see event X262).

(X291) to (X299) Not Used

Immersion Force Fails Vent Valve and Fuel (X300)

A probability of zero was used for this event (see event X50).

Crushing Force Fails Vent Valve and Fuel (X301)

A probability of zero was used for this event (see event X51).

Puncture Probe Strikes Vent Valve and Fuel (X302)

The probability that a puncture probe will strike the vent valve is 1.8×10^{-3}, and to strike the fuel, 0.63. The probability of this event was then estimated to be 1.1×10^{-3}.

Puncture Probe Fails Vent Valve and Fuel (X303)

The probability that a puncture probe fails the vent valve is 8.5×10^{-2} (event X333) and the fuel 1.4×10^{-4} (event X152). The probability of this event was then estimated to be 1.2×10^{-5} per puncture situation.

Side Impact Fails Normal Vent Valve and Fuel (X304)

A velocity change of 65 kph is required to fail the vent valve and 45 kph to fail the fuel in the side impact case. The velocity change required to

fail both the vent valve and fuel would be 65 kph. From event X330, the probability of failure is 9.7×10^{-5} per collision accident for that velocity change.

Side Impact Fails Vent Valve and Fuel when Valve Defective (X305)

A side impact failure of the fuel and a defective vent valve was estimated to be twice as probable as a normal vent valve. A value of 1.9×10^{-4} (twice that of event X304) was used for this event.(a)

Side Impact Fails Vent Valve and Fuel when Valve Damaged During Handling (X306)

A side impact failure of both the fuel and a damaged vent valve was estimated to be twice the probability of failing a normal vent valve. A value of 1.9×10^{-4} (twice that of event X304) was used for this event.(a)

Side Impact Fails Vent Valve and Fuel when Valve Not Installed Properly (X307)

A side impact failure of the fuel and an improperly installed vent valve was estimated to be twice as frequent as a normal valve. A value of 1.9×10^{-4} (twice that of event X304) was used for this event.(b)

Crushing Force Causes LOC from Vent Valve (X308)

A probability of zero was used for this event (see event X87).

End Impact Fails Normal Vent Valve and Fuel (X309)

This event was given a probability of zero (see event X331).

Loss of Coolant from Vent Valve Sufficient to Fail Fuel (X310)

A probability of 1.0 was used for this event (see event X66).

(a) An analysis was performed to determine the sensitivity of the total release probability to the probability value used for this event. It was found that increasing this event probability by a factor of 10 raised the total release probability by less than 0.01%. This is well within the overall accuracy of the analysis.

(b) An analysis was performed to determine the sensitivity of the total release probability to the probability value used for this event. It was found that increasing this event probability by a factor of 10 raised the total release probability by less than 0.1%. This is well within the overall accuracy of the analysis.

Vent Valve Not Installed Properly (X311)

No cases of improper installation of vent valves were found in the survey. Based on a 50% confidence limit, a value of 1.9×10^{-4} was then estimated for this event.

Fuel Does Not Fail when Defective Vent Valve Causes LOC (X312)

The probability of fuel failure when a defective vent valve causes loss of cavity coolant is 3.0×10^{-3} (see event X314). The probability that fuel does not fail is one minus the probability of failure. Therefore, this event was given a conservative value of 1.0.

Fuel Fails when Improperly Installed Vent Valve Causes LOC (X313)

A probability of 3.0×10^{-3} failures per cask shipment was used for this event (see event X78).

Fuel Fails when Defective Vent Valve Causes LOC (X314)

A probability of 3.0×10^{-3} failure per cask shipment was used for this event (see event X78).

Puncture Probe Causes LOC from Vent Valve and Fuel Does Not Fail (X315)

The probability that a puncture probe fails the vent valve is assumed to be 8.5×10^{-2} per puncture situation (see event X333). The probability of restoring the coolant is assumed to be 0.1 (see event X69). Therefore, a value of 8.5×10^{-3} was used for this event.

Fire Causes LOC from Vent Valve and Fuel Does Not Fail (X316)

The probability that a fire accident fails the vent valve is assumed to be 1.0×10^{-7} (see event X329). The probability of restoring the coolant is assumed to be 0.1 (see event X69). Therefore, the value used for this event was 1.0×10^{-8}.

Side Impact Causes LOC from Vent Valve and Fuel Does Not Fail (X317)

A side impact causing failure of the vent valve was determined in event X330 to have a probability of 9.7×10^{-5}. This would result in a loss of

cavity coolant. A valve of 0.1 was used for the estimated frequency of restoring the coolant (see event X69). Therefore, a probability of 9.7×10^{-6} was assigned to this event.

Side Impact Fails Vent Valve Damaged During Handling (X318)

A probability of 3.2×10^{-8} per collision accident was used for this event (see event X268).

Side Impact Fails Improperly Installed Vent Valve (X319)

A probability of 3.2×10^{-8} per collision accident was used for this event (see event X269).

Side Impact Fails Defective Vent Valve (X320)

A probability of 1.1×10^{-7} per collision accident was used for this event (see event X270).

Fuel Does Not Fail when Improperly Installed Vent Valve Causes LOC (X321)

A probability of 1.0 was used for this event (see event X312).

Improperly Installed Vent Valve Causes LOC (X322)

Event X261 gives the failure rate for an improperly installed vent valve based on data from the shipping survey summarized in Section 7. The survey results did not indicate that loss of coolant occurred due to any handling errors. It is conservatively assumed that 1% of the improperly installed vent valves would result in significant leakage. The rate for this event was then set at 1.0×10^{-2} per shipment.(a)

Defective Vent Valve Installed (X323)

The survey showed that two defective vent valves were installed on casks during the time period covered by the survey. Based on the survey, the

(a) An analysis was performed to determine the sensitivity of the total release probability to the probability value used for this event. It was found that increasing this event probability by a factor of 10 raised the total release probability by less than 0.1%. This is well within the overall accuracy of the analysis.

probability that a vent will be defective when installed was estimated to be 5.6×10^{-4} per cask shipment.

Vent Valve Leaks from Wear Causing LOC (X324)

Information provided on this event in the survey showed that five vent valves required replacement due to wear in all of the truck shipments. This gives an occurrence rate of about 1.4×10^{-3} per cask shipment. A rate of 1.0×10^{-2} was used for the probability of a worn vent valve causing a loss of coolant (see event X322). The probability of this event was then estimated to be 1.4×10^{-5} per shipment.(a)

Vent Valve Damaged During Handling (X325)

No cases of damage to the vent valve during handling were found in the survey. Based on a 50% confidence limit, a value of 1.9×10^{-4} was estimated for this event.

Vent Valve Not Closed Causes LOC (X326)

The survey showed that 2 casks were received with the vent valve not closed. This gives a value of 5.5×10^{-4} for the probability of a vent valve being left open. It was learned that none of these occurrences resulted in any loss of coolant. A rate of 1.0×10^{2} was assumed for the probability of an open vent valve resulting in a loss of coolant (see event X322). Thus, the probability of this event was estimated to be 5.5×10^{-6} per shipment.(a)

Puncture Probe Strikes Vent Valve (X327)

Puncture data summarized in Section 5.6 gives the probability of puncture situation for large packages given a truck collision accident. The probability that a puncture probe strikes the vent valve given that the puncture probe strikes the cask is based on the projected area of the valve compared to the

(a) An analysis was performed to determine the sensitivity of the total release probability to the probability value used for this event. It was found that increasing this event probability by a factor of 10 raised the total release probability by less than 0.01%. This is well within the overall accuracy of the analysis.

projected area of the cask. It was estimated that the probability of a puncture probe striking the drain valve would be 1.8×10^{-3}.

Defective Vent Valve Causes LOC (X328)

A probability of 1.0×10^{-2} was used for this event (see event X332).[a]

Fire Temperature and Duration Sufficient to Fail Vent Valve (X329)

The vent valve has a teflon valve seat with a secondary metal seal downstream that prevents leakage. Teflon valve seats can be operated at temperatures up to 285°C. It is conservatively estimated for this event that the teflon valve seats fail if the temperature rises above 285°C. It is assumed that the valve temperature is about equal to the inner wall temperature determined in the thermal analysis summarized in Appendix G. From Section 6.2, it can be seen that a fire must exceed about 30 minutes for the temperature at the valve to cause failure. The probability of a fire exceeding 30-minute length is 4.2×10^{-2}. The probability of the secondary metal seal failing is taken to be about 2.4×10^{-6}.[5] Thus, the probability of this event was then taken to be about 1.0×10^{-7}.

Side Impact Fails Normal Vent Valve (X330)

Threshold side impact velocity changes for vent valves were conservatively assumed to be the same as that required to fail the cask seal. It is also assumed that the impact must occur at the location of the drain valve in the cask flange for failure to occur. A value of 0.25 is assumed for the probability of impacting the drain valve. Based on a velocity change of 65 kph and a side impact probability of 0.145 (see event X85), the probability of this event was then set at 9.7×10^{-5} per collision accident.

(a) An analysis was performed to determine the sensitivity of the total release probability to the probability value used for this event. It was found that increasing this event probability by a factor of 10 raised the total release probability by less than 0.1%. This is well within the overall accuracy of the analysis.

End Impact Fails Normal Vent Valve (X331)

The vent valve is imbedded in the cask bottom and is very well protected from end impact forces. It is assumed that only impacts which would cause a large breach of the cask cavity could fail the vent valve. Therefore, this event was not analyzed and a probability of zero was used.

Damaged Vent Valve Causes LOC (X332)

A probability of 1.0×10^{-2} was used for this event (see event X322).[a]

Puncture Probe Fails Vent Valve (X333)

The equivalent steel thickness of the vent valve was estimated to be about 1.25 cm. Based on data in Reference 2, it was determined that the frequency of puncture that would fail the vent valve would be approximately 8.5×10^{-2} per puncture situation.

Overpressure Fails Vent Valve (X334)

It was conservatively assumed that the vent valve would fail if the pressure exceeds the design pressure of the pressure relief device on the cask. The thermal analysis summarized in Section 6.2 showed that the system would reach 76 atmospheres with a fire of about 15 minutes. The probability of the fire exceeding 15 minutes was determined to be about 0.25. Therefore, the occurrence rate for event X334 was set at 2.5×10^{-1} per fire accident.

Fuel Does Not Fail when Vent Valve Leaks from Wear (X335)

A probability of 1.0 was used for this event (see event X312).

Fuel Does Not Fail when Vent Valve Is Not Closed (X336)

A probability of 1.0 was used for this event (see event X312).

(a) An analysis was performed to determine the sensitivity of the total release probability to the probability value used for this event. It was found that increasing this event probability by a factor of 10 raised the total release probability by less than 0.1%. This is well within the overall accuracy of the analysis.

Fuel Fails when Vent Valve Leaks from Wear Causing LOC (X337)

A probability of 3.0×10^{-3} failures per cask shipment was used for this event (see event X78).

Fuel Fails when Vent Valve Not Closed Causes LOC (X338)

A probability of 3.0×10^{-3} failures per cask shipment was used for this event (see event X78).

Fuel Fails when Vent Valve Not Closed Causes LOC (X339)

A probability of 3.0×10^{-3} failures per cask shipment was used for this event (see event X78).

Fuel Does Not Fail when Damaged Vent Valve Causes LOC (X340)

A probability of 1.0 was used for this event (see event X312).

9.2 RELEASE SEQUENCE PROBABILITIES

The Basic Event Probabilities in Section 9.1 provide the data necessary to calculate the frequency of any event sequence. As explained in Section 8.3, the computer code MFAULT[8] was used to evaluate the release sequences. Fault tree logic and event description, failure rates, and sequence length and probability cutoff values are input to MFAULT (see Figure 9.2). The code determines which sequences will actually result in releases, then eliminates those which contain more elements than the present cutoff level (10 event cut sets are the maximum allowed), and those not surviving the probability cutoff limit. Computer runs were made using different sequence lengths and probability cutoffs. It was determined that a maximum cut set size of 10 elements and a probability cutoff of 10^{-15} allowed all major cut sets to be identified. Redundant release sequences are eliminated automatically. Release sequences with a frequency of occurrence greater than 10^{-15} per shipment are listed in Table 9.1.

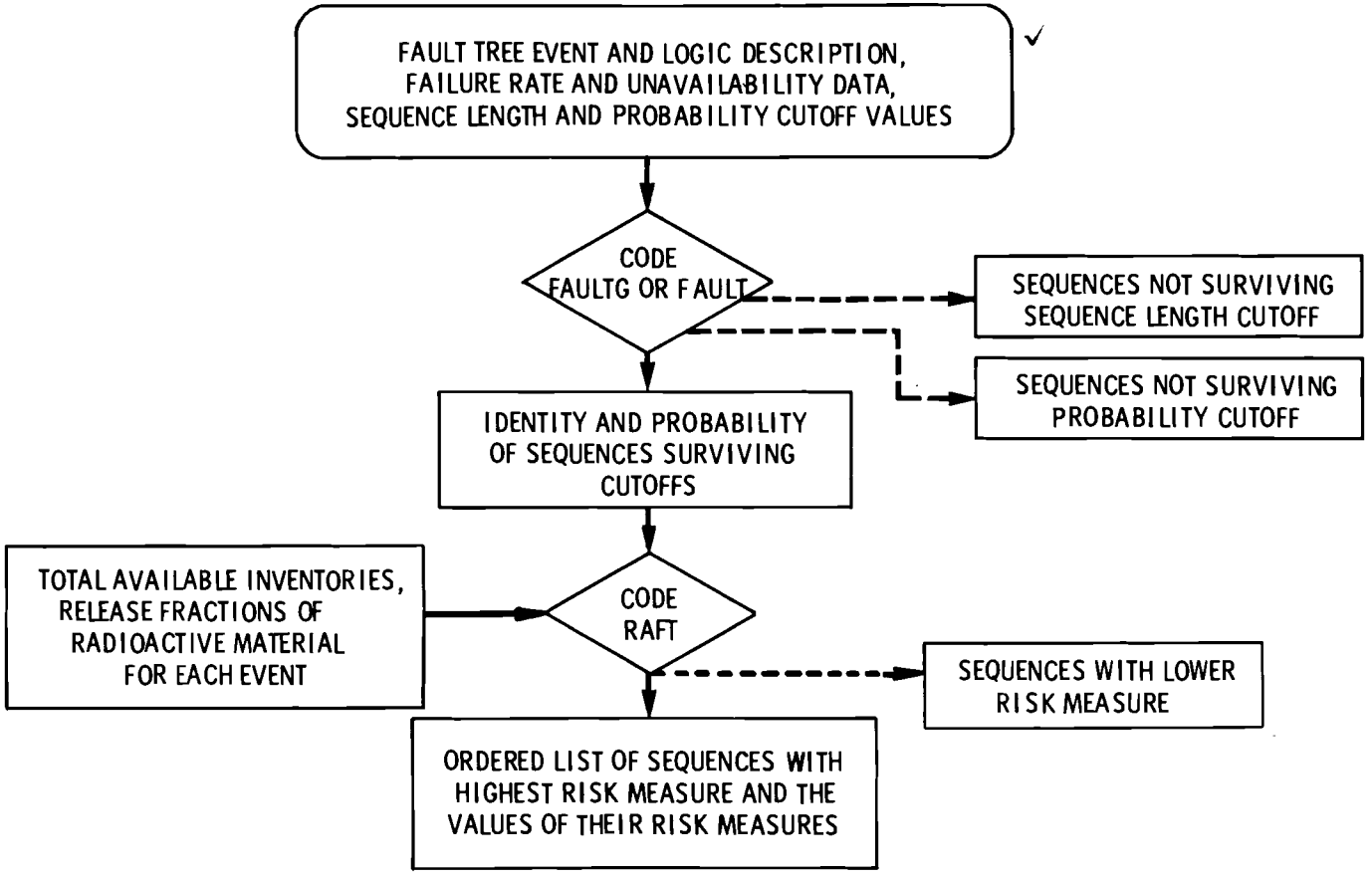

FIGURE 9.2. Screening Process Schematic (The risk sum of all discarded sequences is estimated for later addition to give the total risk in the entire fault tree.)

TABLE 9.1. Release Sequences and Probabilities for Spent Fuel Truck Shipments

Release Sequence Probability	Release Sequence Components*		
5.4450E-06	326	336	
1.6500E-08	326	338	
1.3860E-05	324	335	
4.2000E-08	324	337	
1.8810E-06	276	286	
5.7000E-09	276	288	
2.7720E-05	274	285	
8.4000E-08	274	287	
8.4000E-09	76	80	91
2.9100E-08	74	79	9[illegible]
4.5000E-08	73	78	89
2.7720E-06	76	77	9[illegible]
9.6030E-06	74	75	9[illegible]
1.4850E-05	72	73	8[illegible]
1.4960E-08	2	7	71
3.5200E-08	2	7	7[illegible]
1.4960E-07	2	7	6[illegible]
3.4320E-07	2	7	54
5.7000E-09	325	332	339
1.8810E-06	325	332	34[illegible]
5.5440E-06	312	323	328
1.6800E-08	314	323	328
5.7000E-09	311	313	322
1.8810E-06	311	321	322
8.5360E-09	2	7	317
1.7600E-13	2	4	316
2.3375E-07	2	5	315
8.5360E-08	2	7	304
5.7000E-09	275	282	289
1.8810E-06	275	282	29[illegible]
5.4450E-06	262	273	278
1.6500E-08	264	273	278
5.7000E-09	261	263	272
1.8810E-06	261	271	272
8.5360E-09	2	7	267
1.7600E-13	2	4	266
2.3375E-07	2	5	265
8.5360E-08	2	7	254
5.7000E-09	215	238	239
1.8810E-06	215	238	24[illegible]
2.7720E-06	213	224	236
8.4000E-09	213	226	236
5.7000E-09	214	225	235
1.8810E-06	214	234	235
2.2880E-07	2	7	233
3.4320E-08	2	7	229
5.2800E-07	2	4	228

*See Table 8.2 for listing of components making up these release sequences.

TABLE 9.1. (Cont'd)

Release Sequence Probability	Release Sequence Components			
2.3375E-07	2	5	227	
1.8480E-06	2	7	205	
3.4320E-07	2	7	204	
2.3760E-10	165	167	169	
7.2000E-13	165	168	169	
7.4800E-08	2	7	162	
3.4320E-08	2	7	161	
2.4200E-09	2	5	1[illegible]	
7.4800E-08	2	7	158	
3.4320E-07	2	7	157	
9.0000E-08	127	128	129	
2.9100E-08	123	124	126	
2.9100E-08	118	119	121	
9.6030E-06	123	124	125	
2.9700E-05	127	128	13[illegible]	
9.6030E-06	118	119	12[illegible]	
7.4800E-08	2	7	114	
3.4320E-08	2	7	113	
7.3920E-08	2	4	109	
1.4960E-07	2	7	104	
3.4320E-07	2	7	103	
4.4880E-10	2	7	66	67
2.2880E-10	2	7	66	68
1.4960E-07	2	7	66	92
2.0240E-09	2	7	65	66
1.0560E-09	2	7	6[illegible]	81
3.4320E-07	2	7	66	85
1.4960E-13	2	7	59	82
8.3776E-11	2	7	62	91
2.9022E-10	2	7	61	9[illegible]
2.7826E-10	2	7	11	63
3.4320E-13	2	7	55	82
1.9219E-10	2	7	58	91
6.6581E-10	2	7	57	9[illegible]
1.0296E-09	2	7	56	89
2.8160E-11	2	7	31[illegible]	318
2.8160E-11	2	7	31[illegible]	319
9.6800E-11	2	7	31[illegible]	32[illegible]
8.5360E-08	2	7	31[illegible]	33[illegible]
1.7600E-12	2	4	31[illegible]	329
3.6300E-13	2	5	30[illegible]2	303
3.1768E-11	2	7	306	325
3.1768E-11	2	7	307	311
9.3632E-11	2	7	305	323
2.8160E-11	2	7	26[illegible]	268
2.8160E-11	2	7	26[illegible]	269
9.6800E-11	2	7	260	27[illegible]
8.5360E-08	2	7	26[illegible]	28[illegible]
1.7600E-12	2	4	26[illegible]	279
3.6300E-13	2	5	252	253
3.1768E-11	2	7	256	275
3.1768E-11	2	7	257	261
9.1960E-11	2	7	255	273
2.2880E-06	2	7	212	218

TABLE 9.1. (Cont'd)

Release Sequence Probability	Release Sequence Components				
8.8[illegible]0E-10	2	7	212	222	
1.3200E-09	2	7	212	223	
8.8[illegible]0E-10	2	7	212	237	
3.4320E-07	2	7	212	217	
1.2320E-10	2	7	212	230	
1.2320E-10	2	7	212	231	
1.9360E-10	2	7	212	232	
4.4[illegible]0E-06	2	4	212	221	
3.6300E-13	2	5	202	203	
7.0224E-10	2	7	211	215	
7.0224E-10	2	7	21[illegible]	214	
1.0349E-09	2	7	209	213	
8.3600E-11	2	7	207	215	
8.3600E-11	2	7	208	214	
1.2320E-10	2	7	206	213	
7.4800E-07	2	7	166	170	
8.8[illegible]0E-10	2	7	166	171	
3.4320E-07	2	7	153	166	
3.8500E-10	2	5	6	160	
3.5934E-13	2	7	156	169	
1.6474E-12	2	7	154	169	
2.9040E-10	2	7	112	117	
8.8000E-10	2	7	113	117	
7.4800E-07	2	7	117	131	
2.0240E-09	2	7	11[illegible]	117	
6.6880E-10	2	7	111	117	
3.4320E-07	2	7	117	132	
7.3920E-07	2	4	115	117	
2.9022E-10	2	7	108	118	
8.9760E-10	2	7	107	127	
2.0592E-09	2	7	105	127	
6.6581E-10	2	7	106	118	
5.5000E-15	2	5	52	66	83
4.4880E-14	2	3	7	8	67
2.2880E-14	2	3	7	8	68
7.4800E-12	2	3	7	8	84
2.0240E-13	2	3	7	8	65
1.0560E-13	2	3	7	8	81
3.4320E-11	2	3	7	8	85
4.2075E-09	2	5	31[illegible]	327	333
2.8160E-15	2	3	7	8	318
2.8160E-15	2	3	7	8	319
9.6800E-15	2	3	7	8	320
8.5360E-12	2	3	7	8	330
1.3094E-15	2	4	7	11	329
7.7440E-15	2	4	7	12	329
4.2075E-09	2	5	26[illegible]	277	283
2.8160E-15	2	3	7	8	268
2.8160E-15	2	3	7	8	269
9.6800E-15	2	3	7	8	270
8.5360E-12	2	3	7	8	280
1.3094E-15	2	4	7	11	279
7.7440E-15	2	4	7	12	279

TABLE 9.1. (Cont'd)

Release Sequence Probability	Release Sequence Components					
4.2375E-09	2	5	212	219	220	
2.2880E-10	2	3	7	9	218	
8.8000E-14	2	3	7	8	222	
1.3200E-13	2	3	7	8	223	
8.8000E-14	2	3	7	8	237	
3.4320E-11	2	3	7	8	217	
1.2320E-14	2	3	7	8	230	
1.2320E-14	2	3	7	8	231	
1.9360E-14	2	3	7	8	232	
1.6474E-12	2	7	163	166	169	
3.8500E-09	2	5	5	152	166	
2.3100E-11	2	5	6	159	166	
7.4800E-12	2	3	7	8	155	
3.4320E-11	2	3	7	8	153	
2.9040E-14	2	3	7	8	112	
8.8000E-14	2	3	7	8	113	
7.4800E-11	2	3	7	8	131	
2.0240E-13	2	3	7	8	110	
6.6880E-14	2	3	7	8	111	
3.4320E-11	2	3	7	8	132	
7.3920E-11	2	3	7	8	115	
5.4996E-10	2	4	7	11	115	
3.2525E-09	2	4	7	12	115	
4.4000E-15	2	3	4	8	9	334
3.2736E-14	2	4	7	9	11	334
1.9360E-13	2	4	7	9	12	334
4.2375E-13	2	3	5	8	327	333
3.1304E-12	2	5	7	11	327	333
1.8513E-11	2	5	7	12	327	333
4.4000E-15	2	3	4	8	9	284
3.2736E-14	2	4	7	9	11	284
1.9360E-13	2	4	7	9	12	284
4.2375E-13	2	3	5	8	277	283
3.1304E-12	2	5	7	11	277	283
1.8513E-11	2	5	7	12	277	283
4.2375E-13	2	3	5	8	219	220
3.1304E-12	2	5	7	11	219	220
1.8513E-11	2	5	7	12	219	220
3.8500E-13	2	3	5	6	8	152
2.8644E-12	2	5	6	7	11	152
1.6940E-11	2	5	6	7	12	152
2.3100E-15	2	3	5	6	8	159
1.7186E-14	2	5	6	7	11	159
1.0164E-13	2	5	6	7	12	159

9.3 RELEASE FRACTIONS

The final step in the evaluation of release sequences is the determination of release fractions. For the purpose of this analysis, release fractions are defined as the fraction of the cask inventory that is dispersed into the atmosphere. The release sequences developed from the fault tree were divided into eight accident categories. These categories cover the spectrum of spent fuel transportation accidents which can result in a release of radioactive material. Release fractions were developed for each of the eight accident categories. The release fractions were developed from the results available in existing literature on releases from spent fuel. Published literature reported only experimental accident simulations and known chemical and physical responses of the spent fuel. No actual accidental releases during transport have occurred.[9,10] Accidents are unique events and cannot be experimentally duplicated, so engineering judgment was required to arrive at realistic release estimates.

9.3.1 Material Available for Airborne Release

Interpretations of experimental results which provide a basis for airborne release estimates are summarized below. The basic experimental data are discussed in Appendix B. The evaluation reported here considers releases due to four chemical and mechanical mechanisms as a function of transport cask and fuel cladding conditions.

Radioactive material is available for release from the truck cask under accident conditions postulated for this report in the form of vapors, liquids, and aerosols. The significant radionuclides in the spent fuel are reported in Appendix C. Vapors consist of noble fission gases and elements volatilized under fire conditions. Liquid releases include cavity coolant and volatiles and aerosols that condense. Aerosols are released as a result of vaporizing contaminated cavity coolant or the release of fines from the fuel pellets.

The first barrier to release of the radionuclides from the fuel is the fuel cladding. In order to be available for release from the truck cask, the activity must first escape the fuel rods to the cask cavity. Four mechanisms have been identified which may lead to significant release.

1. Gap Release is the energetic venting of pressurized gases from the fuel element plenum and pellet cladding gap. High temperature creep or mechanical forces can cause the necessary cladding rupture in a spent fuel cask. Available for release are noble gases, volatile halogens and entrained particulates which have migrated from the fuel matrix during irradiation. Information on particulate size is not available. The particulates are conservatively assumed to be less than 10 μm AMAD since particles of that size are biologically significant and easily transported in the atmosphere.

2. Vaporization Release is the volatilization of low melting point fission products and their gaseous transport to the cask cavity. If the high temperature environment occurs before fuel cladding rupture, then a driving force for release is the venting of fuel cladding internal pressure. For mechanical cladding ruptures followed by heating, vapor pressures and diffusion cause the release. Cesium is a primary constituent of the semi-volatile elements.

3. Leaching of fission products from the fuel pellets requires direct contact of aqueous cask cavity coolant. Contact can occur following an impact which ruptures fuel pins while the cask retains its cavity coolant. Also, undetected failed fuel (fuel which outgases in the reactor, but is not detected and overpacked in the spent fuel basin) can release a small amount of fission products to the cask under normal transport conditions. Leached activity escapes the cask with the cavity coolant.

4. Oxidation of some fraction of the UO_2 fuel pellets to ~~of~~ U_3O_8 may take place in the unlikely event of a large cask rupture. Increased releases of fission products occur by this mechanism due to a large increase in surface area. The reaction proceeds at insignificant rates in a steam atmosphere. A cask breech large enough to allow flowing air to contact the fuel is necessary for this type release. Material released would be in the form of noble gases, volatilized fission products and particulates of less than 10 μm AMAD.

9.3.2 Estimated Release Fractions for Various Release Categories

The final barrier to radionuclide release is the transport cask. Very unlikely events must be postulated before a significant pathway exists through this containment. Accident combinations which were postulated in Section 8 may result in releases of activity to the environment. The list of release sequences presented in Section 9.2 have been divided into eight different categories based on postulated accident conditions, and release fractions were assigned to each category.

When forces severe enough to fail the cask wall were assumed, it was conservatively estimated that all material which might escape the cladding would reach the atmosphere.[11] On failure of a closure device, 50% retention of particulates in the cask was estimated. Examples of this type of failure would be a rupture disk venting or a valve failure.

Five different categories based on different release mechanisms from the spent fuel were postulated for fractional release of airborne activity. Those categories were Noble gases, Iodine, Cesium and Ruthenium, Actinides, and all other significant mixed fission products.

Table 9.2 shows the accident spectrum and the associated release fractions. Table 9.3, based on 0.46 MTHM per spent fuel cask shows estimated potential release in curies to the atmosphere. Accidents involving a fire with impact below 30 km/hr or a loss of cavity coolant with resultant fuel rod failure results in the largest potential releases. This occurs because a pressurized creep rupture of the cladding expels much more activity than the less energetic venting following an impact type failure of the fuel.

The following paragraphs present a brief rationale for the release fractions for each of the accidents shown in Table 9.2. Appendix B presents detailed development of the release fractions.

1. All releases involving small undetected losses of cavity coolant were assumed to have a release fraction of 1.4×10^{-11} for Cesium. (Cesium was found to be the primary fission product in the cavity coolant from tests at Savannah River Labs.[11] The release fraction was based on an assumed cavity coolant leak rate of 0.001 cc/sec. It was assumed that

TABLE 9.2. Accident Release Fractions to the Atmosphere from the Truck Transport of Spent Fuel

Accident Case	Cask Condition	Fuel Condition	Release Mechanisms	Release Mechanisms	Fractional Release of Airborne Activity				
					Noble Gases (Kr, Xe)	Iodine[a]	Cesium and Ruthenium	All Other Fission Products[b]	Actinides
1. Small undetected leak of cavity coolant	Closure error	Some undetected failed fuel	Leaching	Leaching	Negligible	Negligible	Cs 3.6×10^{-8} Ci/hr ??	Negligible	Negligible
2. Slow leak of cavity coolant due to gasket failure	Failed head or valve gasket. Leaks for four hours	Some undetected failed fuel	Leaching	Leaching	Negligible	Negligible	Cs 1.2×10^{-9}	Negligible	Negligible
3. Impact and slow leak of cavity coolant	Failed head or valve gasket. Leaks for four hours	All rods fail on impact	1. Gap activity 2. Leaching	1. Gap activity	0.3	0.1	Cs 4.2×10^{-8}	6.5×10^{-9}	5.3×10^{-9}
4. Severe cask impact with a rapid loss of cavity coolant	Cask failure allows entry of flowing air	All rods fail on impact	1. Gap activity 2. Volatilization 3. Oxidation	1. Gap activity	0.31	0.12	Cs 3.0×10^{-4} Ru 1.0×10^{-4}	1.5×10^{-6}	1.0×10^{-6}
5. Cask involved in a 1010°C fire	Cask rupture disk operates venting coolant as a jet flashing to steam	All rods fail by creep rupture	1. Gap activity 2. Volatiles	1. Gap activity	0.3	0.1	Cs 1.5×10^{-4}	1×10^{-5}	1×10^{-5}
6. Cask impact followed by a 1010°C fire	1. Cask unfailed after impact 2. Rupture disk operates venting coolant as a jet flashing to steam	1. Failed by impact	1. Gap activity 2. Volatilization 3. Leaching	1. Gap activity	0.3	0.1	Cs 1.6×10^{-4}	2×10^{-6}	1.5×10^{-6}
7. Severe cask impact followed by a 2-hr. 1010°C fire	Cask fails on impact allows entry of flowing air	Failed by impact	1. Gap activity 2. Volatilization 3. Oxidation	1. Gap activity	0.31	0.12	Cs 3.1×10^{-4} Ru 1.0×10^{-4}	1.5×10^{-6}	1×10^{-6}
8. Rapid loss of cavity coolant due to cask closure device failure	Closure device failed after impact	All rods fail by creep rupture	1. Gap activity 2. Volatiles	1. Gap activity	0.3	0.1	Cs 1.5×10^{-4}	1×10^{-5}	1×10^{-5}

(a) Tritium - same release fraction as Iodine
(b) Carbon-14 - same release fraction as all other fission products

TABLE 9.3 Accidental Atmospheric Releases from the Transport of 0.46 MTHM of Spent Fuel (Ci)

Accident Case No.(a)	Volatiles		Fission Products		Actinides
	Kr,Xe	I,^{3}H	Cesium and Ruthenium	All Other Fission Products(b)	
1	Neg.	Neg.	Cs 3.6×10^{-8} Ci/HR	Neg.	Neg.
2	Neg.	Neg.	CS 1.43×10^{-4}	Neg.	5.7×10^{-4}
3	1200	1.6×10^{-3}	Cs 5×10^{-3} Ru 18.6	8.8×10^{-3}	5.7×10^{-4}
5	1200	1.6×10^{-3}	Cs 17.9	13.6	1.1
6	1200	1.6×10^{-3}	Cs 19.1	2.72	0.16
7	1240	1.9×10^{-3}	Cs 36.9 Ru 18.6	1.76	0.11
8	1200	1.6×10^{-3}	Cs 17.9	13.6	1.1

(a) From Table 9.2
(b) ^{14}C - same release as all other fission products

1% of the released activity in the coolant spilled on the ground would escape to the atmosphere as a sub 10 μm aerosol at ground level. The duration of the release was assumed to be one day since the leak was undetected for the entire length of the transport route. This release category results in very small releases of radioactivity which were determined not to have significant consequences. Thus, this category was not covered further in the analysis.

2. Release sequences in which a leak of cavity coolant would occur due to handling errors were assigned a release fraction of 1.2×10^{-9} for Cesium contained in the cavity coolant. The leak would occur for four hours until discovery and mitigation by the truck driver. This estimate was based on the maximum time allowed between inspections of the transport system by the driver while the cask is in transit. One percent of the activity escaping from the cask was assumed to be released to the atmosphere as a sub 10 μm aerosol at ground level.

3. Failure sequences involving impact with leakage of coolant on the ground were assigned release fractions, with each of the five nuclide release categories. The release fraction values are shown in Table 9.2. This sequence releases gap activity and cavity coolant. The release fractions for coolant activity are based on a time period of three hours for the release to occur following the accident before the fuel overheats. All the gap activity was assumed to be released to the atmosphere. One percent of the activity in the cavity coolant released was assumed to reach the atmosphere. It was conservatively assumed that the gap activity was released at the time of impact at ground level. If the fuel overheats, then the release becomes the same as Case 4 below.

4. Severe impact accidents sequences which rupture the cask and all fuel cladding were assigned release fractions for each of the five nuclide categories. This sequence releases activity from all four mechanisms: gap release, vaporization, leaching, and oxidation. The gap activity was conservatively assumed to be released at the time of impact along with the cavity coolant. Volatilization and oxidation releases would occur about 2 hours later and last for about 1.2 hours. Ground level release was assumed for this category of release sequences.

5. Failure sequences of a cask due to fire accidents with no impact were assigned release fractions for each of the five nuclide release categories. This accident sequence involves release of gap activity, coolant and volatiles. The coolant activity was assumed released when the rupture disk relieves the cask pressure at about 0.6 hours after the fire starts. All of the coolant activity was assumed released to the atmosphere in the fire. The gap activity and volatiles were assumed to be released at 1.9 hours for a duration of about 0.5 hours. Half of the particulates were assumed to remain in the cask. Since the fire was out when the major part of the release occurred, ground level release was assumed except for the coolant activity which was assumed to have a release height of 100 meters.

6. All release sequences involving an impact followed by a fire were assigned release fractions for each nuclide release category. This sequence involves release of the gap activity coolant and volatile cesium. It was assumed that all gas gap and coolant activity products of the release at impact were airborne following the release with an elevated release at an elevation of 100 meters. The remainder of the gap activity and the volatiles were assumed to be released at about 2.0 hours after the accident with a duration of about 1.2 hours. The delayed activity was assumed to be released at ground level.

7. Release sequences which involve a severe impact followed by fire were assigned release fractions for all five of the nuclide release categories. This sequence involves gap, coolant, volatile, and oxidation releases. This release is similar to category 6 except that all the gas gap release occurs at elevated release with 100% emitted to the atmosphere. The release height was assumed to be 100 meters.

8. Sequences involving loss of cavity coolant with resulting failure of the fuel were assigned release fractions for all of the fractional release categories. All of the gap activity is assumed to be released due to creep rupture of the fuel pins with 50% of the particulate remaining in the cask. The release starts about 2 hours after the accident occurs and continues for about 1 hour. Since the fire is out when release occurs, ground level release was assumed.

REFERENCES

1. 10 CFR Part 71, Code of Federal Regulations.

2. A. W. Dennis et al., Severities of Transportation Accidents Involving Large Packages. SAND77-0001, Sandia Laboratories, Albuquerque, NM, May 1978.

3. Trojan FSAR, Safety Analysis Report.

4. K. J. Eger, A. Hulsey, Operating Experience - Irradiated Fuel Storage. GE Morris Operation, June 1975.

5. Reactor Safety Study - An Assessment of the Accident Risks in U.S. Commercial Nuclear Power Plants. WASH-1400 (NUREG-75/014), U.S. Nuclear Regulatory Commission, Washington DC, October 1975.

6. W. F. Hartman et al. Statistical Description of Heavy Truck Accidents on Representative Segments of Interstate Highway, SAND76-0409, Sandia Laboratories, Albuquerque, NM, January 1977.

7. M. Huerta, Analyses, Scale Modeling and Full Scale Tests of a Truck Spent-Nuclear Fuel Shipping System in High Velocity Impact Against a Rigid Barrier SAND77-0270 Sandia Laboratories, Albuquerque, NM, April 1978.

8. P. J. Pelto and W. L. Purcell, MFAULT: A Computer Program for Analyzing Fault Trees, BNWL-2145, Battelle, Pacific Northwest Laboratories, Richland, WA, November 1977.

9. J. W. Langhaar, Transport Experience with Radioactive Materials, E. I. du Pont de Nemours & Company, Inc., from CONF-76-0701, July 1976.

10. A. W. Grella, A Review of Five Years Accident Experience in the U.S. Involving Nuclear Transportation (1971-1975). IAEA-SR-10/5, U.S. Department of Transportation, Washington DC, August 1976.

11. Environmental Survey of Transportation of Radioactive Materials to and from Nuclear Power Plants. WASH-1238, U.S. Atomic Energy Commission, Washington DC, December 1972.

10.0 EVALUATION OF ENVIRONMENTAL CONSEQUENCES

In Section 9 individual release sequences were identified and evaluated by determining their expected frequency of occurrence and the corresponding release fraction. At this point, a risk number could be obtained by multiplying the individual release sequence probabilities and release fractions together, and summing over all release sequences. The resulting risk number, however, would not be in a form suitable for use in comparison with other societal risks. Such a comparison is one of the objectives of the risk assessment.

To express the risk in a form suitable for use in comparison with other societal risks, conversion factors must be developed to evaluate the consequence portion of the risk number in terms of potential fatalities. The purpose of this section is to develop these conversion factors. Areas which must be evaluated in developing this information include: meteorology, demography, quantity of radioactive material made airborne and dispersed, and general population health effects. Analysis of these factors are summarized sequentially in separate parts of this section. The final portion of this section will show how these factors are applied to the risk number to express the risk in a form suitable for comparison with other risks.

10.1 METEOROLOGY

The diffusion climatology along the transport route must be incorporated into any risk analysis where the atmosphere is an important pathway for dosage to man. The important atmospheric variables are 1) wind direction - indicates the initial direction of travel, 2) wind speed - indicates the rate of transport, and 3) atmospheric stability - indicates the rate of dilution and plume rise potential. Certain characteristics of release (e.g., height and temperature) are also important in the evaluation of the atmospheric pathway.

Assuming a postulated accident with a surface release and little or no release-related plume rise, the immediate and greatest impact will be in the region surrounding the location of the event. Transport and diffusion are often determined by local influences. Wind speeds and directions show

considerable variation that cannot always be summarized by large geographic regions. Local influences include topography (surface roughness, channeling), heat island effects, and proximity to large bodies of water. The inclusion of such influences in the present analysis is not possible, principally because the information is not available either from a data base or from current modeling capabilities.

For estimates of long-term diffusion averages, the average persistence of winds by sectors are used. Considering wind direction persistences alone, the actual sector annual-average air concentrations can be considerably higher or lower than an average. Based on reported values from 129 weather bureau surface stations in continental U.S., the concentrations range on the order of from half to 5 times the average. The air concentrations near a particular population center can be expected to vary by the same factor depending on the direction of the population center from the selected route. Such a factor could be quite important in determining the effects of releases near large population centers. Over a sufficiently long route the effect of different wind direction persistences may tend to cancel if there is a random relationship between the prevailing wind directions and population centers. The alternative of picking a route based on known diffusion climatologies to minimize risk could be beneficial; however, at the present time it is not included in the model.

The meteorological data used in this analysis are shown in Table 10.1. The values were developed from micrometeorological data collected for diffusion calculations for reactor sites. Seven sets of micrometeorological data were selected from 26 compilations from reactor sites to account for the range of conditions that could reasonably occur along the route. The use of a single averaged distribution allows for the typical range of windspeeds without undue weighting to any particular site. Although this result cannot be expected to necessarily represent any particular portion of the route, it does represent the type of conditions that may be encountered on the average.

TABLE 10.1. Average Wind Speed/Stability Characteristics

Wind Speed			Pasquill Stability Classification			
			$P_{j/k}$			
U_K m/sec	k	P_k	B(j=1)	D(j=2)	E(j=3)	F(j=4)
1	1	0.255	0.136	0.202	0.299	0.363
3.5	2	0.508	0.243	0.274	0.272	0.211
7	3	0.161	0.190	0.290	0.339	0.181
10	4	0.052	0.240	0.312	0.358	0.090
18	5	0.024	0.276	0.348	0.356	0.020

10.2 DEMOGRAPHY

To determine the number of people affected by a fission product release resulting from a transportation accident, the population distribution along the shipping route must be characterized. This information is needed to determine both the exceeded frequency at which a given population distribution will be exposed to a release and the distribution of the resultant exposure. This data can be developed only after the shipping routes are well defined and realistic population projections have been made.

The population distribution along shipping routes was characterized by dividing the Continental U.S. into four zones based roughly on population density and degree of urbanization. The zones are shown in Figure 4.1 of Section 4. A representative state was chosen for each of the zones. Then for the purpose of the study, the population data of the selected states were used in forecasting population characteristics of their respective zones.

The population densities grouped into three classes: Urban for densely populated urban areas. Suburban for areas of moderate population density, and Rural for the nonurbanized areas. The Suburban area data were obtained by taking the Standard Metropolitan Statistical Area (SMSA) data, which include Urban, and subtracting out the population and land area of the cities.

The initial approach was to establish a set of population data for the representative states. Census data for 1960 were used as a data base and extended to 1970 with information available from the 1970 census. Population projections were also made to the year 2000, and, using the compound interest formula to model population growth, estimates were made for 1980 and 1990.

The fraction of each spent fuel shipment route to its storage location in each of the population zones was identified. Using this, a route population density was calculated for each route for each of the time periods considered: 1980, 1990, 2000.

The techniques employed in each step of the analysis are described in more detail below.

10.2.1 Population Zones Data

The continental U.S. was divided into four population zones (see Figure 4.1, Section 4). A representative state for each zone was chosen and data for the state taken to be representative of the entire zone. The states chosen by zone are shown below:

Zone	Representative State
I - High urbanization	New Jersey
II - Densely populated	Massachusetts
III - Moderately populated	Missouri
IV - Low population	Washington

The population characteristics for each of the representative states based on 1960 census figures[1] is shown in Tables 10.2 through 10.5 respectively.

In Tables 10.2 through 10.5 the city data are based on cities of 25,000 population or greater and the SMSA are all the standard metropolitan statistical areas in the state. The rural population and area values are those of the total state minus those of the SMSA. It should be recognized that since

the SMSA includes many major cities, the cities are in effect counted twice. This shows up in both the land area and total population counts which result in the numbers adding to greater than 100%. For this reason, the Suburban class has been used to illustrate the projected population densities in subsequent tables.

TABLE 10.2. New Jersey Population Characteristics-1960

	Population	Land Area, mi^2	Density People/mi^2	Land Area, %
State	6,066,782	7,532	806	100
Cities	2,440,602	226(a)	10,800	3
SMSA(b)	4,821,032	4,227	1,147	56.1
Rural	1,245,750	3,305	377	43.9

(a) City of Vineland, NJ, showed an area of 67 mi^2. This was corrected to 10 mi^2, which is larger than most cities of comparable population in New Jersey.
(b) Includes cities.

TABLE 10.3. Massachusetts Population Characteristics-1960

	Population	Land Area, mi^2	Density People/mi^2	Land Area, %
State	5,148,578	7,828	657	100
Cities	2,876,806	713	4,035	9.1
SMSA	4,379,477	2,924	1,498	37.3
Rural	769,101	4,904	157	62.6

TABLE 10.4. Missouri Population Characteristics-1960

	Population	Land Area, mi^2	Density People/mi^2	Land Area, %
State	4,319,813	69,046	63	100
Cities	1,715,093	336	5,104	0.5
SMSA	3,414,071	7,967	429	11.5
Rural	905,742	61,079	15	88.5

TABLE 10.5. Washington Population Characteristics-1960

	Population	Land Area, mi^2	Density People/mi^2	Land Area, %
State	2,853,214	66,663	43	100
Cities	1,066,336	226	4,718	0.3
SMSA	1,707,136	7,663	223	11.5
Rural	1,146,078	59,000	19	88.5

The next step was to obtain the same data for 1970 and then determine the population and land area change for major cities (100,000 population) from 1960 to 1970. The 1970 census data were obtained from the Statistical Abstracts of the U.S.[2]

The extrapolation to 2000 was then made based on information presented in an article by J. P. Pickard.[3] Pickard stated that by the year 2000 the urban land area will double. He also states that 85% of the total population growth will occur in major urban areas. Using this, the total population increase is the urban increase divided by 0.85. This leaves the rural increase at 15% of the total growth.

Based on Pickard's projections the land areas and rural populations were calculated for the year 2000. The data for 1980 and 1990 were filled in using the compound interest formula. The resultant population

characteristics for each of the four zones in the years 1980, 1990 and 2000 are presented in Table 10.6. The composite population densities for the four zones are shown in Table 10.7.

10.2.2 Average Size of an Urban Area

The data in Table 10.6 show that urban areas occupy a small fraction of the land area. If a release occurs in a city, it would be incorrect to assume that the release plume is confined completely to an urban area. For that reason, it is important to determine the size of a representative urban area and thereby limit the urban area included in any dose calculation. Using the representative states for each of the four zones, the average urban land area was determined. Only urban areas having a population greater than 25,000 in the year 1960 were used in the analysis. The results of this analysis are summarized in Table 10.8 for the years of interest.

10.2.3 Shipping Route Mileage by Population Zones

The second factor in the characterization of the demography is to relate the shipping routes to the population zones. Spent fuel shipment routes were previously determined in Section 4. Previous parts of 10.2 have characterized the population distribution for the various zones of the country for the same years. This section will develop the information on the route mileage in each zone that is needed to obtain the population density along each shipping route.

TABLE 10.6. Projected Population Density and Land Area by Zone and Population Classes

Zone and Population Classes		1980 Land Area, %	1980 Density People/mi^2	1990 Land Area, %	1990 Density People/mi^2	2000 Land Area, %	2000 Density People/mi^2
I	Urban	3.8	9290	4.8	8390	6.0	7570
	Suburban[(a)]	66.9	822	84.3	893	94.0	1005
	Rural	29.3	612	10.9	696	-	-
II	Urban	11.5	3170	14.5	3130	18.2	2820
	Suburban[(a)]	35.5	845	44.8	762	56.5	686
	Rural	53.0	238	40.7	350	25.3	635
III	Urban	0.8	3980	1.0	3930	1.2	3890
	Suburban[(a)]	17.3	226	21.8	223	27.5	221
	Rural	81.9	17	77.2	24	71.3	29
IV	Urban	0.5	4390	0.6	4480	0.8	4560
	Suburban[(a)]	15.0	131	18.9	144	23.7	147
	Rural	84.5	25	80.6	29	75.5	34

(a) SMSA-Cities.

TABLE 10.7. Average Population Densities by Zone (People/mi^2)

Zone	1980	1990	2000
I	1082	1231	1399
II	824	936	1061
III	84	104	129
IV	62	66	93

TABLE 10.8. Projected Land Area of Urban Areas in the Four Zones of the U.S.

Zone	Number of Urban Areas(a) (Pop >25,000) 1960	Average Urban Land Area, mi(2) 1980	1990	2000
I	36	7.92	9.97	12.56
II	35	25.66	32.34	41.77
III	12	43.92	55.33	69.67
IV	8	37.80	47.63	60.00

(a) Only includes urban areas in representative state.

A map with the population zones and the location of the reactor groups and spent fuel receiving locations (interim storage facilities and reprocessing plants) is shown in Figure 4.1, Section 4. The distance between each reactor group and spent fuel receiver was calculated, and the shipping route was examined for the fraction of the route in each population zone. This data is summarized in Table 10.9.

The shipping routes have been completely characterized. The mileage between any reactor group and the closest interim storage facility or reprocessing plant is shown in Tables H.2 and H.3, Appendix H. Population distributions in each zone along the route can be determined from the data presented in Table 10.6.

The fraction of the route in each zone is shown in Table 10.9, and the population distribution in each zone along the route for a particular year can be determined from the data presented in Table 10.6.

TABLE 10.9. Shipping Route Mileage by Population Zones (Values in Percent)

	Population Zone Number			
	I	II	III	IV
Reactor Group to Interim Storage Facility	9	24	57	10
Reactor Group to Reprocessing Plant	5	13	61	21

10.3 POPULATION DOSE FACTORS

Factors from the meteorological and demographic characteristics of the shipping route are combined with the dose conversion factors developed here to determine the population doses resulting from an accidental release of fission products. There are two parts to the calculation. First, Dose Conversion Factors must be developed to characterize the effect of inhaled activity on an individual's health. Second, using the meteorological data, an Atmospheric Dispersion Model shown in Section 10.4 must be developed to characterize the fission product aerosol concentration downwind from the release point.

The dose to an individual from inhalation of fission product radionuclides is a function of the duration of the release, the concentration during the release period, the particle size, the isotopic composition of the released material the individual's ventilation rate, the solubility of the inhaled material in body fluids, and the retention time of the radionuclide in body organs.

The dose resulting from inhalation of fission product activity is calculated using the lung model recommended by the International Commission

on Radiological Protection (ICRP), Task Group on Lung Dynamics. This model (referred to as the TGLM) characterizes the metabolic pathways of the inhaled material.[7] A computer program has been developed for calculating the dose to lung and other organs using the TGLM.[8]

A detailed discussion of the lung model is presented in Appendix E.

The inhalation dose to an individual exposed to a passing cloud can be expressed by:

$$D_j = K'P$$

where:

K' is the dose conversion factor (rem/ci inhaled)
P is the quantity inhaled

The quantity of material inhaled is dependent upon the time-integrated air concentration as expressed by:

$$P = bc_a\tau = bE \qquad (10\text{-}2)$$

where:

b is human ventilation rate, cm^3/sec
c_a is air concentration, $\mu Ci/cm^3$
τ is duration of inhalation exposure, sec
E is time-integrated air concentration, $\mu Ci.\ sec/cm^3$

The time-integrated air concentration, E is obtained from the Atmospheric Dispersion Model discussed in Section 10.4.

Combining Equation 10-1 with Equation 10-2 and normalizing the result to the quantity released yields:

$$\frac{D_j}{Q} = K' \; b \; \frac{E}{Q} \qquad (10\text{-}3)$$

where:

Q is the quantity released in curies

or

$$\left(\frac{D_j}{Q}\right) = K \left(\frac{E}{Q}\right)$$

where: K is the inhalation dose conversion factor (K'b) for an accidental atmospheric release.

Dose conversion factors for 50-year dose commitments for the most significant isotope in the spent fuel are tabulated in Table 10.10.

The conversion factors presented in Table 10.10 are values of K in Equation 10-3 for the individual isotopes. The particle size is based on an equivalent aerodynamic median diameter (AMAD) of 1 micron. Using this table, one set of conversion factors for any specified isotopic mixture can be obtained.

Table 10.11, Parts A, B, C and D list the isotopic mixtures contained in the various fractional release categories outlined in Section 9. These isotopic mixtures were used for the dose calculations reported in this document. Using the isotopic mixtures outlined, the conversion factors for the mixtures have been calculated and summarized in Table 10.12 using the TGLM conversion factors. The set of K values shown in Table 10.12 convert the amount of material inhaled, expressed in total curies of the various mixtures into 50-year dose commitments to the lung and bone for both soluble and

insoluble particles. The Task Group Lung Model was used in this analysis with cesium metabolized as translocation Class D, all actinides are Class W, and the reference mixture of fission products as a Class D.

The release fractions developed in Section 9.3 are presented as fractions of the total weight of mixed fission products in a container based on the isotopic mixture shown in Table 10.11.

$$Q = (TIA) \times A \times F_r \qquad (10\text{-}4)$$

where:

TIA Total Inventory Available, is the number of curies per gram in the isotopic mixture being shipped. (See Table 10.11)

Q is the curies released

A is the amount of material in a container in grams

Fr is the release fraction for the isotopes dispersed during a release

TABLE 10.10. Population Dose Factors for Individual Isotopes

Isotope	Translocation Class	CONVERSION FACTOR (rem per Ci sec/m^3) Total Body	Bone	Lung	Thyroid
^{85}Kr	--	4.9E-4[a]	--	--	--
^{89}Sr	D	3.4E+0	3.0E+1	1.1E+0	--
	Y	9.9E-1	8.5E+0	6.1E+1	--
^{90}Sr	D	6.9E+2	2.8E+3	9.0E-1	--
	Y	2.8E+2	1.2E+3	6.7E+0	--
^{90}Y	D	2.4E-1	8.8E+0	1.5E+0	--
	Y	2.2E-3	8.1E-2	6.7E+0	--
^{91}Y	D	3.8E+0	1.4E+2	1.2E+0	--
	Y	4.3E-2	1.6E+0	7.5E+1	--
^{95}Nb	D	1.9E+0	5.2E+0	5.1E-1	--
	Y	1.9E-2	5.2E-2	2.1E+1	--
^{95}Zr	D	6.8E+0	2.6E+1	6.4E-1	--
	Y	8.0E-2	3.1E-1	7.8E+1	--
^{103}Rh	D	1.1E-4	1.9E-4	8.0E-3	--
	Y	6.0E-6	1.0E-5	8.5E-3	--
^{103}Ru	D	3.0E-1	6.3E-1	5.2E-1	--
	Y	1.2E-2	2.5E-2	2.3E+1	--
^{106}Ru	D	1.1E+0	8.9E+0	2.8E+0	--
	Y	6.6E-2	5.2E-1	7.1E+2	--
^{123}Sh	D	--	--	--	--
	Y	--	--	--	--
^{125}Sb	D	1.1E+1	3.5E+1	4.2E-1	7.0E-3
	Y	9.0E-1	2.9E+0	2.1E+2	5.7E-4
^{127}Te	D	7.5E-3	3.4E-2	2.1E-1	7.7E+0
	Y	1.3E-3	5.8E-3	3.3E-1	1.3E+0
^{129}I	D	1.8E+0	4.3E-2	1.6E-1	1.4E+3
	W	1.8E+0	4.3E-2	9.9E+0	1.4E+3

(a) External Exposure

TABLE 10.10. (Continued)

Isotope	Translocation Class	CONVERSION FACTOR (rem per Ci sec/m^3) Total Body	Bone	Lung	Thyroid
^{131}I	D	4.7E-1	5.1E-1	5.6E-1	2.6E+2
	W	3.7E-1	4.0E-1	5.4E+0	2.0E+2
^{131m}Xe	--	2.5E-3[a]	--	--	--
^{134}Cs	D	1.1E+1	6.6E+0	3.2E+0	--
^{137}Cs	D	6.0E+0	1.1E+1	2.6E+0	--
^{141}Ce	W	1.3E-1	1.6E+0	8.7E+0	--
	Y	7.0E-3	8.4E-2	1.3E+1	--
^{144}Ce	W	6.4E+0	1.2E+2	1.3E+2	--
	Y	6.3E-1	1.2E+1	5.6E+2	--
^{147}Pm	W	7.3E-1	1.9E+1	7.9E+0	--
	Y	1.4E-1	3.7E+0	5.4E+1	--
^{154}Eu	W	2.1E+1	3.2E+2	1.0E+2	--
	Y	7.1E+0	1.1E+2	9.5E+2	--
^{155}Eu	W	1.4E+0	1.2E+1	1.1E+1	--
	Y	2.2E-1	2.0E+0	6.4E+1	--
^{238}Pu	W	1.5E+4	3.2E+5	1.2E+4	--
	Y	5.6E+3	1.2E+5	1.2E+5	--
^{239}Pu	W	1.7E+4	3.6E+5	1.1E+4	--
	Y	6.4E+3	1.4E+5	1.1E+5	--
^{240}Pu	W	1.7E+4	3.6E+5	1.1E+4	--
	Y	6.4E+3	1.4E+5	1.1E+5	--
^{241}Am	W	1.4E+4	2.0E+5	1.2E+4	--
	Y	5.5E+3	7.6E+4	1.2E+5	--
^{241}Pu	W	2.7E+2	6.6E+3	3.6E+0	--
	Y	8.8E+1	2.1E+3	1.9E+2	--

(a) External Exposure

TABLE 10.10. (Continued)

Isotope	Translocation Class	CONVERSION FACTOR (rem per Ci sec/m^3) Total Body	Bone	Lung	Thyroid
^{242}Cm	W	3.2E+2	4.8E+3	1.0E+4	--
	Y	2.4E+1	3.6E+2	3.3E+4	--
^{242}Pu	W	1.6E+4	3.4E+5	1.1E+4	--
	Y	6.1E+3	1.3E+5	1.1E+5	--
^{244}Cm	W	8.0E+3	1.3E+5	1.3E+4	--
	Y	2.7E+3	4.3E+4	1.2E+5	--

TABLE 10.11. Part A: Reference Mixture of Cesium Isotopes

	Composition by Weight (%)	Activity (Ci/g of Mix)
^{134}Cs	10.8	140.7
^{137}Cs	89.2	77.5

TABLE 10.11. Part B: Reference Mixture of Cesium and Ruthenium Isotopes

	Composition by Weight (%)	Activity (Ci/g of Mix)
^{134}Cs	10.0	129.4
^{137}Cs	82.0	71.4
^{103}Ru	0.1	33.2
^{106}Ru	7.9	265.6

TABLE 10.11. Part C: Reference Mixture of Fission Products

	Composition by Weight (%)	Activity (Ci/g of Mix)
^{89}Sr	0.3	73.8
^{90}Sr	64.6	91.5
^{91}Y	0.5	129.9
^{95}Zr	1.1	230.2
^{95}Nb	1.1	442.7
^{103}Ru	0.2	59.0
^{106}Ru	14.0	472.3
^{127m}Te	0.1	5.6
^{141}Ce	0.8	230.2
^{144}Ce	4.0	126.9
^{147}Pm	13.0	121.0

TABLE 10.11. Part D: Reference Mixture of Actinides

	Composition by Weight (%)	Activity (Ci/g of Mix)
^{238}Pu	1.5	0.27
^{239}Pu	59.0	0.036
^{240}Pu	25.8	0.058
^{241}Pu	12.7	14.2
^{241}Am	0.8	0.026
^{242}Cm	0.1	2.17
^{244}Cm	0.2	0.167

TABLE 10.12. Dose Conversion Factors for Reference Mixtures (rem per Person per Ci sec/m^3)

Isotope	Translocation Class	Total Body	Bone	Lung	Thyroid
Actinide Isotopic Mixture	W	7.0E+2	1.5E+4	1.7E+3	
	Y	2.4E+2	5.0E+3	8.3E+3	
Mixed F.P.	(1)	2.0E+1	1.1E+2	3.2E+1	2.7E-2
	(2)	7.5E+0	3.3E+1	1.8E+2	4.6E-3
Cesium Isotopic Mixture	D	9.2E+0	8.2E+0	3.0E+0	--

(a) These dose conversion factors were generated assuming translocation Class D for Sr, Y, Zr, Nb, Ru, Rh, Sn, Sb, and Te, and Class W for Eu, Pr and Pm.
(b) These dose factors were generated assuming translocation Class Y for all nuclides.

10.4 ATMOSPHERIC DISPERSION MODEL

To affect human life, the products of a release of spent fuel must reach man via some pathway in his environment. For the purpose of this study, only the air pathway was considered. Direct radiation, food chain and aquatic pathways were not considered significant pathways from release of radioactivity. Although material can reach man via these pathways, the consequences from the amount of material following these pathways has been found to be insignificant when compared to the air pathway.[9] Appendix D contains further discussion on pathways of radiation exposure to man.

The radioactive releases were assumed to be neutrally buoyant when airborne. In releases involving fire, the radionuclides were assumed to be carried aloft and released from the fire plume (elevated release).

For releases of short duration, less than a day, the time-integrated air concentration at ground level is evaluated by the bivariate normal diffusion model using Pasquill diffusion parameters.[9] In equation form:

$$E = \frac{Q}{\pi\sigma_y\sigma_z\bar{U}_h} \exp\left[(-y^2/2\sigma_y^2) - (h^2/2\sigma_z^2)\right] \qquad (10\text{-}5)$$

where:

- E is ground level time-integrated air concentration at point x, y, $Ci\cdot sec/m^3$
- x is downwind distance measured from point of release, m
- y is crosswind distance measured horizontally from centerline of cloud, m
- Q is total release from source, curies
- σ_y is crosswind lateral standard deviation of cloud concentration, m
- σ_z is crosswind vertical standard deviation of cloud concentration, m
- $\bar{U}_h$ is average windspeed at the height of release in direction of travel, m/sec
- h is height of release, m.

The values of σ_y and σ_z are a function of the downwind distance x and the Pasquill Stability Category existing at the time of the accident. These values are shown in Tables 10.13 and 10.14, respectively.

The dose to an individual at point (x,y) can now be obtained by specifying the windspeed, height of release and the Pasquill Stability Category. For these conditions, values of σ_y and σ_z at the downwind distance, x, can be obtained from Tables 10.13 and 10.14 by interpolation. Then E/Q can be calculated at x,y using Equation 10-5 and D/Q obtained using Equation 10-3 and Table 10.12.

The population dose could, in theory, be calculated by locating every individual or groups of individuals and going through the above procedure until all individuals receiving a dose have been included in the calculation. In practice, however, Equations 10-3 and 10-5 are used mainly to obtain the individual dose. The population dose is more easily estimated by calculating isopleths of constant dose or time-integrated air concentration. Then the differential area between isopleths and the mean dose received by individuals residing between the two isopleths is calculated.

TABLE 10.13. Values of σ_y for Pasquill Stability Categories

Downwind Distance (meters)	σ_y for Pasquill Type					
	A	B	C	D	E	F
100	21	16	12	8.0	6.0	3.9
250	54	40	28	20	14	9.8
500	100	76	55	37	28	18
1,000	200	150	110	72	52	36
2,500	450	340	240	160	120	81
5,000	830	630	450	310	220	150
10,000	1,600	1,200	850	570	410	280
25,000	3,400	2,600	1,800	1,200	880	610
50,000	6,200	4,700	3,400	2,300	1,600	1,100
100,000	11,000	8,500	6,300	4,100	2,800	2,000

TABLE 10.14. Values of σ_z for Pasquill Stability Categories

Downwind Distance (meters)	σ_z for Pasquill Type					
	A	B	C	D	E	F
100	15	10	7.8	4.7	3.0	1.4
250	43	26	18	10	7.1	4.0
500	140	57	34	19	13	7.6
1,000	670	140	64	33	22	14
2,500	2,000	580	140	62	41	25
5,000	2,000	2,000	260	95	61	35
10,000	2,000	2,000	440	140	84	47
25,000	2,000	2,000	880	220	120	64
50,000	2,000	2,000	1,400	320	140	79
100,000	2,000	2,000	2,000	450	170	94

The isopleth areas outside 100 m from the release are obtained using Equation 10-5. Rather than evaluate E in Equation 10-5 for every Q and every windspeed U, it is more convenient to move Q and U to the other side of the equation and determine isopleths of constant (UE/Q). The isopleths are determined by first selecting a value of UE/Q, obtaining values of σ_y and σ_z for each x beginning at 100, and then solving Equation 10-5 using the k^{th} average wind speed (see Table 10.1) to obtain the value of y for x. The x,y coordinates for an entire isopleth of constant UE/Q can be obtained in the same way. Then by integration, the area enclosed by any isopleth can be determined. The area between two isopleths receives a dose which is intermediate between the two boundary isopleths.

Table 10.15 presents a summary of the isopleth calculations for a 1 m/sec wind speed ($U_k = U_1$), similar tables could be constructed for other wind speeds. Isopleths were calculated for UE/Q values at order of magnitude intervals from 10^{-2} to 10^{-10}. Areas between adjacent isopleths were calculated and are shown as the area values for each Pasquill Stability Class. The mean value of $\overline{UE/Q}$ is set at 2.5 times the value of UE/Q at the outer

isopleth. The n subscript refers to the isopleth number and the j subscript denotes the stability class. A value of j = 1 refers to B stability and j = 2 refers to D stability, etc. The wind speed index, k, is one in the table. In Table 10.15 some of the values of $A_{n,j,1}$ are zero. These zeros are present because the calculations indicate that for those stabilities the isopleth areas lie entirely within the 100-m evacuation distance.

It is assumed that the people residing within 100 m of the accident can be evacuated by transport or emergency personnel. Based on information available for hazardous material transport,[10] transport or emergency personnel should be capable of controlling entry into the 100-m radius circle. Outside that radius many more individuals are needed to control people who may happen onto the accident scene. The model assumes evacuation of all individuals within the 100-m radius circle, who would be in the release plume, to a point where they would receive the centerline dose at 100 m. It is felt

TABLE 10.15. Land Areas Within Isopleths of a Release Plume and More Than 100 m from the Release Point ($U_k = U_1 = 1$ m/sec)

n	$(\overline{UE/Q})_{n,j,1}$	Pasquill Stability Classification			
		B	D	E	F
	m^{-2}	$A_{n,j,1}$ (Area m^2)			
1	2.5×10^{-2}	0	0	0	4.4×10^{3}
2	2.5×10^{-3}	0	1.6×10^{4}	2.2×10^{4}	2.6×10^{4}
3	2.5×10^{-4}	4.1×10^{4}	1.4×10^{5}	3.8×10^{5}	8.0×10^{5}
4	2.5×10^{-5}	1.8×10^{5}	3.0×10^{6}	3.8×10^{6}	2.2×10^{7}
5	2.5×10^{-6}	1.4×10^{6}	7.1×10^{7}	1.9×10^{8}	2.3×10^{8}
6	2.5×10^{-7}	3.3×10^{6}	4.8×10^{8}	3.1×10^{8}	1.5×10^{8}
7	2.5×10^{-8}	2.8×10^{6}	2.9×10^{8}	1.7×10^{8}	1.1×10^{8}
8	2.5×10^{-9}	1.3×10^{7}	2.1×10^{8}	1.3×10^{8}	8.8×10^{7}
9	2.5×10^{-10}	6.0×10^{6}	1.8×10^{8}	1.1×10^{8}	7.7×10^{7}

that giving the centerline dose at 100 m to all evacuated individuals will more than compensate for the dose received by any individuals missed during the evacuation. Based on this model, Table 10.16 shows the area within 100 m which would be in an isopleth for the various stability conditions. Also shown are the values of UE/Q at the centerline 100 m downwind from the release point.

TABLE 10.16. Land Area Contaminated Within 100 m of Accident Scene and Centerline Value of UE/Q at 100 m versus Pasquill Stability Classification

Pasquill Stability Classification	UE/Q m^{-2}	Area m^2
B	2.0×10^{-3}	5.9×10^{3}
D	8.6×10^{-3}	3.3×10^{3}
E	1.9×10^{-2}	2.5×10^{3}
F	5.7×10^{-2}	1.9×10^{3}

10.5 POPULATION HEALTH EFFECTS

The health effects that could be associated with a radioactive release from a spent fuel cask can be divided into three categories. These are early fatalities (fatalities that occur within one year), early illnesses (people needing medical treatment), and late health effects that are estimated from the total population dose. In general, early effects are associated with individual total body doses of 100 rads or more and would be limited to persons in the immediate vicinity of rather large releases of radioactivity, such as reactor accidents covered in WASH-1400.[11] Truck transported spent fuel casks carry relatively small amounts of activity and the public is assumed to be excluded from the immediate area of an accident. On this basis, potential early doses to individuals would be relatively small, thus early health effects were neglected for this study.

Late health effects, including latent cancer fatalities were calculated based on exposure of populations to low levels of radioactivity. The effects of ionizing radiation on large populations are the only applicable data source available to evaluate late health effects. The number of deaths in

the U.S. population which might result from continual exposure to ionizing radiation at a rate of 0.1 rem/yr has been estimated by an advisory committee of the National Academy of Science.[12] Two risk models were used to estimate the number of excess deaths due to radiation-induced cancer. The results for each model are reported here as Tables 10.17 and 10.18. Details of the models can be found in the NAS-BEIR committee report.[12]

TABLE 10.17. Estimated Numbers of Deaths per Year in the U.S. Population Attributable to Continual Exposure at a Rate of 0.1 rem/yr, Based on Mortality from Leukemia and from all Other Malignancies Combined [12]

Irradiation During Period	Absolute Risk Model[a] Deaths Due to: Leukemia	Absolute Risk Model[a] Deaths Due to: All Other Cancer	Relative Risk Model[a] Deaths Due to: Leukemia	Relative Risk Model[a] Deaths Due to: All Other Cancer
In Utero	75	75	56	56
0-9 years	164	73[b] 122[c]	93	715[b] 5,869[c]
10 + years	277	1,062[b] 1,288[c]	589	1,665[b] 2,415[c]
Subtotal	516	1,210[b] 1,485[c]	738	2,436[b] 8,340[c]
Total	1,726 = 0.6% increase 2,001 = 0.6% increase		3,174 = 1.0% increase 9,078 = 2.9% increase	

(a) The figures shown are based on the following assumptions:
- 1967 U.S. vital statistics can be used for age specific death rates from leukemia and all other cancer and for total U.S. population.
- Values for the duration (b or c) of the latent period (the length of time after irradiation before any excess of cancer deaths occur), duration of risk ("plateau region"), and magnitude of average increase in annual mortality for each group are as shown in Table 10.18.

(b) Thirty year duration of plateau (see Table 10.18).
(c) Lifetime duration of plateau (see Table 10.18).

TABLE 10.18. Assumed Values Used in Calculating Estimates of Risk Shown in Table 10.17[12]

Age at Irradiation	Type of Cancer	Duration of Latent Period (years)	Duration of Plateau Region[a] (years)	Risk Estimate	
				Absolute Risk[b] (deaths/10^6/yr/rem)	Relative Risk (% incr. in deaths/rem)
In Utero	Leukemia	0	10	25	50
	All other cancer	0	10	25	50
0-9 years	Leukemia	2	25	2.0	5.0
	All other cancer	15	30 Life	1.0	2.0
10 + years	Leukemia	2	25	1.0	2.0
	All other cancer	15	30 Life	5.0	0.2

(a) Plateau region is the interval following latent period during which risk remains elevated.

(b) The absolute risk for those aged 10 or more at the time of irradiation for all cancer excluding leukemia can be broken down into the respective sites as follows:

Type of Cancer	Deaths/10^6/yr/rem
Breast	1.5
Lung	1.3
GI including stomach	1.0
Bone	0.2
All other cancer	1.0
Total	5.0

A range of risk estimators for the present study was determined as follows. Deaths due to "all other cancers" for all ages were assumed to range from the lower subtotal value of the "Absolute Risk Model" to the upper subtotal value of the "Relative Risk Model." As shown in Table 10.17, the resulting range is from 1210 to 8340 deaths per year due to all cancers other than leukemia. Based on a U.S. population of 200 million people and a dose rate of 0.1 rem/yr the range can be expressed as 6×10^{-5} to 4×10^{-4} in units of deaths per man-rem.

The frequency of cancer death by type of cancer was estimated from Table 10.18 to be:

Type of Cancer	Frequency
Breast	0.30
Lung	0.26
GI including stomach	0.20
Bone	0.04
All other cancer	0.20
Total	1.00

These frequencies of occurrence were then applied to the range of excess deaths previously derived to estimate the range of excess deaths which might occur from radionuclide releases postulated in this study. The resulting range of risk estimators are shown in Table 10.19. Values used for this study were based on the BEIR report statistics.

TABLE 10.19. Health Effects Conversion Factors Population Dose to Maximum Number of Health Effects

Organ of Reference	Estimated Excess Cancer Deaths Per 10^6 man-rem[a] Range of Values	Value Used[b]
Lung	16-110	50
Thyroid	1-15	5
Bone	2-17	6
Total Body	50-450	200

(a) Derived from the BEIR Report.[12]
(b) From EPA-520/4-73-002 based on BEIR statistics.[14]

It is noted that the risk estimators listed in Table 10.19 are based on observed health effects produced at high dose levels, primarily by low linear energy transfer (LET) radiations and a hypothesis of linearity between effect and dose. It is probable that these estimators are significantly dependent on the energy transfer (LET) of the ionizing radiation and upon the dose levels actually encountered.[13] Determination of these factors is not within the scope of this study, therefore, they have been ignored in this analysis.

Conversion of population doses in man-rem to estimated possible excess cancer deaths was based on the factors presented in Table 10.19. These conversion factors enable a comparison to be made of spent fuel shipment risk estimates with other societal risks.

10.6 ESTIMATED EXPOSURE FREQUENCY

The information presented in the previous subsections can be used as conversion factors to modify the release sequence probabilities and release fractions developed in Section 9. The remainder of this section will show how these factors are applied in the risk calculation. The risk calculation

proceeds along two parallel and interrelated paths. One path characterizes the consequences of an accidental release, and the other path determines the frequency of occurrence for each event in the consequence analysis.

As briefly discussed in Section 3, risk is expressed by the equation:

$$R_i = \left(AF_{R_i} \times P_{R_i}\right) \times \sum_q \left(C_{E_{i,q}} \times P_{E_q}\right) \qquad (10\text{-}6)$$

where:

q represents a number of indices as indicated below.

The terms inside the first set of parentheses represent the product of the amount of material present in a shipment (A) times the fraction of that material which is lost to the environment in the i^{th} release sequence (F_{Ri}) times the expected frequency of occurrence of the release sequence (P_{Ri}). All the information needed to evaluate these terms was developed in Section 9. The two terms in the second set of parentheses represent the consequences of a unit release (Ei, q) and the expected frequency of encountering a given set of environmental conditions (PE_q). The primary purpose of previous parts of this section has been to determine the factors required to evaluate the consequences of a release. Simultaneously, the information required to determine the expected frequency that a given environmental consequence will be encountered has been presented. This part of Section 10 will show the development of the frequency of occurrence term.

The analysis presented in this section treated the wind speed, weather stability class and population class as distributed variables. The expected frequency of encountering a given set of environmental conditions can be expressed as:

$$P_{E_{j,k,\ell,m}} = P_{j/k} P_k P_{\ell/m} P_m \qquad (10\text{-}7)$$

where:

j is the atmospheric stability classification index
k is the wind speed index
ℓ is the population density index in zone m of the U.S.
m is the zone index for the shipping routes

The notation j/k indicates that the expected frequency of encountering the j^{th} stability class is a function of the wind speed existing at the time of release. Similarly, the expected frequency of encountering the ℓ^{th} population density is dependent on the expected frequency that a shipment will pass through zone m.

The values for the "P" in Equation (10-7) are obtained from the following tables in this section:

P_k - Table 10.1, Column 3
$P_{j/k}$ - Table 10.1, Columns 4-7
$P_{\ell/m}$ - Table 10.6
P_m - Table 10.9

By specifying a value for j, k, ℓ, and m, one can obtain the expected frequency that an environmental condition will be experienced during a shipment. Associated with that frequency is a corresponding value for the environmental consequences. The relationship is best summarized by the following equation for the environmental term in the risk equation:

$$\sum_{\bar{q}} \left(C_{E_{i,q}} \times P_{E_q} \right) =$$

$$\sum_{j,K,\ell,m,n} C\, K_{1,i} K_2\, A_{n,j,k} (\overline{E/Q})_{n,j,k} N_{\ell/m}\, P_{j/k}\, P_k\, P_{\ell/m}\, P_m \quad (10\text{-}8)$$

where:

C	is the factor to convert grams released to curies (Table 10.11)
$K_{1,i}$	converts curies received to organ dose (Table 10.12) for isotope groupings
K_2	converts organ dose to health effects (Table 10.19)
$A_{n,j,k}$	is the area between two isopleths n and n-1 (Tables 10.15 and Table 10.16)
$(\overline{E/Q})_{n,j,k}$	is the time integrated air concentration received in $A_{n,j,k}$ per curie released
$\overline{E/Q} = \overline{UE/Q}$	(Tables 10.15 and 10.16) divided by $\overline{U}$ (Table 10.6)
$N_{\ell/m}$	is the population density in the release plume (Table 10.6)

The subscripts and the values for P in Equation 10-8 have been defined following Equation 10-7. The product ($C_{E_{i,q}} \times P_{E_q}$) has units of fatalities per gram of material released. If several organs receive a dose as a result of a release, then the product $K_{1,i}K_2$ for each organ receiving a dose must be summed to get the overall effect to the individual.

Equation 10-8 summarizes the information presented in this section. In Section 11, these results will be used in conjunction with the release sequences developed in Section 9 to obtain the risk of shipping spent fuel by truck in the United States.

REFERENCES

1. County and City Data Book 1967. U.S. Dept. of Commerce, 1968.

2. Statistical Abstracts of the U.S. 1970. Census Division, U.S. Dept. of Commerce, Washington DC, 1971.

3. J. P. Pickard, Urban Land and New Trends in Land Development. Dept. of Housing and Urban Development, January 1970.

4. Rand McNally Standard Highway Mileage Guide No. 10. Household Goods Carrier's Bureau, Arlington, VA, 1973.

5. Report of Committee II on Permissible Dose for Internal Radiation. ICRP Publication 2, Pergamon Press, 1959.

6. Recommendations of the International Commission on Radiological Protection. ICRP Publication 6, Pergamon Press, 1962.

7. The Metabolism of Compounds of Plutonium and Other Actinides. A report prepared by a Task Group of Committee II of the International Commission on Radiological Protection, ICRP Publication 19, Pergamon Press, May 1972.

8. J. Houston, D. L. Strenge, and E. C. Watson, DACRIN Computer Program for Calculations of Organ Dose from Acute or Chronic Radionuclide Inhalation. BNWL-B-389, Battelle, Pacific Northwest Laboratories, Richland, WA, December 1974. (Reissued April 1976)

9. David H. Slade, Ed., Meteorology and Atomic Energy, 1968. TID 24190, Office of Information Services, U.S. Atomic Energy Commission, Washington DC, 1968.

10. Highway Accident Report - Automobile-Truck Collision Followed by Fire and Explosion of Dynamite Cargo on U.S. Highway 78, near Waco, Georgia, on June 4, 1971. NTSB-HAR-72-5, National Transportation Safety Board, Washington, DC, September 21, 1972.

11. Reactor Safety Study - An Assessment of the Accident Risks in the U.S. Commercial Nuclear Power Plants. WASH-1400 (NUREG-75/014), U.S. Nuclear Regulatory Commission, Washington DC, October 1975.

12. The Effects on Populations of Exposure to Low Levels of Ionizing Radiation. Report of the Advisory Committee on the Biological Effects of Ionizing Radiations, National Academy of Science, November 1972.

13. National Council on Radiation Protection and Measurements, Review of the Current State of Radiation Protection Philosophy. NCRP Report No. 43, Washington DC, January 15, 1975.

14. Environmental Radiation Dose Commitment: An Application to the Nuclear Power Industry. EPA-520/4-73-002, U.S. Environmental Protection Agency, Washington DC, June 1974.

11.0 THE RISK OF SHIPPING SPENT FUEL BY TRUCK

In this section, the risk of shipping spent fuel by truck will be discussed. The risk was calculated using the methodology presented in Section 3. The probability of an accidental release occurring during transport was determined in Section 9, and the consequences of such a release were discussed in Section 10. Section 11.1 presents the risk of shipping spent fuel in the reference year, based on the shipping system model given in Section 4. Major contributors to the overall risk are discussed in Section 11.2 and the results of sensitivity studies will be presented in Section 11.3.

11.1 RISK EVALUATIONS FOR SPENT FUEL SHIPMENTS

The risk calculated for spent fuel shipment is presented in this section. Section 11.1.1 presents a detailed development of the risk equation and a discussion of measures of risk. The annual risk in the mid 1980's from the shipment of spent fuel for two shipping scenarios, the "once through" fuel cycle and fuel reprocessing, are given in Section 11.1.2.

11.1.1 The Risk Equation

As described in Section 3, the total risk is defined as:

$$R = \sum_i R_i \qquad (11\text{-}1)$$

where:

$$R_i = \left(AF_{R_i} \times P_{R_i}\right) \times \sum_q \left(C_{E_{i,q}} \times P_{E_q}\right) \qquad (11\text{-}2)$$

The subscript "i" refers to the i^{th} release sequence. In Section 10, a general equation was developed for the terms in the second set of parenthesis in Equation (11-2). Substituting this expression into Equation (11-2) results in the following equation.

$$R_i = \left(AF_{R_i} \times P_{R_i}\right) \sum_{j,k,\ell,m,n}$$

$$C\ K_{1,i}\ K_2\ A_{n,j,k}(\overline{E/Q})_{n,j,k}\ N_{\ell/m}\ P_{j/k}\ P_k\ P_{\ell/m}\ P_m \quad (11\text{-}3)$$

The total risk of shipping spent fuel then becomes:

$$R = \sum_{i,j,k,\ell,m,n} \left[C\ K_{1,i}\ K_2\ AF_{R_i}\ A_{n,j,k}\ (\overline{E/Q})_{n,j,k}\ N_{\ell/m}\right] \times$$

$$\left[P_{R_i}\ P_{j/k}\ P_k\ P_{\ell/m}\ P_m\right] . \quad (11\text{-}4)$$

Equation (11-4) has been arranged so that the frequency of occurrence terms are separated from the consequence terms.

In Equation (11-4) the frequencies of occurrence and the consequences of all accidents are summed to obtain a single annual risk number. This number can be thought of as the expected frequency of occurrence of a fatality attributable to spent fuel transport. As discussed in Section 1, the risk spectrum must also be considered because it differentiates between an event which occurs once a year and results in one fatality and an event which occurs once in a thousand years but results in 1000 fatalities. In order to distinguish between these two events which have the same risk but different severities, curves are constructed which plot accident severity versus the expected frequency of accidents with greater severity. The two events described above have discrete contributions to the graph. Thus for the risk of two operations to be truly comparable, they must have both the same risk and the same risk spectrum.

Both the risk and the risk spectrum can be obtained from the terms in Equation (11-4). The number of fatalities from an accident release sequence is expressed by the term inside the first set of brackets in Equation (11-4). The frequency of the consequence (i.e., number of fatalities) is obtained by calculating the terms within the second set of brackets. These two terms

can be thought of as pairs of numbers. The risk spectrum curves can be obtained by choosing a value for N, the number of fatalities, and then scanning the paired sets of numbers for any first terms which exceed N. The summation of all second terms which have a first term greater than or equal to N is the expected frequency of occurrence of accidents which result in N or more fatalities. This is one point on the risk spectrum curve. This operation is continued until points on the risk spectrum curve are calculated for selected values of N down to one fatality.

11.1.2 The Risk of Shipping Spent Fuel in the Mid-1980s

A summary of the shipping system details given in Section 4 and Appendix H which were used in the analysis of spent fuel shipments is shown in Table 11.1. The estimated risk involved with shipping spent fuel was based on this information. Accidents involving truck shipments of spent fuel would be expected to occur at a rate of 1.5×10^{-6} per shipment km or about once in 645,000 shipment km. The expected frequency of accidents involving truck shipments of spent fuel would be about 1 in 935 shipments to interim storage facilities and 1 in 694 shipments to reprocessing plants. At this frequency a truck accident involving spent fuel would be expected to occur about once every 1.1 years for shipments to interim storage and 0.8 years for shipments to reprocessing plants. Based on the release sequence probabilities determined in Section 9, the analysis shows that 1 out of 3.6×10^{4} spent fuel shipments to interim storage would be estimated to release a small amount of radioactive material. An example of this type of release would be a very small leak of cavity coolant which would not result in any consequence to the general public. An accident resulting in some small release would thus be expected to occur about once every 41 years. Since accidents are expected at a rate of once per 935 shipments, 1 accident in 39 can be expected to result in some release of radioactive material. The probability of a release resulting in one or more deaths per year due to shipment of 180-day cooled spent fuel to interim storage facilities by truck was estimated to be 2.2×10^{-5} or about once in every 41,000 years. For 4-year cooled fuel the probability of a release resulting in one or more deaths was estimated to be 3.6×10^{-6} which is about an 84% reduction in the risk level. For spent fuel

TABLE 11.1 Shipping Characteristics for Spent Fuel by Truck

		Once Through Fuel Cycle	Spent Fuel Reprocessing
Amount spent fuel per container (MTHM)	PWR	0.461	0.461
	BWR	0.394	0.394
Shipment origin/destination		Reactor/ Interim storage	Reactor/ Reprocessing plant
Material shipped per year (MTHM)		380	380
Number of shipments[a] per year by truck		885	885
Average shipment[b] distance (km)		690	930
Accident probability[c] number/km		1.5×10^{-6}	1.5×10^{-6}

(a) Number of shipments determined in Appendix H.
(b) Shipment distances determined in Appendix H.
(c) Reference 1.

shipped to reprocessing plants, the probability of a release resulting in one or more deaths per year was estimated to be 1.7×10^{-5}. These results are summarized in Table 11.2.

The risk spectrum curves for shipment of spent fuel to interim storage are shown in Figure 11.1. Also shown in the figure are the risk spectra for meteorites, dam failures, persons on the ground killed in air crashes, the total of all natural disasters and the total of all man-caused disasters. These curves were taken from Reference 1. For comparison, the risk spectrum curves from several previous risk assessment studies[2,3,4] in this series are also shown in Figure 11.1.

The total risk due to the radiation exposure in the mid 1980s from the truck shipment of spent fuel is 4.5×10^{-5} fatalities per year. Using the estimated U.S. population at risk for spent fuel shipment, the individual risk per year is about 1.7×10^{-12} fatalities per person year or one in

TABLE 11.2. Summary of Risk of Transporting Spent Fuel by Truck

	Once Through Fuel Cycle		
	180-day Cooled Fuel	4-year Cooled Fuel	Spent Fuel Reprocessing
Probability of accident (events/year)	9.2×10^{-1}	9.2×10^{-1}	1.2
Probability of a radioactive release (events/year)[(a)]	2.5×10^{-2}	2.5×10^{-2}	3.4×10^{-2}
Probability of release resulting in one or more deaths per year	2.2×10^{-5}	3.6×10^{-6}	1.7×10^{-5}

(a) A release which has no measurable consequence to the general public.

6×10^{11}. The total risk from truck accidents involving spent fuel is compared to the risk from other kinds of accidents and natural disasters in Table 11.3.

Figure 11.2 shows the risk spectrum from spent fuel shipments to both interim storage and reprocessing plants for 180-day cooled fuel. The risk for shipment to reprocessing plants is slightly less than that for shipping to interim storage. The difference of about 20% is due to the different shipping routes for the two scenarios. Although the average shipment distance for shipping to reprocessing plants is longer, the difference in population distributions along the shipping routes accounts for the lower risk.

The results of this study indicate that the risk of shipping spent fuel by truck is lower than the risk of shipping plutonium by air, but somewhat higher than the risk of shipping plutonium by rail. The spent fuel risk is about the same as that of shipping uranium hexafluoride (UF_6) by truck and train.[(5)] The risk of shipping spent fuel is well below the spectrum presented for man caused events. The spent fuel risk spectrum is also below natural occurring risks such as the risk of fatality from being struck by a meteorite. The likelihood of one or more fatalities from a

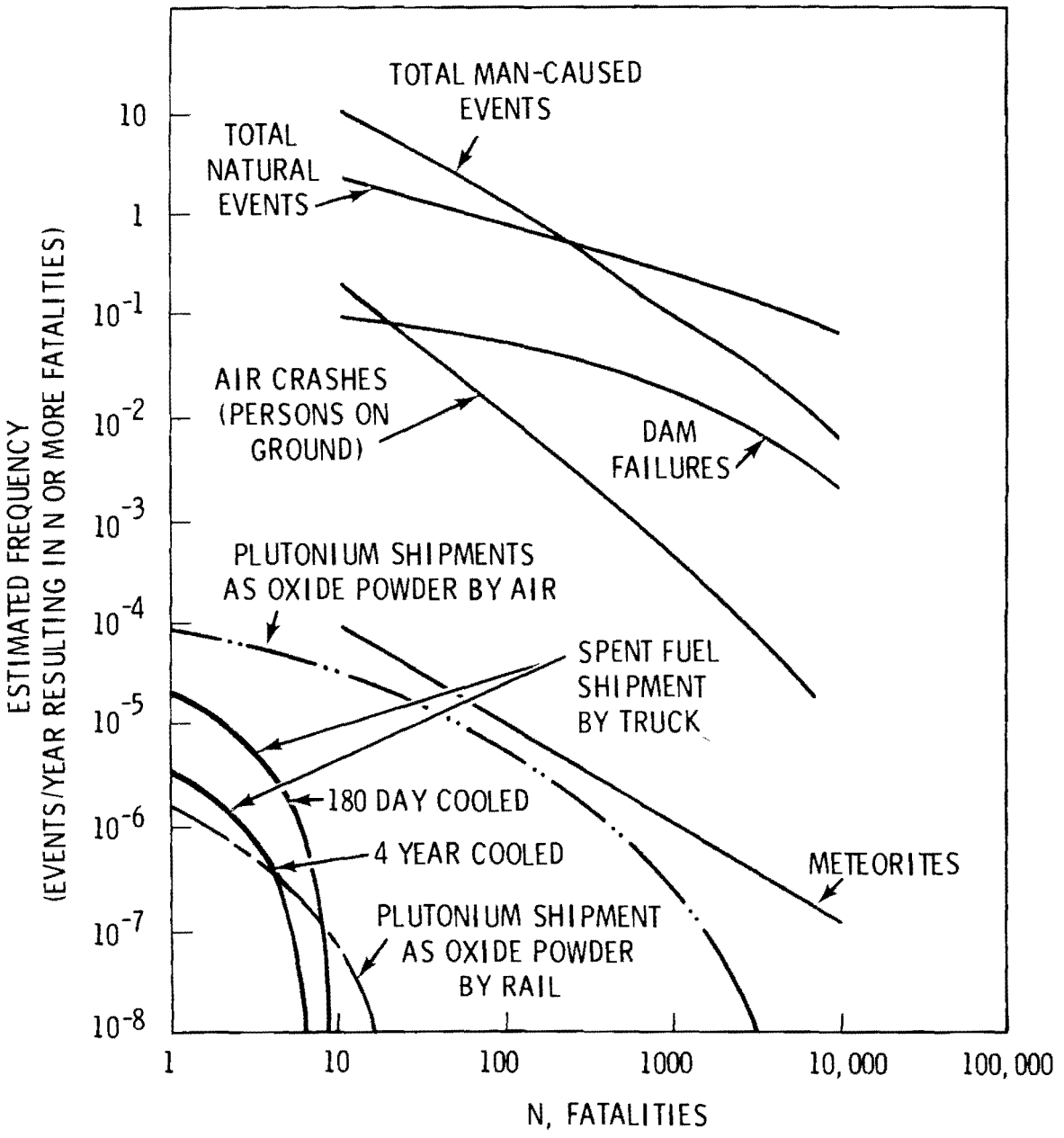

FIGURE 11.1. Risk Spectrum for Shipment of Spent Fuel to Interim Storage and Other Risk Spectra

TABLE 11.3 Average Total and Individual Risk from Various Accidents and Natural Disasters

Event	Total Risk (Fatalities/year)[a]	Individual Risk[b]
All accidents	103,030	1 in 2,000
Motor vehicle accidents	46,700	1 in 4,000
Air crashes	1,552	1 in 130,000
Dam failures	35[c]	1 in 5,700,000
Air crashes (persons on ground)	6[d]	1 in 33,000,000[e]
Meteorites	1.0×10^{-3}[f]	1 in 2×10^{11}
Spent fuel truck shipments, 180-day cooled (excess cancer fatalities)	4.5×10^{-5}	1 in 6×10^{11}[e]

(a) Based on 1975 statistics unless otherwise noted.
(b) Based on total U.S. population.
(c) Average for dam failures 1889-1972 (ref. 1).
(d) Average for years 1960-1973 (ref. 1).
(e) Based on population at risk
(f) From Reference 1.

spent fuel release from one truck shipment is about 1 in 15.5 million. Calculations for this risk analysis showed that the highest number of fatalities occurred under very stable atmosphere conditions (Pasquill F stability) and at one meter per second wind speeds.

The risk values derived in this study are believed to represent a conservative upper limit because of the assumptions used in the analysis. These assumptions include:

- Conservative failure thresholds based on maximum decay heat load
- Conservative accident environment data
- Conservative release fractions
- No corrective action taken in loss of cavity cooling situations

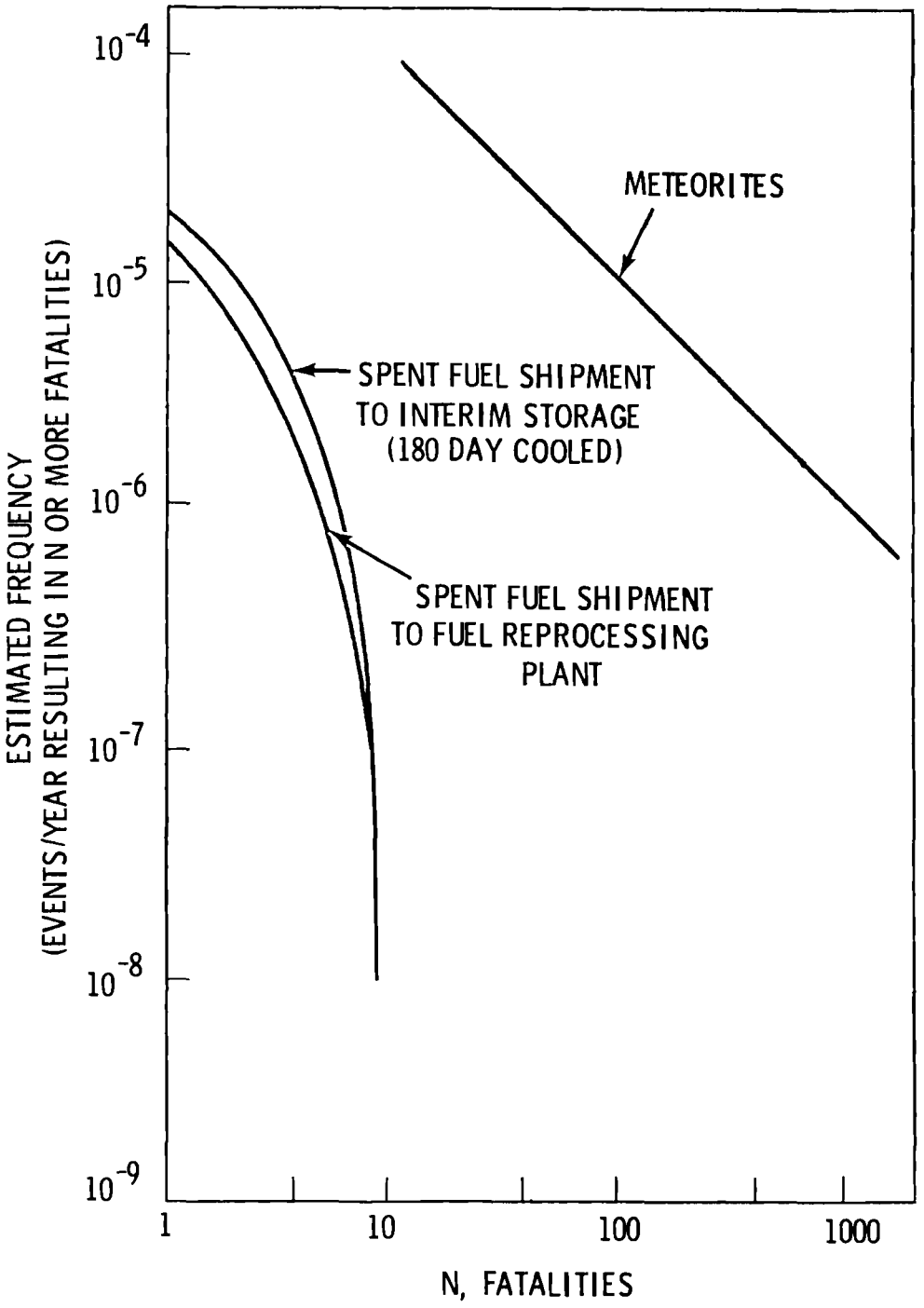

FIGURE 11.2. Risk Spectra for Spent Fuel Shipments in the Mid-1980's

The risks from spent fuel shipment by truck are significantly smaller than many other man-caused and natural risks to which society and individuals are exposed. Society commonly accepts risks which represent a hazard significantly greater than the shipment of spent fuel. It should be noted that the spectra for other societal risks include both latent (long term) and acute (short term) fatalities, whereas there are no acute fatalities related to the radiological consequences of shipping spent fuel.

11.2 MAJOR CONTRIBUTORS TO OVERALL RISK

The release sequences developed from the fault tree were categorized into eight accident scenarios and assigned release fractions based on the different scenarios. The dominant release sequences were ordered using a risk fraction determined from the computer code RAFT[7] based on the product of the probability of occurrence of the sequence and the release fraction. The risk fraction is a relative measure of the risk of each release sequence. The highest ordered release sequence involved a fire accident which resulted in a loss of coolant from the rupture disk with consequent fuel failure. This release sequence accounted for about 24% of the accumulative risk fraction. Fire is also involved in the 6th ranked release sequence which results in failure of the closure seal and accounted for about 4% of the risk. Eighteen out of the 20 highest release sequences involved an impact accident with resulting fuel failure. The highest 20-release sequences accounted for about 96% of the accumulative risk fraction. The remaining 4% of the release sequences primarily involve failures in accidents that occur when nonstandard packaging conditions are present.

11.3 RISK SENSITIVITY STUDIES

Before analyzing the sensitivity of the risk evaluation to the value of certain system parameters, it is important to note a fundamental sensitivity of the risk evaluation. The calculated risk is a function of the shipping assumptions. Use of different shipping routes, different containers, changes in the predicted industry growth rate, etc., would result in a different risk. In general, reevaluation of the risk would be required for these changed conditions.

Risk sensitivity evaluations permit analysis of the importance of the various factors that contribute to the risk. They can be used to identify and quantify the effects of the major contributors to the risk and study the effects of possible design or regulatory changes on the risk. Most sensitivity studies are performed by repeating the risk calculation with a changed value for the parameter of interest. In general, the dependence of the risk on a particular parameter is complex. In some cases, however, the parameter enters simply and directly into the risk calculation and the sensitivity can be determined directly.

The results of the risk sensitivity studies for the shipment of spent fuel in the reference cask are presented in Table 11.4. The effects on the risk spectrum of the sensitivity studies are shown in Figure 11.3. In the base case failure of the cask and components by impact forces contributed to 69% of all releases, failure of the rupture disk and closure seal due to fire, 28%, and accidents that occur when packaging deficiencies are present to about 3% of the releases. Changes in the values of the parameters which affect these release sequences could have a significant effect on the total risk.

The sensitivity of the risk to impact failure threshold forces was determined by assuming that the cask could absorb more impact energy before failing, thus increasing the failure threshold velocities. A 27% reduction in risk level resulted by assuming that 20% more impact energy could be absorbed by the cask. Since the failure thresholds were conservatively calculated, the risk values for the base case are believed to represent a conservative upper limit.

For short-cooled fuel, two possible methods of reducing the effect of fire were investigated. Both involve replacement of equipment on the reference cask which is vulnerable to high temperatures caused by fire. In a 1010°C fire lasting longer than 15 minutes, the cask will overheat and after 4.5 hours the rupture disk on the cask will relieve allowing cavity coolant to escape. It was conservatively assumed that all the coolant would be released instantaneously. If the rupture disk is replaced with a relief valve, the pressure can be relieved without expelling all of the coolant. A fire would

TABLE 11.4 Risk Sensitivity Cases for Spent Fuel Shipments for U.S. in Mid-1980's

Description of Sensitivity Case	Risk Level (Estimated Annual Frequency of Occurrence of One or More Fatalities)	Risk Level Relative to Base Case
Base case[a] (180-day cooled fuel)	2.2×10^{-5}	--
Corrective action to provide cask cooling	1.4×10^{-5}	0.64
Increased impact failure threshold (20% more energy)	1.6×10^{-5}	0.73
Install pressure relief valve (no rupture disk)	1.7×10^{-5}	0.76
Install high temperature O-ring closure seal (no release from seal in fire)	2.11×10^{-5}	0.96
Zero packaging condition deficiencies	2.13×10^{-5}	0.97
All release fractions times factor of 10	1.8×10^{-4}	8.0

(a) Shipment in mid-1980's as described in Section 11.1.2.

then have to burn an estimated 1.5 hours to cause fuel clad failure in the cask with a pressure relief valve installed.[6] This results in a decrease in probability for the accident sequence leading to a release due to loss of cavity coolant through the rupture disk. It was determined that a 24% reduction in risk level would result if the rupture disk is replaced with a pressure relief valve. This also shows that the failure sequence which includes the rupture disk has a significant effect on the risk.

The cask closure seal, consisting of a set of teflon O-rings, was estimated to fail in a fire accident lasting longer than 30 minutes. If the teflon O-rings were replaced with a high temperature material, no release from the seal would result in a fire accident. The risk would be reduced

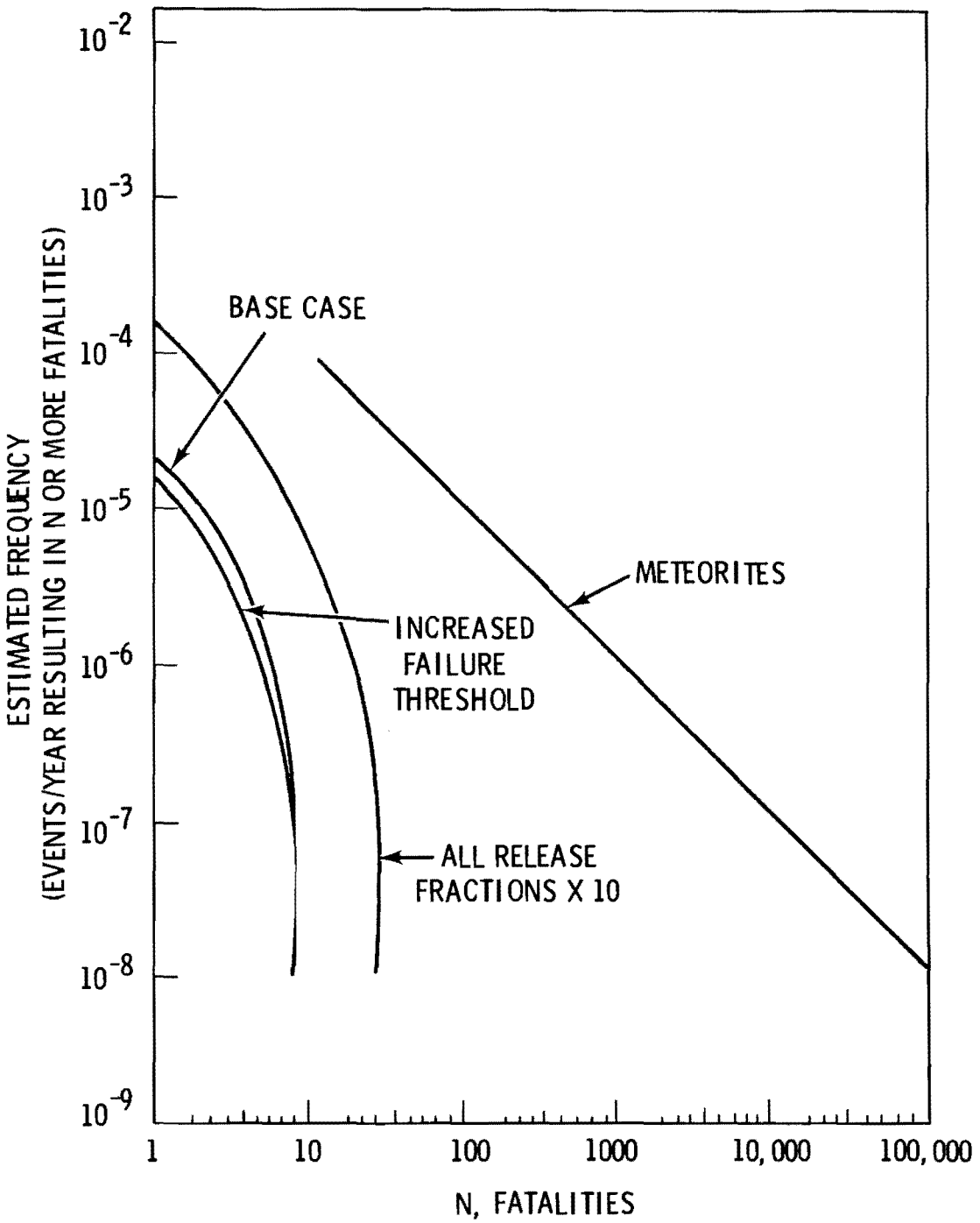

FIGURE 11.3. Risk Spectra for Sensitivity Cases

about 4% in this case. The failure sequence which includes this component is a contributor to the risk, but is not a controlling factor.

A sensitivity study was performed to determine the effects of packaging errors on the risk. The case was evaluated assuming no packaging errors were present during the shipment. Only a 3% reduction in risk level would occur, indicating that packaging deficiencies are not a controlling factor.

It was assumed in the base case that no corrective action by transport or emergency personnel could be taken at an accident scene to replace cavity coolant that was lost. This corrective action could reduce the risk by preventing fuel overheating and subsequent fuel clad failure. Sensitivity analysis showed a 36% reduction in risk level if corrective action could be taken to provide cask cooling within two hours of the accident. To assure that corrective action could be taken if an accident occurred would entail that trained emergency personnel be available at the accident scene within two hours.

To illustrate the sensitivity of the risk to the release fractions used in the base case, it was assumed that all release fractions were increased by a factor of 10. This case represents an upper limit example since the release fractions developed in Section 9 are believed to be conservative. Increasing all the release fractions by a factor of 10 makes them very conservative. It is seen from the sensitivity analysis that this increases the risk by a factor of eight. Conservative extensions of existing data on the fractions of radioactivity released under simulated extreme accident conditions could increase the certainty of the risk evaluation.

These sensitivity studies have identified the major contributors to the shipment risk, potential methods of significantly reducing the risk and areas in which further studies could result in increased knowledge of events and processes which affect the risk assessment.

REFERENCES

1. Reactor Safety Study - An Assessment of the Accident Risks in U.S. Commercial Nuclear Power Plants. WASH-1400 (NUREG-75/014), U.S. Nuclear Regulatory Commission, Washington DC, October 1975.

2. T. I. McSweeney, R. J. Hall et al., An Assessment of the Risk of Transporting Plutonium Oxide and Liquid Plutonium Nitrate by Train. BNWL-1846, Battelle, Pacific Northwest Laboratories, Richland, WA, August 1975.

3. R. J. Hall et al., An Assessment of the Risk of Transporting Plutonium Dioxide and Liquid Plutonium Nitrate by Train. BNWL-1996, Battelle, Pacific Northwest Laboratories, Richland, WA, February 1977.

4. T. I. McSweeney and J. F. Johnson, An Assessment of the Risk of Transporting Plutonium Dioxide by Cargo Aircraft. BNWL-2030, Battelle, Pacific Northwest Laboratories, Richland, WA, June 1977.

5. J. F. Johnson et al., An Assessment of the Risk of Transporting Uranium Hexafluoride by Truck and Train. PNL-2211, Battelle, Pacific Northwest Laboratories, Richland, WA, August 1978.

6. S. R. Fields, Thermal Analysis of a One Element PWR Spent Fuel Shipping Cask. HEDL-TME78-105, Hanford Engineering Development Laboratory, April 1977.

7. G. D. Seybold, RAFT: A Computer Program for Fault Tree Risk Calculations. BNWL-2146, Battelle, Pacific Northwest Laboratories, Richland, WA, November 1977.

APPENDIX A

DESCRIPTION OF REFERENCE SPENT FUEL SHIPPING CASK

The reference cask used for analysis in this study is a legal weight truck cask which is designed to handle the large size and high burn up present generation reactor fuel. It is water filled and air cooled and designed to transport 1-PWR or 2-BWR spent fuel assemblies. This cask can be transported across country without restriction as to legal weight limits.

Table A.1 summarizes some of the significant parameters of the reference cask. Figure A.1 shows a cutaway view of the cask and Figure A.2 shows the cask and trailer in schematic form. Figure A.3 shows the cask assembly drawing and Figure A.4 shows a cross section of the cask. Detailed data on the cask are presented in Tables A.2 and A.3. Material properties of the cask used in calculations for failure thresholds are presented in Table A.4.

TABLE A.1. Reference Cask Operational and Fuel Limitations

Operations		
Fuel Decay - Minimum		120 Days
Fuel Burnup - Maximum		40,000 MWD/MTU
Decay Heat - Maximum		11.5 KW
Fuel Assembly	PWR F/A	BWR F/A
No. of Assemblies	1	2
Envelope, cm(a)	21.84 (8.60 in.)	13.82 (5.44 in.)
Length, cm(a)	450 (177 in.)	450 (177 in.)
Active Length, cm(a)	381 (150 in.)	366 (144 in.)
Enrichment, w/o ^{235}U(a)	3.6	3.0
Weight U, Kg(a)	461.4	188.7

(a) Indicates maximum value.

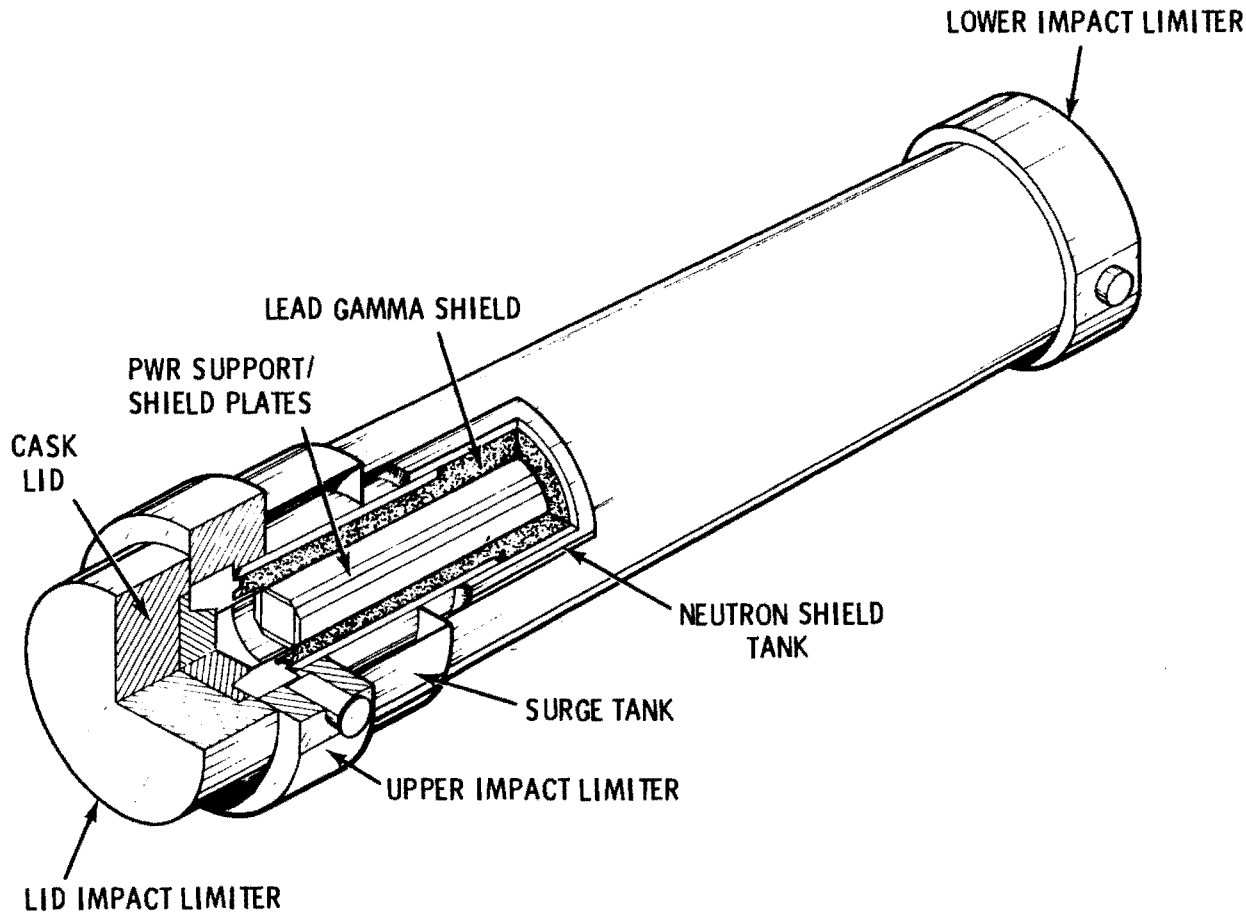

FIGURE A.1. Reference Spent Fuel Shipping Cask

The overall dimensions of the cask include a length of 544 cm (214 in.) and a diameter of 96.5 cm (38 in.). The cask has an inner cavity of 452 cm (178 in.) in length and 34.3 cm (13 1/2 in.) in diameter. Spent reactor fuel is supported inside of the inner cavity by interchangeable fuel baskets (see Figure A.4) for 1-PWR or 2-BWR assemblies. The fuel assembly is supported by four removable 2.5-cm (1 in.) support plates. The support plates rest on support tabs permanently attached to the cavity interior. The cavity is filled with water which transfers the decay heat from the spent fuel elements by convection to the 0.8-cm (5/16-in.) thick stainless steel inner cavity wall and through the wall by conduction. Immediately outside of this wall is a 16.8-cm (6 5/8-in.) thick lead gamma-ray shield surrounded by a 3.2 cm (1 1/4-in.) thick stainless steel outer shell penetration barrier. Heat

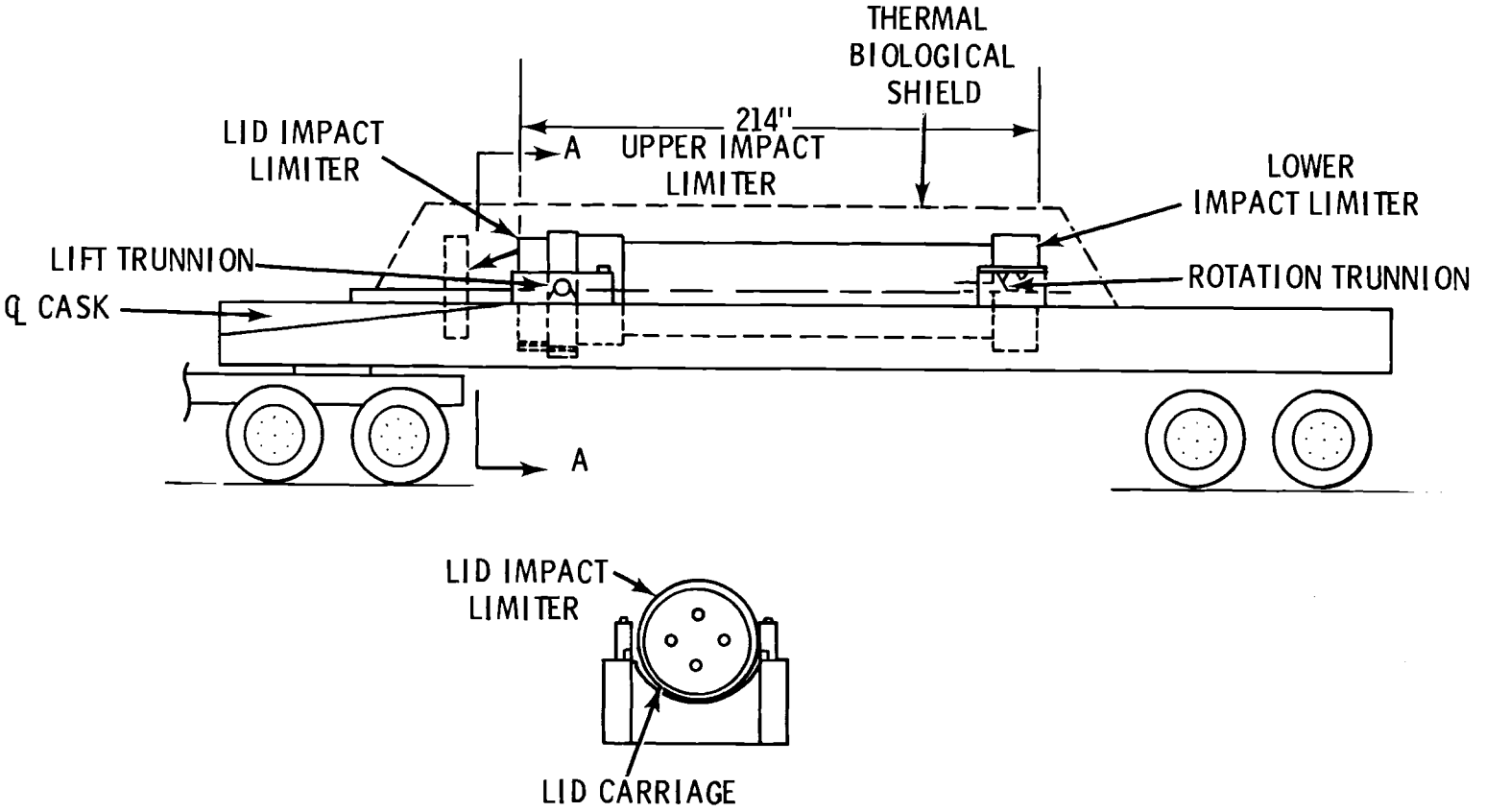

FIGURE A.2. Reference Cask/Trailer Schematic

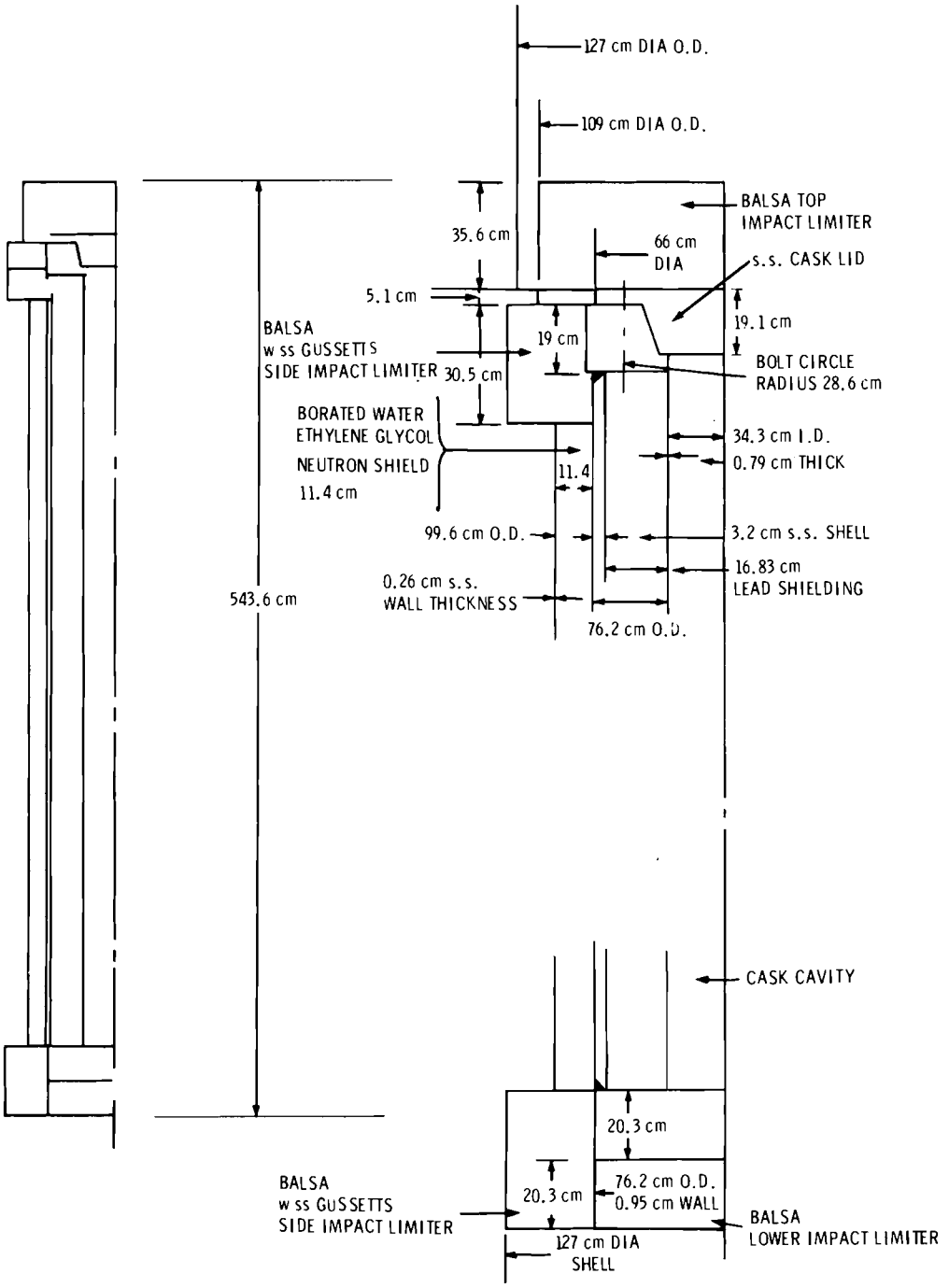

FIGURE A.3. Cask Assembly Drawing

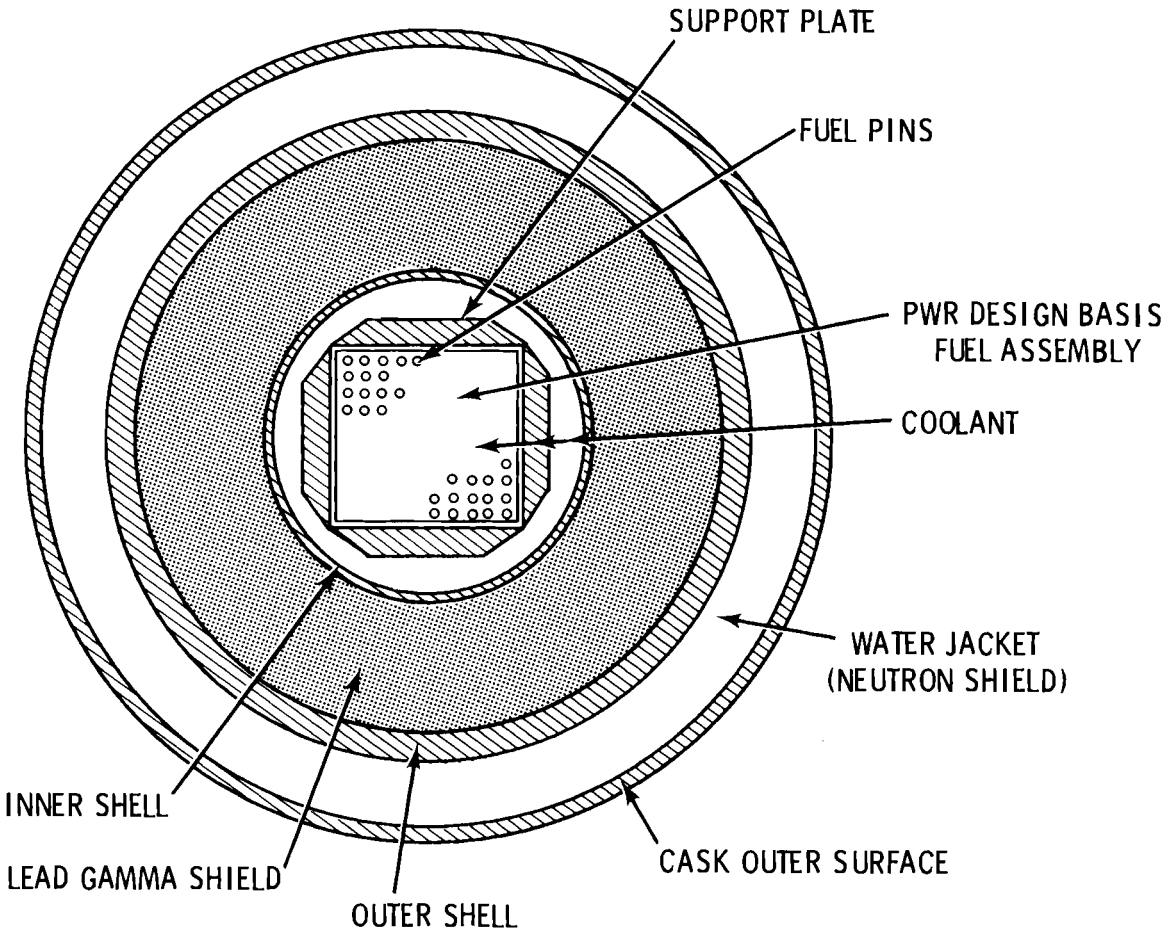

FIGURE A.4. Reference Spent Fuel Shipping Cask Cross Section

passes through both by conduction. Immediately outside of the penetration barrier is the 11.4-cm (4 1/2-in.) thick borated water antifreeze neutron shield solution contained within the 1.27-cm (1/2-in.) thick stainless steel neutron shield tank. The neutron shield consists of an annular region composed of four 90° isolated compartments. Nominal operating pressure in the neutron shield is assumed to be 6.2 atm and the pressure relief valves, set at 6.8 atm, are located midway along the length of the shield. Figure A.1 shows that this tank contains an expansion chamber to assure uniform water shielding thickness at all times.

The heat that is conducted through the penetration barrier is transferred by convection through the water neutron shield. It is conducted through the neutron shield tank wall and enters the atmosphere through radiation and convection. No active cooling is used.

TABLE A.2. Characteristics of Reference Spent Fuel Shipping Cask

Fuel Assembly	
Overall dimensions, inches (slotted envelope)	8.576 x 8.576
Active length	365 cm (144 in.)
Length	386 cm (152 in.)
Number of Fuel Rods	289
Pin Array	17 x 17
Pin Pitch	1.26 cm (0.496 in.)
Pin Diameter	0.949 cm (0.374 in.)
Pin Clad Thickness	0.0572 cm (0.0225 in.)
Pin Clad Material	Zr-4
Weight, Kg	680.4 (1500 lbs)
Enrichment, w/o ^{235}U	3.6
Weight, U	461.4 Kg
H/U Ratio	5.72

TABLE A.3. Characteristics of Design Basis PWR Fuel

Cask		
Cask Length, cm	544	(214 in.)
Cavity Diameter, cm	34.3	(13.5 in.)
Cavity Length, cm	452.1	(178. in.)
Inner Shell Thickness, cm	0.79	(0.312 in.)
Lead Shield Thickness, cm	16.8	(6.625 in.)
Outer Shell Thickness, cm	3.2	(1.25 in.)
Water Jacket Thickness, cm	11.4	(4.5 in.)
Thickness of Outer Shell of Water Jacket, cm	0.27	(0.105 in.)
Maximum Amount of Decay Heat, KW	12.4	
Fuel Support and Shield Plates		
Material	Stainless Steel	
Thickness, cm	2.54	(1.0 in.)
Approximate Distance from Cavity Wall, cm	1.27	(0.5 in.)
Provision for Coolant Circulation	Holes in Both Ends of Plate	

TABLE A.4. Material Properties

Stainless Steel	Yield stress:	2.069×10^4 nt/cm$^{2(a)}$
	E Modulus of elasticity:	2.06×10^7 nt/cm^2
	ν Poisson's ratio:	0.3
	Dynamic flow stress:	3.448×10^4 nt/cm^2
	Ultimate stress:	6.209×10^4 6330 nt/cm^2
Lead	Yield stress:	1.37×10^3 nt/cm^2
	Dynamic flow stress:	3.43×10^3 350 nt/cm^2
Zircaloy	Ultimate stress:	6.209×10^4 nt/cm^2
	E Modulus of elasticity:	8.96×10^6 nt/cm^2
Balsa Wood	Crush strength parallel to the grain	1.09×10^3
	Top disk and top ring impact limiter 112	1.09×10^3 nt/cm^2
	Bottom disk impact limiter 210.0	2.06×10^3 nt/cm^2

(a) 2.413×10^4 nt/cm^2 used to allow for some strain hardening.

The inner cavity is closed by the cask lid which seals and shields the cask cavity. It is solid stainless steel and is attached to the cask by six high strength bolts. Two teflon O-rings, arranged so that each may be pressure tested, provide the head seal. Nominal cavity pressure is 12 atm. A rupture disk vents the cavity to atmosphere when cavity pressure exceeds 76 atm.

Side mounted ring type balsa wood impact limiters, encased in stainless steel, are permanently located at both ends of the cask to provide necessary crash protection in side-on or horizontal impact. At the bottom end of the cask, the ring structure consists of a 0.76 m I.D. x 1.27 m O.D. annular structure with eight 0.95 cm thick radial steel gussets as shown in Figure A.5. This structure is 41 cm long. The internal cylindrical surface of the impact limiter consists of a 0.95 cm thick stainless steel shell. The lower impact limiter also serves as an expanded base when the cask is set vertical.

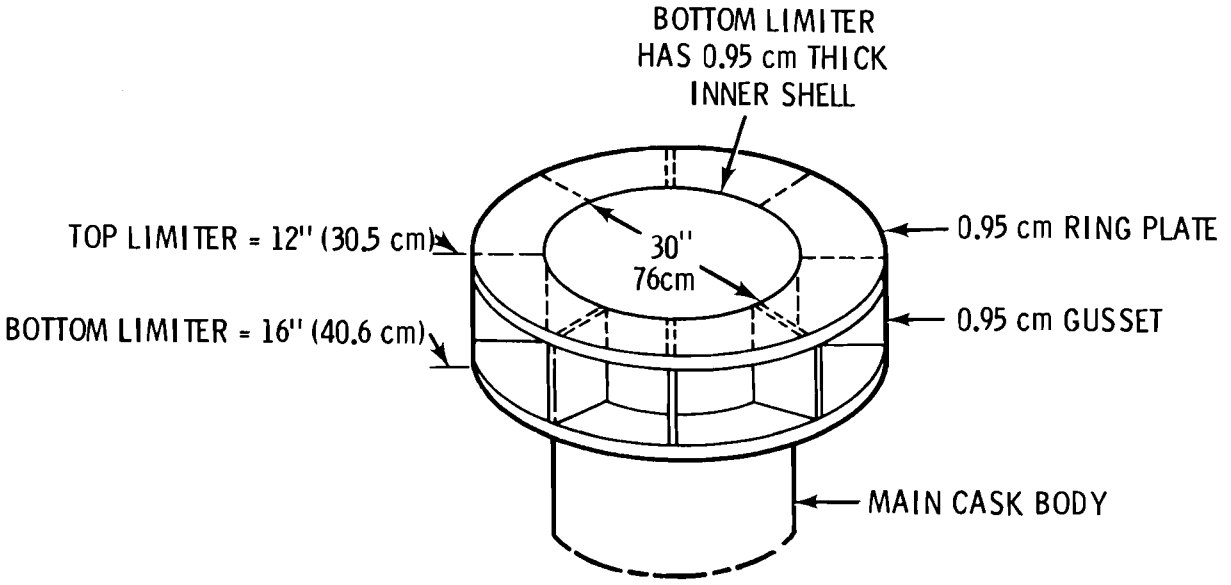

FIGURE A.5. Ring Impact Limiter Details

A removable impact limiter of similar design with 30.5 cm length is used to protect the cask head. The eight cavities in the limiter are filled with balsa wood (grain aligned radially) with a crush strength of 1.09×10^3 nt/cm^2. This limiter is normally removed and stored on the transport trailer during normal unloading operation. Necessary connections to the primary cavity (i.e., vent and drain valves, pressure test connections, and relief valves) are buried within the impact limiter and special structure for protection during accident conditions.

Sacrificial impact limiters exist on both ends of the cask to absorb end impact energy. On the top or lid end, a balsa wood (1.09×10^3 nt/cm^2 crush strength) impact limiter with grain parallel to the cask axis exists and is assumed clad in light gauge sheet metal. This impact limiter is attached to the cask lid by four 3.2 cm bolts.

At the bottom end of the cask, a disk of balsa (2.06×10^3 nt/cm^2 crush strength) is located in a cavity internal to the bottom ring impact limiter. A 0.95 cm thick stainless steel shell which serves as an internal surface of the bottom ring impact limiter surrounds the balsa disk. For end-on and center of gravity impact conditions, the bottom axial impact limiter will be considered equivalent to the top axial impact limiter.

The bottom end of the cask consists of a 20-cm thick disk of stainless steel welded to the main 3.2 cm cask sheel and the inner cavity shell. The top portion of the cask consists of a stainless steel ring flange welded to the cask shells in a similar fashion.

Two sets of trunnions are used for normal cask handling and transport tie-down purposes. The upper set, attached to the upper impact limiter, is used for lifting the cask in conjunction with a special "swing arm" type yoke. This yoke is normally permanently locked to the lift trunnions throughout the complete handling cycle at the reactor or reprocessing site. The lower trunnions are off-set to provide a gravity pivot from the vertical loading position into the horizontal transport mode.

The primary cavity is designed to withstand temperature and pressure conditions of 278°C (532°F) and 67 atm (984 psig) under the fire accident condition [1/2 hr at a temperature of 800°C (1475°F)]. Maximum transport conditions for design basis fuel [i.e., 550°C, (130°F)] direct sunlight, still air, maximum fuel burnup, minimum fuel cooling period) are 174°C (345°F) and 10 atm (150 psig.).

There are two 1/2-inch drain holes in the bottom end of the cask for draining purposes. The drain holes open to the end of the cask cavity and are drilled through the gamma shield to ball valves imbedded in the outer perimeter. Access tubes are provided through the lower impact limiter and are sealed with port covers and o-ring seals. A vent valve similar to the drain valves is also provided in a counter bore in the cavity flange. A 1/2-in. diameter rupture disk is buried in the cavity flange and connected to the cask cavity. The rupture disk assembly is mounted in a counterbore sealed by a cap and also has a safety relief valve as a backup.

APPENDIX B

POTENTIAL RELEASES FROM A TRUCK TRANSPORTED SPENT FUEL CASK DURING POSTULATED ACCIDENT CONDITIONS

B.1 FACTORS INFLUENCING AIRBORNE RELEASE

In the unlikely event of an accident severe enough to release activity from a spent fuel cask, the material, its dispersability and the time of release are of concern. Many factors influence the airborne release of activity from a spent fuel cask. Some, but not necessarily all, are as follows:

- physical and chemical characteristics of the source material and how it is altered during and after the accident.
- container design and post-accident integrity, and
- corrective action taken by persons at the accident scene.

Estimates of the potential releases under postulated accident conditions can be obtained in several ways. The best way to estimate releases would be to use values derived from actual accident experience under similar circumstances. Such data are not available since no releases have occurred. Thus, the data from other than actual accidents must be used. There are two sources of data that can be used; that derived from experimental simulations and that developed from the known chemical and physical responses of the materials involved. The former is preferable since it can encompass some of the conditions postulated for the accident. However, accidents are unique events and cannot be exactly duplicated, so engineering judgment is required to arrive at realistic estimates.

An additional consideration in the quantification of releases is their ultimate use. Release fraction values are only an intermediate step in the assessment of the potential consequences to man. Other physical processes which are influential in determining the quantity of airborne material which effects man are atmospheric transport and respiration rate. Both of these

processes are sensitive to the size of airborne radioactive particles. It is not within the scope of this appendix to discuss either topic, but there are size limitations under various conditions for both.[1,2,3] Considering both processes, the significant size fraction of assumed particulate releases was assumed to be less than 10 μm Aerodynamic Equivalent Diameter.[a]

B.2 POTENTIAL RELEASES

This section summarizes the existing fractional airborne release information applicable to radioactive fission products.

Migration of volatile fission products radially outward to the cooler cladding under reactor conditions is one mechanism of release from the fuel matrix. In the absence of chemical reactions or mechanical damage, the migrated elements are the total potential release. Davies, et al[4] analyzed cladding deposits on rods from a BWR element which was ramped at high power to failure. Table B-1 shows an enhancement factor for the listed fission products over what was expected from peripheral burnup. The extent of fission product release is dependent on reactor operating parameters. Total burnup and linear heat rate histories are important in the generation and release of fission products from the fuel pellets.[5] While these migrated elements represent a potential release, a driving force is necessary for their escape from the fuel cladding. Realistic mechanisms are selective in the radionuclides that are released and would allow only a small fraction of the total gap inventory to escape the cladding.

Fission produce release from a spent fuel element in a cask would probably occur continuously until the system cooled following postulated accidents severe enough to cause damage. Release rates from the fuel would vary over wide limits depending on system temperatures, fission product properties, and the physical condition of the fuel following the accident. It is possible to identify four conditions at which major driving forces for release exist. These periods of high rates would account for most of the total release.

(a) Behaves in air as a sphere of unit density of the stated size.

TABLE B-1. Analysis of Cladding Deposits[4]

Element	Concentration Observed (μgm/gmU)	Predicted (μgm/gmU)	Enhancement Factor
Cesium	119,000	1,940	61
Tellurium	42,600	318	134
Barium	20,000	995	20
Iodine	11,600	201	58
Cadmium	2,700	41.2	66
Cerium	2,410	2,150	1.1
Palladium	1,030	669	1.5
Tin	629	34.3	18
Silver	567	45.9	12
Strontium	577	671	0.9

The four release mechanisms outlined below describe the macroscopic pathways of radionuclide escape from spent fuel elements. Diffusion from the fuel is ignored due to the relatively low temperatures (for solid diffusion) during normal transport conditions and the short high temperature periods of accident conditions.

Retention of radionuclides in the cask cavity is discussed, but is generally difficult to quantify because performance under actual accident conditions is unknown. Conservative assumptions were made to compensate for the uncertainties.

A PWR fuel element is used as the basis for accident source terms in this study. This is conservative for two reasons:

1. The cask can carry 0.4 MTHM of BWR fuel and 0.46 MTHM of PWR fuel.
2. The BWR elements can tolerate higher temperatures before rupture.[6]

GAP RELEASE

Gap release is the energetic venting of pressurized gases from the fuel element plenum and pellet-cladding gap. High temperature creep or mechanical forces may cause the necessary cladding rupture in a spent fuel cask.

Available for release are a fraction of the noble gases, volatile halogens and entrained particulates that have migrated from the fuel during irradiation.

Mathematical models exist for predicting fission gas releases from the fuel pellets in the reactor. Beyer and Hann[7] with burnup correction factors predict an 8% release of the noble gases to the gap from high power (15 kW/ft) PWR rods irradiated to 30,000 MWd/MT. To account for rough handling (fuel pellet fractures) and unusual reactor operating conditions, a 30% release of krypton and xenon was used. Regulation Guide 1.25 suggests this value for krypton. A release of 10% is given for fission product iodine and tritium. Table B.2 summarizes gap inventories available for outgassing.

TABLE B.2. Fraction of Nuclides Available for Release during Outgassing from the Pellet-Cladding Gap

Isotope	Fraction
Kr	0.3
Xe	0.3
I	0.1
^{3}H	0.1
AOFP(a)	
(Impact Failures)	10^{-6}
(Creep Rupture)	2.0×10^{-5}
Actinides(a)	
(Impact Failures)	10^{-6}
(Creep Ruptures)	2.0×10^{-5}
^{14}C	
(Impact Failures)	10^{-6}
(Creep Ruptures)	2.0×10^{-5}

(a) Assume sub 10μm fines.

All Other Fission Products (AOFP), Actinides and Carbon-14 are assumed to be released after an impact or pressurized cladding rupture as particles. The release fraction for impact failures is estimated from work by Smith and Ross.[8] Breakup and release of vitreous high level waste from stainless steel canisters during impact was studied. For an 80-mph test, less than 0.1% of the material was broken into sub-10μm fines. In no case was any weight change detected (detection limit 0.017%) due to material escaping the canister. For impact fuel failures in this study, it was assumed 0.1% of the fines are released as sub-10μm particles. Recent tests have been run to measure releases from fuel elements failed by high temperature creep rupture.

Information from R. A. Lorenz at Oak Ridge National Laboratory (September 1977) indicates that at 900°C up to 0.02% of the fuel in the form of fines may be released during high pressure venting. According to Lorenz (October 1977), ninety per cent of this material settled out near the rupture point which leaves 0.002% available for release in the cask cavity. This value will be used for creep failures in this study. Cubiciotti, et al.[9] reports that UO_2 dust is ejected from fuel in the reactor due to radiation damage.

Advanced fuel designs reduce the linear heat rate and therefore the fission product release. Gap inventories in future fuels may be less than those specified in this study. Actual measurements of fission gas release have been made on fuel irradiated at less than 10 kW/ft to 31,000 MWd/MT. Lorenz, et al[10] examined krypton and xenon releases from irradiated fuel elements and found that less than 2% of the generated gases were released.

The final barrier to atmospheric release is the cask shell. If this containment is breached, essentially all of the noble gases released from the failed fuel elements escape. Iodine would probably be partially retained in the cask cavity but is conservatively assumed to totally escape. For the case of a fire with no breach of the cask except for the rupture disk or valve, 50% retention of particulates is assumed. This value was calculated assuming that the driving forces for escape were the release of pressurized gases and expansion due to heating of steam in the cask cavity.

VAPORIZATION RELEASE

Fission products are released from ruptured fuel elements at elevated temperatures. Low melting point solids volatilize and leave the fuel in gaseous form. If the high temperature environment occurs before cladding failure, then a driving force for release is the venting of internal pressures. For low temperature cladding failures followed by heating, vapor pressures and diffusion cause the release.

Cesium is a primary constituent of the semi-volatile elements. It is estimated that 0.06%[11] of the total is present as metallic cesium on void boundaries before a pressurized element ruptures and that 50% escapes the cladding. This same fraction (0.03%) is conservatively used for passive outgassing following an impact failure and subsequent overheating.

Recent experimental results indicate the conservative nature of the estimates. Lorenz, et al[12] measured cesium release during the heating of pre-drilled high burnup fuel to be less than 6.7×10^{-4}%. Osborne and Parker[13] tested rods to failure which were irradiated to 7,000 MWd/MT and noted releases of 10^{-2}% to 10^{-3}%. Lorenz (September 1977) indicated that 0.03% of the cesium was vented during pressurized rupture of fuel elements.

Partial retention of cesium in the cask cavity is likely. Mechanisms of condensation and plate out or chemical reactions with other materials have been studied. Releases attenuation due to these actions is variable and difficult to quantify, therefore is not used. However, since cesium is a particulate at the lower cask temperatures, cask retention described for the gap particulates was used.

LEACH RELEASE

Leaching of fission products from the fuel pellets requires direct contact of aqueous cask cavity coolant. Contact can occur following an impact which ruptures fuel pins while the cask retains its cavity coolant. Also, undetected failed fuel (fuel which outgasses in the reactor, but is not

detected and overpacked in the spent fuel basin) can release a small amount of fission products to the cask coolant under normal transport conditions.

Releases from fuel contacted by the coolant after an impact failure are presented in Table B-3. The one day and one week data comes from a slow-leach test in deionized water of fuel pellets irradiated to 54,450 MWd/MTU.[14] The releases are conservative since the samples were broken fuel fragments, had free contact with a flowing leachant and enhanced fission product availability due to the high burnup. The one-hour leach releases are outside the experimental data, but were calculated using a logarithmic mechanism model presented in the study. The value listed for all other fission products is based on strontium data. Actinides leached from the pellets are based on plutonium. Ten percent of the fuel in the rods broken by an end-on impact was assumed available for leaching.[15]

TABLE B.3. Fraction of Spent Fuel Constituents Released to Coolant (Deionized Water)

	1 Hour[a]	1 Day	1 Week
Cs	2×10^{-4}	5.5×10^{-4}	1.2×10^{-3}
AOFP[b] (Sr)	3×10^{-5}	7.5×10^{-5}	1.5×10^{-4}
Actinides (Pu)	2×10^{-5}	6×10^{-5}	1.5×10^{-4}

(a) All other fission products.
(b) Calculated from the general equation given in Ref. 14:

Release Fraction = Bt^n

where t is time, and the two isotope constants B and n were given.

Retention of leached radionuclides depends on the integrity of the cask. The cask coolant can escape either as a vapor during venting or as a liquid due to a cask breach. Vaporization external to the cask of the released liquid could also take place. For coolant which escapes the cask and remains a liquid, 1% of the contained activity is assumed to escape as an aerosol.

If an external fire is present, 10% may be in the aerosol.[15] Vaporized coolant vented from the cask is assumed to release all contained activity as sub 10 μm particulates.

OXIDATION RELEASES

Oxidation of some fraction of the UO_2 fuel pellets to U_3O_8 may take place in the unlikely event of a large cask rupture. Increased releases of fission products occur by this mechanism due to a large increase in surface area. The reaction proceeds at insignificant rates in a steam atmosphere.[16] Therefore, a cask breach large enough to allow flowing air to contact the fuel is necessary for this type release.

Experimental data indicate that the rate or oxidation controls the process. After complete oxidation, additional releases were not observed. This study assumed all material contacted by the air is completely oxidized in 90 minutes at 700°C. Table B-4[17] gives release fractions under these conditions. The data are based on fuel irradiated to 7000 MWd/MT heated in air for 90 minutes. The value for all other fission products is based on strontium data. Releases of actinides are assumed negligible because of their low oxidation potential in the fuel matrix.

TABLE B.4. Fission Product Release from PWR-Type UO_2 Irradiated to 7000 MWd/T and Heated in Air to 700°C for 90 Minutes

Fission Product	Percent Release
Kr, Xe	6.
I	15
^{3}H	15
Cs	< 0.005
Ru	0.1
AOFP[a] (Sr)	< 0.0005
^{14}C	< 0.0005

(a) All other fission products.

Containment by the cask of oxidation released fission products is not postulated. Some hold up of the fines is possible, but due to the initiating event of a large cask breach this factor cannot be quantified. However, only fuel pellets contacted by flowing air will be oxidized. For this study, 10% of the fuel rods broken by an end-on impact were available for oxidation. The release is assumed to be in the form of sub 10 μm particles and gases.

B.3 RELEASE CATEGORIES

In order to define the various releases that might occur, a series of release categories were identified for the postulated types of accident conditions or failure of the cask system. Brief descriptions of the various physical processes that define each release category are presented in this section.

Releases from postulated accidents involving the truck transport of spent fuel in a water cooled cask, are reported as fractions of the cask inventory. Releases due to operational errors are reported as curies released. Various failure mode fractions for the fuel elements are defined as follows:

X = Fraction broken on impact

Y = Fraction fail by creep rupture

1. Small, Undetected Leakage of Cavity Coolant[15]

Assume that a truck cask is shipped with an undetected leak of cavity coolant. Due to previously failed fuel which is available for leaching, the cavity coolant is contaminated to a level of 1 μCi/cc with mixed fission products, primarily ^{137}Cs. The cask water volume is estimated to be 1.9×10^5 cc so the contained activity would be 0.19 Ci. The largest leak that would go undetected is estimated to be 0.001 cc/sec. One percent of the released activity would escape to the atmosphere as a sub 10 μm aerosol at ground level.

2. Slow Leak of Cavity Coolant Due to a Gasket Failure

A gasket in the truck cask which retains the cavity coolant fails in transit. A leak 1000 times larger than Case 1 or 1 cc/sec continues, for four hours until discovery and mitigation by the driver. The coolant contains 1 μCi/cc of ^{137}Cs. One percent of the activity which escapes the cask is released to the atmosphere as a sub 10 μm aerosol at ground level.

3. Impact and Slow Leak of Cavity Coolant

The truck cask is involved in an impact which causes some fuel element failures and a small leak of cask cavity coolant to the ground. Ten percent of the fuel in the broken rods is contacted by the cavity coolant. Particulates released from the gap (AOFP) would also be absorbed in the coolant. The leak rate is assumed to be 1 cc/sec. Atmospheric releases are the gaseous gap release fractions (Kr, Xe, I) in Table 2 and 1% of the activity in the escaping coolant.

For three hours following the accident, if the cask is level, all of the fuel elements will be immersed in the coolant. As the water drains away from the fuel, some rods will lose their cooling capacity. Self heating to failure as described in Case 4 (below) could occur. Failures could be avoided by retrieving the cask and implementing emergency measures to stop the coolant leakage. Activity released from the cask during the three hours following the accident before the fuel overheats is listed below. The coefficient in the release to the coolant are due to the holdup in the cask. A factor is needed to convert the leach data and gap activity to a fraction released per hour from the cask.

a. Gap (Kr, Xe, I, ^{3}H only)[(a)] - (Table 2 fractions impact failure) X

b. Coolant[(b)] - $1.9 \times 10^{-2} \times t$ [0.1 (Activity in Table 3 - 1 day)]
+ (AOFP, Actinides and ^{14}C in Table 2 - Impact Failures)

t = time of leak termination (hours) $0 < t < 5$

(a) Gaseous release at ground level.
(b) One percent of activity released to atmosphere as a sub 10 μm aerosol at ground level.

4. Severe Cask Impact With a Rapid Loss of Cavity Coolant

The postulated impact is severe enough to rupture the cask and all fuel cladding. This results in an immediate loss of coolant and air is admitted to the cask cavity. Thermal analysis for this cask indicates that the fuel would reach temperatures above 1050°F in about two hours.

Releases from this accident are due to the loss of coolant, impact releases of the gap activity, volatilization of available cesium and oxidation of exposed pellets. The five hour releases are as follows:

a. Gap[(a)] - (Table 2 fractions - Impact Failure) 1.
b. Coolant[(b)] - 0.19 Ci of mixed fission product (primarily ^{137}Cs).
c. Volatiles[(a)] (cesium) - 0.0003.
d. Oxidation[(a)] - 0.1 (Table 4 fractions) X.

(a) Nongaseous fission products released as sub 10 μm fines at ground level.
(b) 1% of this activity released to the atmosphere as a sub 10 μm aerosol.

5. Cask Involved in a Two Hour 1850°F Fire

This accident postulates an accidental fire external to the cask-truck system. No impact forces are involved. Thermal analysis (Appendix A) indicates that the cask coolant would be lost about 0.6 hours after the fire starts leaving a steam atmosphere in the cask cavity. The rupture disk relieves the cask pressure and does not reseal. Fuel would reach 1050°F in 1.9 hours. Fuel elements begin to creep rupture at this time.[(a)(5)] All pins are assumed failed in 2.6 hours.

During this accident, the cask releases the cavity coolant, all gap inventories and volatile cesium as follows:

(a) Based on a calculation of stresses due to internal pressure. Ten-hour creep failure data used for material properties. Conservatively assumed immediate failure upon reaching 1050°F.

a. Gap[a,b] - (Table 2 fractions - Creep Rupture) 1.
b. Coolant[c,d] - 0.19 Ci of mixed fission products (primarily ^{137}Cs).
c. Volatiles [a,b,c] (cesium) - 0.0003.

(a) Released after fire extinguished at ground level.
(b) Half of these particulates remain in the cask.
(c) Activity released as sub 10 μm fines.
(d) Released to fire plume.

6. Cask Impacted Followed by Two-Hour 1850°F Fire

This accident is the combination of an impact which may fail a fraction of the fuel elements followed by a 2-hr 1850°F fire. No releases are postulated until the pressure relief rupture disk vents the vaporized coolant after 0.6 hours leaving a steam atmosphere in the cask. The coolant contains all nuclides leached from 10% of the impact-failed fuel elements. Fission gases from broken rods are also vented. The remaining unfailed fuel reaches perforation temperatures and fails between 1.9 and 2.6 hours after the fire begins. Cesium isotopes are volatilized from all failed fuel elements. The releases are as follows:

a. Gap[a,b] - (Table 2 fractions - Impact Failure) X.
   [c,b] - (Table 2 fractions - Creep Rupture) Y.
b. Coolant[d,a] - 0.1 (Table 3 fractions - 1 hour) X.
c. Volatiles[b,c,d] (cesium) - 0.0003.

(a) Released to fire plume.
(b) Half of these particulates remain in the cask.
(c) Released after fire extinguished at ground level.
(d) Activity released as sub 10 μm.

7. Severe Cask Impact Followed by a Two-Hour 1850°F Fire

The postulated impact in this accident is severe enough to cause a large breach in the cask and fail all fuel elements. Air is allowed into the cavity. The coolant is immediately lost to the ground. Fission gases from all rods are vented. The fire causes the fuel to reach volatilization temperatures in 1.9 hours. Exposed fuel pellets are oxidized and cesium is volatilized from all failed fuel. The releases are as follows:

a. Gap[a] - (Table 2 fractions - Impact Failure) 1.

b. Coolant - 0.19 Ci (mixed fission products primarily ^{137}Cs). Assume 10% of the activity is released to the fire plume as an aerosol.[b]

c. Volatiles (cesium)[b,c] - 0.0003

d. Oxidation[b,c] - 0.1 (Table 4 fractions) 1.

(a) Released to fire plumes.
(b) Released as sub 10 μm particles.
(c) Released after fire extinquished at ground level.

8. Rapid Loss of Cavity Coolant Due to Cask Closure Device Failure

A cask accident which fails a cask closure device other than the head is possible. An example of this would be a valve failure. The cask was conservatively assumed to be in an orientation which allows complete draining of the cavity coolant to the ground. Thermal analysis for this cask indicates perforation temperatures (1050°F) would be reached within 2 hours by self-heating. All the fuel elements would fail within 3 hours of the accident. This accident may release the gap activity, coolant and volatile elements as follows:

a. Gap[a] - (Table 2 fractions - Creep Rupture) 1.

b. Coolant[b] - 0.19 Ci of mixed fission products (primarily ^{137}Cs).

c. Volatiles[c,a] (cesium) - 0.0003.

(a) Half of these particulates will remain in the cask.
(b) 1% of this activity released as an aerosol at ground level.
(c) Released as sub 10 μm particles at ground level.

REFERENCES

1. "Report of Task Group and Lung Dynamics to ICRP Committee 2. Deposition and Retention Models for Internal Dosimetry to Human Respiratory Tract," Health Physics, 12:173, 1966.

2. D. H. Slade, Meteorology and Atomic Energy, 1968. USAEC Division of Technical Information, July 1968.

3. E. J. Katz, "Atmospheric Diffusion of Settling Particles with Sluggish Response." Journal of Atmospheric Sciences, 23:159, 1966.

4. J. H. Davies et al., Irradiation Tests to Characterize the PCI Failure Mechanism. NEDO-21551, pp. 38-42, General Electric Company, San Jose, CA, February 1977.

5. C. W. Smith, Calculated Fuel Rod Perforation Temperatures Commercial Power Reactor Fuels, NEDO-10093, p. 5, General Electric Company, San Jose, CA, September 1969.

6. Reference 5, p. 9.

7. C. E. Beyer and C. R. Hann, Prediction of Fission Gas Release from UO_2 Fuel. BNWL-1875, Battelle, Pacific Northwest Laboratories, Richland, WA, November 1974.

8. T. H. Smith and W. A. Ross, Impact Testing of Vitreous Simulated High-Level Waste in Canisters. Battelle, Pacific Northwest Laboratories, Richland, WA, May 1975.

9. D. Cubicciotti et al, The Nature of Fission-Product Deposits Inside Light-Water-Reactor Fuel Rods. p. 96, Stanford Research Institute, Menlo Park, CA, November 1976.

10. R. A. Lorenz et al, Quarterly Progress Report on Fission Product Release from LWR Fuel for the Period October-December 1976. ORNL-NUREG-TM-88, p. 29, Oak Ridge National Laboratory, Oak Ridge, TN, March 1977.

11. Potential Releases of Cesium from Irradiated Fuel in a Transportation Accident. NUREG-0069, p. 14, U.S. Nuclear Regulatory Commission, Washington, DC, July 1976.

12. Reference 10, p. 24.

13. Nuclear Safety Program: Annual Progress Report for the Period Ending December 31, 1970. ORNL-4647, p. 46, Oak Ridge National Laboratory, Oak Ridge, TN, May 1971.

14. Y. B. Katayama, Leaching of Irradiated LWR Fuel Pellets in Deionized and Typical Ground Water. BNWL-2057, Battelle, Pacific Northwest Laboratories, Richland, WA, July.

15. Environmental Survey of Transportation of Radioactive Materials to and from Nuclear Power Plants. WASH-1238, U.S. Atomic Energy Commission, p. 44, Washington, DC, December 1972.

16. G. W. Parker et al., Out-of-Pile Studies of Fission-Product Release from Overheated Reactor Fuels at ORNL, 1955-1965. ORNL-39810, p. 85, Oak Ridge National Laboratory, Oak Ridge, TN, July 1967.

17. Reference 16, pp. 85-92.

APPENDIX C

SIGNIFICANT RADIONUCLIDES IN SPENT FUEL

The potential radioactive sources including fission products and actinides in the spent fuel at the time of shipment were obtained from analyses performed with the ORIGEN[1] computer program. The set of equations describing the formation, transmutation, and decay of nuclides from a nuclear reactor is approximated by ORIGEN as a homogeneous set of simultaneous first-order ordinary differential equations with constant coefficients. Rigorously, the set of equations is nonlinear since the neutron flux varies as the composition of the fuel changes at constant power. However, this variation with time is small, and the neutron flux can be considered constant over short time intervals, thus permitting the linear approximation. ORIGEN solves this set of equations by the matrix-exponential method. Radionuclide inventories were calculated by means of the ORIGEN program for a 1200 MWe reference reactor operated 70% of the time to produce 0.84 GWe of electricity per year.

Inventories were calculated for an equilibrium core at a burnup of 29,000 megawatt-days per metric ton of uranium charged. The fuel was assumed to decay for 180 days at which time it is shipped in spent fuel casks.

A nuclear reactor that has operated for many hundreds of hours contains several hundred different radionuclides - almost the full range of the chart of the nuclides. Not all these radionuclides need be considered in the calculation of exposure from an accidental release. With very little decrease in the accuracy of the calculated consequences, the number of radionuclides considered can be reduced significantly.

The elimination of radionuclides from consideration in radiation dose calculations was based on a number of parameters, such as quantity (curies), release fraction, radioactive half-life, emitted radiation type and energy, and chemical characteristics. In addition, it is possible to eliminate radionuclides with half-lives shorter than 15 days.

Since storage is assumed for 180 days, any nuclide with half-lives shorter than 15 days would have negligible activity after 10 or more half-lives had passed.

These eliminations resulted in the list of 24 radionuclides presented in Table C.1, which gives their activity at the time the spent fuel is assumed to be shipped. The table shows the radioactive inventory in the fuel in terms of curies per metric ton of heavy metal. These values were converted to the fuel assembly inventory by multiplying the amount of heavy metal per fuel element, (0.46 MTHM per PWR element).

TABLE C.1. Significant Fission Products in Spent Fuel (180 Days After Discharge)

#	Isotope	Radioactive Inventory Source (Ci/MTHM)	Fuel Assembly Inventory (Ci)	Half Life (Days)
1	Tritium	4.4×10^{2}	2.0×10^{2}	4,511
2	Carbon 14[(a)]	7.4×10^{-1}	3.4×10^{-1}	2.1×10^{6}
3	Krypton 85	9.5×10^{3}	4.4×10^{3}	3,950
4	Strontium 89	5.5×10^{4}	2.5×10^{4}	52.1
5	Strontium 90	6.7×10^{4}	3.1×10^{4}	11,030
6	Yttrium 91	9.5×10^{4}	4.4×10^{4}	59.0
7	Zirconium 95	1.7×10^{4}	7.8×10^{4}	65.2
8	Niobium 95	3.3×10^{5}	1.5×10^{5}	35.0
9	Ruthenium 103	4.3×10^{4}	2.0×10^{4}	39.5
10	Ruthenium 106	3.4×10^{5}	1.6×10^{5}	366
11	Tellurium 127m	4.2×10^{3}	1.9×10^{3}	109
12	Iodine 129	3.3×10^{-2}	1.5×10^{-2}	6.2×10^{9}
13	Cesium 134	1.7×10^{5}	7.8×10^{4}	750
14	Cesium 137	9.4×10^{4}	4.3×10^{4}	11,000
15	Cerium 141	2.4×10^{4}	1.1×10^{4}	32.3
16	Cerium 144	6.1×10^{5}	2.8×10^{5}	284
17	Promethiom 147	9.0×10^{4}	4.1×10^{4}	956
18	Plutonium 238	2.1×10^{3}	9.7×10^{2}	32,500
19	Plutonium 239	2.9×10^{2}	1.3×10^{2}	8.9×10^{6}
20	Plutonium 240	4.5×10^{2}	2.1×10^{2}	2.4×10^{6}
21	Plutonium 241	1.1×10^{5}	5.1×10^{4}	5,350
22	Americium 241	2.0×10^{2}	9.2×10^{1}	1.5×10^{5}
23	Curium 242	1.7×10^{4}	7.8×10^{3}	163
24	Curium 244	1.3×10^{3}	6.0×10^{2}	6,630

(a) Not a Fission Product ^{14}C is formed by neutron activation of ^{14}N impurity in fuel.

REFERENCE

1. M. J. Bell, 1973, ORIGEN, The ORNL Isotope Generation and Depletion Code. ORNL-4628, Oak Ridge National Laboratory, Oak Ridge, TN.

APPENDIX D

PATHWAYS OF RADIATION EXPOSURE TO MAN

To evaluate the risks involved in shipping spent fuel, the impact of radiological releases to man must be determined. Exposure pathways to man must be identified in order to evaluate the impact of releases. The pathways by which man can be exposed to radiation from a transportation accident are illustrated in Figure D.1. The exposure pathways can be grouped into those associated with gaseous effluents, liquid effluents and direct radiation from the transport system. Table D.1 lists the various pathways of exposure to man.[1]

TABLE D.1. Pathways of Exposure to Man[1]

Water Pathways

External

Water immersion and water surface
Exposure to shoreline

Internal

Ingestion of water
Ingestion of aquatic foods
Ingestion of irrigated food crops
Ingestion of products from animals fed irrigated foods

Air Pathways

External

Air submersion
Exposure to deposited materials

Internal

Inhalation of initial plume
Ingestion of food crops
Ingestion of animal products
Inhalation of resuspended material

Direct Radiation Pathways

External

Exposure during transport of fuels

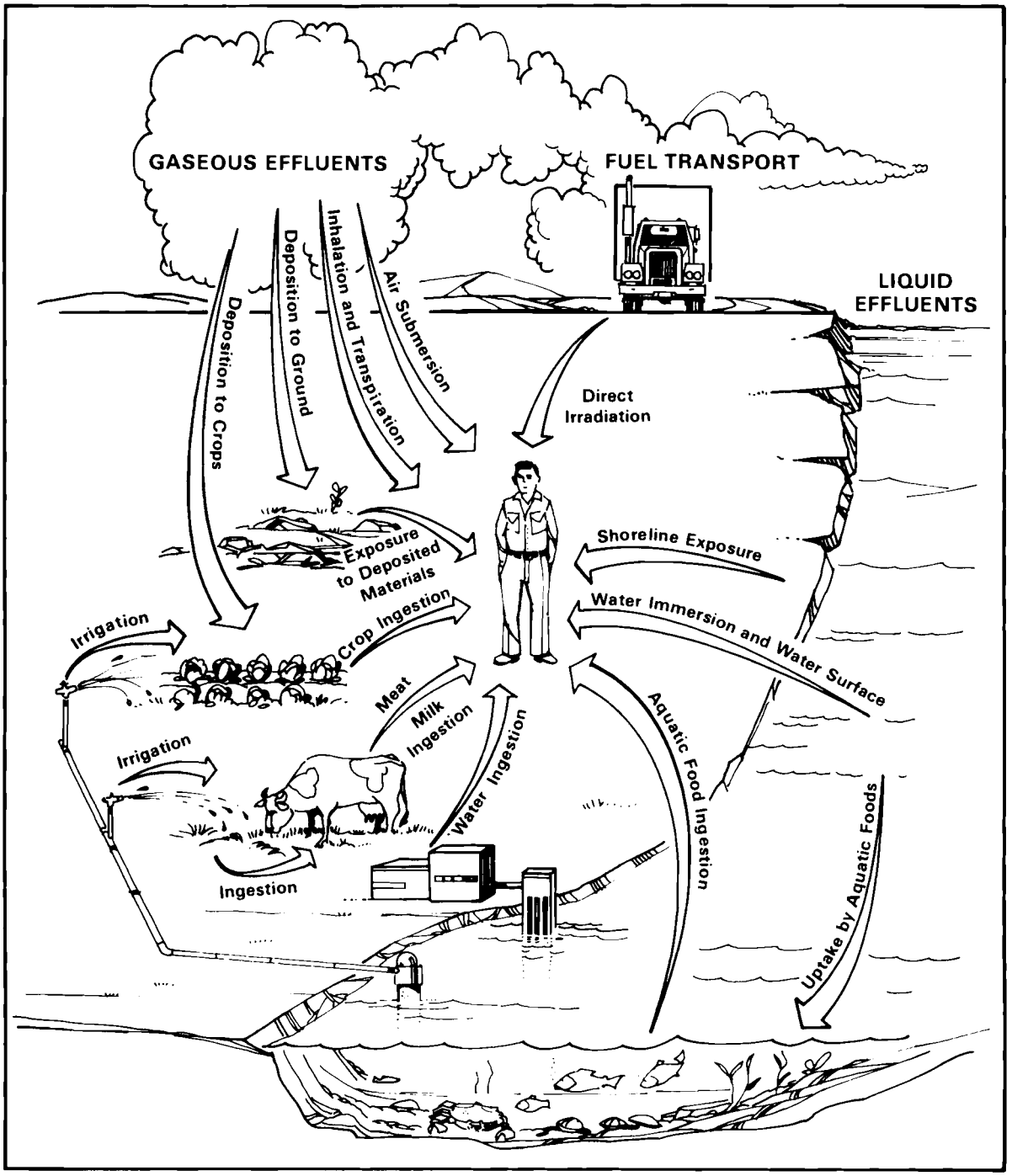

FIGURE D-1. Exposure Pathways to Man

The fundamental equation for calculating radiation dose rate from the pathways listed in Table D.1 is:

$$R_{ipr} = C_{ip} U_p D_{ipr} \quad (1)$$

where

R_{ipr} is the dose rate to organ r from nuclide i via pathway p,

C_{ip} is the concentration of nuclide i in the medium pathway p,

U_p is the usage: the exposure or intake rate associated with pathway p,

and

D_{ipr} is the dose rate factor: a number specific to a given nuclide i, pathway p, and organ r which can be used to calculate radiation dose rate from exposure to a given radionuclide concentration or a radionuclide intake.

Equations tailored to each specific exposure pathway are derived from this equation. The principal difference between pathways is the manner in which the radionuclide concentrations are calculated.

The liquid effluent pathway for transportation accidents is not considered to be a significant hazard to the population. The only releases that involve liquids in a transportation accident are those accidents where leakage of cavity coolant containing small amounts of activity occurs. This release does not constitute a significant hazard to the public.

Direct radiation is not assumed to be a hazard since the population is assumed to be evacuated for 100 meters from the accident point. At that distance, there is negligible direct radiation dose even with no neutron shield in place around the cask.

For purposes of this study only the air pathway was considered significant. It is assumed in transportation accident analysis that contaminated crops can be confiscated to reduce the threat from the deposition--ingestion pathway. Thus it can be seen that the airborne inhalation dose dominates all the other exposure pathways for transportation accidents.

In WASH 1400,[2] approximate percentages of latent cancer fatalities attributable to each type of airborne exposure mode are shown in Table D.2,[2] both on a whole body and organ by organ basis. It is evident from those results that lung cancer due to inhalation of radioactive material in the passing cloud is the dominant contribution to the total latent cancer fatalities. This illustrates that latent health effects due to an accident should be calculated on an organ-by-organ basis. The results given in Table D.2 show that the inhalation dose is the dominant pathway in determining the consequence of a release of fission products from reactor fuel.

TABLE D.2. Contribution of Different Exposure Modes to Latent Cancer Fatalities[2]

	Leukemia	Lung	Breast	Bone	GI Tract	All Other	Total	Whole Body[a]
External cloud	0.2	0.5	0.5	0.1	0.1	0.3	1	3
Inhalation from cloud	0.5	59.0	10.0	0.2	1.0	0.2	71	15
External ground (7 days)	4.0	8.0	8.0	1.0	1.0	3.0	25	47
External ground (7 days)	2.0	2.0	6.0	1.0	1.0	2.0	13	30
Inhalation of resuspended contamination	0.1	3.0	0.1	0.1	0.1	0	3	2
Ingestion of contaminated foods	0.2	0.2	0.5	0.1	0.1	0.2	1	4
Total	7	72.7	16	2.5	3	6	114	100

(a) Whole body values are proportional to 50-year whole-body man-rem.

REFERENCES

1. D. L. Brenchley, et al., Environmental Assessment Methodology for the Nuclear Fuel Cycle. BNWL-2219, Battelle, Pacific Northwest Laboratories, Richland, WA, June 1977.

2. Reactor Safety Study, An Assessment of the Accident Risks in U.S. Commerical Nuclear Power Plants. WASH-1400 (NUREG-75/014) U.S. Nuclear Regulatory Commission, Washington, DC, October 1975.

APPENDIX E

INHALATION MODELS FOR CALCULATING THE DOSE FROM INTERNAL DEPOSITION OF RADIONUCLIDES

The information for this appendix was taken from the text of Reference 3. The mathematical model for calculating the dose to an organ of interest via inhalation using the ICRP Task Group Lung Model, TGLM[2, 4] is considerably more complex than that utilized by the lung model initially proposed by the ICRP.[1] In the TGLM, the respiratory tract is divided into three regions, the nasopharyngeal (NP), the tracheobronchial (TB), and the pulmonary (P). The schematic representation of the respiratory tract used in the development of the mathematical model for the deposition and clearance of inhaled radionuclides is shown in Figure E.1. Deposition is assumed to vary with the aerodynamic properties of the aerosol distribution and is described by the three parameters D_3, D_4, and D_5. These parameters represent the fraction of the inhaled material initially deposited in the NP, TB and P regions, respectively. Each of the three regions of deposition is further subdivided into two or more subcompartments, each representing the fraction of material initially in a compartment that is subject to a certain clearance process. This fraction is represented by f_k, where k indicates the clearance pathway. The quantity of material in the TB region, for example, cleared by process (c) is then represented by the product $f_c D_4 Q_I$. Values of the (f_k) and the clearance half times T_k for each clearance process for the three translocation classes of aerosols used in the computer code[3] are shown in Table E.1.[2] Values of the deposition fractions D_3, D_4, and D_5 as functions of activity median aerodynamic diameter have been published in the form of a graph.[4]

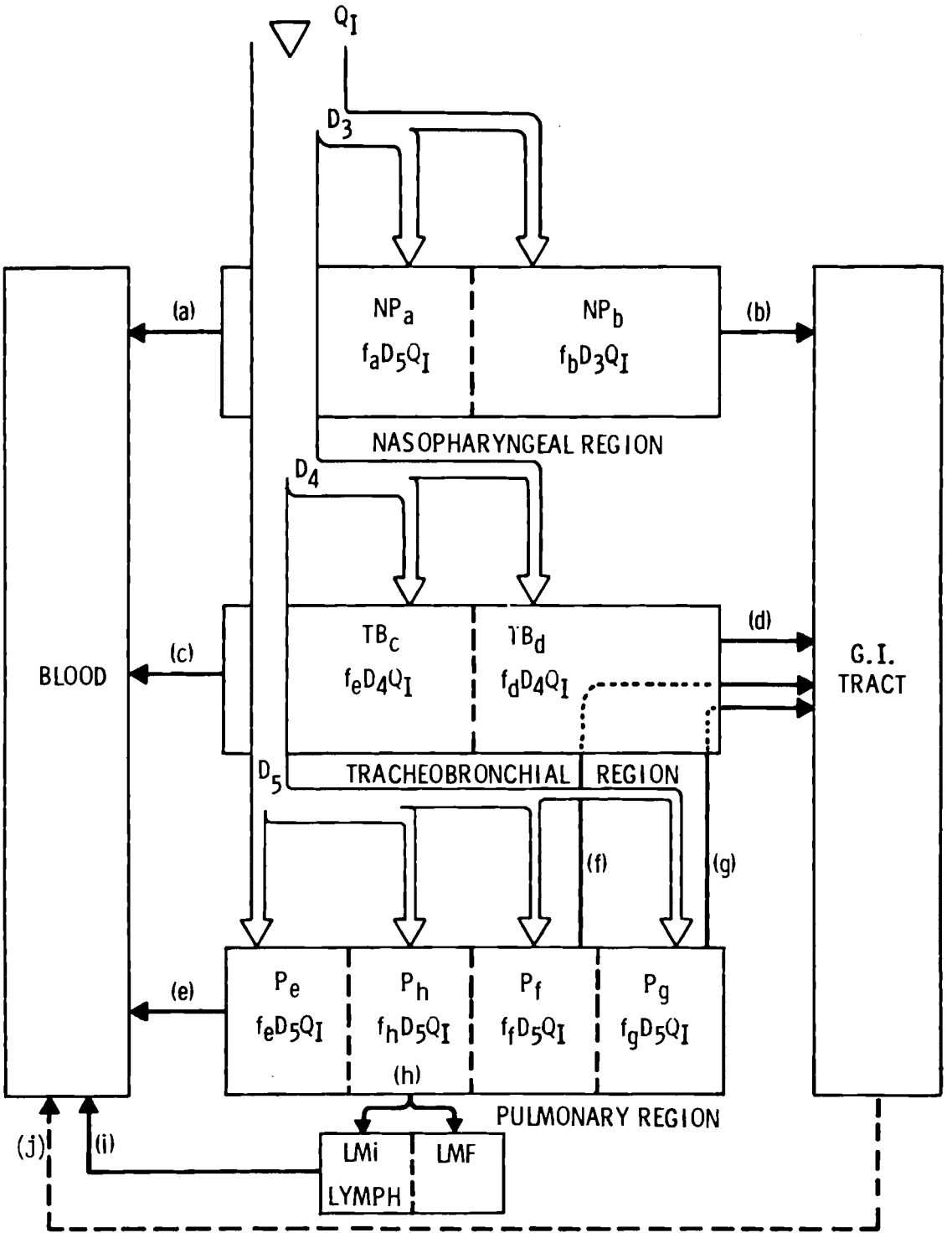

FIGURE E-1. Schematic Diagram of the Task Group Lung Model

TABLE E 1. Values of the Clearance Parameters for the Task Group Lung Model

Compartment	k[a]	Translocation Class D T_k[b]	D f_k[c]	W T_k	W f_k	Y T_k	Y f_k
NP	a	0.01	0.5	0.01	0.1	0.01	0.01
	b	0.01	0.5	0.40	0.9	0.4	0.99
TB	c	0.01	0.95	0.01	0.5	0.01	0.01
	d	0.2	0.05	0.2	0.5	0.2	0.99
P	e	0.5	0.8	50	0.15	500	0.05
	f	n.a.	n.a.	1	0.4	1	0.4
	g	n.a.	n.a.	50	0.4	500	0.4
	h	0.5	0.2	50	0.05	500	0.15
L	i	0.5	1	50	1	1000	0.9

(a) Metabolic pathways from lung.
(b) Removal half time in days from compartment via pathway k.
(c) Fraction removed from compartment via pathway k.

Transport of the radionuclides from the respiratory tract, lymphatic systems, and gastro-intestinal tract to other organs and tissues where significant accumulations of the inhaled radionuclide occur, is assumed to take place via the blood. This translocation from the respiratory tract and lymphatic system to the blood has been described in considerable detail.[4] Of the material clearing from the respiratory tract through the GI tract, a constant fraction is assumed to be taken up by the blood. Uptake by the n^{th} organ or tissue is assumed to be a constant fraction of the amount entering the blood stream at any time. Once in the n^{th} organ, the activity is assumed to clear the organ and the body at a constant rate.

Notation for the equations found in this section is as follows:

- $D_{1n}(T_1)$ • is the dose equivalent in rem received by the n^{th} organ tissue by time T_1 during continuous inhalation of a radioactive aerosol.
- $D_{2n}(T_2)$ • is the dose equivalent in rem received by the n^{th} organ or tissue by time T_2 following the termination of continuous inhalation of a radioactive aerosol.
- $Q_{1n}(T_1)$ • is the quantity of radioactive material in μCi present in the n^{th} organ or tissue as a function of time during continuous inhalation of radioactive aerosol.
- $Q_{2n}(T_2)$ • is the quantity of radioactive material in μCi present in the n^{th} organ or tissue following the termination of continuous inhalation of radioactive aerosol.
- E_n • is the effective absorbed energy per disintegration in $\frac{\text{MeV}\cdot\text{rem}}{\text{dis}\cdot\text{rad}}$ for the n^{th} organ or tissue.
- M_n • is the mass in grams of the n^{th} organ or tissue over which the dose is to be averaged.
- λ_j^b • is the biological removal rate constant for the j^{th} subcompartment of the respiratory tract, sec.^{-1}
- λ • is the radiological decay constant of the nuclide of interest, sec.^{-1}
- λ_j • is the total removal rate constant for the j^{th} subcompartment of the respiratory tract, sec.^{-1} (Note: $\lambda_j = \lambda_j^b + \lambda$)
- λ_n^b • is the biological removal rate constant for the n^{th} organ or tissue, sec.^{-1}
- λ_n • is the total effective removal rate constant for the n^{th} organ or tissue, sec.^{-1} (Note: $\lambda_n = \lambda_n^b + \lambda$)

- f_2' • is the fraction of material in the blood that reaches the organ or tissue of interest.
- f_1 • is the fraction of material in the G.I. tract that reaches the blood.
- P_o • is the rate at which the radioactive aerosol is inhaled in μCi/sec.
- f_j • is the fraction of the material in a deposition region, NP, etc., that clears by the j^{th} pathway.
- D_3 • is the fraction of the material inhaled deposited in the NP region.
- D_4 • is the fraction of the material inhaled deposited in the TB region.
- D_5 • is the fraction of material inhaled deposited in the P region.
- T_1 • is the total uptake time in seconds.
- T_2 • is the time following termination of uptake.

Developing the equations to describe the lung clearance model was divided into two parts. The first part is concerned with describing the organ burdens and the organ doses in the time interval during which the inhalation of radionuclides is taking place. The second part, requiring a different set of equations, describes the organ burdens and the organ doses for the contiguous time interval following the cessation of radionuclide intake.

During uptake, the equations for computing the quantity of radionuclide in the eight subcompartments (j) of the respiratory tract have the form:

$$Q_{j,k}(t) = f_j \, D_k \, Q_I \, \frac{(1-e^{-\lambda_j t})}{\lambda_j} \qquad (5)$$

The equations for the removable quantity in the pulmonary lymph nodes are complicated by the fact that both equal and unequal rates for transfer paths

into and out of the system are involved. This is due to the dependence of transfer rate upon the solubility class of the radionuclide. Thus, two equations are needed to compute the quantity in the lymph compartment.

For the case $\lambda_h \neq \lambda_i$, i.e., class Y solubility in the current version of the model:

$$Q_{LMi}(t) = \frac{\lambda_h^b f_i f_h P_o D_5}{\lambda_h} \left[\frac{(1-e^{-\lambda_i t})}{\lambda_i} - \frac{(e^{-\lambda_i t}-e^{-\lambda_h t})}{\lambda_h-\lambda_i} \right] \quad (6)$$

and for the case $\lambda_h \doteq \lambda_i$, i.e., class D and W in the current version of the model:

$$Q_{LMi}(t) = \frac{\lambda_h^b f_i f_h P_o D_5}{\lambda_h} \left[\frac{(1-e^{-\lambda_i t})}{\lambda_i} - te^{-\lambda_i t} \right] \quad (7)$$

With the preceding equations, the equations describing the quantity of radionuclide in the n^{th} organ as a function of time during uptake can be derived by:

$$Q_{1n}(t) = P_o \left\{ \sum_{j=a}^{g} f_2' C_i \left[\frac{(1-e^{-\lambda_n t})}{\lambda_n} - \frac{(e^{-\lambda_n t}-e^{-\lambda_j t})}{(\lambda_j-\lambda_n)} \right] + L \right\} \quad (8)$$

where:

L is the contribution to the organ burden from material passing through the lymphatic system,

and:

$$C_a = \lambda_a^b f_a D_3/\lambda_a$$

$$C_b = \lambda_b^b f_b D_3 f_1/\lambda_b$$

$$C_c = \lambda_c^b f_c \, D_4/\lambda_c$$

$$C_d = \lambda_d^b f_d \, D_4 f_1/\lambda_d$$

$$C_e = \lambda_e^b f_e \, D_5/\lambda_e$$

$$C_f = \lambda_f^b f_f \, D_5 f_1/\lambda_f$$

$$C_g = \lambda_g^b f_g \, D_5 f_1/\lambda_g \, .$$

The lymph pathway contributions to the n^{th} organ burden for the two situations are calculated as follows:

$$L = f_2' C_h \left\{ \frac{1}{\lambda_i} \left[\frac{(1-e^{-\lambda_n t})}{\lambda_n} - \frac{(e^{-\lambda_n t}-e^{-\lambda_i t})}{(\lambda_i-\lambda_n)} \right] - \frac{1}{(\lambda_i-\lambda_n)} \left[\frac{(e^{-\lambda_n t}-e^{-\lambda_i t})}{(\lambda_i-\lambda_n)} - \frac{(e^{-\lambda_n t}-e^{-\lambda_h t})}{(\lambda_h-\lambda_n)} \right] \right\} \quad \text{for } \lambda_h \neq \lambda_i \qquad (9a)$$

$$L = f_2' C_h \left\{ \frac{1}{\lambda_i} \left[\frac{(1-e^{-\lambda_n t})}{\lambda_i} - \frac{(e^{-\lambda_n t}-e^{-\lambda_i t})}{(\lambda_i-\lambda_n)} \right] - \frac{e^{-\lambda_n t} - \left[(\lambda_i-\lambda_n)\, t + 1\right] e^{-\lambda_i t}}{(\lambda_i-\lambda_n)^2} \right\} \quad \text{for } \lambda_h \neq \lambda_i \qquad (9b)$$

where:

$$C_h = \frac{\lambda_{i\,h} f_i f_h D_5}{\lambda_h} \, .$$

The calculation of the dose equivalents to organs burdened by the radionuclide are based on the following:

$$D_{1n}(t) = \frac{5.92 \times 10^{-4} E_n}{M_n} \int_0^t Q_{1n}(\tau) d\tau \qquad (10)$$

where the constant is a combination of the conversion factors:

$$3.7 \times 10^{4} \left(\frac{\text{dis/sec}}{\mu\text{Ci}}\right) \; 1.6 \times 10^{-6} \left(\frac{\text{ergs}}{\text{MeV}}\right) \; 10^{-2} \left(\frac{\text{rads}}{\text{erg/g}}\right) = 5.92 \times 10^{-4}.$$

The dose to the pulmonary lung at the end of inhalation intake of a radionuclide is determined by:

$$D_{1p}(T_1) = \frac{5.92 \times 10^{-4} E_p}{M_p} \; P_o D_5 \sum_{j=e}^{h} \frac{f_j}{\lambda_j} \left(T_1 - \frac{1-e^{-\lambda_j T_1}}{\lambda_j} \right) \qquad (11)$$

where M_p is the mass of the lung in grams

For the n^{th} organ or tissue, the dose is computed by:

$$D_{1n} = 5.92 \times 10^{-4} \; \frac{E_n P_o f_2'}{M_n} \left\{ \sum_{j=a}^{g} C_j \left[\frac{T_1 - A_n}{\lambda_n} - \left(\frac{A_n - A_j}{\lambda_j - \lambda_n} \right) \right] + \right.$$

$$\frac{C_h}{\lambda_i} \left[\frac{T_1 - A_n}{\lambda_n} - \frac{A_n - A_i}{(\lambda_i - \lambda_n)} \right] - \frac{C_h}{(\lambda_h - \lambda_i)}$$

$$\left. \left[\frac{A_n - A_i}{(\lambda_i - \lambda_n)} - \frac{A_n - A_h}{(\lambda_h - \lambda_n)} \right] \right\} \quad \text{for } \lambda_h \neq \lambda_i \qquad (12)$$

or:

$$D_n(T_1) = 5.92 \times 10^{-4} \; \frac{E_n P_o f_2'}{M_n} \left(\sum_{j=a}^{q} C_j \left(\frac{T_1 - A_n}{\lambda_n} - \frac{A_n - A_j}{\lambda_j - \lambda_n} \right) + \right.$$

$$\frac{C_h}{\lambda_1} \left(\frac{T_1 - A_n}{\lambda_n} - \frac{A_n - A_i}{\lambda_i - \lambda_n} \right) - \frac{C_h}{(\lambda_i - \lambda_n)^2} \left\{ A_1 - A_n + \right.$$

$$\left. \left. \frac{(\lambda_i - \lambda_n)}{\lambda_i^2} \left[1 - (\lambda_i T_i + 1) \, e^{-\lambda_i T_1} \right] \right\} \right) \quad \text{for } \lambda_h = \lambda_i \qquad (13)$$

where:

$$A_n = \frac{1 - \exp(-\lambda_n T_1)}{\lambda_n}$$

$$A_j = \frac{1 - \exp(-\lambda_j T_1)}{\lambda_j}$$

$$A_i = \frac{1 - \exp(-\lambda_i T_1)}{\lambda_i}$$

$$A_h = \frac{1 - \exp(-\lambda_h T_1)}{\lambda_h}$$

and C_j and C_h are as previously defined.

Now for the time following cessation of radionuclide inhalation, the equations used to calculate the respiratory tract burden and the other organ or tissue burdens become:

$$Q_{2j}(T_2) = Q_{1j}(T_1)e^{-\lambda_j T_2} \qquad (14)$$

where:

$Q_{2j}(T_2)$ is the respiratory tract subcompartment burden at a time T_2 following the termination of inhalation uptake.

$Q_{1j}(T_1)$ is the respiratory tract subcompartment burden at the end of inhalation uptake for a time T_1.

The burden in the n^{th} organ can be described by:

$$Q_{2n}(T_2) = Q_{1n}(T_1)e^{-\lambda_n T_2} + f_2'\lambda_i^b \, Q_{1LMi}(T_1) \, \frac{(e^{-\lambda_i T_2} - e^{-\lambda_n T_2})}{(\lambda_n - \lambda_i)} +$$

$$f_2' \left\{ \sum_{j=a}^{g} \frac{C_j'}{(\lambda_j - \lambda_n)} \, (e^{-\lambda_n T_2} - e^{-\lambda_j T_2}) + \frac{C_j'}{(\lambda_h - \lambda_i)} \right.$$

$$\left. \left[\frac{(e^{-\lambda_n T_2} - e^{-\lambda_i T_2})}{(\lambda_i - \lambda_n)} - \frac{(e^{-\lambda_n T_2} - e^{-\lambda_h T_2}}{(\lambda_h - \lambda_n)} \right] \right\} \quad \text{for } \lambda_h \neq \lambda_i \quad (15)$$

or by:

$$Q_{2n}(T_2) = Q_{1n}(T_1)e^{-\lambda_n T_2} + f_2'\lambda_i^b \, Q_{1LMi}(T_1) \, \frac{(e^{-\lambda_i T_2} - e^{-\lambda_n T_2})}{(\lambda_n - \lambda_i)} +$$

$$f_2' \left(\sum_{j=a}^{g} \frac{C_j'}{(\lambda_j - \lambda_n)} \, (e^{-\lambda_n T_2} - e^{-\lambda_j T_2}) + \frac{C_j'}{(\lambda_i - \lambda_n)} \right.$$

$$\left. \left\{ \frac{e^{-\lambda_n T_2} - e^{-\lambda_i T_2}}{\lambda_i - \lambda_n} - T_2 e^{-\lambda_i T_2} \right\} \right) \quad \text{for } \lambda_h = \lambda_i \quad (16)$$

where:

$$C_e' = \lambda_e^b Q_{1e}(T_1)$$

$$C_f' = \lambda_f^b Q_{1f}(T_1) f_1$$

$$C_g' = \lambda_g^b Q_{1g}(T_1) f_1$$

$$C_h' = f_i \lambda_h^b \lambda_i^b Q_{1h}(T_1)$$

The pulmonary lung dose from inhalation of a radionuclide for a time T_1 followed by no additional radioactive intake for a time T_2 is determined by:

$$D_p = D_{1p}(T_1) + 5.92 \times 10^{-4} \frac{E_p P_o D_5}{M_p} \sum_{j=a}^{h} f_j A_j B_j \qquad (17)$$

where:

$$B_j = \frac{1-e^{-\lambda_j T_2}}{\lambda_j}$$

and $D_{1p}(T_1)$ and A_j are the same as previously defined by Equation (11).

The effective dose to the n^{th} organ as a result of inhalation uptake for time T_1 followed by no additional radioactive intake for a time T_2 is determined by:

$$D_n = D_{1n}(T_1) + 5.92 \times 10^{-4} \frac{E_n}{M_n} \left\{ Q_{1n}(T_1)B_n + f_2' \left[\frac{\lambda_i^b Q_{1LMi}(T_1)}{(\lambda_n - \lambda_i)} (B_i - B_n) + G \left[\frac{(B_n - B_i)}{(\lambda_i - \lambda_n)} - Z \right] + \sum_{j=a}^{g} \frac{C_j'}{(\lambda_j - \lambda_n)} (B_n - B_j) \right] \right\} \qquad (18)$$

where:

$$B_n = \frac{1 - e^{-\lambda_n T_2}}{\lambda_n}$$

$$B_n = \frac{1 - e^{-\lambda_n T_2}}{\lambda_h}$$

$$B_i = \frac{1 - e^{-\lambda_i T_2}}{\lambda_i}$$

$$B_j = \frac{1 - e^{-\lambda_j T_2}}{\lambda_j}$$

also, for $\lambda_h \neq \lambda_i$:

$D_{1n}(T_1)$ is determined by Equation (12)

$Q_{1n}(T_1)$ is determined by Equations (i, 9a)

$$G = \frac{C_h'}{(\lambda_h - \lambda_i)}$$

$$Z = \frac{B_n - B_h}{(\lambda_h - \lambda_n)}$$

and for $\lambda_h = \lambda_i$:

$D_{1n}(T_1)$ is determined by Equation (13)

$Q_{1n}(T_1)$ is determined by Equations (8, 9b)

$$G = \frac{C_h'}{(\lambda_i - \lambda_n)}$$

$$Z = \lambda_i^{-2} \left[1 - (\lambda_i T_2 + 1)\, e^{-\lambda_i T_2}\right]$$

Provision is made in the code to calculate the dose equivalent to the pulmonary lung as a result of primary deposition, i.e., that occurring directly on the lung surfaces during inhalation and also for secondary deposition, i.e., that occurring as a result of solubilization and redeposition in the lung tissue itself, in this respect the pulmonary lung is treated as any other organ.

Weighted values of the effective energy of daughter radionuclides, ε_i were calculated using the ICRP equations[4] for three biological clearance half times of 1 day, 50 days and 500 days. The effective energy of the i^{th} daughter is determined by:

$$\varepsilon_i = \sum_i F_i \left[E(RBE)\, n\right] i$$

where:

$$F_i = \frac{\prod_{j=1}^{i} T_j/T_j^r}{1-e^{-\lambda_o t}} \sum_{n=1}^{i} \frac{T_n^i \left(1-e^{-\lambda_n t}\right)}{\prod_{\substack{p=o \\ p\neq n}}^{i} \left(T_n - T_p\right)}$$

and:

- F_i • the ratio of the number of distintegrations of daughter atoms to the number of disintegrations of parent atoms in the lung over a time t.
- λ_o • the effective decay constant of the parent, the subscript, zero, refers to the parent.
- λ_i • the effective decay constant of the i^{th} daughter in the lung.
- T_i • the effective half life of the i^{th} daughter in the lung.
- T_i^r • the radioactive half life of the i^{th} daughter.
- t • the time of interest over which the dose is to be calculated.
- E • the total energy absorbed in the organ per disintegration of the radionuclide.
- RBE • the relative biological effectiveness of the radiation
- n • the relative damage factor for radionuclides deposited in the bone.

REFERENCES

1. Report by Task Group of Committee II, on ICRP, Permissible Dose for Internal Radiation, ICRP Publication 2, Pergamon Press, 1952.

2. Task Group of Committee II, ICRP, The Metabolism of Compounds of Plutonium and Other Actinides, ICRP Publication 19, Pergamon Press, Oxford, 1972.

3. J. Houston, D. L. Strenge and E. C. Watson, DACRIN Computer Program for Calculations of Organ Dose from Acute or Chronic Radionuclide Inhalation, BNWL-B-389, Battelle, Pacific Northwest Laboratories, Richland, WA, December 1974.

4. Task Group of Committee II, ICRP, "Task Group on Lung Dynamics for Committee II of the ICRP," Health Physics, Vol. 12, p. 173, 1966.

APPENDIX F

CALCULATIONS OF MECHANICAL FAILURE THRESHOLDS FOR REFERENCE CASK

Regulatory conditions used to calculate shipping cask performance in an accident environment are not actual tests. Licensing requires that analyses be performed to show that radionuclides will be contained during certain extreme conditions. These licensing requirements do not address failure thresholds (a point below which all "identical" packages will survive and above which they would fail). As a result, for most casks, failure points are largely unknown. In the case of spent fuel shipping casks, actual tests more extreme than those required for licensing have been performed at Sandia.[1] Results of the cases treated (end impacts) for a similar cask in the testing program[2] have been compared to the analytical results presented here. Generally, the analytical results were found to be more conservative than the test results indicated. The analysis tended to produce failure thresholds which were lower than the test results indicated failure would occur.

Failure thresholds calculated in this appendix are of two types. The first uses dynamic elastic and energy absorption analyses to estimate cask failure thresholds which are assumed for purposes of this study to result in a release of radioactive material (Cases 1-5). The second uses an energy absorption model and assumptions of material behavior to estimate impact velocities which may result in a larger opening of the cask cavity to the surrounding atmosphere (Case 6). Fuel cladding failure thresholds are also calculated in Case 7 by elastic and energy absorption analyses.

All cask failure thresholds calculated in this appendix are reported as cask velocities except Case 5 (crush loading). Recent full scale testing[2] indicates substantial energy may be absorbed by the tractor-trailer structures. For a 20410 kg cask on a 5000 kg trailer and pulled by a 5900 kg tractor, 3.19×10^6 joules of energy were absorbed during a

125 km/hr (84 mph) impact before the cask tie down ratings were exceeded.[2] An identical impact at 98 km/hr (61 mph) absorbed 3.97×10^6 joules. If the same energy absorption values were applied to the reference cask, the impact velocities would be 26.8 km/hr (16.7 mph) and 15.5 km/hr (9.7 mph) below the incident truck velocities.

The degree of accuracy of the calculations contained in this appendix is difficult to assess. Due to the complex nature of cask behavior under dynamic conditions, the values can only be expected to provide estimates of actual behavior. Some of the failure velocities could deviate from actual values as much as 50%. However, a conservative approach was used which produced thresholds believed to be on the low side of expected failure velocity ranges. Sophisticated, but expensive, computer techniques such as the finite element method were not employed in the calculations. It was felt that simpler and more economical computational techniques would be sufficiently accurate in view of the risk assessment uncertainties.

The reference spent fuel truck cask considered for analysis in this appendix is described in Appendix A. The gross weight of the cask and contents is 22,680 kg so that transport without special permit is possible. Material properties of the cask used in calculations for the failure thresholds are shown in Table A.4 of Appendix A.

Casks of this type are mounted lengthwise on the flat bed trailers by means of special tie-down devices. These devices are usually designed so as to facilitate vertical loading and unloading of the cask from the trailer. Typically, one end of the tie-down configuration consists of a trunnion type mount and the other end provides cradling support.

The tie-down mechanism must be strong enough to provide the following g level forces without failure:

- 10 g's axial
- 5 g's lateral
- 2 g's vertical

Reference 1 stipulates that the cask must withstand the following hypothetical mechanical conditions without loss of containment:

Impact - A 30-ft (9.14 m) free-fall onto an essentially unyielding flat surface in an orientation so as to sustain maximum damage.

Puncture - A 40-in. (1 m) drop onto a 6-in. (15.2 cm) diameter steel pin.

Immersion - Immersion to a depth of 3-ft (0.9 m) for a period of 8 hours.

SPENT FUEL CASK FAILURE THRESHOLDS

Case 1. Determine the velocity for cask failure during an end-on impact onto a rigid planar target. A conservative estimate of the initial cask velocity necessary to fail the cask in an end impact accident was made using preliminary results of full scale testing conducted at Sandia Laboratories, Albuquerque, New Mexico, during 1977 and the CASK computer program.[3] Energy absorbed by the truck frame was neglected. The energy necessary to crush the impact limiter was added to the energy absorbed by the cask body to estimate the failure threshold.

The maximum initial cask velocity which could be mitigated before the cask was involved in a rigid impact was calculated by assuming that all kinetic energy is dissipated by crushing the top impact limiter to a depth of 30.5 cm. The cask kinetic energy is equated to the product of volume and crush stress for the impact limiter:

$$E = 1/2\ Mv^2 = L\ \pi\ \frac{D^2}{4}\ \sigma_c$$

where:

E = energy absorbed in impact limiter (3.15×10^6 J)

D = impact limiter diameter (109 cm)

σ_c = balsa wood crush strength (1096 nt/cm^2)

L = length of impact limiter (30.5 cm)

M = Cask mass: $\frac{2.22 \times 10^5}{980.7}\ \frac{\text{nt - sec}^2}{\text{cm}}$

v = 1667 cm/sec (60 km/hr) (37.3 mph)

The rate of deceleration for this impact condition (Ng) is calculated to be 46.5 g's and is independent of initial impact velocity so long as the 30.5 cm depth of the impact limiter is not totally consumed:

$$Ng = \frac{4W}{\sigma_{cl} D^2}$$

where:

W = 22,680 kg

The CASK[3] computer program calculates the energy absorbed in deforming both the shielding lead and shell material during an end impact with a rigid planar target. The impact is modeled as a constant acceleration process. Stressed due to inertial loading are calculated as a function of the distance along the cask length. Using strain dependent material properties and assuming incompressible material flow, local deformations are predicted. Shell-lead bonding as used in the reference cask was not considered. Energy absorbtion and rigid constraints in the cask head were neglected. The inner shell of the cask was considered rigid. It is believed that these simplifications cause the model to predict conservatively large deflections and smaller accelerations.

To provide an estimate of the error associated with this program, a run was made using characteristics of a cask subjected to full-scale impact tests at Sandia Laboratories.[1] For an impact velocity of 26.8 m/s (60 mph), the program predicts a centerline deformation of 33 cm (13 in.). The shell hoop strain for this deformation would be 11%. An acceleration of 100 g would be required to stop the cask. Personal communication in September 1977 with M. Huerta of Sandia Laboratories indicated that the cask sustained a 27.8 m/s (62 mph) hardened impact with a centerline deformation of 6 cm (2.4 in.). The maximum hoop strain was 3%. Maximum accelerations were about 70 g's. About 100 cc of cask cavity coolant were detected on the trailer wreckage. No sustained leakage occurred. The CASK program predicted

conservative deformations and accelerations. The lower accelerations recorded in the full scale test may be due to deviation from a rigid target.

A run of the CASK program for the reference cask predicts 3% hoop strain could occur if the cask sustains a 13.8 m/s (30.8 mph) impact at 46 g's after the impact limiter is crushed. This would require 2.17×10^6 J (1.6×10^6 ft-lb) of kinetic energy. The impact velocity predicted by the program to cause 3% hoop strain is believed to be a conservative failure threshold for the cask.

The initial impact velocity to fail the cask is obtained from the total energy absorbed in the cask-impact limiter system.

E = TOTAL ENERGY ABSORBED

$= E_{\text{impact limiter}} + E_{\text{cask body}}$

$= 3.15 \times 10^6 J + 2.17 \times 10^6 J$

$= 5.32 \times 10^6 J$

$E = 1/2\ Mv^2$

$M = 22680$ kg

$v = 21.7 \frac{m}{s}$ (48.5 mph)

Case 2. Determine the cask impact velocity to actuate the 76 atm rupture disk located in the top end of the cask.

The analysis for this case assumed pressures caused by three influences:

- P_1 = normal operating pressure, 12 atm
- P_2 = pressure caused by a constant deceleration rate during crush of the top impact limiter

  $P_2 = L\ Ng\ \rho = 20.1$ atm

  $L = 452$ cm

  $Ng = 46.5$

  $\rho = 1$ kg/li

- P_3 = water hammer pressure caused by instantaneous velocity change assumed to occur after the impact limiter has bottomed out.

$$P_3 = \Delta v \sqrt{E\rho} = 43.8 \text{ atm} = 444.2 \text{ nt/cm}^2$$

E = bulk modulus of water, 220,720 $\frac{\text{nt}}{\text{cm}^2}$

ρ = density of water = 1×10^{-5} nt sec^2/cm^4

It was thus concluded that an instantaneous velocity change of 300 cm/sec occurred:

$$\Delta v = 44.2 \left[(220{,}720)(1 \times 10^{-5})\right]^{-1/2}$$

$$\Delta v = 300 \text{ cm/sec}$$

The initial impact velocity of the cask which would yield this cask velocity after crush of the forward impact limiter can be computed as follows:

initial kinetic energy - final kinetic energy = crush energy of impact limiter

$$1/2 \, M \left[v_i^2 - 3^2\right] = \sigma_c h \, \frac{\pi D^2}{4}$$

v_i = 16.94 m/sec (61 km/hr) (37.9 mph)

M = cask mass, 22680 kg

v_i = initial velocity m/sec

σ_c = crush strength of impact limiter, 1.125×10^6 n/m^2

h = height of impact limiter, 0.30.5 m

D = diameter of impact limiter, 1.09 m

Case 3. Determine the cask velocity for a failure during a side impact onto a flat rigid target.

For this analysis, it was assumed that all of the kinetic energy due to initial velocity was dissipated by:

- crush of the top ring impact limiter,
- crush of the bottom ring impact limiter,
- flattening of the main 3.2 cm shell and lead column.

The top solid impact limiter covering the cask lid was conservatively neglected from consideration. It was felt that the attachment method of this impact limiter was inadequate for providing significant shear restraint forces. Also, energy absorbtion by the 0.26 cm thick neutron shield outer shell was conservatively neglected.

After the crush plane reaches the 76.2 cm inside diameter of the two ring-type impact limiters, it was assumed the remainder of the kinetic energy was absorbed totally by deformation of the lead column and the main shell. Energy absorbtion by deformation of the ring flange and bottom disk (see Appendix A, Figure A.3) was neglected. Due to the length of the cask being considered and the large stiffness of these structural components, this assumption seems appropriate. Cask failure was assumed to occur when an approximate average of this deformation becomes equal to the shell thickness of 3.2 cm.

In most real targets the flanges would penetrate the material. This would tend to shear the shell from the flange in the direction of impact. Since the mass of the cask head is small relative to the cask body, this effect is not expected to cause significant damage.

Energy absorbtion by the two ring type impact limiters involves plastic collapse behavior of the annual plates and radial rectangular gusset plates (see Appendix A, Figure A.5). In addition, for the top ring impact limiter, balsa wood between the radial gussets also absorbs substantial crush energy.

The mean crush stress in an open steel structure (such as the ring structures) is governed by plastic buckling behavior. An expression for this mean crush stress for axial collapse of circular tubes is given in Reference 4.

$$\bar{\sigma}y = 15.19\ \sigma y\ \frac{t}{s}$$

$\bar{\sigma}y$ = effective crush stress (16370 nt/cm^2) based on steel cross section

σy = material dynamic yield stress (34490 nt/cm^2 assumed)

t = wall thickness 0.95 cm

c = tube diameter (30.5 cm assumed)

This expression was used with the values indicated above to arrive at a crush stress of (16370 nt/cm^2) for the steel components of the ring structures.

For the bottom ring impact limiter, an equivalent crush energy density was computed as:

$$E_{eqB} = \frac{(\text{vol steel})\ \bar{y}}{\text{total volume}} = 1.16 \times 10^3\ \text{nt/cm}^2$$

where:

$$\text{vol steel} = 20.3 \times 0.95 \times 25.4 \times 40.6 + 2 \times 0.95 \times \pi\ (63.5^2 - 38^2)D\ \text{cm}^3$$

$$\text{total volume} = 40.6\pi\ (63.5^2 - 38.1^2)\ \text{cm}^3$$

For the top ring impact limiter which is filled with 1.15 x 10^3 nt/cm^2 balsa,

$$E_{eq_T} = \frac{\text{vol steel}}{\text{total volume}}\ \bar{\sigma}y + 1.103 \times 10^3\ \text{nt/cm}^2 = 2.52 \times 10^3\ \text{nt/cm}^2$$

Energy absorbed by the two ring type impact limiters as a function of crush depth may now be computed by determining the volume of the impact limiters consumed as a function of crush depth. Referring to Figure F.1, this expression takes the form:

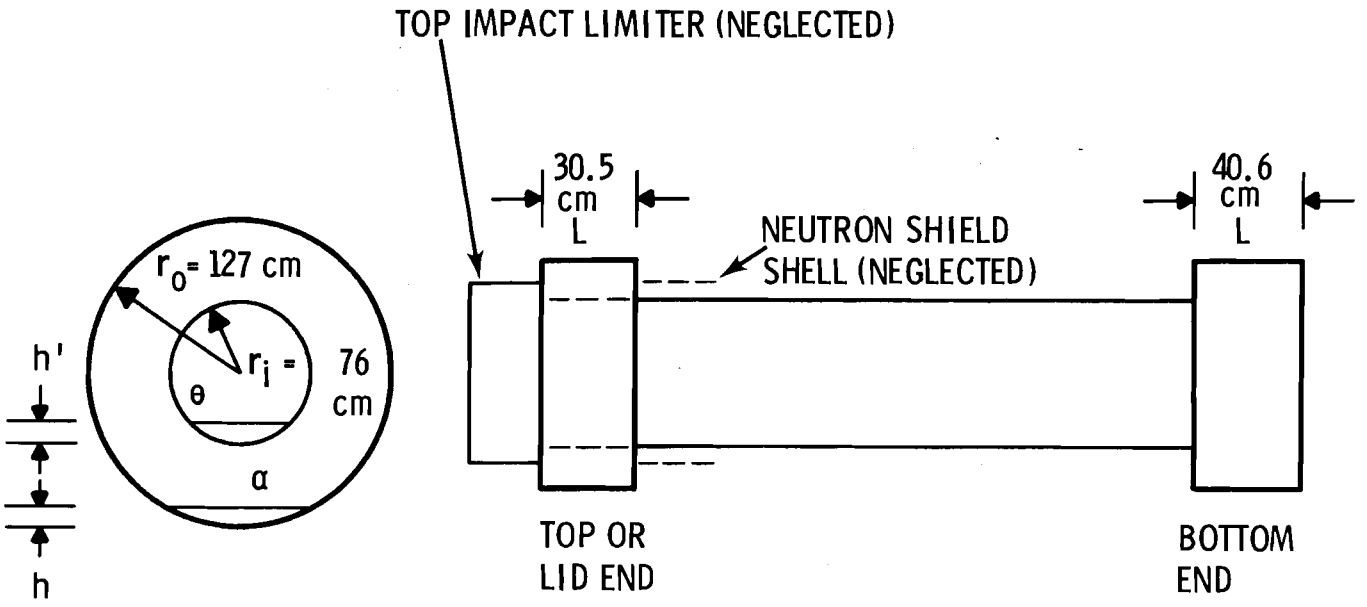

FIGURE F.1. Volume Consumption of Ring Impact Limiters and Main Shell Structure

$$E_{IL} = r_o^2 \left[E_{eq_B} L_B + E_{eq_T} L_T\right] [\alpha - \sin\alpha\cos\alpha]$$

where:

$$\alpha = \cos^{-1} \frac{r_o - h}{r_o} \quad \alpha_{max} = \cos^{-1} \frac{25-10}{25} = 0.927 \text{ rad } (53.13°)$$

L_B = width of bottom impact limiter, 40.6 cm

L_T = width of top impact limiter, 30.5 cm

E_{IL} = energy consumption of sacrificial ring impact limiters

r_o = impact limiter outside radius, 63.5 cm

$E_{IL}max = 2.231 \times 10^6$ nt - m

The impact force as a function of crush depth during this impact phase was approximated by differentiating the energy with respect to h. Applying the chain rule for differentiation, this force takes the form:

$$F_{IL} = \frac{dE}{d\alpha}\frac{d\alpha}{dh}$$

$$F_{IL} = 2r_o[E_{eq_B}L_B + E_{eq}+L_T] \sin \alpha$$

$$F_{IL\ max} = 1.282 \times 10^6 \text{ kgf @ } \alpha = 53°$$

In arriving at this expression, the assumption was made that crush depths of both ring structure were idnetical. The bottom ring structure, while wider than the top ring does not contain balsa wood inserts and will therefore not be as stiff. For this reason, the bottom ring will have a greater crush penetration than the top. Symmetrical behavior was assumed, however, and crush depth h of Figure A.5 of Appendix A represents somewhat of an average for the two rings.

After crushing of the ring type impact limiters to a depth of 25.4 cm, further kinetic energy of the cask is assumed to be absorbed by lead movement and circumferential plastic stretching of the 3.2 cm shell. An expression for this energy may be found in the "Cask Designer's Guide".[5] Referring to Figure A.5 this expression is:

$$E_c = r_i^2 L\ \sigma_{pb}\ (\Theta - 1/2 \sin 2\Theta)$$

$$+ r_i t_s L\ \sigma_s[\sin\Theta(2 - \cos\Theta) - \Theta]$$

where:

r_i = shell radius (38.1 cm)

L = shell length (452 cm)

σ_{pb} = dynamic flow stress of lead (3.45×10^3 nt/cm^2 assumed)

$\Theta = \cos^{-1}\frac{r_i - h'}{r}$

t_s = shell thickness (3.2 cm)

σ_s = dynamic flow stress of shell material (3.4×10^4 nt/cm^2 assumed)

By differentiating this expression with respect to h' (of Figure F.1), the impact force due to this deformation component becomes:

$$F_i = r_i L \sigma_{pb} \frac{(1-\cos 2\,\Theta)}{\sin \Theta}$$

$$+ \frac{t_s\, L\sigma s}{\sin \Theta} [2 \cos \Theta - \cos 2\,\Theta - 1]$$

Impact velocities and maximum g level as a function of crush depth may now be computed for side-on impact onto a rigid target. For penetration depths less than 25.4 cm, these two parameters become:

$$v = \left(\frac{2E_{IL}}{M}\right)^{1/2}$$

where:

v = impact velocity

E_{IL} = energy absorbed by top and bottom ring impact limiters

M = mass of cask (22680 kg)

$$Ng = \frac{F_{IL}}{M}$$

Ng = maximum decleration rate, g's

M = cask mass.

For penetration depth greater than 25.4 cm, the analogous expressions are:

$$v = \left[\frac{2(E_{IL(max)} + E_L)}{M}\right]^{1/2}$$

$$Ng = \frac{F_{IL(max)} + F_c}{M}$$

Graphs of impact velocity and maximum g level versus penetration distance are shown in Figure F.2. For a penetration depth (and assumed failure) of 28.6 cm (3.2 cm penetration into the main shell), the cask impact velocity and assumed failure threshold was 1796 cm/sec (64.7 km/hr) (40.2 mph).

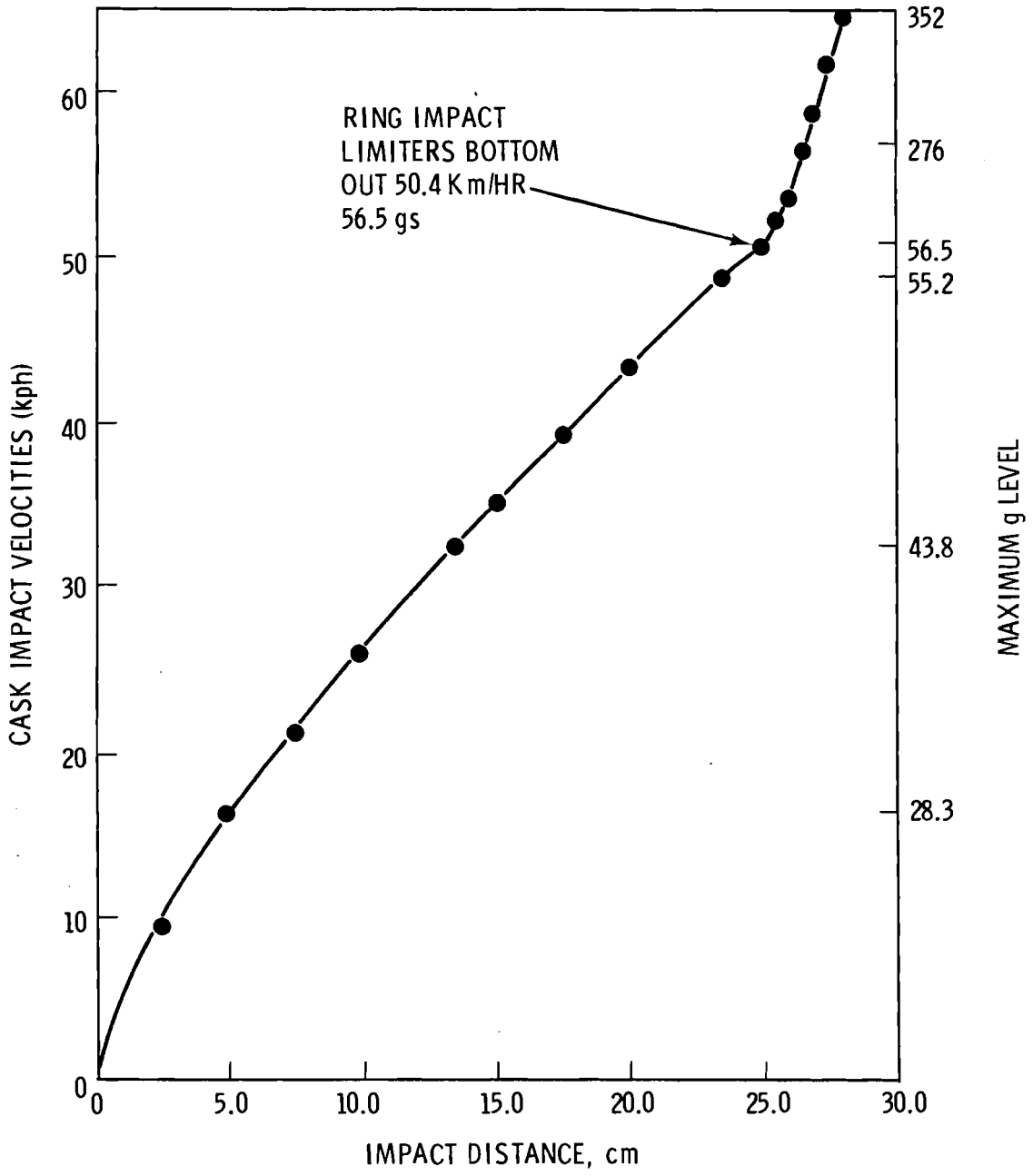

FIGURE F.2. Impact Velocity and Maximum g Level versus Impact Distance

Case 4. Determine the cask failure threshold for a side-on impact against a rigid, 1.5 m diameter column.

This impact case considers cask behavior for accidents in which the cask becomes detached from the trailer and strikes a rigid column such as an overpass support. Such a condition could occur, for example, when the trailer jackknifes and the column is assumed not to yield.

The impact condition under consideration is shown in Figure F.2. Due to the length of the generic cask being considered, impact severity is highly dependent upon the proximity of the cask center of mass and the point of impact. For this reason, failure velocities will be computed as a function of this electricity value (e of Figure F.3).

The cask motion before impact is assumed to the pure translation; no rotational velocity considerations are made. In addition, the cask geometry was idealized. It was assumed that the cask could be treated as a right circular cylinder of uniform density. The diameter of the cylinder was

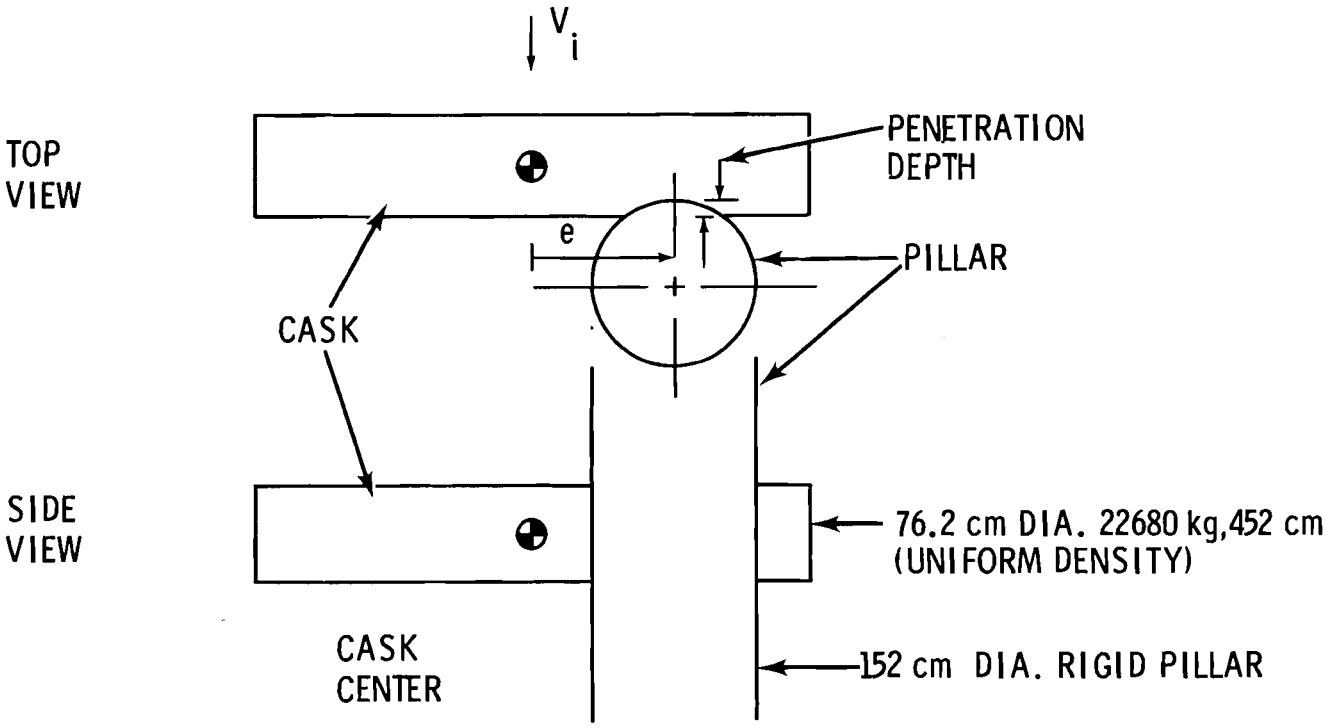

FIGURE F.3. Impact Configuration for Side-On Impact into a Pillar

chosen to be 76 cm, the OD of the main 3.2 cm thick shell. The length was assumed to be 452 cm, the length of the lead column. In addition, the mass of the cylinder was assumed to be 22680 Kg, the mass of the generic cask being considered.

An assumption of idealized impact was made. This implies that the separation velocity of the impact point on the cask relative to the column is zero after impact, or:

$v_f = \omega e$

v_f = final velocity of cask center of gravity

ω = final angular velocity of cask.

By assuming that the impact force acts over a small length of the cask, the following expression results from impulse considerations:

$$I_{cg}\omega = Me(v_i - v_f)$$

where:

I_{cg} = moment of inertia of cask about the center of gravity, $1/12\ ML^2$

M = cask mass

From these last two expressions, it can be shown that the kinetic energy lost due to impact is:

$$\text{Energy Loss} = \frac{Mv_i^2}{2} \quad \frac{L^2}{L^2 + 12e^2}$$

Thus, if a central impact occurs, all of the cask kinetic energy must be absorbed, whereas only about one-fourth is absorbed if the point of impact occurs near the cask end.

This impact energy causes permanent deformation of the cask. The following assumptions were made regarding this deformation energy:

- All of the energy dissipated went into the formation of a local dent in the side of the cask.
- The geometrical shape of the dent corresponded to the common volume of the two right circular cylinders composed of the 1.5-m diameter column and the 0.76-m diameter cask model.
- The energy consumed in the formation of this dent is equal to the dent volume multiplied times the dynamic flow stress of lead (3.46×10^3 nt/cm^2 assumed).

Maximum impact force was computed for this case by differentiating the deformation energy as described above by the penetration depth. Deformation energy and maximum force computed in this fashion are plotted against penetration depth in Figure F.4 and F.5.

For a central impact (corresponding to e = o) the gross bending moment incurred at the central cask section could be substantial. As an approximation to the worst case condition, the "plastic moment" of the cask model cross section will not be computed. Neglecting any contribution due to the neutron shield shell, this maximum moment is:

$$M = 4\sigma_{ys} \frac{r_{os}^3 - r_{is}^3}{3} + 4\sigma_{yl} \frac{r_{ol}^3 - r_{il}^3}{3}$$

$$+4\sigma_{ys} \frac{r_o^3 - r_i^3}{3}$$

$$M = 5.001 \times 10^6 \text{ nt - m}$$

where: σ_{ys} = steel yield stress (2.41×10^4 nt/cm^2 assumed)
σ_{yl} = lead yield stress (1.38×10^3 nt/cm^2 assumed)
r_{os} = 38.0 cm
r_{is} = 34.9 cm
r_{ol} = 34.9 cm

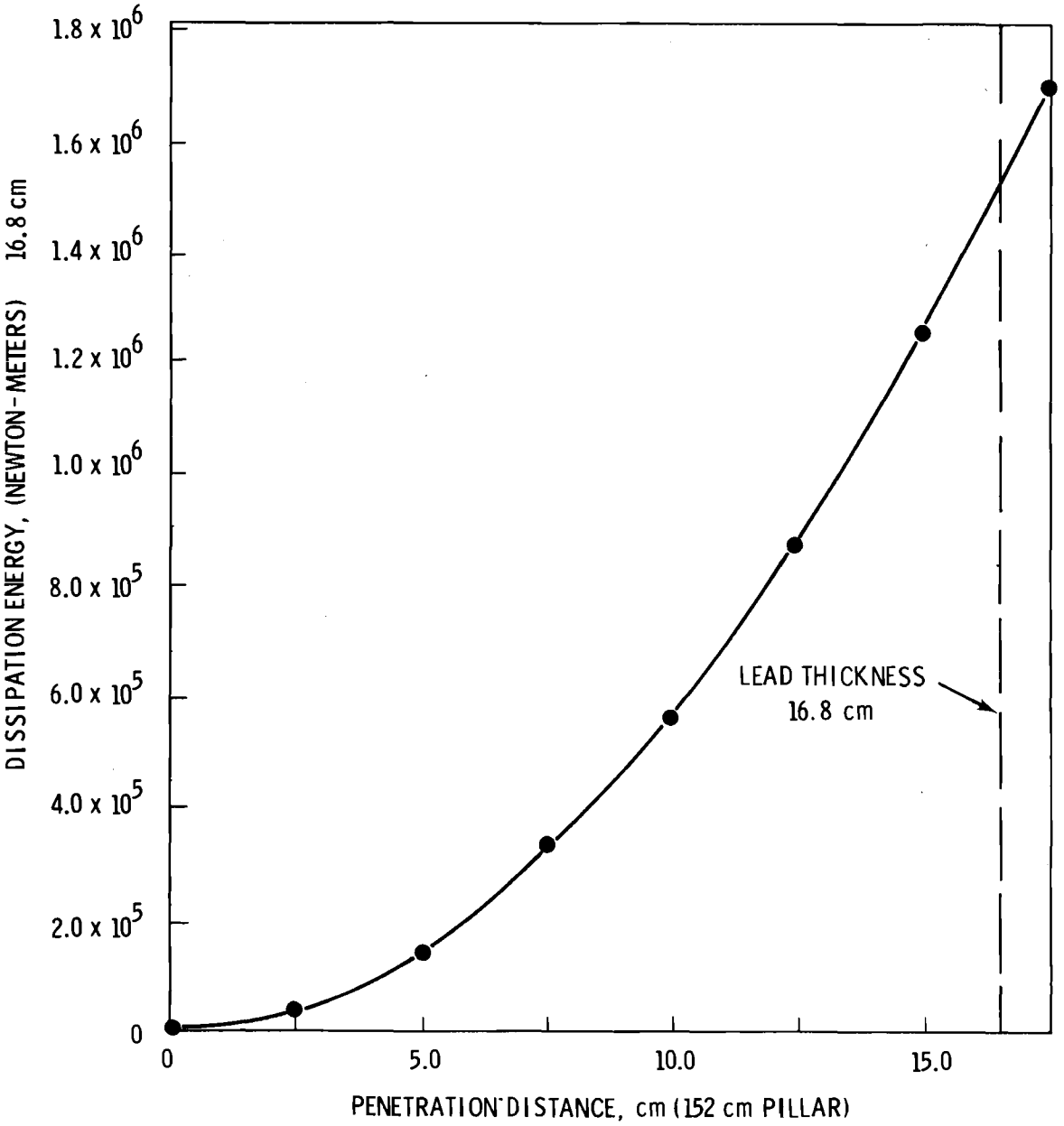

FIGURE F.4. Dissipation Energy versus Penetration Distance for Side-On Impact into a 152-cm Diameter Pillar

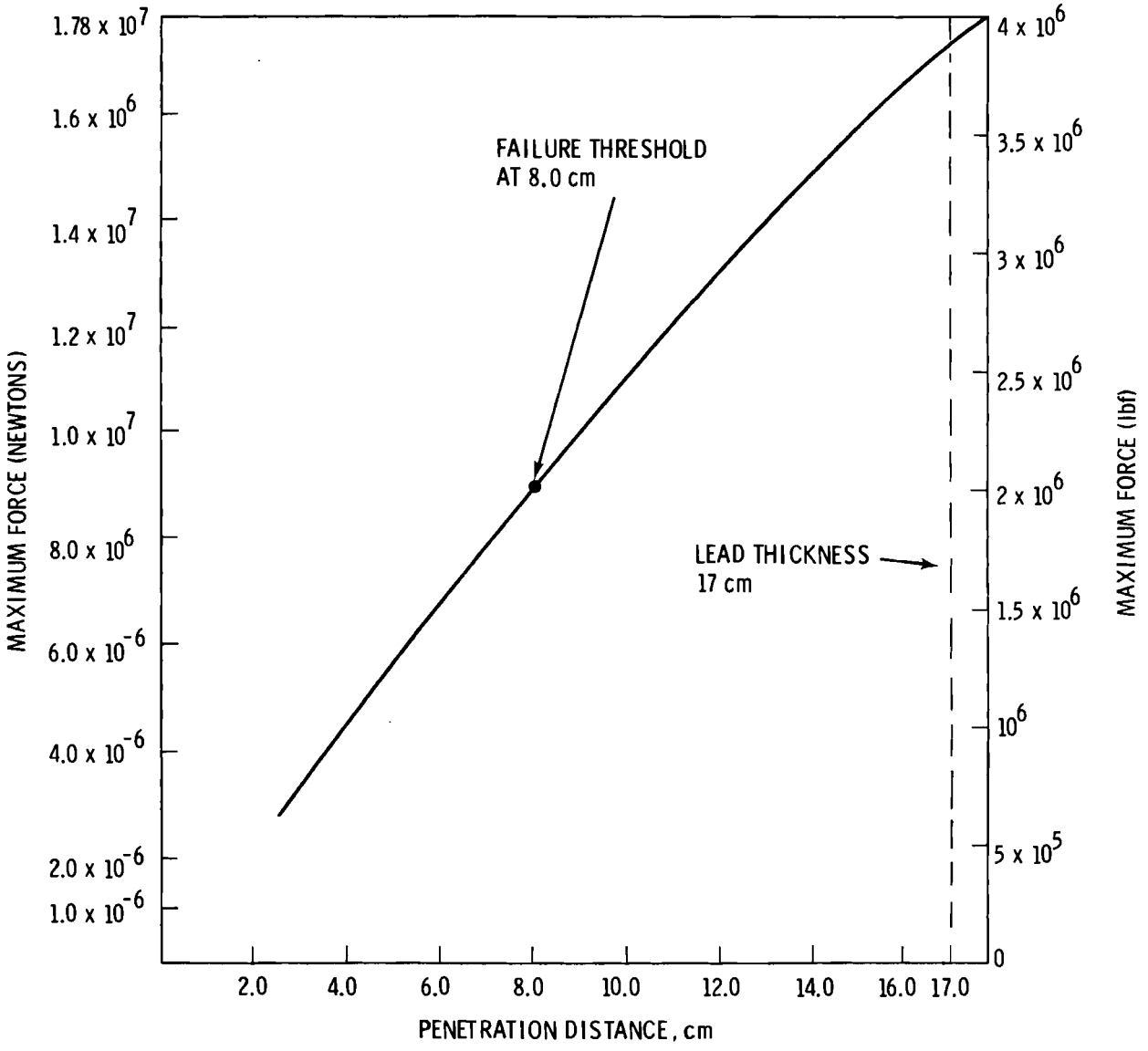

FIGURE F.5. Maximum Force versus Penetration Distance for Side-On Impact into a 152-cm Diameter Pillar

r_{il} = 17.9 cm
r_o = 17.9 cm
r_i = 17.1 cm

The impact force required to cause this moment (for central impact) is:

$$F = \frac{8M}{L} = 8.848 \times 10^6 \text{ nt}$$

From Figure F.4, this force level corresponds to a penetration distance of 8 cm and an impact dissipation energy of 3.6×10^5 nt-m.

Since this penetration distance is less than half of the lead thickness (16.83 cm), it was decided that a penetration distance of 8 cm or a penetration energy of 3.6×10^5 nt m represented a conservative failure threshold for central as well as eccentric impact. From the previous expression relating energy lost as a function of impact velocity and eccentricity, failure velocities were computed as a function of eccentricity. These failure velocities are plotted in Figure F.6.

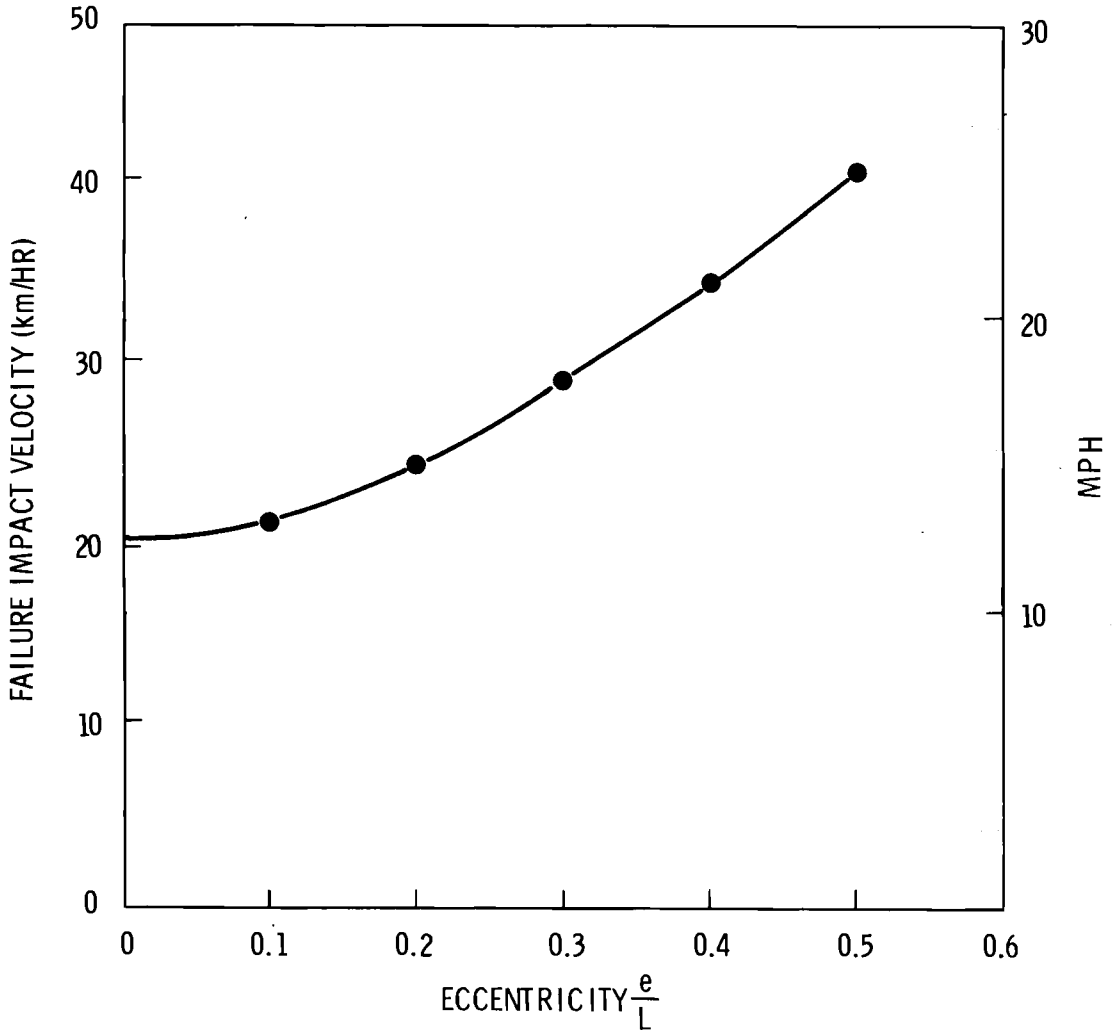

FIGURE F.6. Failure Velocity versus Impact Eccentricity for Side-On Impact into a 152-cm Diameter Pillar

It should be mentioned that a central impact, dent formation will reduce the bending section of the cask and hence some plastic bending may occur. It is believed, however, that local strain hardening and the decrease in inertial loading accompanying plastic bending will prevent gross bending behavior for velocities below those of Figure F.6.

Case 5. Determine the load per unit length that the cask can withstand without crushing.

The neutron shield shell was not assumed to support any appreciable crush load. For calculation of the crush load, the main 3.17-cm shell was considered the only structural member. This is a very conservative assumption which shows that crush forces in transportation accidents will not fail the cask.

The crush configuration analyzed is shown in Figure F.7. A very conservative analysis for this case assumes crush failure when the ring flexure stress in the main shell exceeds the yield stress of the shell. This crush load was found to be 2.86×10^3 nt/cm (1.76×10^6 nt over the entire cask) by using the following expressions found in Reference 6.

$$M_{max} = \frac{WR}{\Pi}, \quad \sigma_{max} = \frac{6M}{t^2} \text{ max}$$

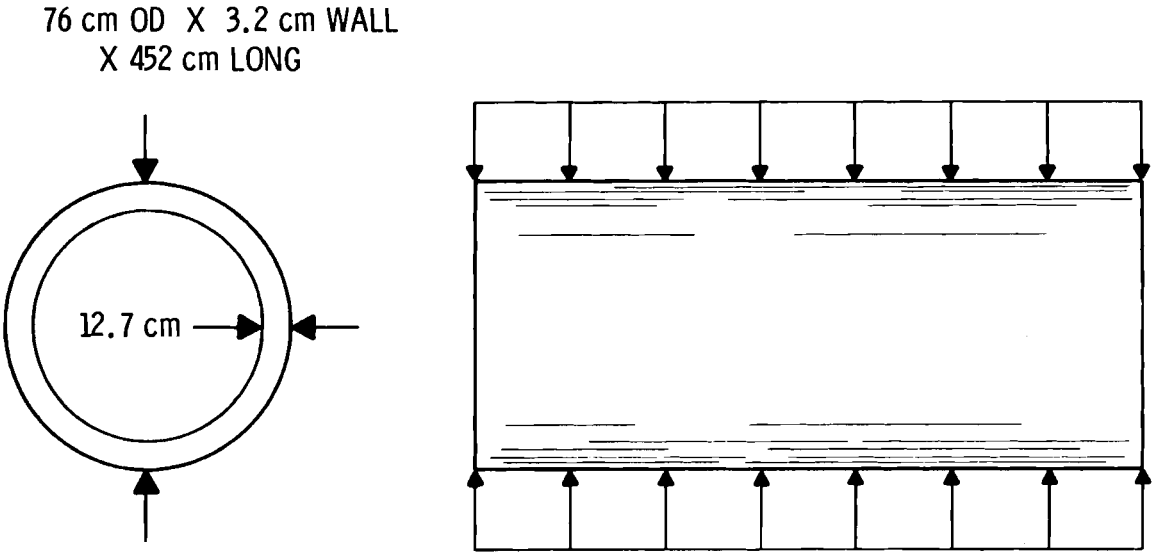

FIGURE F.7. Crush Model for 3.2-cm Thick Main Shell

where: M = bending moment per unit length

W = crush load/unit length

σ_{max} = flexure stress (2.070×10^4 nt/cm^2 assumed)

t = shell thickness (3.18 cm)

R = cylinder radius (38.1 cm)

Case 6. Determine the cask impact velocity necessary for failure of the cask body.

The threshold levels for cask failure by impact derived in other sections of this appendix are based on cask failure which results in release of radioactive materials. In this case, a failure where the cask cavity is opened to the surrounding atmosphere is analyzed. Credible accidents involving impact within the known truck accident environment that could produce this type of failure would be extremely rare and have never occurred.

The CASK computer program (discussed in Case 1) was used to estimate a lower limit of energy required to breach the outer cask shell. Energy absorbed by the transport vehicle and impact limiters was neglected.

Type 321 or type 347 stainless steel is used for constructing the outer cask shell. Experimental tensile test data[7] indicates that both types of stainless can tolerate greater than 50% strain (in a 2" sample) before rupture. A conservative failure point for the cask wall was assumed to occur at 20% hoop strain in the outer shell. The CASK program predicts that this may occur at about 42.7 m/s (95.5 mph) impact velocity with a rigid planar target. This is equivalent to drop height of 95 m.

SPENT FUEL ELEMENT FAILURE THRESHOLD

Case 7. Determine the cask velocities for fuel pin failure during end-on and side-on impact against a rigid target.

PWR fuel bundles (and fuel pins) differ greatly in design. A diagram showing basic fuel pin features is shown in Figure F.8. The fuel pins are transversely supported by grid spacers along the length of the fuel bundle. The hollow plenum end is typically quite short and serves as a gas containment region to prevent excessive pressure buildup.

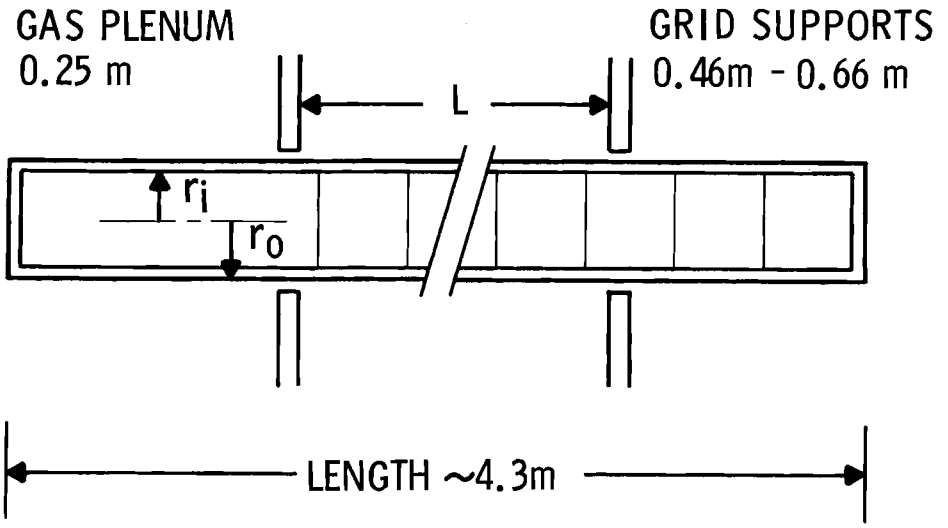

FIGURE F.8. Fuel Pin Diagram

It should be emphasized that no consideration was given to pin differences within a fuel bundle. Poison rod pins were not considered. In addition, the potentially significant stress enhancing effects of appurtenances such as fuel pin end caps and fuel bundle end fixtures were not considered.

Three different pin designs were analyzed for impact effects. Geometries and weights for these pins were taken from Reference 8 and are shown in Table F.1.

For all three pin designs, cladding was Zircaloy. Failure stress for the irradiated Zircaloy was assumed to be 6.209×10^4 nt/cm^2. This value was assumed after reviewing tube test rupture data for irradiated Zircaloy contained in Reference 9. It was further assumed that the stress failure mode was that of maximum shear stress. thus, for the pin cladding being considered, failure was assumed to occur when the maximum shear stress exceeded 3.103×10^4 nt/cm^2.

The cladding was assumed to be stress-free during normal transport conditions except for stresses caused by internal gas pressure. In particular, stresses caused by pellet swelling and stresses corresponding to residual stress states were neglected.

TABLE F.1. Fuel Failure Thresholds

	Bundle I	Bundle II	Bundle III
Tube inside radius (cm) r_i	0.479	0.474	0.493
Tube outside radius (cm) r_o	0.546	0.536	0.559
Grid span length (cm) L	53.3	66.0	45.7
ω (kg/m)	0.8768	0.8590	0.9608
Pressure stress nt/cm^2			
Axial σ_{pa} (tensile)	2911.	3143.	3053.
Circumferential σ_{pc} (tensile)	5821.	6288.	6107.
End-On Impact			
Inertial force (nt)	1806.	1766.	1979.
Buckling force (nt) (static)	889.	507.	1281.
Inertial stress nt/cm^2 (axial compressive)	8668.	9768.	9435.
Traveling wave stress (nt/cm^2) σ_{ra}	5.284×10^4	5.189×10^4	5.192×10^4
Incremental velocity for end-on failure			
Δv cm/s	844.3	797.1	795.0
Δv km/hr (mph)	30.25 (18.8)	28.64 (17.8)	28.64 (17.8)
Cask velocities for fuel failure			
m/s	18.68	18.48	18.47
km/hr (mph)	67.2 (41.8)	66.4 (41.3)	66.4 (41.3)
Side-On Impact			
g level for fuel failure, Ng	75.82	45.11	111.4
Fundamental period (sec.)	0.0147	0.0239	0.0110
Cask velocity for fuel failure			
m/s	14.02	9.45	14.05
km/hr (mph)	50.5 (31.4)	34.1 (21.2)	50.7 (31.5)
Midspan deflection @ failure (cm)	1.07	1.65	0.88

Precise structural modeling of fuel pin behavior under dynamic conditions is a difficult task. Knowledge regarding the cladding-fuel bond and the degree of structural continuity in the pellet stack would be needed in order to accomplish this. The following simplifying assumptions were, therefore, made:

- stiffness effects of the fuel pellet stack were neglected, and
- the mass of the fuel pellets was assumed to be uniformly distributed along the length of the fuel pin cladding.

Gas pressure inside the fuel pin was assumed to be 80.8 atm. This value was taken from Reference 10 and reflects a correction so as to correspond to a nominal pin temperature of 177°C.

Nominal stress levels due to pressure were conservatively computed by neglecting cavity pressure (normally 10.9 atm). This was done since primary coolant pressure could possibly be lost during an impact condition. Considering only internal gas pressure, the axial and circumferential stresses were computed as:

$$\sigma_{pa} = \frac{Pr_i}{2(r_o - r_i)}$$

$$\sigma_{pc} = \frac{Pr_i}{r_o - r_i}$$

$$p = 818.6 \text{ nt/cm}^2$$

Pressure stresses computed for the three pins being considered are shown in Table F.1.

END-ON IMPACT

Cladding stresses for end-on impact were assumed to be composed of the following three stress conditions:

- stresses caused by a nominal internal pin pressure of 818.6 nt/cm^2,
- stresses caused by body force loading during that phase of impact for which the impact limiter is being crushed,

- traveling wave stresses caused by an assumed instantaneous velocity change when the impact limiter bottoms out.

The pins were assumed to be perfectly straight before and during impact. If the pins are sufficiently warped, then failure would most likely occur well below the failure velocities listed in Table F.1. The decrease in failure velocity threshold due to pin eccentricity would depend upon:

- The degree of eccentricity,
- the duration of impact,
- the degree of lateral motion allowed by neighboring pins,
- the degree by which the primary coolant and grid spacers would retard lateral motion.

Some insight regarding the likelihood of buckling can be gained by considering the question of static buckling of an idealized model. For a perfectly straight fuel pin having multiple and equally spaced support points, the critical buckling force is:[11]

$$F_{cr} = \frac{\Pi^2 EI}{L^2}$$

where: E = cladding modulus of elasticity (8.96×10^6 nt/cm^2)
L = distance between grid supports
I = area moment of inertia $\frac{\Pi}{4}(r_o^4 - r_i^4)$

This equation assumes that support grids provide only lateral and no rotational constraint. Values of F_{cr} were computed for the pins being considered and are tabulated in Table F.1.

As a comparison load level, the axial force required for 46.47 g deceleration was computed. This deceleration rate corresponds to that level caused by crushing of the end impact limiter and represents the axial force near the impact end of the pin.

$$F_{Ng} = 46.47\ (w)\ (L_p)$$

where: L_p = pin length 452 cm, assumed
w = pin weight per unit length (Table F.1)

Values of F_{Ng} corresponding to each of the three pins analyzed are also shown in Table F.1.

For each of the cases considered, F_{Ng} was substantially larger than F_{cr}. This implies that pin failure due to dynamic buckling could be a likely failure mechanism. However, consideration of pin failure due to dynamic buckling is beyond the scope of this analysis, and stable pin behavior was assumed.

Axial stresses caused by uniform deceleration during end-on crush of an impact limiter were computed as:

$$\sigma_{Ia} = \frac{-Ng\ w\ L_p}{A_{cl}}$$

where; Ng = g level of deceleration (46.47 assumed from Case 1 calculations)
w = weight per cm Table F.1)
L_p - pin length (assumed same as cavity length, 452 cm)
A_{cl} = cladding cross sectional area, $\pi(r_o^2 - r_i^2)$

Axial stresses computed in this fashion are shown in Table F.1 for the three fuel pins being considered.

If end impact limiters are sufficient to completely absorb the kinetic energy of the cask, then only stresses in fuel pins caused by internal pressure and deceleration will occur. For cask velocities in excess of this amount, it was assumed that the pins were instantaneously stopped when the impact limiter became fully crushed.

An instantaneous velocity change at the end of a uniform bar induces an axial stress wave of magnitude:

$\sigma_T = \Delta v\sqrt{E\rho}$, (Ref. 12)
E = bar modulus of elasticity
ρ = bar material density.

In keeping with the assumption that pellet stiffness is neglected and that pellet mass is uniformly distributed along the pin cladding, these two parameters become:

E = modulus of elasticity of Zircaloy (8.96×10^6 nt/cm^2)

ρ_{eq} = equivalent cladding density

$$\frac{w}{\pi(r_o^2 - r_i^2)\, 10^4} \quad \left(\frac{nt\ sec^2}{cm^4}\right)$$

Instantaneous fuel pin velocity changes required to cause pin failure were computed from the following expression:

$$6.209 \times 10^4\ nt/cm^2 = \sigma_{pc} - \sigma_{pa} + \sigma_{Ia} - \sigma_T$$

Values of σ_T and Δv required for pin failure are shown in Table F.1.

Initial cask impact velocity required for fuel pin failure was computed by using the following energy balance relationship:

initial kinetic energy	=	energy absorbed by impact limiter	=	kinetic energy remaining after crush of impact limiter

$$1/2\ mv_i^2 = \sigma_c L \frac{\pi D^2}{4} + 1/2\ m\ (\Delta v)^2$$

where: m = cask mass 22680 $\frac{nt\ sec^2}{m}$

σ_c = crush stress of impact limiter, $1.103 \times 10^3 \times 10^3$ nt/cm^2

D = diameter of impact limiter, 109 cm

L = thickness of impact limiter, 30.5 cm.

Initial cask velocities required for fuel failure of the three pin configurations are shown in Table F.1.

SIDE-ON IMPACT

Cladding stresses occurring during side-on impact were conservatively assumed to be caused by:

- internal pin pressure (80.77 atm),
- dynamic stresses due to inertial loading.

Stresses caused by internal gas pressure were computed for the end-on impact pin analysis and are tabulated in Table F.1.

Flexure stresses due to inertial loading were computed by assuming a model illustrated in Figure F.9. Symmetrical behavior on either side of a grid support was assumed. Thus, the model consists of a clamped beam segment corresponding in length to the grid spacing distance.

The pin motion was assumed to be small relative to the cask stop depth.

Stress levels in the cladding were not computed by considering the dynamic response of the fuel pins. Instead, stresses corresponding to an approximately equivalent static load were computed.

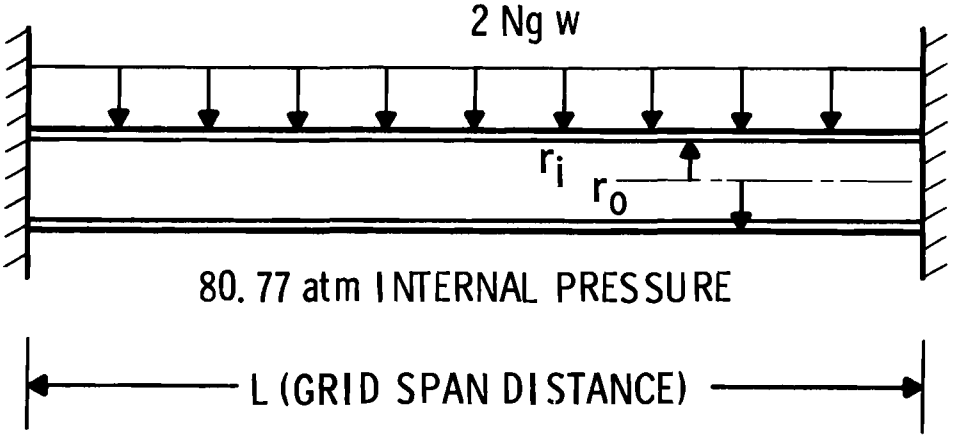

FIGURE F.9. Fuel Pin Model for Side-On Impact Failure

Fundamental periods for each of the pin designs were computed as follows:

$$T = \frac{2\Pi L^2}{4.730^2} \left[\frac{P}{EI}\right]^{1/2} \quad \text{(Ref. 13)}$$

where: T = fundamental period
L = grid support length
P = pin mass/unit length
E = cladding modulus
I = pin moment of inertia

These periods are shown in Table F.1.

Impact duration (the duration of pin loading) will depend on impact velocity. An estimate, for impact duration, is 19 milliseconds. (This corresponds to the time to traverse 25 cm at 48 km/hr). As can be seen from Table F.1, this is roughly equivalent to one period for the pins being considered. For this reason, a dynamic amplification factor of two was used to compute pin inertial loads. Thus, pin loading for a given cask impact velocity will be assumed to be:

$$W = 2Ng\ w$$

where: W = pin loading, nt/m
Ng = g level from Figure F.2
w = pin weight per unit length

It should be pointed out that this equivalent static load is conservative since Ng values used are assumed to be maximum g levels.

The maximum flexure stress for a beam loaded as shown in Figure F.9 occurs at the support points. This stress level and the midspan deflection are:(6)

$$\sigma_f = \frac{MC}{I}$$

$$y_{max} = \frac{2Ng\ wL^4}{384\ EI}$$

$$M = \frac{2wNgl^2}{12}$$

$$I = \frac{\pi}{4}(r_o^4 - r_i^4)$$

E = cladding modulus

$C = r_o$

L = pin grid span length

w = pin weight/unit length

Ng values for pin failure were computed from the following equation:

$$6.209 \times 10^4\ nt/cm^2 = \sigma_{pa} + \sigma_f$$

Cask impact velocities corresponding to these g levels were obtained from Figure F.2. Cask impact velocities, g levels and pin midspan deflections for the three cases considered are shown in Table F.1.

REFERENCES

1. H. Richard Yoshimura, Michael Huerta, Full-Scale Tests of Spent-Nuclear Fuel Shipping Systems, IAEA-SR-10/17, Sandia Laboratories, Albuquerque, NM, July, 1976.

2. M. Huerta, Analysis, Scale Modeling, and Full Scale Tests of a Truck Spent-Nuclear-Fuel Shipping System in High Velocity Impacts Against a Rigid Barrier, SAND 77-0270, Sandia Laboratories Albuquerque, NM, April 1978.

3. J. H. Evans, Structural Analysis of Shipping Casks, Volume 13. CEIR: A Fortran Program for Estimation of the Response of Cylindrical Lead Shielded Casks, ORNL-TM-1312 (Vol. 13), June 1974.

4. R. J. Burion and E. C. Lusk, Compact Metallic Impact Limiters for Shipping Containers, International Journal of Radiation Engineering, 1971, 1(4), pp. 349-364.

5. L. B. Shappert, A Guide to the Design, Fabrication and Operation of Shipping Casks for Nuclear Applications, ORNL-NSIC-68, Feb 1970.

6. R. J. Roark and Warren C. Young, Formulas for Stress and Strain, 5th edition, McGraw-Hill Book Co., NY, 1975.

7. W. F. Simmons, H. C. Cross, The Elevated-Temperature Properties of Stainless Steels, Special Technical Publication No. 124, Americal Society for Testing Materials, 1952.

8. Design and Analysis Report - IF 300 Shipping Cask, Nuclear Fuel Department, The General Electric Company, San Jose, CA, 1973.

9. P. J. Pankaskie, Irradiation Effects on the Mechanical Properties of Zirconium and Dilute Zirconium Alloys, A Review, Pacific Northwest Laboratory, BN-SA-618, 1976.

10. Wisconsin Utilities Project 1975, PSAR, Vol. 2, Fig. 4.2.5.

11. S. Timoshenko and J. Gera, Theory of Elastic Stability, 2nd edition, McGraw-Hill Book Co., NY, 1961.

12. S. P. Timoshenko, J. N. Goudier, Theory of Elasticity, 3rd edition 1970, McGraw-Hill Book Co., NY, 1975.

13. S. Timoshenko, D. H. Young, and W. Weaver, Vibration Problems in Engineering, 4th edition, John Wiley and Sons, NY, 1974.

APPENDIX G

THERMAL ANALYSIS OF REFERENCE CASK

INTRODUCTION

The transient thermal behavior of the reference spent fuel cask containing one spent PWR bundle under various postulated accident conditions is summarized in this appendix.

The objectives of this study were to determine the transient behavior of the cask and its spent fuel assembly during and after several fire and loss of cavity cooling situations. Calculated maximum fuel and cavity temperatures as a function of time obtained from the analysis allow failure sequences and releases of radionuclides to be estimated.

Title 10, Chapter 1, Code of Federal Regulations, Part 71, describes basic qualification tests for spent fuel packages. The thermal test requires that a cask with a surface absorptance of 0.8 retain its integrity for 0.5 hours in a 800°C (1475°F) fire with an emittance of 0.9. Additional mechanical tests are specified. Tests to license a shipping cask demonstrate that the cask can withstand certain conditions with only nominal damage. These are not failure tests. Calculated failure thresholds presented here are based on postulated conditions in excess of licensing requirements and are a representation, based on conservative (pessimistic) assumptions of the cask performance.

DESCRIPTION OF SHIPPING CASK

The reference spent fuel shipping cask analyzed is described in Appendix A. Information necessary for thermal analysis (e.g., general configuration, dimensions, materials of construction, etc.) are also given in Appendix A. A schematic of the cross section of the shipping cask with fuel assembly in place is shown in Figure A.3 of Appendix A. Thermophysical property data required for the analysis was taken from Reference 1.

DESCRIPTION OF FUEL ASSEMBLY

The particular fuel assembly selected for use in this analysis is a current design with the characteristics listed in Table A.3 of Appendix A.

The total heat generation rate of the fuel assembly is 11.5 kW and is considered to be uniformly distributed among all rods over their active length. The surface of the clad was assumed to be a diffuse emitter with a constant emittance of 0.4. Other thermophysical properties were taken from Reference 1.

ANALYTICAL APPROACH

The analysis employed a special purpose code designed to handle radiation and conduction heat transfer including an estimate of the effects of convection. The code utilizes an implicit finite difference technique and, as a consequence, time steps may be set according to desired accuracy rather than limited by stability criteria.

One portion of the code places nodes along cartesian axes and is therefore, naturally compatible with the square array of rods in the fuel assembly. Each node within the fuel assembly is centered on a fuel rod. Nodes exterior to the fuel assembly are identified with appropriate portions of the support/shield or the inner surface of the cask cavity.

The radiation heat transfer is calculated in the manner described in Reference 2 for interchange among gray surfaces. This method requires the calculation of view factors for applicable enclosures. The enclosure for a rod entirely within the fuel assembly is formed by considering nearest-neighbor rods and next-nearest-neighbor rods. The enclosure for rods on the exterior of the fuel assembly consists of the support/shield in addition to neighboring rods. Radiation heat transfer between the support/shield and the inside surface of the cavity was determined using an enclosure consisting of the cavity surface and neighboring support/shield surface. Water is considered opaque in the wave length range of interest and steam is considered as completely transparent.

Convection within the cavity is calculated on a local basis according to the expression $Nu = 0.037\ G_r^{0.37}$ as indicated in Reference 3. This method approximates, in what is believed to be a conservative fashion, the bulk circulation of fluid throughout the cavity.

The other portion of the code calculates the heat transfer through the cask proper. Continuity of temperature and equality of heat transfer rate is enforced at the inner surface of the cask cavity for both portions of the overall code. The nodal system for the cask is laid out conventionally in cylindrical coordinates. One or more nodes are assigned to each cylinder component of the cask depending on the thickness of that component.

Radiation heat transfer within the neutron shield cavity with steam present was modeled for two concentric cylinders. Convection heat transfer within the cavity is determined by means of the above expression relating Nusselt number with Grashof number for either liquid or gas. Convection heat transfer at the cask exterior is determined using the conventional heat transfer coefficient for a vertical plate whose length is equal to the diameter of the cask.

ACCIDENT CONDITIONS

Prior to accident occurrence, the fuel assembly and cask are in thermal equilibrium with the ambient conditions. These ambient conditions include convection and radiation to a 37.8°C (100°F) environment and insolation of 45.85 Btu/ft^2hr average over the entire cask surface or 144 Btu/ft^2hr to a surface normal to the sun.

At the beginning of the accident, the cask outer surface is breached allowing the neutron shield liquid to drain out. The vapor from the liquid remains in the neutron shield cavity for the duration of the accident.

At the initiation of a fire, the emittance of the cask outer surface increases from 0.3 to 0.8. Both convection and radiation heat transfer with the fire (effective emittance of 0.9) commence. At the conclusion of the fire, the emittance of the cask outer surface remains at 0.8, but convection and radiation heat transfer (including isolation) are now to a 37.8°C environment.

The cask cavity coolant will be released when the internal pressure reaches 76 atm (1115 psig) by means of a rupture disc. The analysis conservatively assumes that the rupture disc is in such a position that essentially all of the coolant is expelled at the moment of rupture. Based upon the volumes of the cavity and coolant and the vapor pressure of water, loss of coolant will occur at a mean coolant temperature of 285°C (545°F). After loss of coolant, steam at atmospheric pressure remains within the cavity.

When an initial loss of coolant with no fire occurs, ambient temperatures and heat transfer coefficients would apply to the outside of the cask. The cask internal temperatures were initially based on ambient conditions (with coolant), but the heat transfer coefficients were for a vapor atmosphere.

Calculations were made for the following accident assumptions:

1. 1/2-hr fire at 1010°C
2. 2-hr fire at 1010°C
3. No fire with initial loss of coolant
4. 1/2-hr fire at 1010°C with initial loss of coolant
5. 2-hr fire at 1010°C with initial loss of coolant
6. Minimum duration fire at 1010°C that causes a loss of coolant.

RESULTS

Steady state temperatures in the cask before the accident are shown in Figure G.1. The maximum fuel temperature is 177.8°C and the water in the cask cavity is at about 177.2°C. The inner and outer surface of the cask wall are at temperatures of about 172°C and 157°C respectively. The coolant in the outer jacket is at a temperature of 154°C and the temperature of the outer jacket wall is about 153°C.

The transient behavior of the cask and its spent fuel assembly during and after the fire was determined for six different cases which are summarized in the following paragraphs.

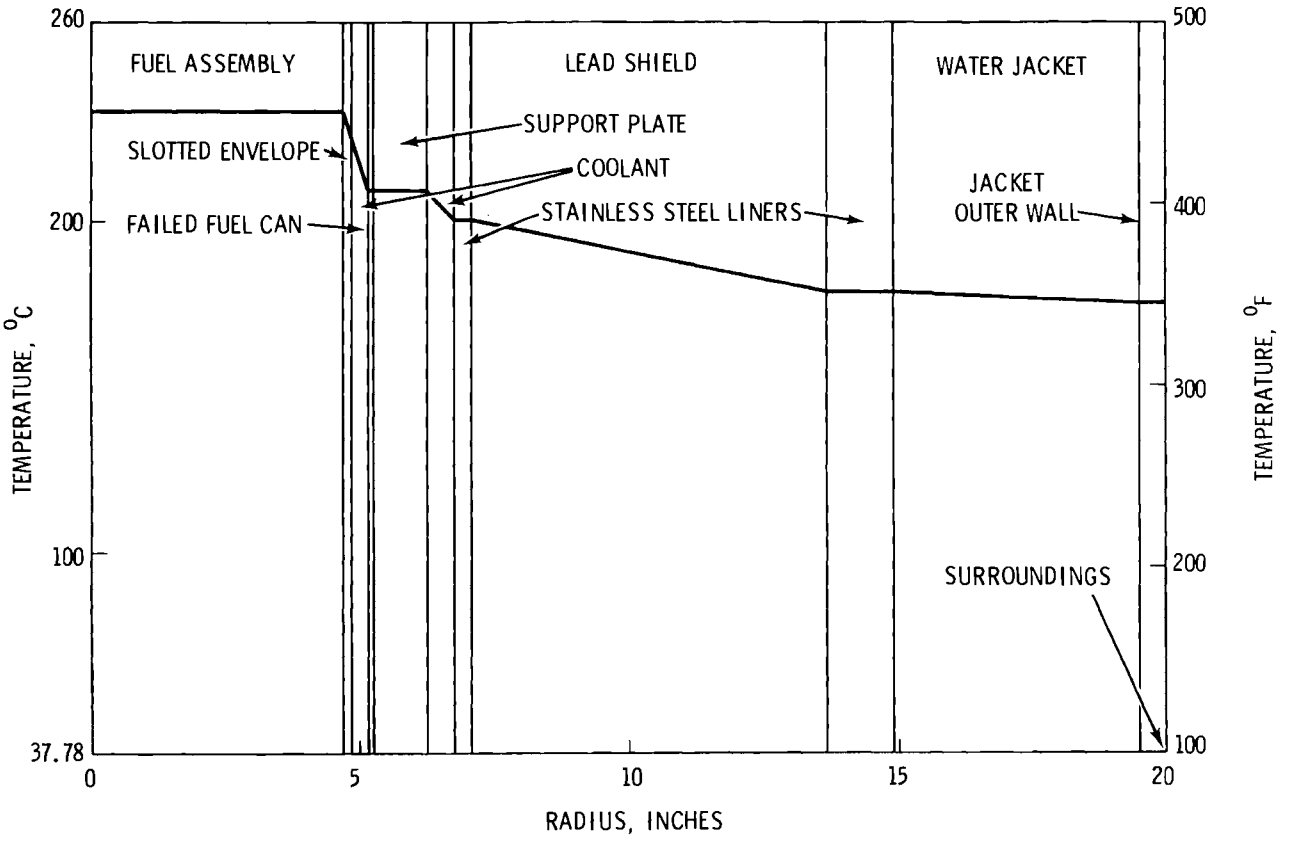

FIGURE G.1. Steady-State Temperatures in the Cask Before the Accident

Case 1 - 1/2 hr Fire at 1010°C

Temperatures in the cask as a function of time after the accident are shown in Figure G.2 for this case. The temperature of the surroundings were at the fire temperature of 1010°C for 0.5 hrs which then drop to ambient at 37.8°C. As the temperature of the cavity coolant increases, the pressure in the cavity also increases. At about 0.8 hrs at a coolant temperature of about 285°C and a pressure of 76 atm (1115 psia), the pressure rupture disk bursts relieving the cask internal pressure and expelling the cavity coolant to atmosphere. Failure of the rupture disk results in an instantaneous drop to atmospheric pressure in the cask cavity. The coolant left in the cask exists as a residual vapor.

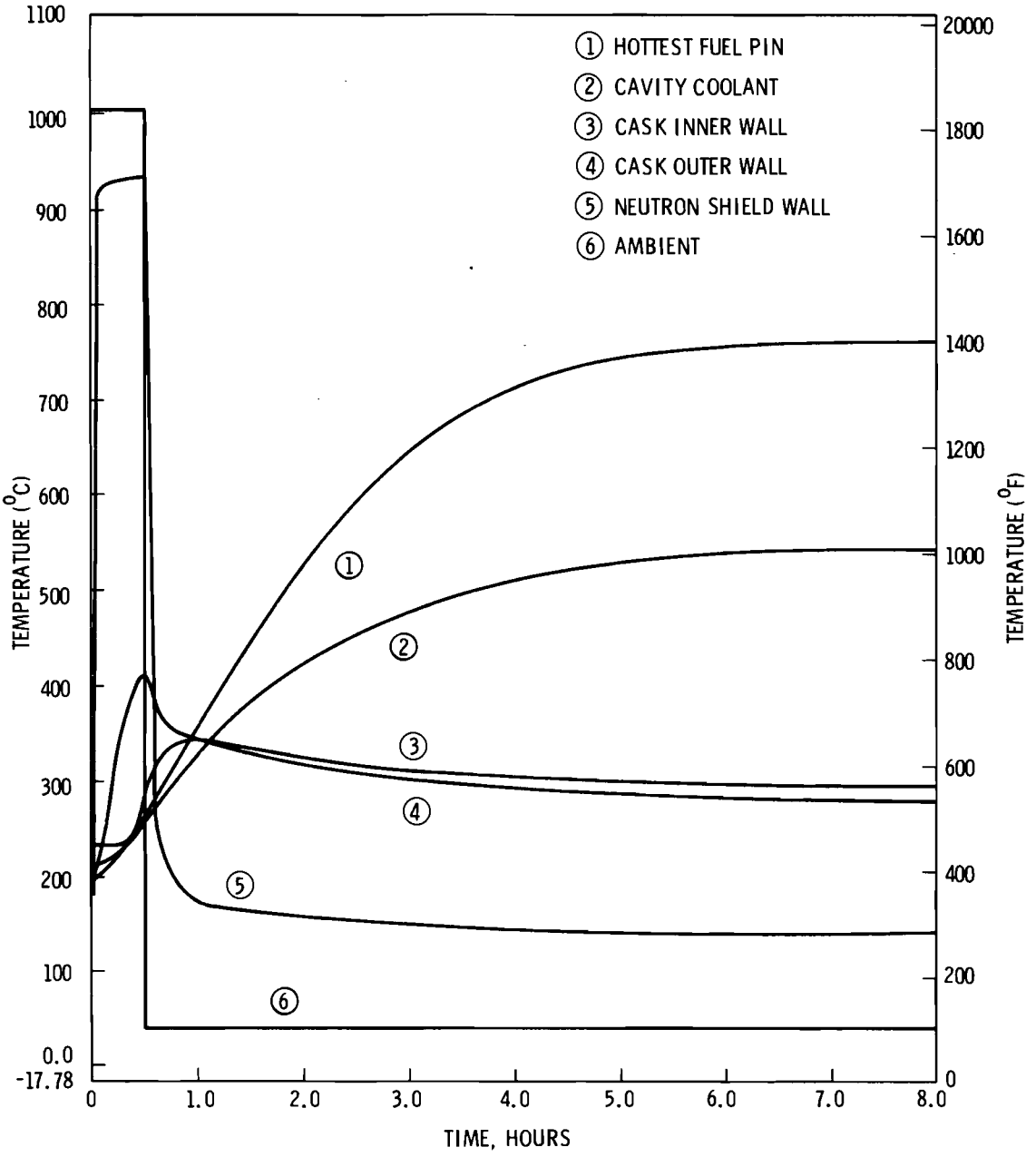

FIGURE G.2. 1/2-Hour Fire at 1010°C

As the fuel temperature increases, the pressure in the fuel pins increases which results in a hoop stress in the fuel pin clads. Fuel pin failure occurs when the hoop stress exceeds the creep rupture strength of the Zircaloy-4 tubing. Smith[4] estimates that some PWR cladding will start to fail above 565°C and all elements will fail above 675°C. Fuel cladding failures start to occur at about 2.6 hours after the start of the fire and by 4.0 hours, all are assumed to fail. The maximum fuel pin temperature would occur at about 8 hours after the fire starts at a temperature of about 760°C.

Case 2 - Two Hour Fire at 1010°C

Figure G.3 shows the temperature in the cask as a function of time for the case. The fire temperature surrounding the cask was assumed to last for two hours and then drop to ambient temperature conditions. At about 0.4 hours, after the fire starts, the cavity coolant would be lost. The fuel cladding starts to fail at 2.1 hours and was assumed to be all failed at about 3.1 hours after the start of the fire. The maximum temperature of the fuel for this case would be about 835°C which would occur at about 4 hours after the start of the fire.

Case 3 - No Fire With an Initial Loss of Cavity Coolant

Cask temperatures for this transient case are shown in Figure G.4. This case covers accidents where an initial loss of coolant occurs due to a cask failure. Coolant is drained from the cavity allowing the fuel element to self heat due to radioactive decay of fission products. Initial failure of fuel rod cladding would occur at about 2.2 hours after loss of coolant and all clad was assumed to fail at about 3.5 hours. The maximum temperature of the hottest fuel rods reached were 738°C at about 7 hours after loss of coolant.

Case 4 - 1/2 Hour Fire at 1010°C with Initial Loss of Cavity Coolant

In this case, a loss of coolant in the cavity was assumed to occur, followed by a 1/2 hour fire at 1010°C. Cask temperatures as a function of time after the accident are shown in Figure G.5. Initial fuel clad failure

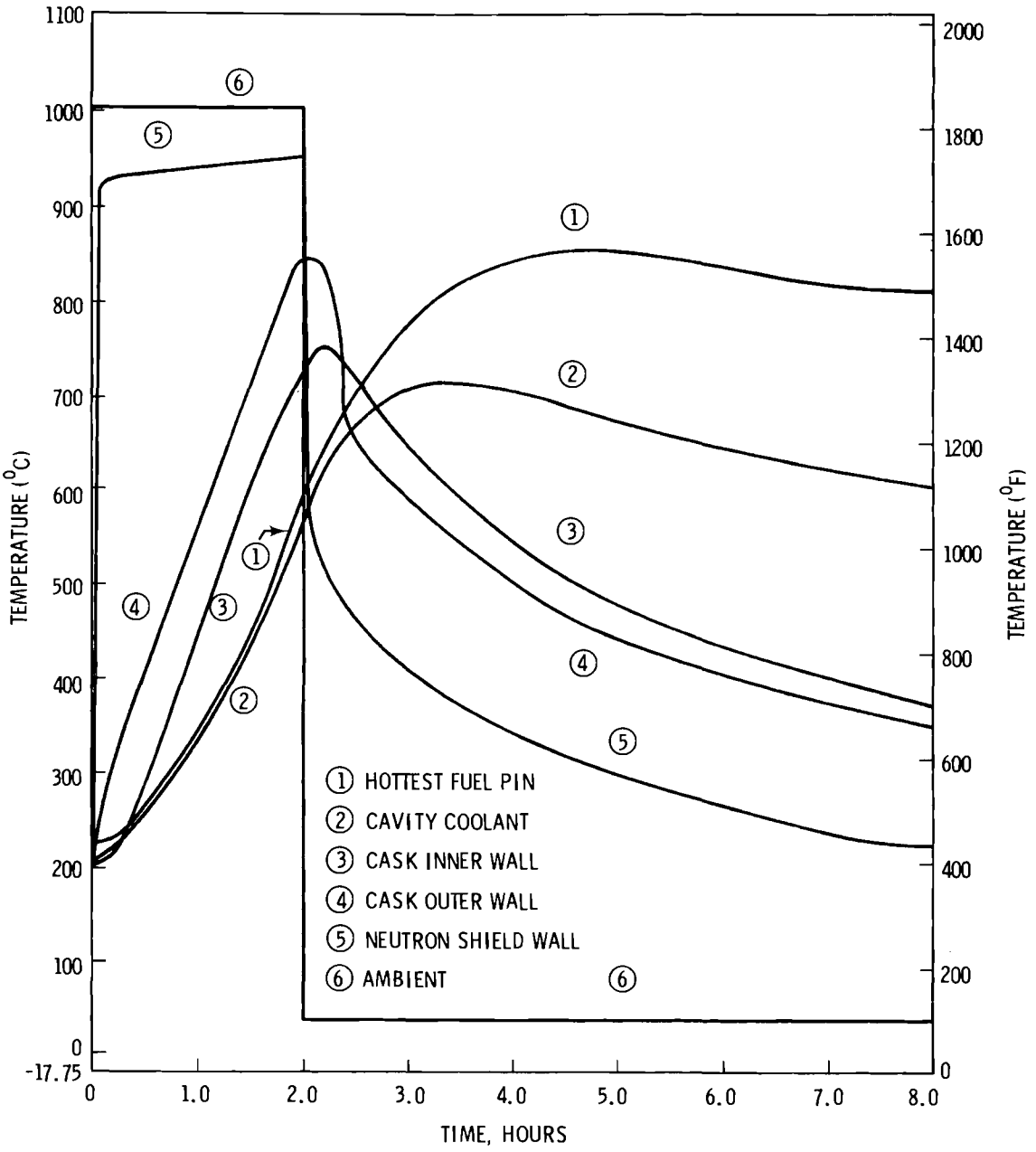

FIGURE G.3. Two-Hour Fire at 1010°C

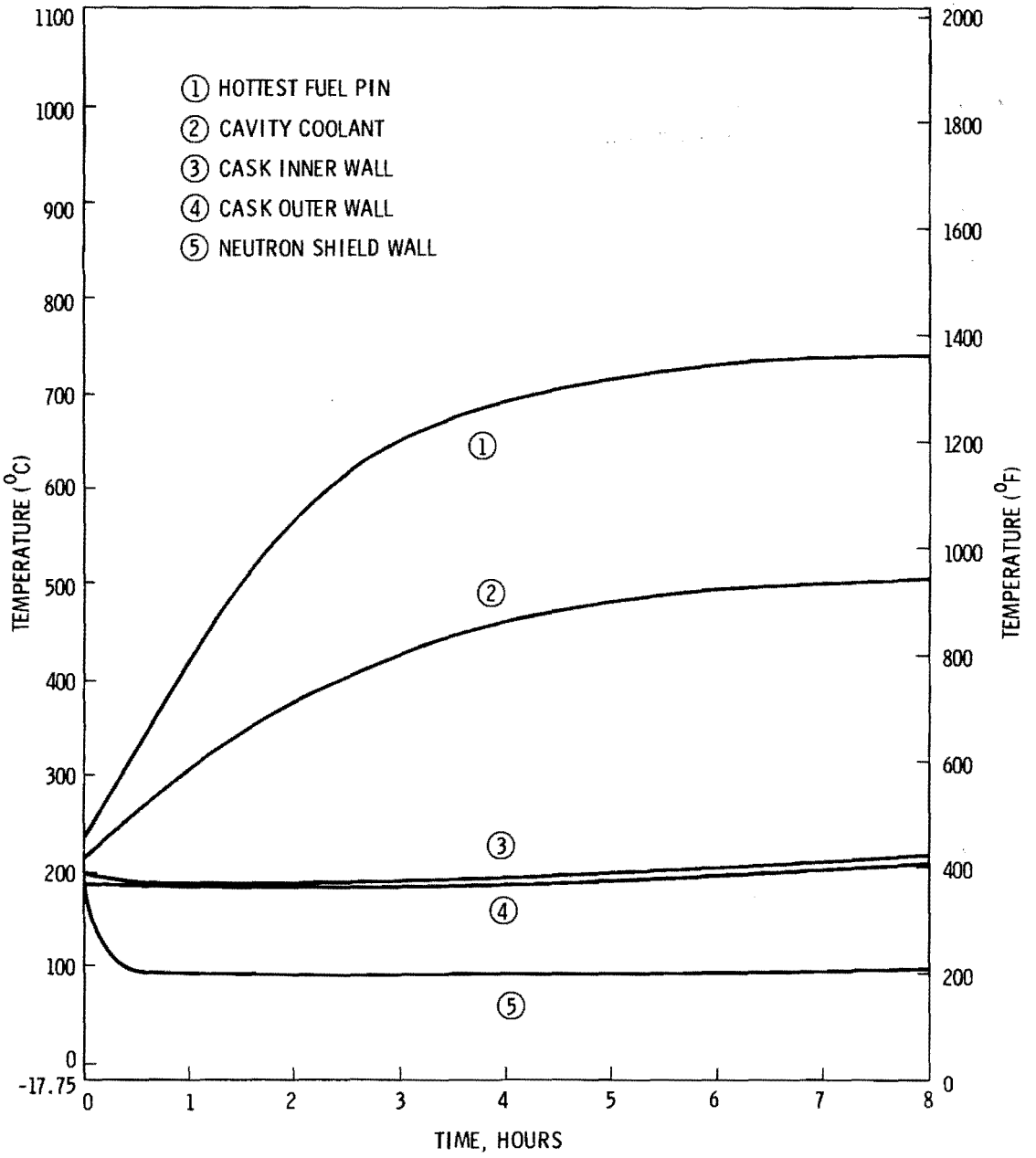

FIGURE G.4. Initial Loss of Coolant

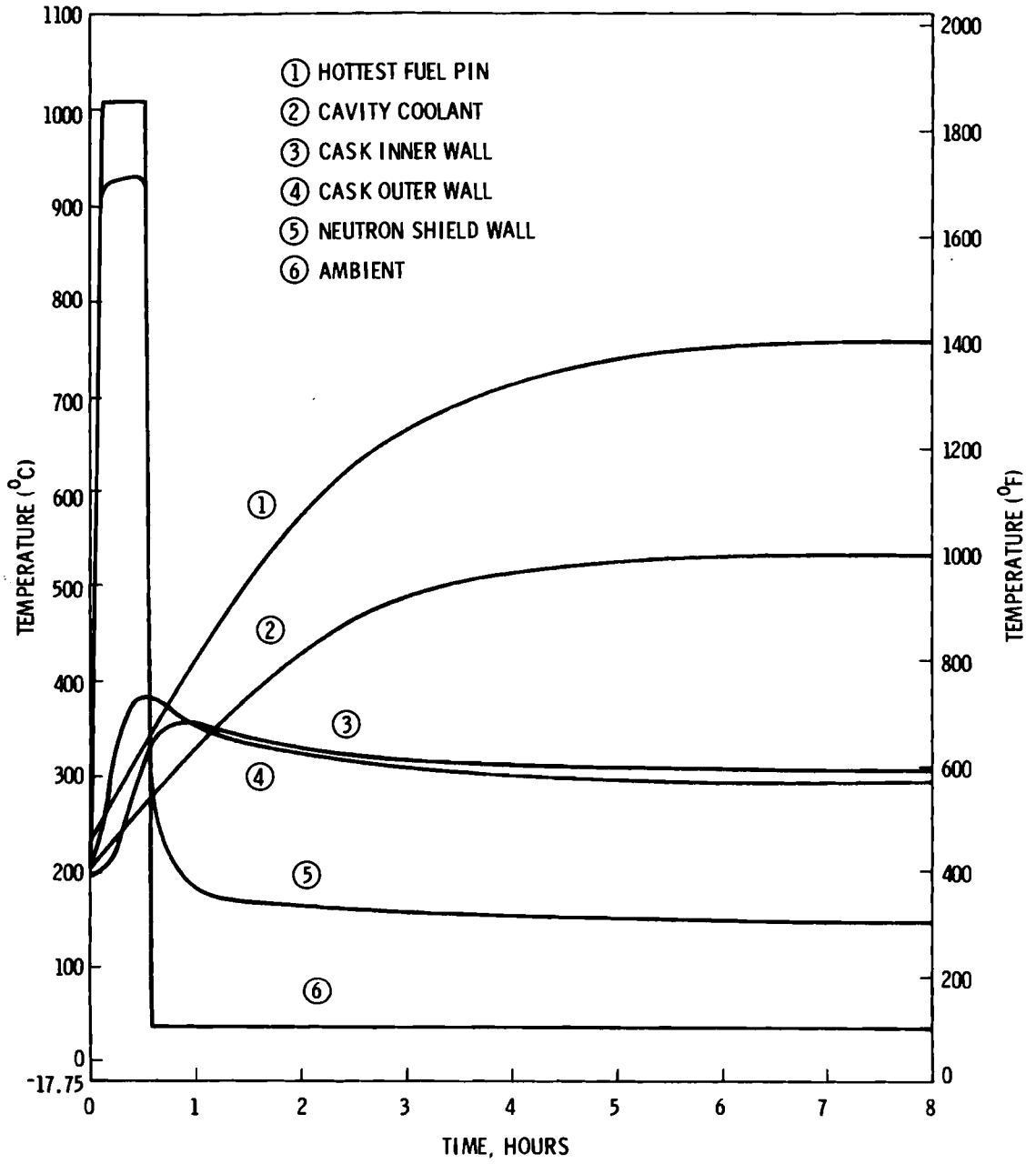

FIGURE G.5. 1/2-Hour Fire with Initial Loss of Coolant

occurred at about 2 hours after the accident and all cladding was assumed to fail by 2.8 hours following the accident. The maximum fuel clad temperature occurred about 6 hours after the accident at a temperature of 760°C.

Case 5 - Two Hour Fire at 1010°C With an Initial Loss of Cavity Coolant

For this case, a loss of coolant was also assumed, followed by a two hour fire at 1010°C. Figure G.6 shows the temperature in the cask as a function of time for this case. At approximately 1.8 hours from the start of the accident, the first fuel clad failure would occur. All cladding would be assumed to fail by about 2.1 hours after the accident. Maximum fuel temperature would occur about 4.5 hours after the accident at a temperature of 870°C.

Case 6 - Minimum Duration Fire to Cause Loss of Coolant to Occur

In this case, the cask thermal characteristics were analyzed to determine what minimum duration fire would result in the occurrence of a loss of cavity coolant. The thermal analysis showed that a fire would have to exceed 15 minutes length to heat the cask sufficiently to result in a loss of cavity coolant. The pressure would increase to 76 atm (1115 psia) which would cause the rupture disk to fail releasing hot coolant to the atmosphere.

Any fire which exceeds 15 minutes at 1010°C will result in a loss of cavity coolant in about 2.5 hours from the start of the fire. A release of radionuclides would then be possible because the rupture disk remains open. Curves for various fire durations giving the temperature of the hottest fuel are shown in Figure G.7.

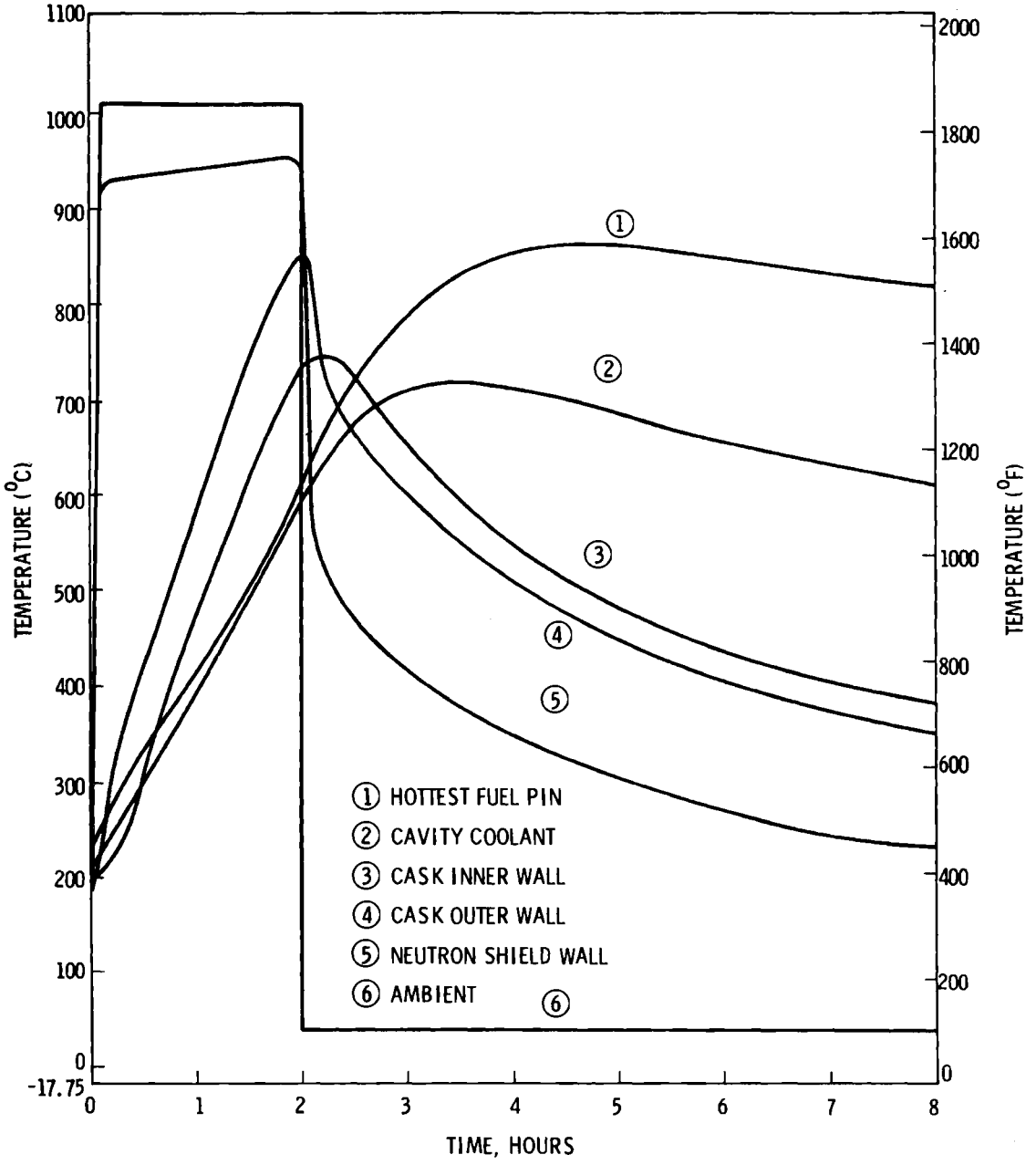

FIGURE G.6. Two-Hour Fire with Initial Loss of Coolant

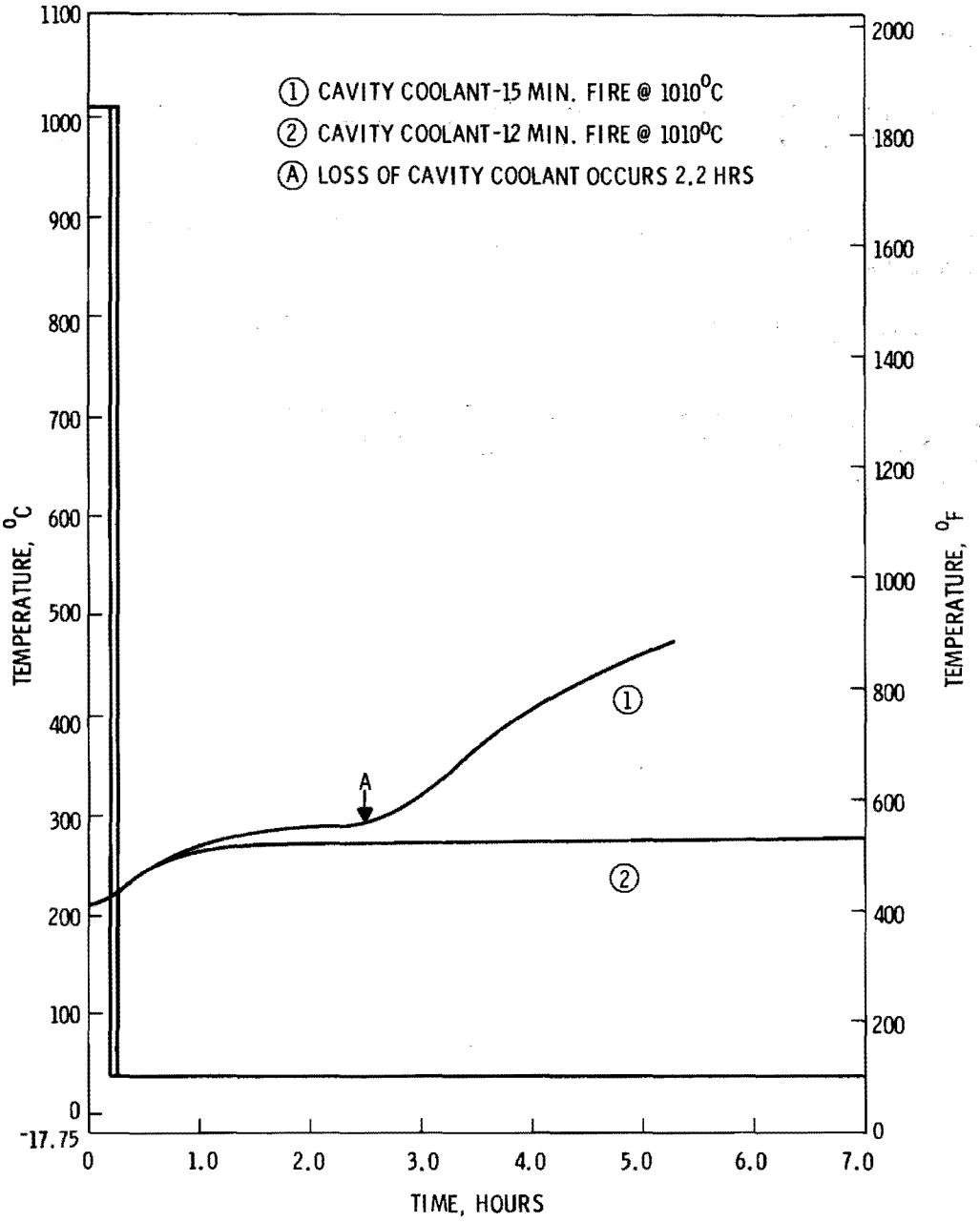

FIGURE G.7. Minimum Duration Fire to Cause Loss of Cavity Coolant

REFERENCES

1. Y. S. Touloukian, C. Y. Ho, Thermophysical Properties of Matter. Thermophysical Properties Research center (TPRC), Purdue University, 1970.

2. E. M. Sparrow and R. D. Cess, Radiation Heat Transfer, Brooks/Cole, Belmont, CA, 1966.

3. F. Kreith, Principles of Heat Transfer, Second Ed., International Textbook Company, Scranton, PA, 1965.

4. C. W. Smith, Calculated Fuel Rod Perforation Temperatures Commercial Power Reactor Fuels, NEDO-10093, General Electric Company, San Jose, CA, September 1969.

APPENDIX H

SPENT FUEL SHIPPING MODEL

In order to determine shipping distances between reactors and interim storage facilities or reactors and reprocessing plants, a shipment system model was developed. To simplify the analysis and reduce computer time, reactors either currently operating or planned for operation during the reference year,[1] were grouped according to reactor type (BWR or PWR) and location. A listing of the reactor groups is presented in Table H.1. Interim spent fuel storage facilities were assumed to be located at:

- Hanford, Washington
- Oak Ridge, Tennessee
- Morris, Illinois
- Barnwell, South Carolina

Reprocessing plants were assumed to be operating at Oak Ridge, Tennessee, and Barnwell, South Carolina. A map showing the locations of reactor groups and spent fuel shipment receiving sites is shown in Figure 4.1 of Section 4.

Estimates of the amounts of spent fuel shipped per year from each reactor group were made based on the number, size and type of reactors in each group. From these amounts, the number of assemblies shipped and the number of shipments by truck were calculated. Truck shipments were assumed to account for 20% of all spent fuel shipped during the reference time period. The results of these calculations are tabulated in Tables H.2 and H.3.

REFERENCE

1. Nuclear News, 20(10):73, August 1977..

TABLE H.1. Tabulation of Reactors and Reactor Groups

Group No.	Reactor Name	Type	State
1	Monticello	BWR	Minnesota
1	La Crosse	BWR	Wisconsin
2	Dresden 1	BWR	Illinois
2	Dresden 2	BWR	Illinois
2	Dresden 3	BWR	Illinois
2	Lasalle 1	BWR	Illinois
2	Lasalle 2	BWR	Illinois
2	Bailly	BWR	Indiana
2	Clinton 1	BWR	Illinois
2	Clinton 2	BWR	Illinois
3	Quad Cities 1	BWR	Illinois
3	Quad Cities 2	BWR	Illinois
3	Duane Arnold 1	BWR	Iowa
4	Enrico Fermi 2	BWR	Michigan
4	Perry 1	BWR	Ohio
4	Perry 2	BWR	Ohio
5	Nine Mile Point 1	BWR	New York
5	Fitzpatrick 1	BWR	New York
5	Nine Mile Point 2	BWR	New York
5	Somerset 1	BWR	New York
5	Somerset 2	BWR	New York
6	Grand Gulf 1	BWR	Mississippi
6	Riverbend 1	BWR	Louisiana
6	Riverbend 2	BWR	Louisiana
6	Grand Gulf 2	BWR	Mississippi
7	Browns Ferry 1	BWR	Alabama
7	Browns Ferry 2	BWR	Alabama
7	Browns Ferry 3	BWR	Alabama
7	Barton 1	BWR	Alabama
7	Barton 2	BWR	Alabama
7	Barton 3	BWR	Alabama
7	Yellow Creek 1	BWR	Mississippi
7	Yellow Creek 2	BWR	Mississippi

TABLE H.1. Continued

Group No.	Reactor Name	Type	State
8	Oyster Creek 1	BWR	New Jersey
8	Hope Creek 1	BWR	New Jersey
8	Hope Creek 2	BWR	New Jersey
8	Peach Bottom 2	BWR	Pennsylvania
8	Peach Bottom 3	BWR	Pennsylvania
8	Limerick 1	BWR	Pennsylvania
8	Limerick 2	BWR	Pennsylvania
8	Susquehanna 1	BWR	Pennsylvania
8	Susquehanna 2	BWR	Pennsylvania
8	Douglas Point 1	BWR	Maryland
8	Douglas Point 2	BWR	Maryland
9	Millstone 1	BWR	Connecticut
9	Pilgrim 1	BWR	Massachusetts
9	Shoreham	BWR	New York
9	Vermont Yankee	BWR	Vermont
9	Montague 1	BWR	Massachusetts
9	Montague 2	BWR	Massachusetts
10	Hatch 1	BWR	Georgia
10	Hatch 2	BWR	Georgia
11	Brunswick 2	BWR	North Carolina
11	Brunswick 1	BWR	North Carolina
12	Zimmer 1	BWR	Ohio
12	Zimmer 2	BWR	Ohio
13	Hartsville 1	BWR	Tennessee
13	Hartsville 2	BWR	Tennessee
13	Hartsville 3	BWR	Tennessee
13	Hartsville 4	BWR	Tennessee
14	Allens Creek 1	BWR	Texas
14	Allens Creek 2	BWR	Texas
15	Black Fox 1	BWR	Oklahoma
15	Black Fox 2	BWR	Oklahoma
16	Skagit 1	BWR	Washington
16	Skagit 2	BWR	Washington
17	Cooper	BWR	Nebraska
18	Big Rock Point	BWR	Michigan

TABLE H.1. Continued

Group No.	Reactor Name	Type	State
19	Humboldt Bay	BWR	California
20	WPPSS 2	BWR	Washington
21	Trojan	PWR	Oregon
21	WPPSS 3	PWR	Washington
21	WPPSS 5	PWR	Washington
22	WPPSS 1	PWR	Washington
22	Pebble Springs 1	PWR	Oregon
22	Pebble Springs 2	PWR	Oregon
22	WPPSS 4	PWR	Washington
23	Prairie Island 1	PWR	Minnesota
23	Prairie Island 2	PWR	Minnesota
23	Tyrone 1	PWR	Wisconsin
24	Zion 1	PWR	Illinois
24	Zion 2	PWR	Illinois
24	Palisades	PWR	Michigan
24	Cook 1	PWR	Michigan
24	Cook 2	PWR	Michigan
24	Braidwood 1	PWR	Illinois
24	Braidwood 2	PWR	Illinois
24	Byron Township 1	PWR	Illinois
24	Byron Township 2	PWR	Illinois
24	Koshkonong 1	PWR	Wisconsin
24	Koshkonong 2	PWR	Wisconsin
25	Point Beach 1	PWR	Wisconsin
25	Point Beach 2	PWR	Wisconsin
25	Kewaunee 1	PWR	Wisconsin
26	Midland 1	PWR	Michigan
26	Midland 2	PWR	Michigan
26	Davis Besse 1	PWR	Ohio
26	Greenwood 2	PWR	Michigan
26	Greenwood 3	PWR	Michigan
26	Davis Besse 2	PWR	Ohio
26	Davis Besse 3	PWR	Ohio
27	Ginna 1	PWR	New York
27	Sterling	PWR	New York

TABLE H.1. Continued

Group No.	Reactor Name	Type	State
28	Comanche Peak 1	PWR	Texas
28	Comanche Peak 2	PWR	Texas
28	Blue Hills 1	PWR	Texas
28	Blue Hills 2	PWR	Texas
28	South Texas 1	PWR	Texas
28	South Texas 2	PWR	Texas
29	Turkey Point 3	PWR	Florida
29	Turkey Point 4	PWR	Florida
29	St. Lucie 1	PWR	Florida
29	St. Lucie 2	PWR	Florida
29	South Dade 1	PWR	Florida
29	South Dade 2	PWR	Florida
30	Harris 1	PWR	North Carolina
30	McGuire 1	PWR	North Carolina
30	McGuire 2	PWR	North Carolina
30	Robinson 2	PWR	South Carolina
30	Oconee 1	PWR	South Carolina
30	Oconee 2	PWR	South Carolina
30	Oconee 3	PWR	South Carolina
30	Virgil Summer 1	PWR	South Carolina
30	Harris 2	PWR	North Carolina
30	Harris 3	PWR	North Carolina
30	Harris 4	PWR	North Carolina
30	Catawba 1	PWR	South Carolina
30	Catawba 2	PWR	South Carolina
30	Perkins 1	PWR	North Carolina
30	Perkins 2	PWR	North Carolina
30	Perkins 3	PWR	North Carolina
30	Cherokee 1	PWR	South Carolina
30	Cherokee 2	PWR	South Carolina
30	Cherokee 3	PWR	South Carolina
31	Farley 1	PWR	Alabama
31	Farley 2	PWR	Alabama
31	Barton 4	PWR	Alabama
32	Sequoyah 1	PWR	Tennessee
32	Sequoyah 2	PWR	Tennessee
32	Watts Bar 1	PWR	Tennessee
32	Watts Bar 2	PWR	Tennessee
32	Belefonte 1	PWR	Tennessee
32	Belefonte 2	PWR	Tennessee
32	Phipps Bend 1	PWR	Tennessee
32	Phipps Bend 2	PWR	Tennessee

TABLE H.1. Continued

Group No.	Reactor Name	Type	State
33	Calvert Cliffs 1	PWR	Maryland
33	Calvert Cliffs 2	PWR	Maryland
33	Salem 1	PWR	New Jersey
33	Salem 2	PWR	New Jersey
33	Forked River 1	PWR	New Jersey
33	Three Mile Island	PWR	Pennsylvania
33	Three Mile Island	PWR	Pennsylvania
33	Atlantic 1	PWR	New Jersey
33	Atlantic 2	PWR	New Jersey
33	Atlantic 3	PWR	New Jersey
33	Atlantic 4	PWR	New Jersey
34	Connecticut Yankee	PWR	Connecticut
34	Millstone 2	PWR	Connecticut
34	Yankee	PWR	Massachusetts
34	Indian Point 1	PWR	New York
34	Indian Point 2	PWR	New York
34	Indian Point 3	PWR	New York
34	Jamesport 2	PWR	New York
34	Jamesport 1	PWR	New York
34	Pilgrim	PWR	Massachusetts
34	Seabrook 1	PWR	New Hampshire
34	Seabrook 2	PWR	New Hampshire
34	Nep 1	PWR	Rhode Island
34	Millstone 3	PWR	Connecticut
34	Nep 2	PWR	Rhode Island
34	Green County	PWR	New York
35	Main Yankee	PWR	Maine
35	Sears Island	PWR	Maine
36	Surry 4	PWR	Virginia
36	Surry 1	PWR	Virginia
36	Surry 2	PWR	Virginia
36	North Anna 1	PWR	Virginia
36	North Anna 2	PWR	Virginia
36	North Anna 3	PWR	Virginia
36	North Anna 4	PWR	Virginia
36	Surry 3	PWR	Virginia
37	Diablo Canyon 1	PWR	California
37	Diablo Canyon 2	PWR	California
37	Rancho Seco	PWR	California

TABLE H.1. Continued

Group No.	Reactor Name	Type	State
38	Beaver Valley 1	PWR	Pennsylvania
38	Shippingport	PWR	Pennsylvania
38	Beaver Valley 2	PWR	Pennsylvania
39	Arkansas 1	PWR	Arkansas
39	Arkansas 2	PWR	Arkansas
40	San Onofre 1	PWR	California
40	San Onofre 2	PWR	California
40	San Onofre 3	PWR	California
41	Fort Calhoun 1	PWR	Nebraska
41	Fort Calhoun 2	PWR	Nebraska
42	Callaway 1	PWR	Missouri
42	Callaway 2	PWR	Missouri
43	Palo Verde 1	PWR	Arizona
43	Palo Verde 2	PWR	Arizona
43	Palo Verde 3	PWR	Arizona
44	Marble Hill 2	PWR	Indiana
44	Marble Hill 1	PWR	Indiana
45	Crystal River 3	PWR	Florida
46	Waterford 3	PWR	Louisiana
47	Wolf Creek	PWR	Kansas

TABLE H.2. Spent Fuel Shipments by Truck from Reactors to Storage Facilities

R.G.	Reactor Type	Miles to Nearest Storage Facility	MT Shipped/ Year	Number Of Ass. Shipped	Number Shipped By Truck (20%)	Truck Shipments	Shipment-Miles(a)
1	BWR	470	8	48	10	5	2.35×10^3
2	BWR	130	80	483	97	49	6.37×10^3
3	BWR	200	32	193	39	20	4.00×10^3
4	BWR	410	45	272	54	27	1.11×10^4
5	BWR	660	37	223	45	23	1.52×10^4
6	BWR	480	28	169	34	17	8.16×10^3
7	BWR	210	49	296	59	30	6.30×10^3
8	BWR	560	110	664	133	67	3.75×10^4
9	BWR	790	40	241	48	24	1.90×10^4
10	BWR	70	27	163	33	27	1.89×10^3
11	BWR	230	24	145	29	15	3.45×10^3
12	BWR	230	12	72	14	7	1.61×10^3
13	BWR	120	50	302	60	30	3.60×10^3
14	BWR	780	30	181	36	18	1.40×10^4
15	BWR	420	0	0	0	0	0
16	BWR	180	16	97	19	10	4.20×10^3
17	BWR	360	12	72	14	7	2.52×10^3
18	BWR	460	2	12	2	1	4.60×10^2
19	BWR	470	2	12	2	1	4.70×10^2
20	BWR	10	17	103	21	11	1.10×10^2
21	PWR	180	41	83	17	17	3.06×10^3
22	PWR	40	42	85	17	17	6.80×10^2
23	PWR	410	14	28	6	6	2.46×10^3
24	PWR	200	131	264	53	53	1.06×10^4
25	PWR	350	22	44	9	9	1.80×10^3
26	PWR	380	52	105	21	21	7.98×10^3
27	PWR	670	7	14	3	3	2.01×10^3
28	PWR	730	53	107	21	21	1.53×10^4

TABLE H.2. Continued

R.G.	Reactor Type	Miles to Nearest Storage Facility	MT Shipped/ Year	Number Of Ass. Shipped	Number Shipped By Truck (20%)	Truck Shipments	Shipment-Miles(a)
29	PWR	450	59	119	24	24	1.08×10^4
30	PWR	190	127	256	51	51	9.69×10^3
31	PWR	200	21	42	8	8	1.60×10^3
32	PWR	100	95	191	38	38	3.80×10^3
33	PWR	570	93	187	37	37	2.11×10^4
34	PWR	780	152	306	61	61	4.76×10^4
35	PWR	1000	25	50	10	10	1.00×10^4
36	PWR	420	78	157	31	31	1.30×10^4
37	PWR	730	40	81	16	16	1.17×10^4
38	PWR	410	22	44	9	9	3.42×10^2
39	PWR	360	24	48	10	10	3.60×10^3
40	PWR	920	24	48	10	10	9.20×10^3
41	PWR	400	19	38	8	8	3.20×10^3
42	PWR	160	26	52	10	10	1.60×10^3
43	PWR	980	13	26	5	5	4.90×10^3
44	PWR	190	13	26	5	5	9.50×10^2
45	PWR	260	13	26	5	5	1.30×10^3
46	PWR	520	15	30	6	6	3.12×10^3
47	PWR	370	13	26	5	5	1.85×10^3
Total			1854			885	3.80×10^5

(a) 1 Mile = 1.61 km

TABLE H.3. Spent Fuel Shipments by Truck from Reactors to Fuel Reprocessing Plants

R.G.	Reactor Type	Spent Fuel Receiver	Miles[a] to Nearest Reprocessing Plant	MT Shipped/ Year	Number Of Ass. Shipped	Number Shipped By Truck (20%)	Truck Shipments	Shipment-Miles[a]
1	BWR	M	820	8	48	10	5	4.10×10^3
2	BWR	M	440	80	483	97	49	2.16×10^4
3	BWR	M	550	32	193	39	20	1.10×10^4
4	BWR	M	460	45	272	54	27	1.24×10^4
5	BWR	M	660	37	223	45	23	1.52×10^4
6	BWR	O	480	28	169	34	17	8.16×10^3
7	BWR	O	210	49	296	59	30	6.30×10^3
8	BWR	O	560	110	664	133	67	3.75×10^3
9	BWR	O	790	40	241	48	24	1.90×10^4
10	BWR	B	70	27	163	33	27	1.89×10^3
11	BWR	B	230	24	145	29	15	3.45×10^3
12	BWR	O	230	12	72	14	7	1.61×10^3
13	BWR	O	120	50	302	60	30	3.60×10^3
14	BWR	M	790	30	181	36	18	1.42×10^4
15	BWR	M	620	0	0	0	0	0
16	BWR	H	2100	16	97	19	10	2.10×10^4
17	BWR	M	700	12	72	14	7	4.90×10^3
18	BWR	M	680	2	12	2	1	6.80×10^2
19	BWR	H	2170	2	12	2	1	2.17×10^3
20	BWR	H	1950	17	103	21	11	2.15×10^4
21	PWR	H	2140	41	83	17	17	3.64×10^4
22	PWR	H	1960	42	85	17	17	3.33×10^4
23	PWR	M	750	14	28	6	6	4.50×10^3
24	PWR	M	490	131	264	53	53	2.60×10^4
25	PWR	M	630	22	44	9	9	5.67×10^3
26	PWR	M	480	52	105	21	21	1.01×10^4
27	PWR	O	670	7	14	3	3	2.01×10^3
28	PWR	M	760	53	107	21	21	1.60×10^4
29	PWR	B	450	59	119	24	24	1.08×10^4
30	PWR	B	190	127	256	51	51	9.69×10^3
31	PWR	B	200	21	42	8	8	1.60×10^3
32	PWR	O	100	95	191	38	38	2.80×10^3
33	PWR	O	570	93	187	37	37	2.11×10^4
34	PWR	O	780	152	306	61	61	4.76×10^4
35	PWR	O	1000	25	50	10	10	1.00×10^4
36	PWR	B	420	78	157	31	31	1.30×10^4
37	PWR	H	2030	40	81	16	16	3.25×10^4
38	PWR	O	410	22	44	9	9	3.42×10^2
39	PWR	M	500	24	48	10	10	5.00×10^3
40	PWR	H	1890	24	48	10	10	1.89×10^4
41	PWR	M	750	19	38	8	8	6.00×10^3
42	PWR	M	470	26	52	10	10	4.70×10^3
43	PWR	H	1620	13	26	5	5	8.10×10^3
44	PWR	M	230	13	26	5	5	1.15×10^3
45	PWR	B	260	13	26	5	5	1.30×10^3
46	PWR	O	520	15	30	6	6	3.12×10^3
47	PWR	M	650	13	26	5	5	3.25×10^3
Totals				1854			885	5.12×10^5

(a) 1 Mile = 1.6 km

DISTRIBUTION

No. of Copies

OFFSITE

A. A. Churm
Chicago Patent Group
DOE Chicago Operations Office
9800 South Cass Avenue
Argonne, IL 60439

171 DOE Technical Information Center

K. A. Trickett
Division of Reactor Development and Demonstration
Department of Energy
Germantown, MD 20014

25 W. Brobst
Transportation Branch
Division of Environmental Control Technology
Department of Energy
Washington, DC 20545

J. Counts
Transportation Branch
Division of Environmental Control Technology
Department of Energy
Washington, DC 20545

R. F. Garrison
Transportation Branch
Division of Environmental Control Technology
Department of Energy
Washington, DC 20545

J. A. Sisler
Transportation Branch
Division of Environmental Control Technology
Department of Energy
Washington, DC 20545

No. of Copies

R. B. Chitwood
Division of Fuel Storage and Transfer
Department of Energy
Washington, DC 20545

E. C. Hardin, Jr.
Office of the Assistant Secretary for Energy Technology
Department of Energy
Washington, DC 20545

R. M. Moser
DOE Chicago Operations Office
9800 South Cass Avenue
Argonne, IL 60439

W. G. O'Quinn
DOE Savannah River Operations Office
P.O. Box A
Aiken, SC 29801

N. Stetson
DOE Savannah River Operations Office
P.O. Box A
Aiken, SC 29801

L. L. Turner
DOE Savannah River Operations Office
P.O. Box A
Aiken, SC 29801

D. Davis
DOE Albuquerque Operations Office
P.O. Box 5400
Albuquerque, NM 87115

No. of
Copies

Sidney Firarman
Brookhaven National
Laboratory
Bldg. 197 C
Upton, NY 11973

Susan Metzler
System Communications
N. E. Utilities
P.O. Box 270
Hartford, CT 06101

L. Blalock
DOE Oak Ridge Operations
Office
P.O. Box E
Oak Ridge, TN 37830

J. J. Schreiber
DOE Oak Ridge Operations
Office
P.O. Box E
Oak Ridge, TN 37830

G. R. Swindell
International Atomic Energy Agency
A-1011 Vienna, AUSTRIA

J. L. Russell
Office of Radiation Programs
AW-459, EPA
401 M. St. S.W.
Washington, DC 20460

R. L. Ferguson
Director, Nuclear Energy
Programs
Department of Energy
Washington, DC 20545

T. K. Keenan
University of California
Los Alamos Scientific Laboratory
P.O. Box 1663
Los Alamos, NM 87545

No. of
Copies

T. A. Butler
University of California
Los Alamos Scientific Laboratory
P.O. Box 1663
Los Alamos, NM 87545

G. Kinchin
UKAEA
Risley, Lancaster
ENGLAND

L. Benner
National Transportation
Safety Board
Department of Transportation
Washington, DC 20594

E. J. Wilson
Department of Transport
Dangerous Goods Branch
2 Marsham St.
London SW 1
ENGLAND

Ichiro Yabe
Nuclear Safety Research
Association
Room 1037, National Press
Building
14th and F St. N.W.
Washington, DC 20004

A. L. Schmieg
National Transportation
Safety Board
Department of Transportation
Washington, DC 20594

P. J. Eicker
Sandia Laboratories, Livermore
Livermore, CA 94550

J. W. Langhaar
E. I. Dupont de Nemours &
Company
Savannah River Plant
Aiken, SC 29801

No. of
Copies

L. D. Santman
Materials Transportation Bureau
Department of Transportation
2100 Second St. S.W.
Washington, DC 20590

Dr. H. C. Thompson
Battelle Memorial Institute
Washington Operations
20301 M St. N.W.
Washington, DC 20036

W. Rowe
Environmental Protection Agency
401 M St.
Washington, DC 20460

A. J. Nertney
Aerojet Nuclear Company
550 2nd St.
Idaho Falls, ID 83401

Dr. J. Jacquemin
Office of Minister für Arbeit,
Gesundheit, und Sociales des
Landes NRW
Landeshaus
4000 Dusseldorf
FEDERAL REPUBLIC OF GERMANY

C. Starr
Electrical Power Research Inst.
P.O. Box 10412
Palo, Alto, CA 94304

C. Comar
Electric Power Research Inst.
P.O. 10412
Palo Alto, CA 94304

E. Zebrowski
Electrical Power Research Inst.
P.O. Box 10412
Palo, Alto, CA 94304

No. of
Copies

R. Williams
Electrical Power Research Inst.
P.O. Box 10412
Palo, Alto, CA 94304

Combustion Engineering, Inc.
Windsor, CT 06095

J. Desmond
Babcock & Wilcox, Co.
P.O. Box 1260
Lynchburg, VA 24505

C. Woods
Babcock & Wilcox Co.
P.O. Box 1260
Lynchburg, VA 24505

Prof. Norman C. Rasmussen
Massachusetts Institute of
Technology
Cambridge, MA 02139

J. K. Cole
Sandia Laboratories
P.O. Box 5800
Albuquerque, NM 87115

J. T. Foley
Sandia Laboratories
P.O. Box 5800
Albuquerque, NM 87115

J. Freedman
Sandia Laboratories
P.O. Box 5800
Albuquerque, NM 87115

W. F. Hartmann
Sandia Laboratories
P.O. Box 5800
Albuquerque, NM 87115

R. M. Jefferson
Sandia Laboratories
P.O. Box 5800
Albuquerque, NM 87115

No. of
Copies

R. Luna
Sandia Laboratories
P.O. Box 5800
Albuquerque, NM 87115

T. G. Priddy
Sandia Laboratories
P.O. Box 5800
Albuquerque, NM 87115

A. W. Snyder
Sandia Laboratories
P.O. Box 5800
Albuquerque, NM 87115

R. Yoshimura
Sandia Laboratories
P.O. Box 5800
Albuquerque, NM 87115

R. F. Baker
Nuclear Regulatory Commission
Washington, DC 20555

C. B. Bartlett
Nuclear Regulatory Commission
Washington, DC 20555

S. H. Hanauer
Nuclear Regulatory Commission
Washington, DC 20555

S. Levine
Nuclear Regulatory Commission
Washington, DC 20555

R. B. Minogue
Nuclear Regulatory Commission
Washington, DC 20555

C. McDonald
Nuclear Regulatory Commission
Washington, DC 20555

W. E. Vesely
Nuclear Regulatory Commission
Washington, DC 20555

No. of
Copies

I. Wall
Nuclear Regulatory Commission
Washington, DC 20555

M. J. Steindler
Argonne National Laboratory
9800 South Cass Avenue
Argonne, IL 60439

D. S. Joy
Union Carbide Corporation
Oak Ridge National Laboratory
P.O. Box X
Oak Ridge, TN 37830

Bill Pardue
Battelle Memorial Institute
Office of Nuclear Waste
Isolation
505 King Avenue
Columbus, OH 43201

R. A. Robinson
Battelle Memorial Institute
Office of Nuclear Waste
Isolation
505 King Avenue
Columbus, OH 43201

Atomics International
8900 DeSoto Avenue
Conoga Park, CA 91304

A. L. Kaplan
General Electric Co.
Nuclear Fuel Division
P.O. Box 780
Wilmington, NC 28401

G. Lapier
Babcock & Wilcox Co.
Apollo, PA 15613

R. D. Seagren
Union Carbide Corporation
Oak Ridge National Laboratories
P.O. Box X
Oak Ridge, TN 37830

No. of Copies

L. Shappert
Union Carbide Corporation
Oak Ridge National Laboratories
P.O.Box X
Oak Ridge, TN 37830

J. Duckworth
Nuclear Fuel Service, Inc.
P.O. Box 124
West Valley, NY 14171

G. L, Stukenbroeker
N. L. Industries, Inc.
Nuclear Transportation Dept.
P.O. Box 2046
Wilmington, DE 19899

J. R. Marshall
Union Carbide Corporation
Oak Ridge National Laboratory
P.O. Box X
Oak Ridge, TN 37830

M. M. Heiskel
Union Carbide Corporation
Oak Ridge National Laboratory
P.O. Box X
Oak Ridge, TN 37830

H. G. Shealy
Bureau of Radiological Health
South Carolina Department of Health and Environmental Control
Columbia, SC 29405

J. S. Corbett
ChemNuclear Systems, Inc.
P.O. Box 1866
Bellevue, WA 98009

J. A. Hebert
Battelle Seattle Research Center
P.O. Box 5395
Seattle, WA 98105

No. of Copies

P. T. Tuite
Hittman Nuclear and Development Corporation
9190 Red Branch Rd.
Columbia, MD 21045

D. A. Edling
Mound Laboratories
P.O. Box 32
Miamisburg, OH 45342

J. W. Doty
Mound Laboratories
P.O. Box 32
Miamisburg, OH 45342

D. Okrent
Department of Engineering and Applied Science
University of California
Los Angeles, CA 90024

J. Walker
California Energy Resources Conservation and Development Commission
1111 Howe Avenue
Sacramento, CA 95825

B. Jost
Mail Stop 18
California Energy Commission
111 Howe Ave.
Sacramento, CA 95825

R. H. Jones
Transportation Systems
Nuclear Energy Programs Division
General Electric Company
175 Curtner Avenue
San Jose, CA 95125

M. Gordon
Atomic Industrial Forum
7101 Wisconsin Avenue
Washington, DC 20014

No. of Copies

A. L. Babb
Department of Nuclear Engineering
Benson Hall
University of Washington
Seattle, WA 98195

W. S. Fellows
Southern Interstate Nuclear Board
One Exchange Place, Suite 1230
Atlanta, GA 30341

D. G. Maxwell
N. L. Industries
Nuclear Division
Foot of West Street
Wilmington, DE 19801

W. R. Teer
Transnuclear Inc.
One N. Broadway
White Plains, NY 10601

S. Hartwig
Battelle Institute, e.v.
Am Romerhof 35
600 Frankfurt Main 90
GERMANY

M. Stammler
Battelle Institute, e.v.
Am Romerhof 35
600 Frankfurt Main 90
GERMANY

R. S. Lowrie
Union Carbide Corporation
Office of Waste Isolation
P.O. Box Y
Oak Ridge, TN 37830

J. L. Ridihalgh
Ridihalgh, Eggers & Associates
2112 Iuka Avenue
Columbus, OH 43201

No. of Copies

S. C. Cohn
Teknekron
4701 Sangamore Rd.
Washington, DC 20016

I. N. Lafontaine
Belgonucleaire
Rue de Champ de Mars 25
B-1050 Bruxelles
BELGIUM

K. R. Shultz
Atomic Energy Control Board
P.O.B. 1046
Ottawa KIP 5S9
CANADA

W. R. Taylor
Atomic Energy of Canada Ltd.
Chalk River Laboratories
Chalk River, Ontario KOJIJO
CANADA

Y. Sousselier
CEA/CEN
B.P. No. 6
F-92260 Fontenay-aux-Roses
FRANCE

H. Hubner
Bundesanstalt für Material-prufung
Unter den Eichen 87
D-1000 Berlin 45 (West)
GERMANY, FED. REPUBLIC

B. Schulz-Forberg
Bundesanstalt für Material-prufung
Unter den Eichen 87
D-1000 Berlin 45 (West)
GERMANY, FED. REPUBLIC

H. F. McDonald
CEGB
Berkeley Nuclear Labs
Berkeley
Gloucestershire GL139PB
UNITED KINGDOM

No. of
Copies

R. G. Deshpande
Isotope Division
Bhabha Atomic Research Centre
Trombay, Bombay 400 085
INDIA

S. Aoki
Research Laboratory for
Nuclear Reactors
Tokyo Institute of
Technology
Ookayamá, Meguroku, Tokyo 152
JAPAN

G. D. Bell
United Kingdom Atomic Energy
Authority
Safety and Reliability
Directorate
Warrington WA3 4NE
UNITED KINGDOM

A. Ondedera
Hitachi Shipbuilding and
Engineering Co., Ltd.
5-4 Kakurajima, Kitano-cho
Konohana-ku, Osaka-shi
JAPAN

K. Ikeda
Science and Technology Agency
2-2-1 Kasumigaseki,
Chiyoda-ku, Tokyo
JAPAN

M. Tomlinson
White Shell Nuclear Research
Establishment
Pinewa, Manitoba ROE ILO
CANADA

S. A. Mayman
Fuel Recycle Waste
Management Program
Whiteshell Nuclear Research
Establishment
Pinewa, Manitoba ROE ILO
CANADA

No. of
Copies

Dr. R. Girardi
Euratom
21020 Centro Euratomdi
Ispra (Varesse)
ITALY

Ake Hultgren
AB Atomenergi, Studsvik
Fack
S-611 01 Nyköping 1
SWEDEN

B. Gustafson
c/o Ake Hultgren
AB Atomenergi, Studsvik
Fack
S-611 01 Nyköping 1
SWEDEN

Dr. Schmidt-Kuester
Beim Bundesminister für
Forschung and Technologie
Stresemannstrasse 2
5300 Bonn
GERMANY

R. W. Peterson
Battelle Memorial Institute
Office of Nuclear Waste
Isolation
505 King Avenue
Columbus, OH 43201

A. Carson
General Electric Company
175 Curtner Avenue
San Jose, CA 95125

R. A. Koynenburg
University of California
Lawrence Livermore Laboratories
P.O. Box 808
Livermore, CA 94551

No. of
Copies

R. E. Best
Nuclear Assurance Corporation
24 Executive Park West
Atlanta, GA 30329

M. Pollock
Oregon Department of Energy
Salem, OR 97301

W. M. Rogers
Western Interstate Nuclear
Board
1300 Carr
Denver, CO 80226

G. P. Jones
University of Southern
California
University Park
Los Angeles, CA 90007

E. A. Straker
Science Applications, Inc.
P.O. Box 2351
La Jolla, CA 92038

R. C. Erdman
Science Applications, Inc.
2680 Hanover St.
Palo, Alto, CA 94304

N. C. Harris
Imperial Chemical Industries, Ltd.
Mond Division
P.O. Box No. 47 Brunner House
Winnington Northwich
Cheshire CW8 40J
ENGLAND

G. Waymire
Exxon Nuclear Company, Inc.
P.O. Box 3990
MS 8A-68
Seattle, WA 98124

No. of
Copies

W. R. Rhyne
Science Applications Inc.
P.O. Box 843
Oak Ridge, TN 37830

Hubert Baker
E. I. DuPont de Nemours & Co.
Savannah River Laboratory
Aiken SC 29801

C. A. Mayer
Tri-State Motor Transit Co., Inc.
P.O. Box 113
Joplin, MO 64801

J. Edlow
Edlow International
1100 17th Street N.W.
Washington, DC

W. F. Black
Hazardous Materials Branch
Federal Railroad Administration
Department of Transportation
Washington, DC

Dr. C. Furber
Research and Test Department
Association of American Railroads
1920 L. Street N.W.
Washington, DC 20036

R. R. Rawl
Materials Transportation Bureau
U.S. Department of Transportation
Washington, DC 20545

E. P. Goldfinch
Safeguards Branch
Nuclear Health and Safety
Department
Courtenay House
18 Warwick Lane
London F C4P 4EB
UNITED KINGDOM

No. of
Copies

N. Darmstader
American Trucking Association
1616 P St. N.W.
Washington, DC 20036

R. A. Kaye
Director Bureau of Motor
Carrier Safety
Federal Highway Administration
U.S. Department of Transportation
Washington, DC 20590

M. Parrot
Oregon State Health Division
Radiation Control Section
1400 S. W. 5th
Portland, OR 97201

H. Latham
Oregon Emergency Services
Division
Rm. 43 State Capitol Bldg.
Salem, OR 97310

No. of
Copies

ONSITE

6 DOE Richland Operations Office

T. A. Bauman
R. B. Goranson
P. E. Lamont
J. M. Peterson
H. E. Ransom
D. J. Squires

3 Rockwell Hanford Company

W. G. Bevan
W. M. Harty
D. D. Woodrich

3 United Nuclear Industries, Inc.

J. A. Adams
P. A. Crosetti
T. E. Dabrowski

2 Washington Public Power Supply System

G. F. Bailey
J. B. Vetrano

3 Exxon Nuclear Company, Inc.

E. Mays
R. Nilsen
R. K. Robinson

Hanford Engineering Development Laboratory

A. W. DeMerschman

No. of
Copies

58 Pacific Northwest Laboratory

W. B. Andrews
W. J. Bair
C. L. Brown
N. M. Burleigh (25)
S. H. Bush
N. E. Carter
J. G. DeSteese
H. K. Elder
A. L. Franklin
J. Friley
C. A. Geffen
R. J. Hall
H. Harty
S. W. Heaberlin
H. L. Henry
W. S. Kelley
S. N. Liu
R. McCann
T. I. McSweeney
J. Mishima
E. S. Murphy
R. E. Rhoads
J. W. Voss
E. C. Watson
R. D. Widrig
L. D. Williams
W. K. Winegardner
Technical Information (5)
Publishing Coordination (2)